SHIBUYA

ISSN 0385-2520

# ROCK MAGNETISM and PALEOGEOPHYSICS

volume 7

1980

Published by the

ROCK MAGNETISM AND PALEOGEOPHYSICS RESEARCH GROUP IN JAPAN

# PREFACE

This volume is the annual progress report of the Rock Magnetism and Paleogeophysics Research Group in Japan for the year 1980. As the previous volumes were so, this volume is a collection of summaries or extended abstracts of various research works carried in our group. Many of the reports contain substances which may be revised or updated as the research activity continues. In this respect, this volume contains many tentative results.

Except for the ones written as pure progress reports, most of the papers in this volume will ultimately be published elsewhere in full detail and length. This volume may be referenced, but if a paper is published in an academic journal, the readers are requested to quote the paper from such a journal. We hope that this volume is a useful source of advance information of recent works on rock magnetism and paleogeophysics in Japan.

We would like to express our gratitude to three institutions (Department of Earth Sciences, Kobe University; Ocean Research Institute, University of Tokyo; Geophysical Institute, University of Tokyo) for partial financial supports in the publication of the last (Vol. 6) and the present volumes. We also thank Dr. T. Nakajima who kindly arranged for the printing and Mrs. T. Osaki who helped in editing.

December 1980

Masaru KONO
Editor

## ROCK MAGNETISM AND PALEOGEOPHYSICS SYMPOSIUM 12

The Twelfth Rock Magnetism and Paleogeophysics Symposium was held on 18th and 19th July, 1980 at the Library Building, Toyama University. The following papers were presented.

18 July Morning

| | |
|---|---|
| I. Katsura (Kyoto Univ.) | Paleomagnetism of Tamba Belt. |
| H. Shibuya (Kyoto Univ.) | Paleomagnetism of Mino Belt. |
| K. Kodama, T. Tosha (Tokyo Univ.), A. Taira (Kochi Univ.) and S. Saito (Natl. Science Museum) | Paleomagnetism of green rocks in Shimanto Belt in Shikoku. |
| J. Nishida (Otani Univ.) | Paleomagnetism of Mesozoic rocks from Hong Kong. |
| S. Sasajima, T. Hirashima, M. Kitamura and N. Morimoto (Kyoto Univ.) | Magnetic minerals in layers with low paleolatitudes. |

18 July Afternoon

| | |
|---|---|
| I. Hattori (Fukui Univ.) | An interpretation of formation mechanism of Paleozoic-Mesozoic Mino Belt. |
| S. Nomura, Y. Koido and N. Yamada (Gumma Univ.) | Paleomagnetism of the Permian Nohi rhyolites. |
| M. Yoshida (Hokkaido Univ.) | Paleomagnetic stratigraphy of Central Hokkaido (Ashiyoro-Tokachi area). |
| S. Mukoyama (Hokkaido Univ.) | Paleomagnetic stratigraphy of Central Hokkaido (Central Plateau-Tokachi area). |
| H. Tanaka (Tokyo Inst. Tech.) | A geomagnetic reversal at 30,000 y.B.P. found in Shibutami. |
| A. Hayashida, I. Katsura and H. Shibuya (Kyoto Univ.) | On the paleomagnetic data base. |
| T. Yokoyama (Doshisha Univ.), A. Hayashida, S. Nishimura (Kyoto Univ.), Sapri and Wahue | Paleomagnetic stratigraphy and radiometric ages of Sangiran and Trunir area, Indonesia. |

19 July Morning

| | |
|---|---|
| K. Noritomi (Akita Univ.) and J.N. Almasco | Paleomagnetism of rocks from Sebu Island, the Phillipines. |
| A. Hayashida (Kyoto Univ.) | Biwa I event and upper Pleistocene formations in Kinki area. |
| K. Manabe (Fukushima Univ.) | Relation between the geomagnetic excursion in late Pleistocene and climatic change inferred from botanical fossils (pollens). |
| N. Niitsuma (Shizuoka Univ.) | The VGP's at the time of geomagnetic reversal and changes in environment. |
| I. Muroi (Osaka Sci. Educ. Center) | Magnetic field induced by a spherical coil. |

19 July Afternoon

| | |
|---|---|
| T. Fujii (Toyama Univ.) | Submerged fossil-forest in Toyama bay. |
| H. Inokuchi (Kobe Univ.) | Geomagnetic surveys on the islands in the Southern Pacific. |
| N. Niitsuma (Shizuoka Univ.) | Evolution of TTT triple junction off the Kanto coast. |
| N. Niitsuma (Shizuoka Univ.) | The boring plan in post-GDP program. |

# CONTENTS

Preface i

Rock Magnetism and Paleogeophysics Symposium 12 ii

Contents iv

ANALYSES OF GEOMAGNETIC SIGNALS

Y. Matsubara and J. Matsuda — On the Determination of "Paleolongitude" in Paleomagnetism 1

H. Sakai — Spherical Harmonic Analysis of the Geomagnetic Field During the Last 2,000 years 8

T. Sato and K. Kobayashi — Spectral Analysis of Geomagnetic Field Intensity Derived from Four Deep-Sea Cores 16

M. Kono, Y. Hamano, T. Nishitani and T. Tosha — A New Spinner Magnetometer : Principles and Techniques 22

N. Isezaki, J. Matsuda, H. Inokuchi, and K. Yaskawa — Shipboard Measurement of Three Components of Geomagnetic Field 30

M. Hyodo, T. Ishizawa, Y. Hase, H. Inokuchi, N. Isezaki, and K. Yaskawa — Preliminary Report on the Magnetic Survey in Niue Island 36

MAGNETIC PROPERTIES OF ROCKS

Y. Otofuji, I. Katsura and S. Sasajima — Note on Effects of Drying on Post Depositional Remanent Magnetization of Sediments 40

M. Yoshida — Thermomagnetic Properties of the Pleistocene Pyroclastic Fall Deposits in the Yatsugatake Volcanoes, Central Japan 46

Y. Fujiwara, S. Mukoyama and T. Koshimizu — Identification of Pyroclastic Flow by Thermomagnetic and Neutron Activation Analysis 49

T. Nakajima and K. Hirooka — Anomalous Remenent Magnetization Caused by Thunderbolts Found in Ojima Andesite, Fukui Prefecture 52

H. Domen — Chemical and Alternative Magnetic Field Cleaning of Holocene Basalt from Kasa-Yama, Yamaguchi, Japan 59

PALEOMAGNETISM : RECENT TO QUATERNARY

H. Sakai — Variation of the Geomagnetic Field Intensity Deduced from Archaeological Objects 61

H. Inokuchi, H. Morinaga and K. Yaskawa — Paleomagnetism of Flowstone Collected at Gujo-Hachiman 68

K. Heki — Paleomagnetic Study of Secular Variation in Japan During the Last 40,000 Years 72

K. Hirooka — Palaeomagnetic Correlation of the Late Pleistocene Tephra Sediments in Japan 78

J. Furuya, H. Akai and T. Furuta Magnetic Properties of the Old Somma Lavas of Hakone Volcano 82

A. Hayashida Confirmation of a Magnetic Polarity Episode in the Brunhes Normal Epoch : A Preliminary Report 85

S. Sasajima, S. Nishimura and K. Hirooka Studies of the Blake Episode with Special Emphasis to East Asian Results Obtained 90

K. Maenaka On the Existence of Pre-Jaramillo Event in Matuyama Epoch 94

I. Kaneoka, H. Mehnert, S. Zashu and S. Kawachi Pleistocene Volcanic Activity in the Fossa Magna Region, Central Japan — K-Ar Age Studies of Yatsugatake Volcanoes — 100

PALEOMAGNETISM : TERTIARY AND EARLIER

M. Torii and Y. Tatsumi Paleomagnetic Study of the Setouchi Volcanic Belt. Part 1. Shodo-Shima Island (Preliminary Report) 105

S. Tonouchi and K. Kobayashi Magnetic Anomaly and Paleomagnetism of the Hayama-Mineoka Ophiolite 107

H. Ito, K. Tokieda and Y. Notsu A Paleomagnetic Approach to Possible Tilting Movements of Kitakami Mountains and Oshima Peninsula of Hokkaido 113

H. Shibuya and S. Sasajima A Paleomagnetic Study on Triassic-Jurassic System in Inuyama Area, Central Japan (Part I) 121

S. Sasajima and M. Torii Preliminary Paleomagnetic Studies on the Permian and Triassic Rocks from Okinawa-Jima, Ryukyus, Southern Japan 126

I. Katsura, J. Nishida and S. Sasajima Paleomagnetism of Permian Red Chert in the Tamba Belt, Southwest Japan (Preliminary Report) 130

Author Index 136

ON THE DETERMINATION OF "PALEOLONGITUDE" IN PALEOMAGNETISM

Yoshikazu MATSUBARA and Jun-ichi MATSUDA

Department of Earth Sciences, Faculty of Science,
Kobe University, Nada, Kobe 657, Japan

## 1. Introduction

Since Sclater and Cox (1970) opened the discussion on the "paleolatitude" from the variation of inclinations on DSDP samples, there have been a number of reports about it. Meanwhile, the declination has not been paid attention to as much as the inclination. One of the reason is that some method of sampling needs to rotate the corer. Therefore, a soft sample in the corer might be rotated during the sampling. The data of declination from such a core were not reliable.

Recently, a new technique of core sampling without rotating the corer has been developed, and we have now reliable data of declination of the magnetization in some cases. A precise measurement of three components of the geomagnetic field has just started (Isezaki et al., 1980), and we discuss the magnetization of the whole island obtained from geomagnetic anomalies.

So far, a change of declination seems to be interpreted in two ways; (1) The polar wondering... the geomagnetic pole was in a different position from the present site. (2) The rotation of island itself.

As the secular variation of the geomagnetic field is randomized for the period as long as $\sim$1 m.y. (Kobayashi, 1977), the geomagnetic field is regarded only due to the geocentric dipole for such a long term. Therefore, it is reasonable to assume that the geomagnetic pole is in accordance with the geographic pole for the magnetization of sediment core with slow sedimentation or of the magnetization of a whole island, if it takes $\sim$1 m.y. to acquire the magnetization as the whole island. Actually this assumption is used to get the paleolatitude from the inclination of the magnetization. Therefore, the interpretation (1) is not reasonable for the magnetization of a whole island or the site of slow sedimentation.

Meanwhile, we must be careful in discussing the rotation of the island. If the island drifts as the plate moves, the declination of the magnetization of the island changes. The change of this declination depends on the plate motion, the geomagnetic pole (which, we can assume, is the geographic pole) position and the site where the island got its magnetization. In this paper, we calculated how the declination changes as the plate moves. These change of declination should be corrected when we discuss the local rotation of the island itself. If the island did not rotate locally, we can get the "paleolongitude" of the island or the site from this calculation.

## 2. The equation of the change of declination

As we discussed in the previous section, the assumption that the geomagnetic pole agrees with the geographic pole is quite reasonable, in case we discuss the magnetization of the whole island. We consider the case that an island acquired its magnetization to the direction of the normal geomagnetic pole (= geographic pole), then drifts as the plate rotates by its rotational vector (Fig. 1). When the island got the magnetization, the declination of the magnetization of the island is zero. The angle of the magnetization from the great circle through the site of the island and the rotational pole of the plate is constant to the plate rotation. From the theories of spherical triangles, we can get the equation of the declination change as follows,

$$
\begin{aligned}
D_1 - D_0 = & \left[\tan^{-1}\left\{\frac{\cos 1/2(\theta_p-\theta_s)}{\cos 1/2(\theta_p+\theta_s)}\cot\left(\frac{A-B}{2}\right)\right\}\right. \\
& \left. + \tan^{-1}\left\{\frac{\sin 1/2(\theta_p-\theta_s)}{\sin 1/2(\theta_p+\theta_s)}\cot\left(\frac{A-B}{2}\right)\right\}\right] \\
& - \left[\tan^{-1}\left\{\frac{\cos 1/2(\theta_{I_0}-\theta_p)}{\cos 1/2(\theta_{I_0}+\theta_p)}\cot\left(\frac{\phi_{I_0}-\phi_p}{2}\right)\right\}\right. \\
& \left. - \tan^{-1}\left\{\frac{\sin 1/2(\theta_{I_0}-\theta_p)}{\sin 1/2(\theta_{I_0}+\theta_p)}\cot\left(\frac{\phi_{I_0}-\phi_p}{2}\right)\right\}\right]
\end{aligned}
$$

and

$$
\begin{aligned}
A = & \tan^{-1}\left\{\frac{\cos 1/2(\theta_{I_0}-\theta_p)}{\cos 1/2(\theta_{I_0}+\theta_p)}\cot\left(\frac{\phi_{I_0}-\phi_p}{2}\right)\right\} \\
& + \tan^{-1}\left\{\frac{\sin 1/2(\theta_{I_0}-\theta_p)}{\sin 1/2(\theta_{I_0}+\theta_p)}\cot\left(\frac{\phi_{I_0}-\phi_p}{2}\right)\right\}
\end{aligned}
$$

$$\theta_s = \cos^{-1}\{\cos\theta_p\cos\theta_{I_0} + \sin\theta_p\sin\theta_{I_0}\cos(\phi_{I_0}-\phi_p)\}$$

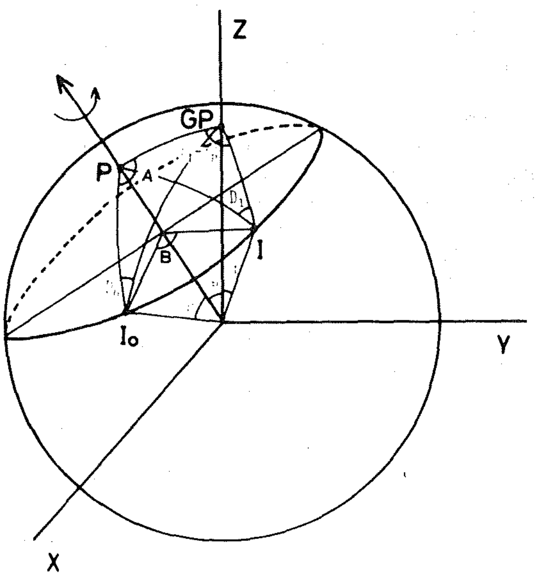


Fig. 1. The island gets its magnetization at $I_0$ and drifts to I as the plate rotates. GP is the geographic pole. P is the rotation pole of the plate.

where,

$\theta_I$: The colatitude of the present position of island

$\phi_I$: The longitude of the present position of the island

$\theta_{I_0}$: The colatitude of the site where the island acquired its magnetization

$\phi_{I_0}$: The longitude of the site where the island acquired its magnetization

$\theta_p$: The colatitude of the rotational pole of the plate

$\phi_p$: The longitude of the rotational pole of the plate

(a)

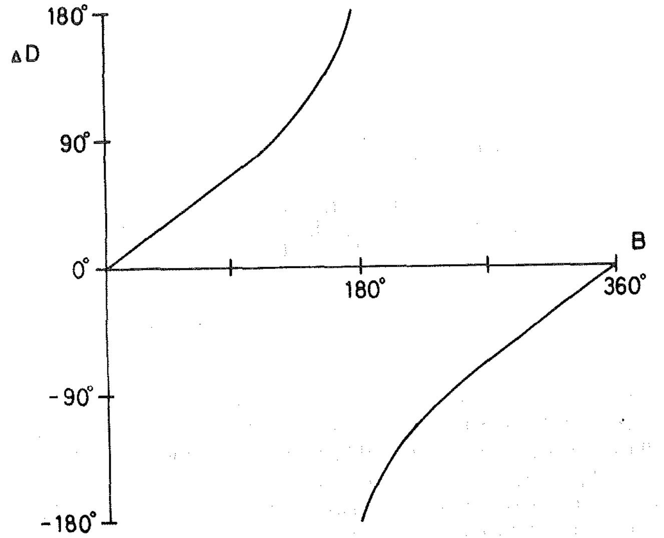


(b)

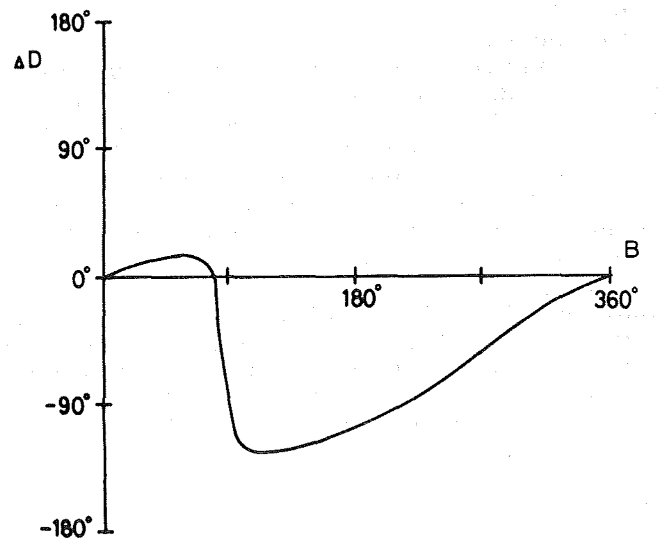


Fig. 2. The change of declination (ΔD) for the rotation angle (B) of the plate in two typical cases; (a) Rotation pole (44°N, 155°E) and the island(17°N, 155°E). (b) Rotation pole (45°N, 10°E) and the island (30°N, 70°E). The explanation for the difference of two curves is in the text. In (a) the island got its magnetization on the great circle through the geomagnetic pole and the rotation pole, because the longitudes of the island and the rotation pole are the same. Therefore, there is no phase shift of the curve.

$\theta_s$: The great circle distance between the rotation pole and the island

A: The angle between $\overset{\frown}{GP \cdot P}$ and $\overset{\frown}{P \cdot I_0}$

B: The rotation angle of the plate (In this equation B<A)

The longitude and colatitude of the present position of the island are

$$\theta_I = \cos^{-1}\{\cos\theta_s\cos\theta_p + \sin\theta_s\sin\theta_p\cos(A-B)\}$$

$$\phi_I = \phi_p + [\tan^{-1}\{\frac{\cos 1/2(\theta_p-\theta_s)}{\cos 1/2(\theta_p+\theta_s)} \cot(\frac{A-B}{2})\} - \tan^{-1}\{\frac{\sin 1/2(\theta_p-\theta_s)}{\sin 1/2(\theta_p+\theta_s)} \cot(\frac{A-B}{2})\}]$$

The change of declination have been calculated as a function of rotation angle of the plate in two typical cases (Fig. 2). The great circle distance between the island and the rotation pole is smaller than the great circle distance between the rotation pole and the geomagnetic pole in Fig. 2-(a). In this case, the declination changes from -180° to +180° as the plate moves. In Fig. 2-(b), the great circle distance between the island and the rotation pole is larger than the distance between the rotation pole and the geomagnetic pole. The amplitude of the change of the declination is determined by the relation among sites of the island, the rotational pole, and the geomagnetic pole.

Another constrain to determine the curve comes from the condition that the declination is zero when the island acquired its magnetization. This is because we assume that the geomagnetic pole is located at the geocentric pole. Thus, the curve directly depends on where the island got the magnetization. The "whole" shape of the curve is the same, if the great circle distances between the island and the rotation pole and between the rotation pole and the geomagnetic pole are the same, respectively.

The equations in this section are useful only in the case that the geomagnetic pole, the island, and the rotation pole are all in the same hemisphere. In an actual problem only the rotation pole may be in the different hemisphere. The equations are different case by case. We will calculate the actual cases in the next section.

## 3. Two examples

(a) The Hawaiian and the Society islands on the Pacific plate.

Recently McDougall and Duncan (1980) got a rotation pole and a rate of rotation for the Pacific palte to the mantle. Using this rotation vector ${}_{PA}\omega_{M}$* we can see how the declination of the island changes by time. We calculated for the Hawaiian islands and the Society islands for past 40 m.y. As the great

* We defined a rotation vector ${}_{A}\omega_{B}$ as follows; "When we looked at from the center of the Earth, the direction of the rotation of A to B is clockwise around the rotation vector."

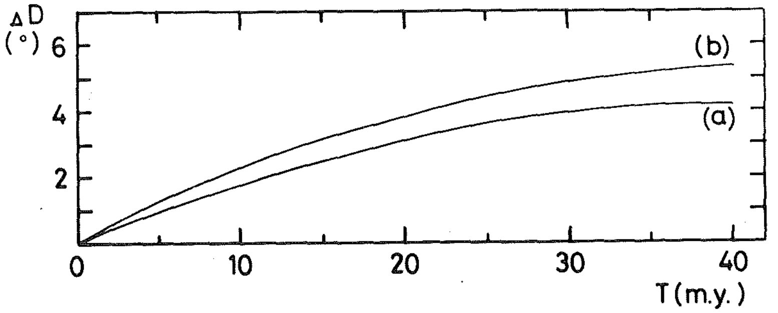


Fig. 3. The declination changes for (a) the Hawaiian islands and (b) the Society islands for past 40 m.y. As the rotation pole of the Pacific plate is close to the geomagnetic pole, the change is quiie small.

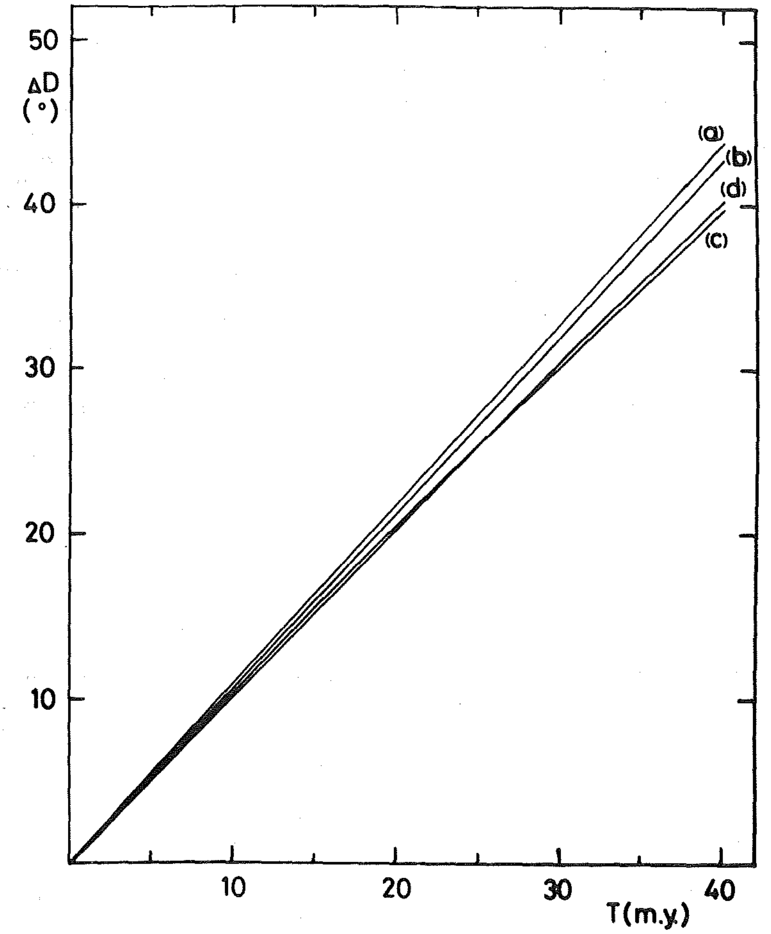


Fig. 4. The declination changes for the four sites on the Philippine Sea plate; (a) (30°N, 133°E), (b) (20°N, 142°E), (c) (20°N,124°E) and (d) (9°N, 133°E). The scale of ΔD axis is smaller than that in Fig. 3 by factor 2. We had hoped that the difference of the sites might be quite effective to the declination change, because the rotation pole of the mantle to the Philippine Sea plate is close to the plate. The spherical angles ($D_I$ and $D_0$ in section 2) of the island for the geomagnetic pole and the rotation pole are quite different each other for individual cases. However, ΔD ($=D_I-D_0$) were similar for all sites.

circle distances from the rotation pole are different for these two islands, there should be different declination curves(Fig. 3). In the Hawaiian islands, we assume that the initial site where the island acquired the magnetization was in Kirauea. The site where the islands in the Society islands got the magnetization is calculated from the present position and the age of 0.77 m.y. of Tahiti (McDougall and Duncan, 1980). The motion of the Pacific plate had changed its direction at about 40 m.y. ago (Dalrymple and Clague, 1976), we only compared the results for past 40 m.y. Such a kind of curves should be used as an another proof of the Pacific plate motion. Here, the change of declination was rather small for there islands. This is because the rotation pole of the Pacific plate is close to the geomagnetic pole and there islands are far from the poles.

(b) The sites on the Philippine Sea plate.

Seno (1977) calculated the rotation vector (${}_{PH}\omega_{PA}$) of the Philippine Sea plate to the Pacific plate from the available fault-plane solutions of the earthquakes. If we assume the instantaneous motion for these plates, the rotational vector (${}_{PH}\omega_{M}$) of the Philippine plate to the mantle has a relation of ${}_{PH}\omega_{M} + {}_{PA}\omega_{PH} + {}_{M}\omega_{PA} = 0$. The rotation pole of 44°S, 25°W and the rate of rotation of 1.42°/m.y. have been calculated for ${}_{PH}\omega_{M}$ using ${}_{PH}\omega_{M}$ of McDougall and Duncan (1980) and ${}_{PA}\omega_{PH}$ of Seno (1977). We calculated the declination changes for 4 sites, which are almost the eastern, the western, the southern, and the northern edges on the Philippine Sea plate (Fig. 4). The sites where the magnetization had been acquired were calculated from the present position of these sites and the rotational vector of the mantle to the Philippine Sea plate. As the rotation pole of the mantle to the Philippine Sea plate is located off Hokkaido, the rotation is quite effctive to the changes of declinations. We compared the results for past 40 m.y., again.

## 4. Discussion

The equation of declination changes consists of many parameters such as rotation pole position, age, the site where the magnetization was acquired. It seems difficult to get the unique solutions for these many parameters. However, we can get the information of the paleolatitude from the inclination change of the magnetization. If we know the rotation vector precisely, declination and inclination are independent informations to determine the age of the island.

Although these calculations are based on the assumption that the island or the site have been moved tightly with the plate, the island might have been rotated within the plate as the plate grows. In discussing such a kind of local rotation of the island itself, we need to do the correction of the change of declination by the plate motion.

## References


Dalrymple, G.B. and Clague, D.A. (1976) Earth Planet. Sci. Lett., 31, 313.

Isezaki, N. et al. (1980) (Submitted to J. Geomag. Geoelectr.)

Kobayashi, K. (1977) "KAIYOTEI CHIKYUKAGAKU", p. 87 (in Japanese).
McDougall, I. and Duncan, R.A. (1980) Tectonophysics, 63, 275.
Seno, T. (1977) Tectonophysics, 42, 209.

Spherical harmonic analysis of the geomagnetic field during the last 2,000 years

Hideo SAKAI

Department of Earth Sciences, Faculty of Science, Toyama University, Toyama 930.

## 1. Introduction

Spherical harmonic analysis initiated by Gauss early in the 19th century is a very powerful tool for the study of the geomagnetic field. It is not only a convenient way of representing the earth's magnetic field but also one of the most useful expressions for studying its secular variation. Since Gauss, considerable sets of spherical harmonic coefficients of the geomagnetic potential have been accumulated by many investigators.

The analytical method used by them needs the geomagnetic field components X,Y,Z or those calculated from F,I,D, where X,Y,Z denote the northward, eastward and downward components and F,I,D denote the intensity inclination and declination of the geomagnetic field, respectively.

Prior to the 19th century, the instrumental observation of field intensity indispensable for completing an analysis was lacking and only the directions of the field were available, so that the applicability of such method is limited to the ages of Gauss and later.

Bauer (1894) proposed a method to determine the relative magnitude of spherical harmonic coefficients only from the magnetic direction data. Many authors have tried to obtain the geomagnetic potential from the magnetic direction data. Yukutake (1971) and Benkova (1974) proposed a method to use some archaeomagnetic intensity data together with observational data, and determined the absolute magnitude of the set of the coefficients back to 16th century. Kono (1973) developed the new mathematical expressions and applied to archaeo and palaeomagnetic data.

The number of localities where the archaeo and palaeomagnetic direction data are obtained is limited. So that the variation of the potential of the interval of few handred years has been hardly discussed.

In the present paper, a new cmethod of spherical harmonic analysis is used to perform the analysis of the archaeomagnetic data from 0 to 1,600 A.D. Then, using the Gaussian coefficients obtained in this way, secular variation of the geomagnetic field is investigated.

## 2. Method

Potential W due to the geomagnetic field with internal origin is given by

$$W = a \sum_{n=1}^{\infty}\sum_{m=0}^{\infty} (a/r)^{n+1}(g_n^m \cos m\phi + h_n^m \sin m\phi)P_n^m(\cos\theta) \qquad (1)$$

where a is the radius of the earth and $\theta$ , $\phi$ are the geographic colatitude and east longitude, respectively, $P_n^m(\cos\theta)$ are quasi-normalized associated Legendre polynomials (Schmidt, 1935), and $g_n^m$ ,$h_n^m$ are generally referred to as the Gaussian coefficients. The geomagnetic field elements at $(r,\theta,\phi)$ are:

$$X = (1/r)x(\partial W/\partial\theta), \quad Y = -(1/r)x(\partial W/\partial\theta), \quad Z=(\partial W/\partial\theta) \qquad (2)$$

where X, Y, and Z are respctively the north, east, and vertically-down components of the field. At the surface of the earth, r = a, and the values of X, Y, and Z at colatitude $\theta$ and longitude $\phi$ are :

$$X = \sum\sum (g_n^m \cos m\phi + h_n^m \sin m\phi) \times (dP_n^m(\cos\theta)/d\theta)$$

$$Y = \sum\sum m \times (g_n^m \sin m\phi - h_n^m \cos m\phi) \times (P_n^m(\cos\theta)/\sin\theta) \qquad (3)$$

$$Z = \sum\sum (n+1) \times (g_n^m \sin m\phi - h_n^m \cos m\phi) \times P_n^m(\cos\theta)$$

In the archaeomagnetic data, there are many pairs of (F, I). To use these data for the analysis, the relation

$$F \sin I = Z \qquad (4)$$

is utilized in this study.

That is, we intend to obtain the potential (1) which will minimize the sum

$$\sum_{i=1}^{N1} (X_i \sin D_i - Y_i \cos D_i) + \sum_{j=1}^{N2} (Z_j \cos I_j - X_j \sin I_j/\cos D_j) + \sum_{k=1}^{N3} (F_k \sin I_k - Z_k)$$

where subscripts i, j, and k denote the data points. The number of data sites where (D), (D, I), and (F, I) are known is denoted by N1, N2, and N3 respectively.

Differentiation of (2) by coefficients ($g_n^m$ , $h_n^m$ ) yields the minimization conditions. Then the gausian coefficients are obtained.

## 3. Test of the Validity of the Method

In order to test the validity of the method, the procedure referred in (2) was applied to calculate the geomagnetic potential for the year 1958 from the data of magnetic observations in the world (Nagata and Sawada, 1963). The number of locations where data were collected was 123. The present method was applied in the following three cases;
(A) data sets (D, I) were available,
(B) data sets (F, I) were available,
(C) all the data were available.

The analyzed result was compared to the result obtained by the conventional method using X,Y,Z data, where X,Y,Z data calculated from the D,I and F data were used. Spherical harmonic analysis was truncated in the maximum degree and order of 4.

In Fig. 1, the results in the case of (A) and (C) are compared to the results by the conventional method, respectively. In these figures, closed circles denote the coefficients $g_n^m$ and open circles $h_n^m$ . If the coefficients estimated by both methods are equal, the plots of the coefficients should be on the straight line whose slope is unity.

The results indicate that the coefficients obtained by new methods will coincide with those by conventional, although small deviations are seen in terms of higher order.

## 4. Results of Sherical Harmonic Analysis

The present method was used to find the geomagnetic potential of the age from 0 to 1,600 A.D.

The archaeomagnetic data used were obtained at 18 locations shown in Fig. 2. Since the number of data was rather small, the spherical harmonic series was truncated in the second degree and order. The gathered data were grouped in the following range of the age where data minimally required for analysis were obtainable. They were 0-300, 0-400, 300-600,

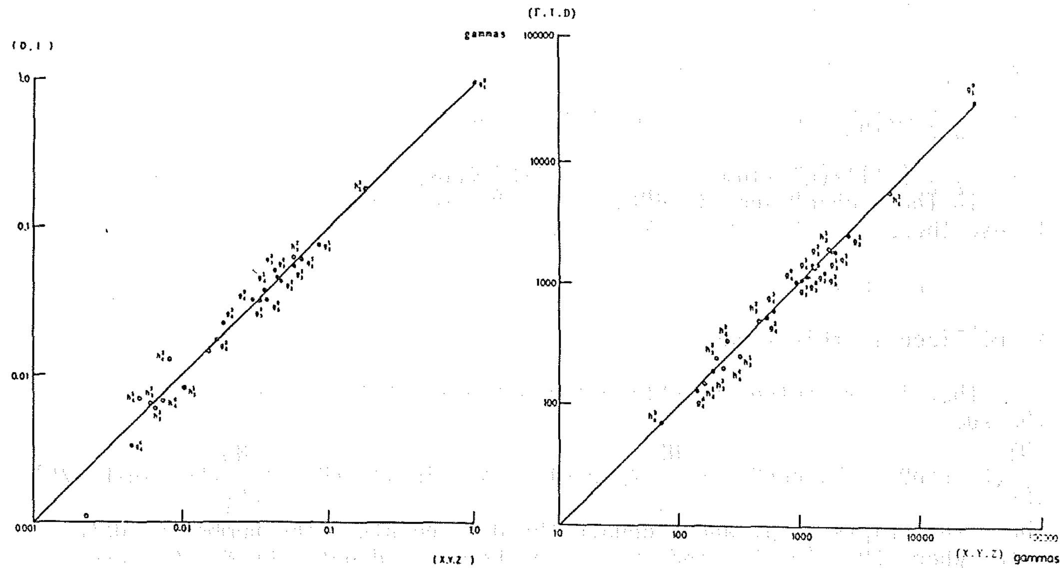


Fig. 1. Results of harmonic analysis using the recent observational data.

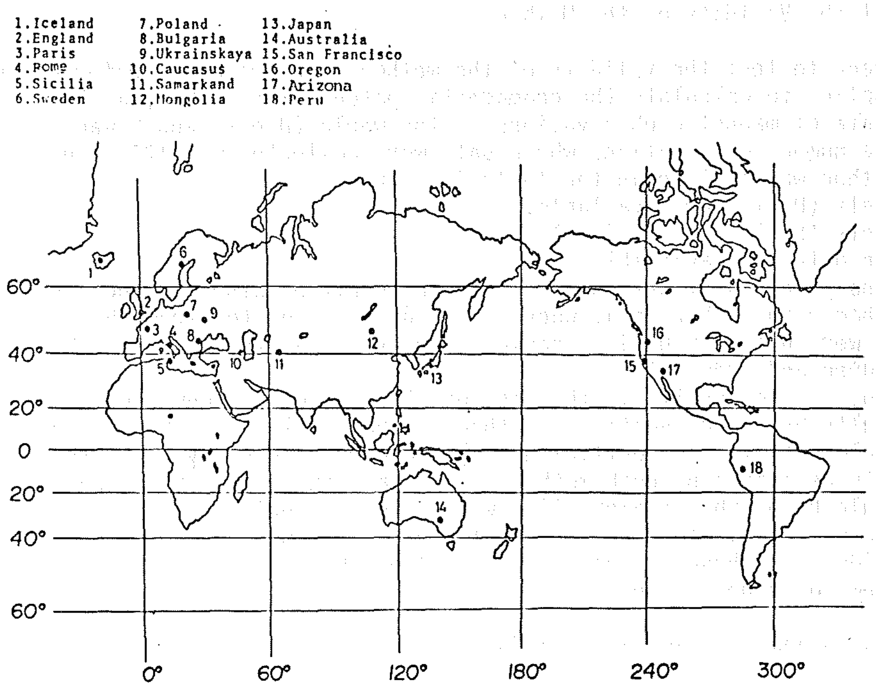


Fig. 2. Locations where the archaeomagnetic data used for analysis were obtained.

400-800, 600-900, 800-1,000, 900-1,100, 1,000-1,200, 1,100-1,300, 1,200-1,400, 1,300-1,500, 1,400-1,600 years, respectively.

The archaeomagnetic data used for analysis were taken from Brynjolfsson (1957), Irving (1964), Watanabe (1964), Watanabe et al. (1965) Aitken et al. (1965), Coe (1967), Tunguy (1970), Hirooka(1971), Kovacheva( 1972), Heinrichs (1973), Rusakov et al.(1973 a,b), Ayuushzhav et al. (1976 Barbetti (1977), Sakai (1980).

The obtained coefficients are shown in Fig. 3, where the magnitude of the coefficients are shown in the ordinates. In Fig. 4, the archaeomagnetic data used for analysis and the calculated data from the coefficients are compared.

The root mean squares of the errors in a fitting method are calculatd The average deviation is 0.043 Oe(8 %) in F, 4,4° in I, and 6.5° in D, respectively.

Since the palaeomagnetic data usually contain errors of the order, 10% for F, 3-5 % for D and I, the results shown above are proved to be useful for the analysis of archaeomagnetism. It may be said that the estimation of the geomagnetic potential from the archaeomagnetic data was successful.

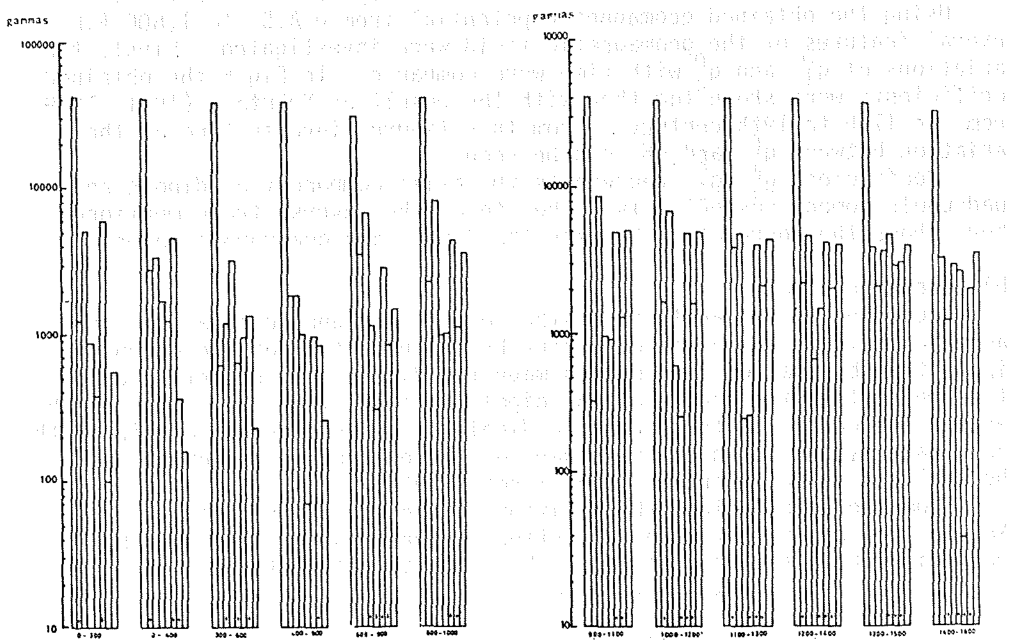


Fig. 3. Gaussian coefficients obtained from archaeomagnetic data of 0 A.D. to 1,000 A.D. Eight coefficients in each group represent $g_1^0, g_1^1, h_1^1, g_2^0, g_2^1, h_2^1, g_2^2, h_2^2$ from the left to the right.

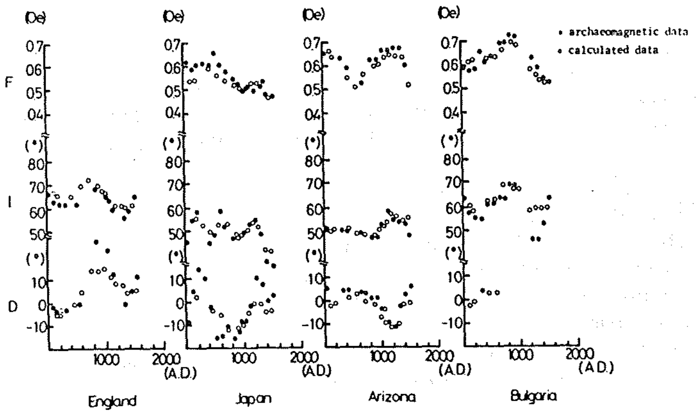


Fig. 4. Archaeomagnetic data used for analysis and the data calculated from the Gaussian coefficients of some sites.

## 5. Several Features of Geomagnetic Field

(a) Intensity variation of the dipole and quadrupole moment with time

Using the obtained geomagnetic potential from 0 A.D. to 1,600 A.D., several features of the geomagnetic field were investigated. First, the variations of $g_1^0$ and $g_2^0$ with time were compared. In Fig.5 the obtained coefficients were shown together with the result of Yukutake (1971, 1979) from the 17th to 19th century. From this figure, inverse tend of the variation between $g_1^0$ and $g_2^0$ can be seen.

Coefficient $g_1^0$ ,$g_2^0$ represents the axial component of dipole and quadrupole moment respectively. Therefore, the inverse trend mentioned above shows the correlation between the dipole and quadrupole moment.

(b) Eccentric dipole

According to the analysis of the recent geomagnetic data, the geomagnetic field is approximated better by the potential of the eccentric dipole than by that of the centred magnetic dipole. By eccentric dipole it is meant that the centre of the dipole is apart from the centre of the earth. The centre of the eccentric dipole is defined as the origin of the coordinate system in which the square of the quadrupole potential has the smallest value. (Bartles 1936, Schmidt 1936)

From the calculation, the position of the eccentric dipole (Xo, Yo, Zo) can be estimated. Distance between the position of the eccentric dipole and the centre of the earth is calculated as

$$d = \sqrt{(x_0)^2+(y_0)^2+(z_0)^2} \tag{5}$$

Fig.6 shows the variation of the distance of the eccentric dipole from the earth's centre. The distance is about 700 km around 1,400 A.D., which is at most one tens of the radius of the earth.

Fig. 7 shows the variation of the positions of eccentric dipole with time where variation of the positions during the last 300 years obtained by Yukutake (1979) and Barraclough (1976) is also shown. This figure indicates that the eccentric dipole seems to have moved westward since the 17th century to the present. Its movement is more complicated before the 17th century, but a trend of eastward movement is more predominant.

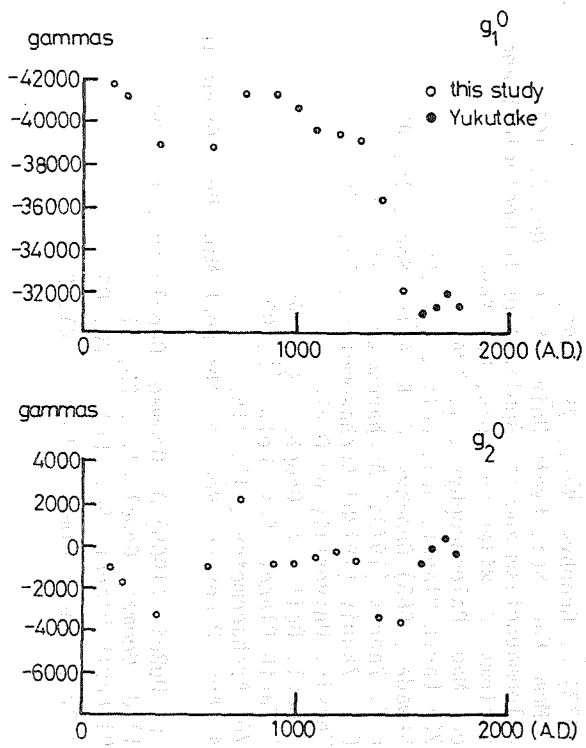


Fig. 5. Time variation of $g_1^0$ and $g_2^0$ .

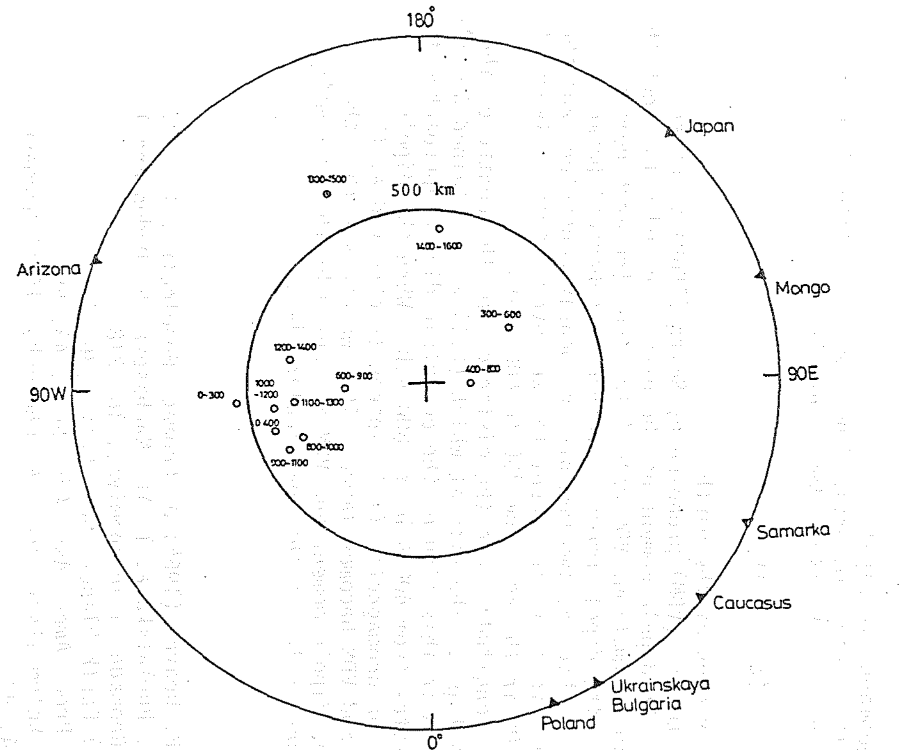


Fig. 6. Variation of the positions of the eccentric dipole with time; closed triangles show the locarities where the data set (F,I) are obtained. Distance of the eccentric dipole from the earth s centre was culculatd from eq.(5).

(c) Moment of the geomagnetic dipole

The moment of the earth s magnetic dipole was calculated from the 3 Gaussian coefficients of the first degree namely,

$$M = a\{(g_1^0)^2 + (g_1^1)^2 + (h_1^1)^2\}$$

where a denotes the radius of the earth.

Virtual dipole moment (VDM) proposed by Smith (1969) is often used to approximate the dipole moment of the past. In order to check the efficiency of the approximation, VDM calculated from the archaeomagnetic data was compared to the dipole moment obtained by spherical harmonic analysis. As shown in Fig. 8, two moments are nearly consistent and the approximation appears to be valid except for an inverce trend between the dipole moment and VDM in the age from 450 to 600 years.
The dipole with the longitude $\phi$ and the distance from the centre of the earth is plotted in Fig.7. The site at which (F,I) were obtained are also shown here. As shown in this figure, the eccentric dipole approached the majority of these sites from 400 A.D. to 600 A.D. When the dipole approaches a site, the geomagnetic field intensity observed at that location increases and VDM becomes large. Thus we can say that the inverse trend of the dipole moment and VDM is caused by the proximity of the dipole to these sites at that particular time.

## References


Aitken, M.J. and G.H. Weaver (1965) J. Geomag. Geoelectr., 17, 391.

Ayuushzhav, G., S.P. Burlatskaya, I. YE. Nachasova, G. Dodon and I. Balbar (1976) Geomagn. i aeronomiya., 16, 318.

Barbetti, M., (1977) Earth Planet. Sci. Lett., 36, 207.

Bauer, L.A., (1894) Proc. Amer. Ass. Adv. Sci., 43, 55.

Benkova, N.P., G.I. Kolomiitseva and T.N. Cherevko (1974) Geomagn. i aeronomiya 14, 93.

Brynjolfsson, A., (1957) Adv. Phys., Quart. Suppl. Phil. Mag., 6, 247.

Coe, R.S., (1967) J. Geophys. Res., 72, 3247.

Heinrichs, D.F., (1973) J. Geophys. Res., 78, 5983.

Hirooka, K., (1971) Mem. Fac. Sci. Kyoto Univ,. S. G., No. 2, 167.

Irving, E.,(1964) Paleomagnetism and its Application to Geological and Geophysical Problems, J. Wiley and Sons, New York.

Kono, M., (1973) Rock Mag. Paleogeophys., 1, 124.

Kovacheva, M., (1972) Earth Planet. Sci. Lett., 17, 199.

Nagata, T. and M. Sawada (1963) Geophys. J. R. Astr. Soc., 19, 417.

Rusakov, O.M. and G.F. Zagniy (1973a) Archaeometry., 15, 153.

Rusakov, O.M. and G.F. Zagniy (1973b) Archaeometry., 15, 275.

Sakai, H., (1980) Thesis, University of Osaka

Schmidt, A., (1943) Gerl. Beitr. z. Geophs., 41, 346.

Smith, D.J., (1969) Earth Planet. Sci. Lett., 2, 99.

Tunguy, J. C., (1970) Archaeometry., 12, 115.

Watanabe, N., (1964) Ann. Progress. Rep. of the Rock Mag. Res. Group in Japan., 30.

Watanabe, N. and R.L. DuBois (1965) J. Geomag. Geoelectr., 17, 395.

Yukutake, T., (1971) J. Geomag. Geoelectr., 23, 11.

Yukutake, T., (1979) Earth Planet. Sci. Lett., 20, 83.

Bartles, J., (1936) Terr. Magn. Atmos. Electr., 41, 225.

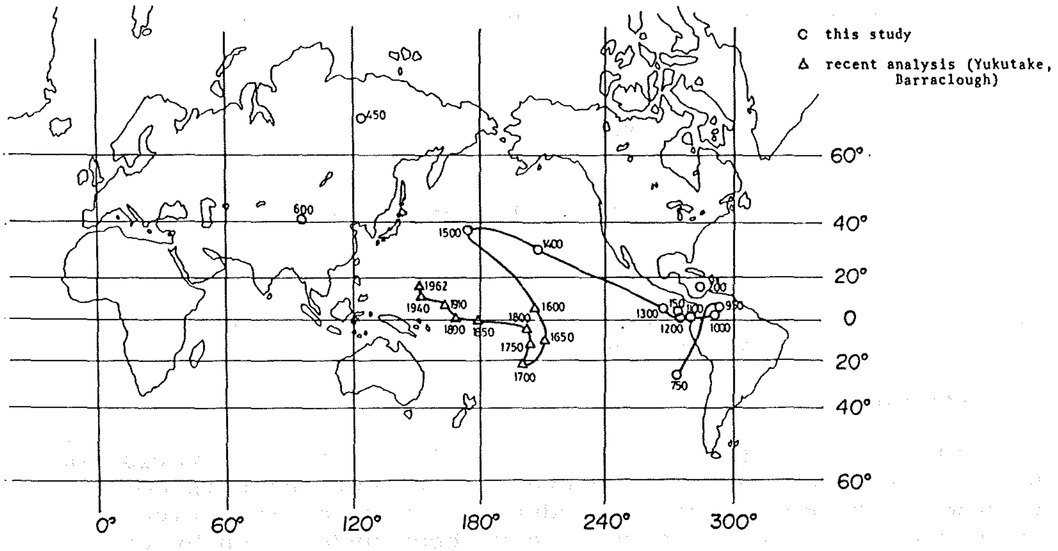


Fig. 7. Variation of the position with time where the eccentric dipole put through the earth's surface.

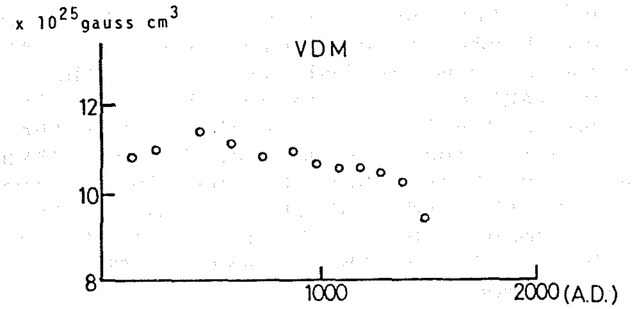


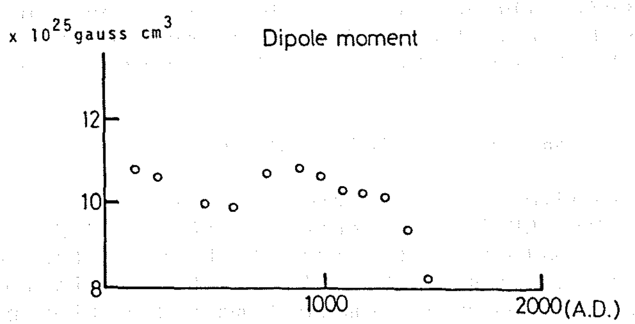


Fig. 8. Variation of the dipole moment and VDM with time.

SPECTRAL ANALYSIS OF GEOMAGNETIC FIELD INTENSITY DERIVED FROM FOUR DEEP-SEA CORES

Takaharu SATO

Department of Physics, Faculty of Engineering Science, Osaka University, Toyonaka, Japan

Kazuo KOBAYASHI

Ocean Research Institute, University of Tokyo, Nakano-ku, Tokyo, Japan

## Introduction

The periodicity of geomagnetic field intensity variations has received considerable interest in recent years in conection with the mechanism of geodynamo. Several investigations on geomagnetic field intensity have been undertaken by use of deep-sea cores (Opdyke et al., 1973; Kawai et al., 1976, 1977; Kent and Opdyke, 1977; Sueishi et al., 1979; Sato and Kobayashi, 1979). Spectral analyses of these results have been reported (Kent and Opdyke, 1977; Okubo and Takeuchi, 1979). However, general agreement about the periodicity is not given.

In recent years, the maximum entropy method (MEM) introduced by Burg (1967, 1968) has been used for the spectral analysis of various kinds of geophysical data. In this method, an important parameter remains indefinite. On the other hand, the autoregressive (AR) model introduced by Yule (1927) has been developed independently. It was shown that these two methods for time series analysis were equivalent (Akaike, 1969; Van den Bos, 1971) and that the indefinite parameter in the MEM was equal to the order of the AR model. An information criterion (AIC) introduced by Akaike (1973, 1974) can be used for finding the best order of the AR model. The AIC is minimized in this order of the model.

In this study, the spectra of the variations in paleomagnetic intensity recorded in four deep-sea cores were obtained from the AR model by using the computer program of Akaike et al. (1976).

## Variations in paleomagnetic field intensity

The cores studied in this paper were KH 73-4-7 (core A), KH 73-4-8 (core B), KH 72-2-2 (core C) and KH 72-2-58 (core D). Correspondence of paleomagnetic results between the four cores was shown by Sato and Kobayashi (1979). The variations in the intensity of the natural remanent magnetization normalized by the content of magnetic minerals in each core are shown in Fig. 1. These variations in the normalized intensity clearly show a number of alternating intensity stages. It will be convenient to label tentatively the strong-intensity stage immediately after the Brunhes-Matuyama boundary as FB 1 and the following stages with increasing integers. The strong-intensity stage immediately before the boundary is tentatively labeled as FM 1 and preceding stages are labeled

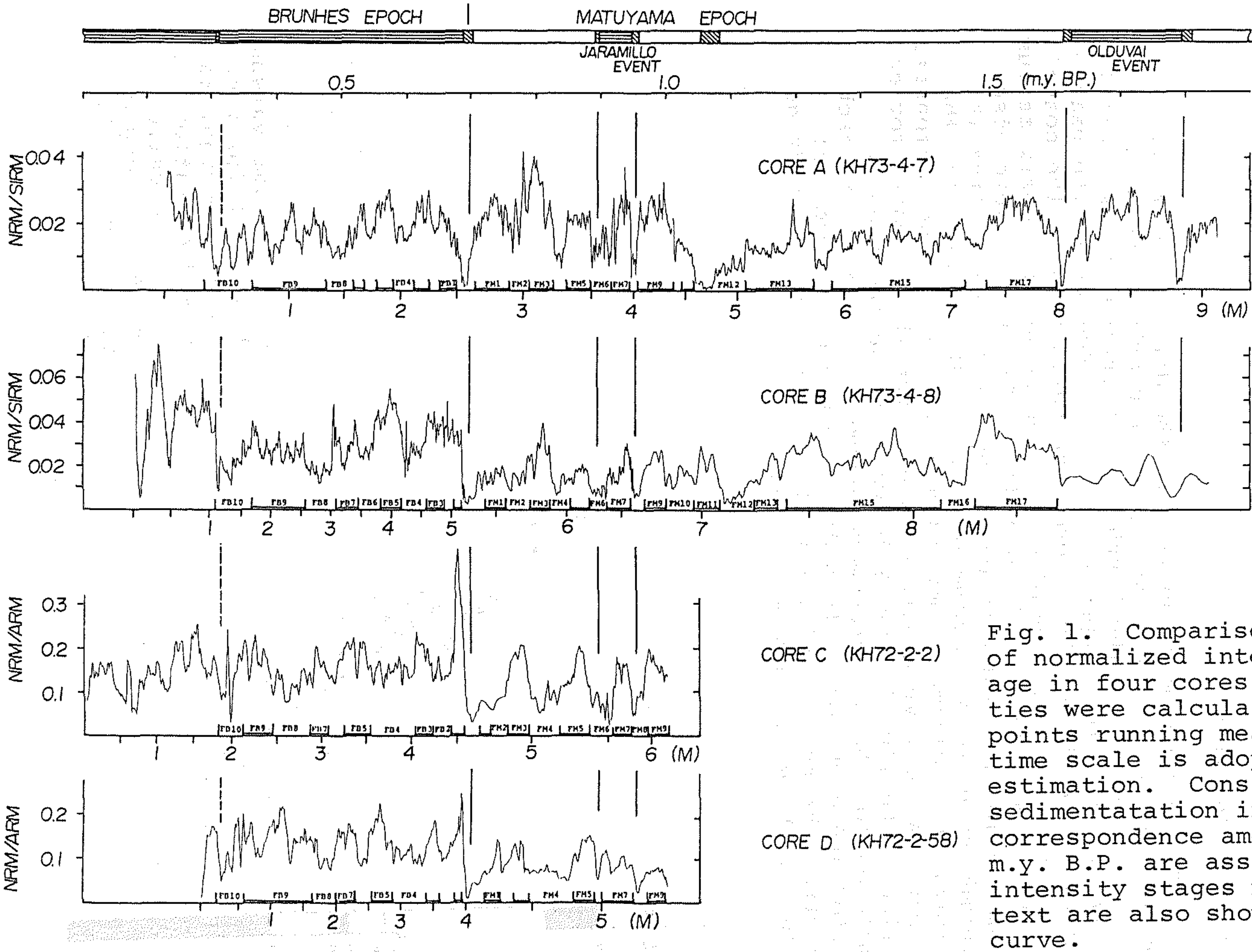


Fig. 1. Comparison of variations of normalized intensities versus age in four cores. The intensities were calculated from three points running mean. The standard time scale is adopted for the age estimation. Constant rate of sedimentatation in core A and a correspondence among cores at 0.3 m.y. B.P. are assumed. Normalized intensity stages mentioned in the text are also shown below each curve.

with increasing integers. The numbers are odd for strong-intensity stages and even for weak-intensity ones, following the paleoclimate stages introduced by Arrhenius (1952) and designated by Emiliani (1955). The rates of sedimentation for the Matuyama epoch were estimated from the ages of the distinct polarity boundaries in terms of the standard magnetic time scale as shown in Fig. 2. On the basis of nearly a constant rate of sedimentation in whole core A and correspondence between cores, the rate for each core in the Brunhes epoch was estimated.

Spectral analyses

The analyses were applied to the data of the normalized intensities in the four cores, particularly to those in the periods involved in the Brunhes and Matuyama epochs. Within these periods, there appeared no large changes in the paleomagnetic direction. Therefore, the variations in the normalized intensity were considered to represent stationary features of the geomagnetic field intensity. The spectra were also examined for the order in which the AIC increased from the minimum value to an increment of ten. The spectra for the saturation isothermal remanent magnetization (SIRM) intensities in cores A and B were also obtained from the AR model for each period. The time intervals between the adjacent points employed for the analyses were assumed to be equal in each period and each core. In order to compare the power of spectra, the normalized intensities divided by the average value of the whole core were used.

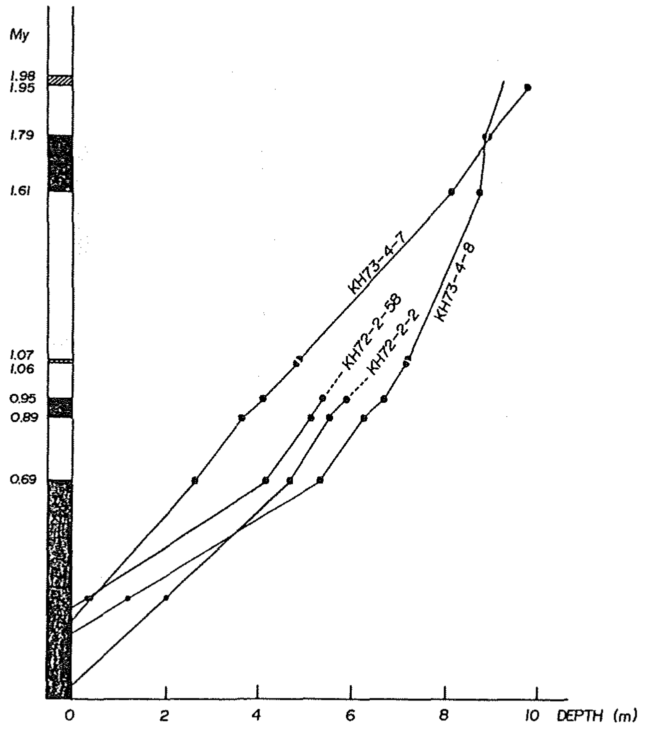


Fig. 2. Time versus depth plot for four cores. Constant rate of sedimentation for core A and correspondence among cores at 0.31 m.y. B.P. are assumed.

## Results and disccusion

### a) Periodicity

Table 1 gives the numbers of samples (N), the average normalized intensities ($R_{av}$), the locations of samples in a core, the sampling time intervals ($\Delta t$), the mean rates of sedimentation and the orders in which the AIC is minimized (M). M is between 2 and 5. There is no significant peak in the spectrum for any of the above analyses as shown in Figs. 3a and 3b.

As the order increased from M, the AIC increased gradually and some peaks in the spectrum are observable. One peak may be significant for each core in the Brunhes epoch. The periods of the peaks for cores A, B, C and D in the Brunhes epoch are 25,000, 3,800, 5,000 and 6,700 yr., respectively. For the Matuyama epoch, two peaks (10,500, and 5,800 yr.) may be significant for core A. However, the spectrum for core B shows a monotonic decrease with increase in frequency. It appears that no distinct correspondence is seen between the peaks in another spectra. Periodicities of 25,000 and 18,000 yr. are mentioned by Okubo and Takeuchi (1979) for the portions of the Brunhes and the upper Matuyama epochs in core A from analyses using the MEM with much higher orders. However, the spectra for the portion of the middle Matuyama epoch on the same core exhibit no peak around the period of 25,000 yr. Similarly, no periodicity of 25,000 yr. appears for the remaining cores. So predominant periodicity of 25,000 yr. is higher questionable. A periodicity around 18,000 yr. is unobservable in the present analyses.

### b) Trend of spectra

The spectra show the concentration of power dencity to

Table 1, Data for spectral analyses.

| Period | Brunhes epoch | | | | Matuyama epoch | |
|---|---|---|---|---|---|---|
| Core | A | B | C | D | A | B |
| N | 161 | 432 | 545 | 377 | 371 | 172 |
| $R_{av}$ ($\times 10^{-2}$) | 1.68 | 2.45 | 14 | 11 | 1.68 | 2.45 |
| Location of samples (depth in cm) | 36-254 | 115-493 | 8-457 | 34-399 | 476-803 | 715-871 |
| $\Delta t$ (yr.) | 2330 | 854 | 1120 | 951 | 1430 | 3020 |
| Mean rate of sedimentation (cm/1,000 yr.) | 0.57 | 1.05 | 0.71 | 0.90 | 0.60 | 0.31 |
| M | 2 | 5 | 3 | 2 | 3 | 2 |

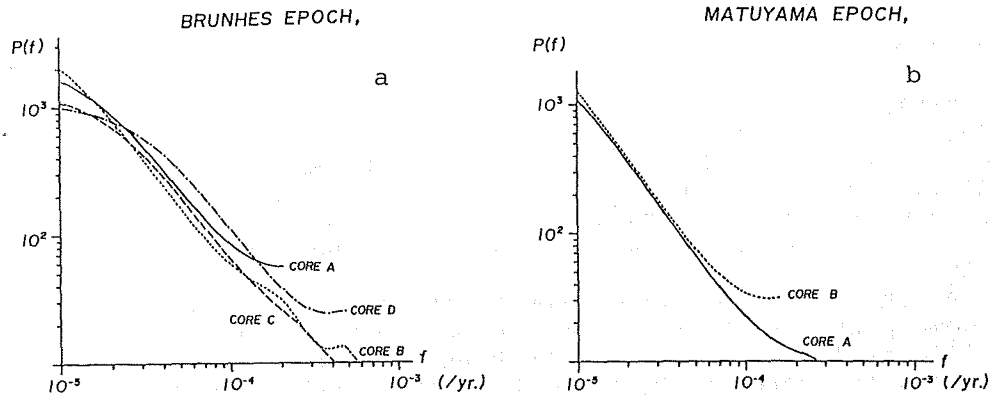


Fig. 3. AR spectra of the normalized intensities for four cores in the Brunhes (a) and the Matuyama (b) epoch. AIC is used to choose the AR order.

the lower frequency side. Possible reasons for this are as follows: first, due to the acquisition process of depositional remanent magnetization (DRM) as described by Løvlie (1976): second, due to characteristics of the geomagnetic field. If the intensity of the DRM acquired by compaction is independent of time required for compaction as shown by Otofuji and Sasazima (1980), the influence of the acquisition process results in that the shapes of spectra should be analogous to each other. The spectra should agree with each other if the spectra are calculated as a function of width of sediment. These presume the same behavior of acquiring DRM. On the other hand, the second is thought to result in that the shapes of the spectra should be analogous and the spectra should agree with each other, if the period analysed is the same. Figs. 4a and 4b show the spectra calculated as a function of width of sediment. The actual spectra almost agree with each other in

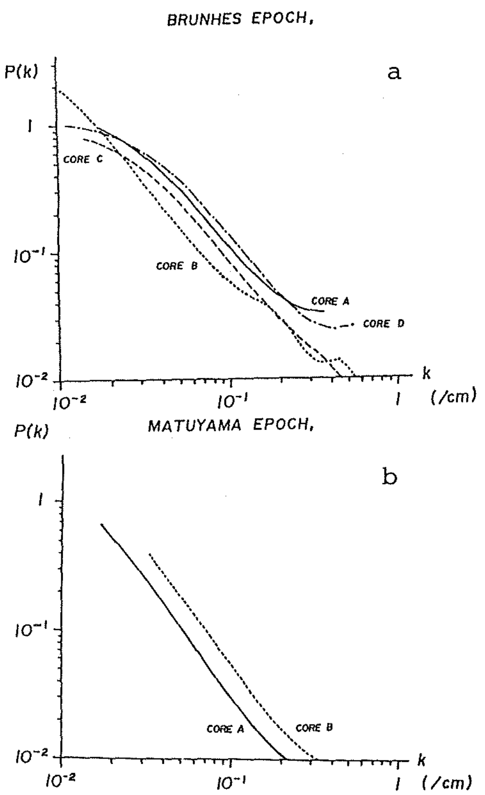


Fig. 4. AR spectra of the normalized intensities for four cores versus width of sediment in the Brunhes (a) and the Matuyama (b) epoch. AIC is used to choose the AR order.

the region of $2 \times 10^{-5}$ c/yr. ~ $1 \times 10^{-4}$ c/yr. in spite of the difference of rates of sedimentation for the same periods. It becomes evident that the high frequency components of the spectra in the Brunhes epoch are much larger than those in the Matuyama epoch. The shapes of the spectra are also analogous for the same periods. In spite of the difference of the concentration for the normalized intensity, there is no significant difference among the intensity of SIRM in the two periods. On the basis of these results, it can be concluded that the influence of acquiring process of DRM extends to a very small region and that the general trend of variations in the earth's magnetic field intensity have probably changed between the periods.

## References


Akaike, H. (1969) Ann. Inst. Statist. Math., 21, 243.

Akaike, H. (1973) Proc. 2nd Int. Symp. Inf. Theory, p. 267, eds., Petrov, B. N. and F. Csaki, Akadeniai Kiado, Budapest.

Akaike, H. (1974) IEEE trans. Automatic Control, AC-19, 6, 716.

Akaike, H., E. Arahata and T. Ozaki (1976) Computer science monographs No. 6, a publication of the Inst. Statist. Math.

Arrhenius, G. (1952) Swedish Deep-Sea Exped. Repts., 5, 6.

Burg, J. P. (1967) paper presented at the 37th Annual International Meeting. Soc. of Explor. Geophys., Oklahoma City, Okla., Oct. 31.

Burg, J. P. (1968) paper presented at Advanced Study Institute on Signal Processing, NATO, Enschede, Netherlands.

Emiliani, C. (1955) Jour. Geol., 63, 538.

Kawai, N., Y. Otofuji and K. Kobayashi (1976) J. Geomag. Geoelectr., 28, 395.

Kawai, N., T. Sato, T. Sueishi and K. Kobayashi (1977) J. Geomag. Geoelectr., 29, 211.

Kent, D. V. and N. D. Opdyke (1977) Nature, 266, 156.

Løvlie, R. (1976) Earth Planet. Sci. Lett., 30, 209.

Okubo, S. and H. Takeuchi (1979) Geophys. J. R. astr. Soc., 56, 309.

Opdyke, N. D., D. V. Kent and W. Rowrie (1973) Earth Planet. Sci. lett., 20, 315.

Otofuji, Y. and S. Sasajima (1980) Geophys. J. R. astr. Soc., in press.

Sato, T. and K. Kobayashi (1979) Rock Mag. Paleogeophys., 6, 41.

Sueishi, T., T. Sato, N. Kawai and K. Kobayashi (1979) Phys. Earth Planet. Inter., 19, 1.

Van den Bos, A. (1971) IEEE Trans. Inf. Theory, IT-17, 493.

Yule, G. U. (1927) Philos. Trans. R. Soc. London, A, 226.

A NEW SPINNER MAGNETOMETER : PRINCIPLES AND TECHNIQUES

Masaru KONO, Yozo HAMANO, Tadashi NISHITANI*, and Toshiyuki TOSHA

Geophysical Institute, University of Tokyo,
Bunkyo-ku, Tokyo 113, Japan

## 1. Introduction

Spinner magnetometer is one of the most widely used instruments in rock magnetic and paleomagnetic laboratories. The basic idea is rather old (e.g., Johnson, Murphy and Torreson 1948; Graham 1955), but it may be said that it became standard instrument only after a significant development was made by Foster (1966) and by Molyneux (1971). Foster used modern electronic techniques such as phase sensitive amplification and also employed fluxgate sensors. The most developed of the Foster-type spinners is the one commercially available from Schonstedt, in which much sophistication exists both in mechanism and in electronics, but is still a basically identical instrument. Molyneux introduced the idea of digital sampling and real-time computation of the results by a computer. This idea is materialized as Digico magnetometers. By the use of a computer, it is possible to employ such numerical techniques as stacking of signals and fast Fourier transform (FFT).

One of the basic differences between the above two types of magnetometers which received little attention until now is that the former is a frequency sensitive machine while the latter is not. In fact, analog-digital (AD) converters used in digital sampling have such a short settling time that they can be considered to have a flat frequency response within the frequency range of practical interest. This means that the digital spinner magnetometers can be used with variable rotation speed. More important, this also means that several different frequency components in a signal spectrum can be measured at the same time with a same accuracy and with negligible distortion.

In this paper, we exploit this nature of the digital spinner magnetometers by rotating the sample around two orthogonal axes simultaneously. It can be shown in general case that complete description of sample magnetization is possible through the analysis of amplitudes and phases of various frequency components.

In the new spinner magnetometer, we used a microcomputer (Digital Equipment Corporation, LSI-11) not only to sample and process fluxgate data as is done by Digico spinners but also to control all the procedure needed for completing measurements; i.e., on/off switching of the moter, selection of the appropriate gain of the amplifier, and so on. Since the sample need not be taken out and replaced as in conventional spinners before the measurement is complete, the whole process is conveniently controled by the computer.

## 2. Magnetic Signals

Consider a sample which is rotated around two axes which are orthogonal to each other (Fig. 1). We shall use two cartesian coordinate systems (X, Y, Z) and (x, y, z) to describe the coordinates fixed to the magnetometer and those rotating with the sample. If the angles of rotation around the vertical and the horizontal axes are $\alpha$ and $\beta$, the relation between the

* Now at Department of Mining Geology, Akita University, Akita 010.

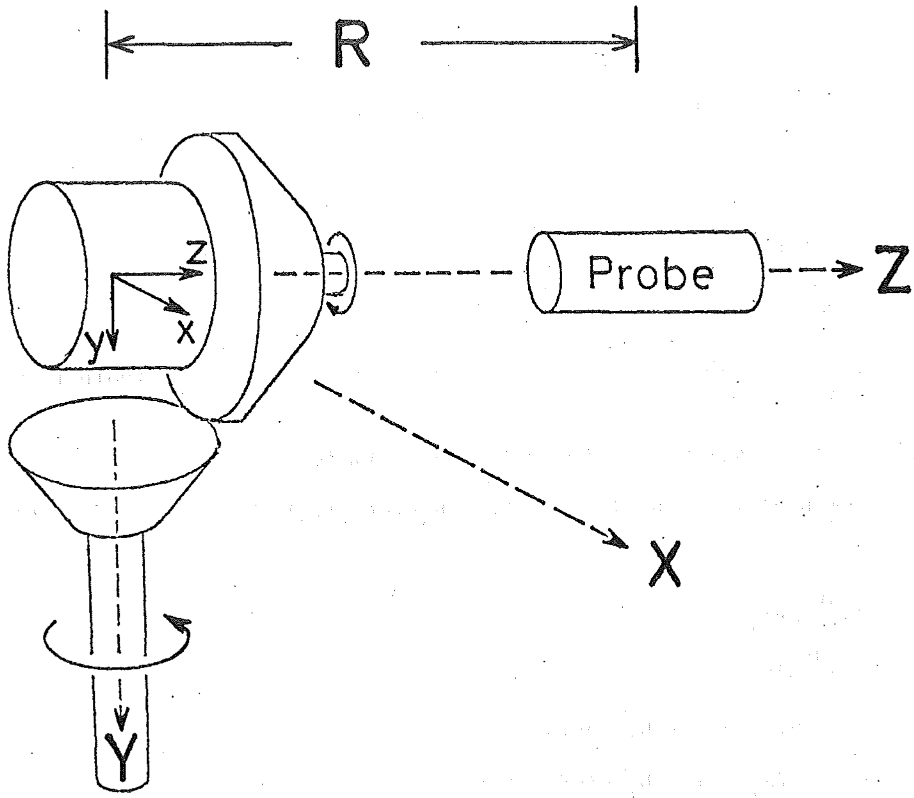


Fig. 1. Schematic diagram of two-axis tumbler system.

two coordinate system is

$$\begin{pmatrix} X \\ Y \\ Z \end{pmatrix} = \begin{pmatrix} \cos\alpha\cos\beta & \cos\alpha\sin\beta & -\sin\alpha \\ -\sin\beta & \cos\beta & 0 \\ \sin\alpha\cos\beta & \sin\alpha\sin\beta & \cos\alpha \end{pmatrix} \cdot \begin{pmatrix} x \\ y \\ z \end{pmatrix} \tag{1}$$

The magnetic potential of a sample can be expressed in the usual form by spherical harmonic expansion,

$$W = R \sum_{n=0}^{\infty} \sum_{m=0}^{n} (a/R)^{n+1} P_n^m(\cos\theta)(a_n^m \cos m\phi + b_n^m \sin m\phi) \tag{2}$$

where R is some length scale included to make the dimension of $a_n^m$ and $b_n^m$ that of the field, r, $\theta$, $\phi$ are spherical coordinates with the polar axis directed toward z, and $P_n^m$ are associated Legendre functions. Since spherical coordinates are related to sample coordinates by

$$\cos\theta = z/r = \cos\alpha$$

$$\tan\phi = y/x = \sin\alpha\sin\beta/\sin\alpha\cos\beta = \tan\beta$$

we can simply equate

$$\Theta = \alpha = \omega_1 t + \delta_1$$

$$\phi = \beta = \omega_2 t + \delta_2$$

where $\omega_1$, $\omega_2$, $\delta_1$, $\delta_2$ are angular velocities and offsets for the two axes, and $\omega_1$ and $\omega_2$ are related to each other by $\omega_2 = -(n_1/n_2)\omega_1$ where $n_1/n_2$ is the gear ratio of the bevel gears driving the two axes (Fig. 1).

Thus, the magnetic signal picked up hy a sensor ar (0, 0, R) is

$$H(t) = \sum_{n=0}^{\infty} \sum_{m=0}^{\infty} (n+1)\, P_n^m\{\cos(\omega_1 t + \delta_1)\}$$

$$\{a_n^m \cos m(\omega_2 t + \delta_2) + b_n^m \sin m(\omega_2 t + \delta_2)\} \tag{3}$$

in the radial direction. When the potential contains only the dipole term (n=1), eq.(3) is simplified to

$$H_1(t) = [a_1\cos\omega_1 t + a_2\cos(\omega_1-\omega_2)t + a_3\cos(\omega_1+\omega_2)t$$

$$+ b_1\sin\omega_1 t + b_2\sin(\omega_1-\omega_2)t + b_3\sin(\omega_1+\omega_2)t] \tag{4}$$

with

$$a_1 = 2a_1^0\cos\delta_1$$

$$b_1 = -2a_1^0\sin\delta_1$$

$$a_2 = a_1^1\sin(\delta_1-\delta_2) + b_1^1\cos(\delta_1-\delta_2)$$

$$b_2 = a_1^1\cos(\delta_1-\delta_2) - b_1^1\sin(\delta_1-\delta_2)$$

$$a_3 = a_1^1\sin(\delta_1+\delta_2) - b_1^1\cos(\delta_1+\delta_2)$$

$$b_3 = a_1^1\cos(\delta_1+\delta_2) + b_1^1\sin(\delta_1+\delta_2)$$

Therefore, by measuring the amplitudes and phases of the three frequency components, $\omega_1$, $\omega_1 \pm \omega_2$, we can completely determine the dipole moment ($a_1^0$, $a_1^1$, $b_1^1$).

The magnetic field due to a quadrupole is more complicated; they contain, apart from the DC component, six frequency components $2\omega_1$, $2\omega_2$, $2\omega_1 \pm \omega_2$, $2\omega_1 \pm 2\omega_2$ corresponding to five Gauss coefficients $a_2^0$, $a_2^1$, $b_2^1$, $b_2^1$, $a_2^2$, $b_2^2$. In general, the order n term in (3) contains frequency components produced by summing or subtracting one of ($0$, $\omega_2$, $2\omega_2$, ...., $n\omega_2$) from one of ($n\omega_1$, $(n-2)\omega_1$, ....., $\omega_1$ or 0); for example, $n\omega_1$, $n\omega_1 \pm \omega_2$, $n\omega_1 \pm 2\omega_2$, etc. As shown later, it is usually satisfactory to assume that the magnetization is dipolar.

## 3. Practical Techniques

The basic idea of the new magnetometer is quite simple as explained earlier. In this section, we shall discuss some of the practical problems and techniques involved in the construction of such systems, and show some examples of actual operation.

### 3.1. Gear Ratio

The rotation in two orthogonal axes is made possible by the use of bevel gears. The gear ratio $n_1/n_2$, where $n_1$ and $n_2$ are irreducible integers, should be chosen to satisfy (1) that measurement is done as uniformly in direction as possible, (2) that the frequency components of especially dipole term are distinct from other signals or noise, and (3) that problems in production and operation are avoided.

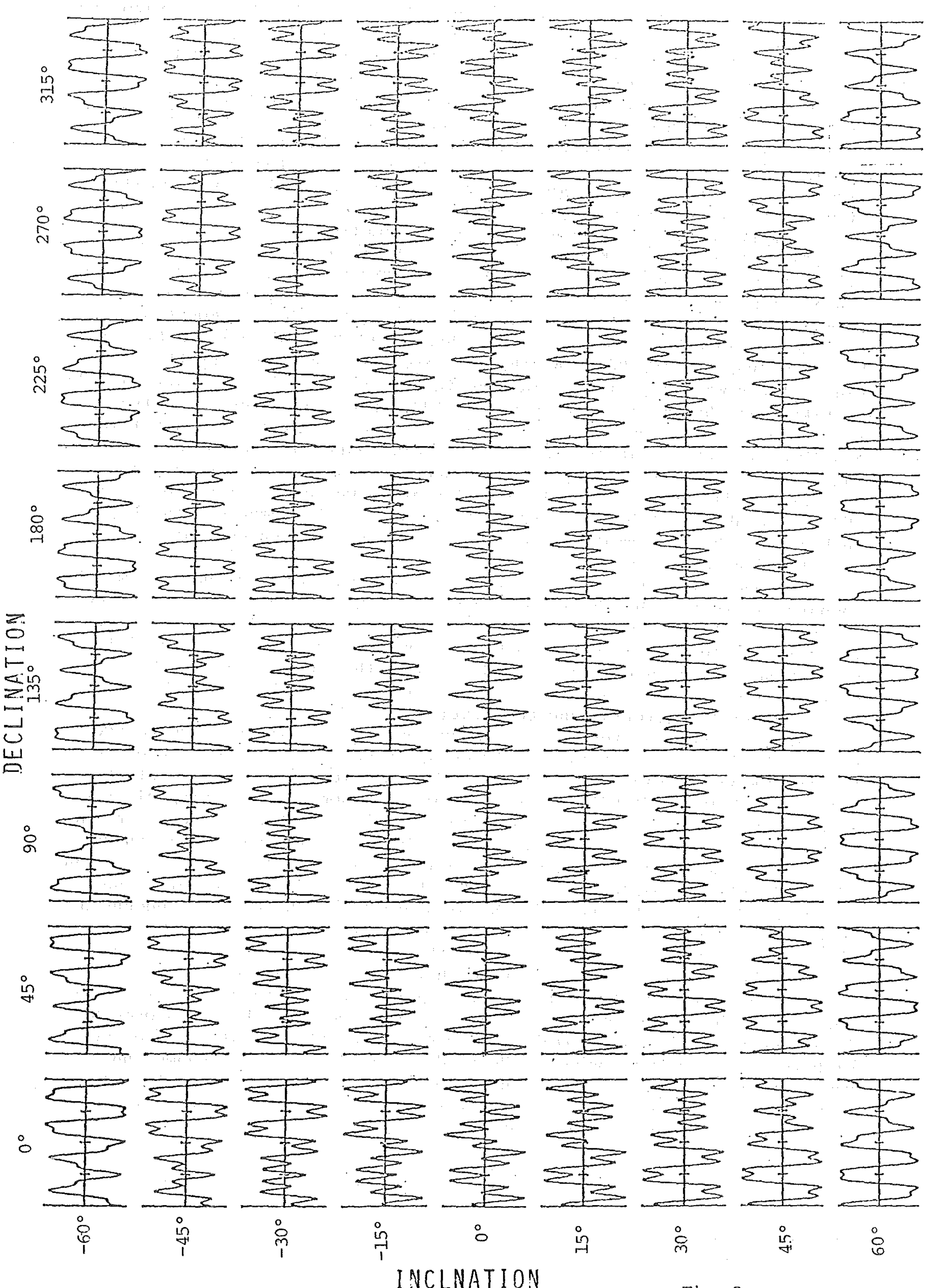
DECLINATION
0°
45°
90°
135°
180°
225°
270°
315°
-60°
-45°
-30°
-15°
0°
15°
30°
45°
60°
INCLNATION

Fig. 2

Some of the above requirements conflict with each other. A compromise should be sought between directional uniformity, shorter measurement time, and so on. We chose a ratio of 4 : 7 for our system as it appears good enough for all the requirements. Theoretical signals for various inclination ($\tan I = a_I^0 / \sqrt{(a_I^1)^2 + (b_I^1)^2}$ ) and declination ($\tan D = b_I^1 / a_I^1$ ) of magnetization is shown for this gear ratio (Fig. 2). As seen from the figure, the 4 Hz signal becomes dominant when inclination becomes very steep, while 3 Hz and 11 Hz signals has the same amplitude with no 4 Hz signal present if I = 0. Samples with intermediate inclinations produce signals of mixtures of the three frequencies.

### 3. 2. Amplification, Synchronization, and Sampling.

The following is a brief description of the present system. The signal from the fluxgate sensor (Schonstedt MND-5C-25) is filtered through a band eliminate filter (BEF) to reduce 50 Hz noise, amplified by a programmable gain instrumentation amplifier (PGIA, Burr Brown 3606 AG), passed through a sample/hold amplifier (Burr Brown SHC 80), and sampled by a 12-bit AD converter (ADC 80). As the data are later processed by FFT technique, the number of sampling must be in the form of $2^n$. A rotary encorder (Ishikawajima-Harima Industries REI-9z-102) which generates 512 pulses per revolution in addition to a zero signal is used to trigger S/H amplifier and AD converter. Sampling is done at every fourth of the pulses (starting at zero) from the rotary encorder and 512 readings in 4 revolutions completes a data set. The PGIA has 11 stage power-of-2 gains from 1 to 1024 selectable by 4 bits of input data. Hence, the computer can choose such a gain that the amplitude of the signal is large enough and yet overflow does not occur.

The operation is done as follows. After switching on the system, the computer waits for the absolute zero signal. When zero is received, the computer starts to sample data with the lowest (x 1) amplification. If the gain is found to be not enough, the computer changes to appropriate gain by setting gain bits of the PGIA. Once the gain is fixed, the computer samples the signal until predefined stack number is reached.

### 3.3. Numerical Filtering and Computation

As discussed earlier, digital magnetometers are insensitive to frequency of signals. This lack of frequency sensitivity is not a problem in discriminating signal from noise. The technique used here is stacking, same as in Molyneux (1971). Fig. 3 shows an example of stacking signals. In our laboratory, a noise of about 15 nT peak to peak exists even in the three-layer permalloy shield. It is mainly 50 Hz line noise and its overtones. When a sample with a magnetization of $7 \times 10^{-6}$ Am$^2$ is measured, the signal is almost completely covered by the noise if only one set of data is taken (Fig. 3). However, S/N becomes greater with increased number of stacking, and the signal is quite apparent with stackings of 32 or greater. The noise level in the present system changes as $n^{-1/2}$, where n is the stack number, as it should do for incoherent, random noise.

The data are processed by FFT technique. Fig. 4 shows the amplitude spectra of the data given in Fig. 3. It is noteworthy that even when S/N is not very good, correct amplitudes are obtained for dipole frequencies with very small stack numbers. Phase data (not shown) also shows the same situation. Amplitudes of quadrupole frequencies are also consistent from about n = 16. Evidently staking and FFT are quite effective in discriminating signals from incoherent noise.

---

Fig. 2. Theoretical signal shapes for dipole with various inclinations and declinations.

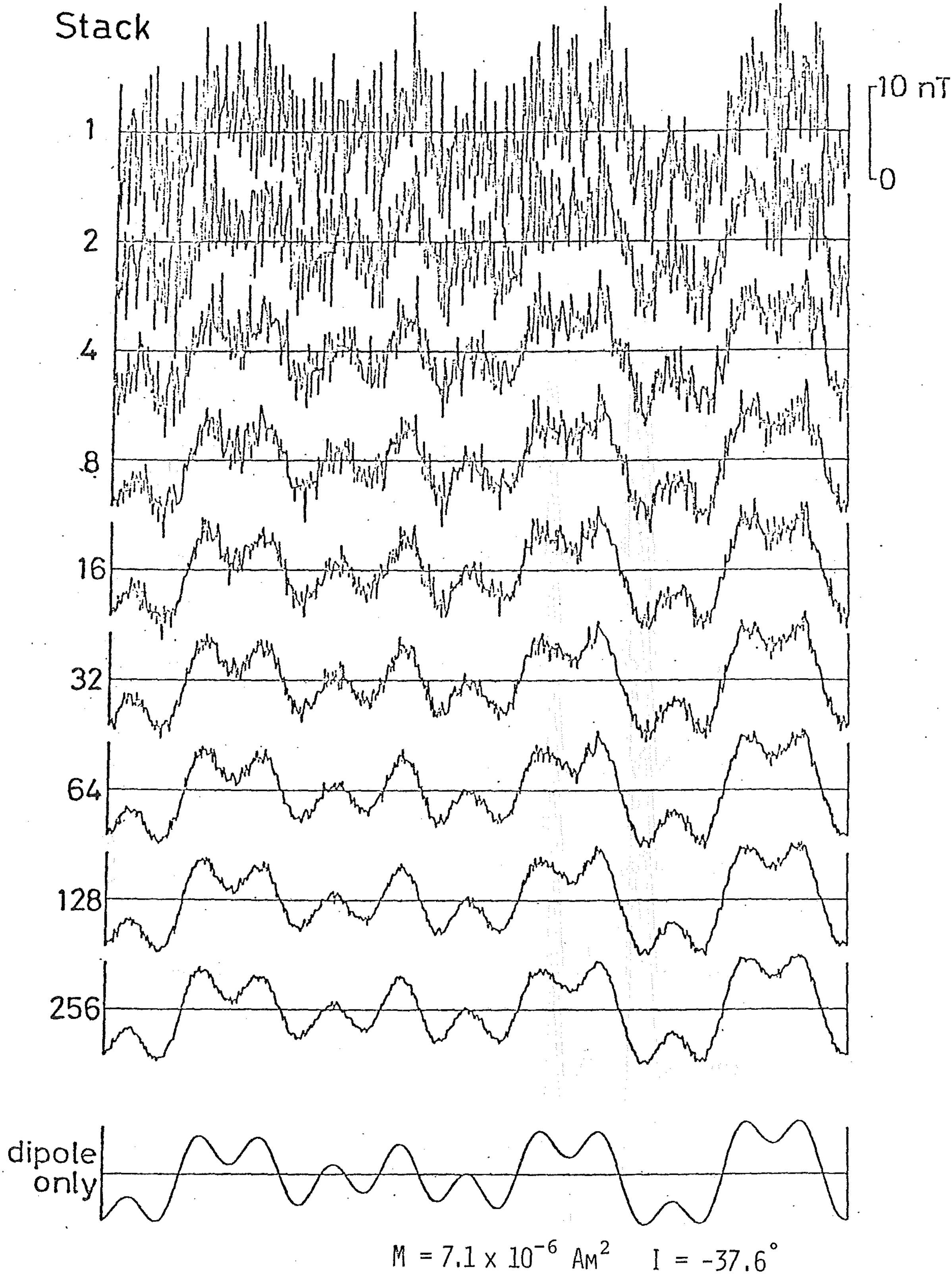


Fig. 3. The effect of stacking the signals of a volcanic sample from Izu penninsula, Japan. The curve at the bottom shows the teoretical wave form reconstructed from the dipole component in Fourier transform.

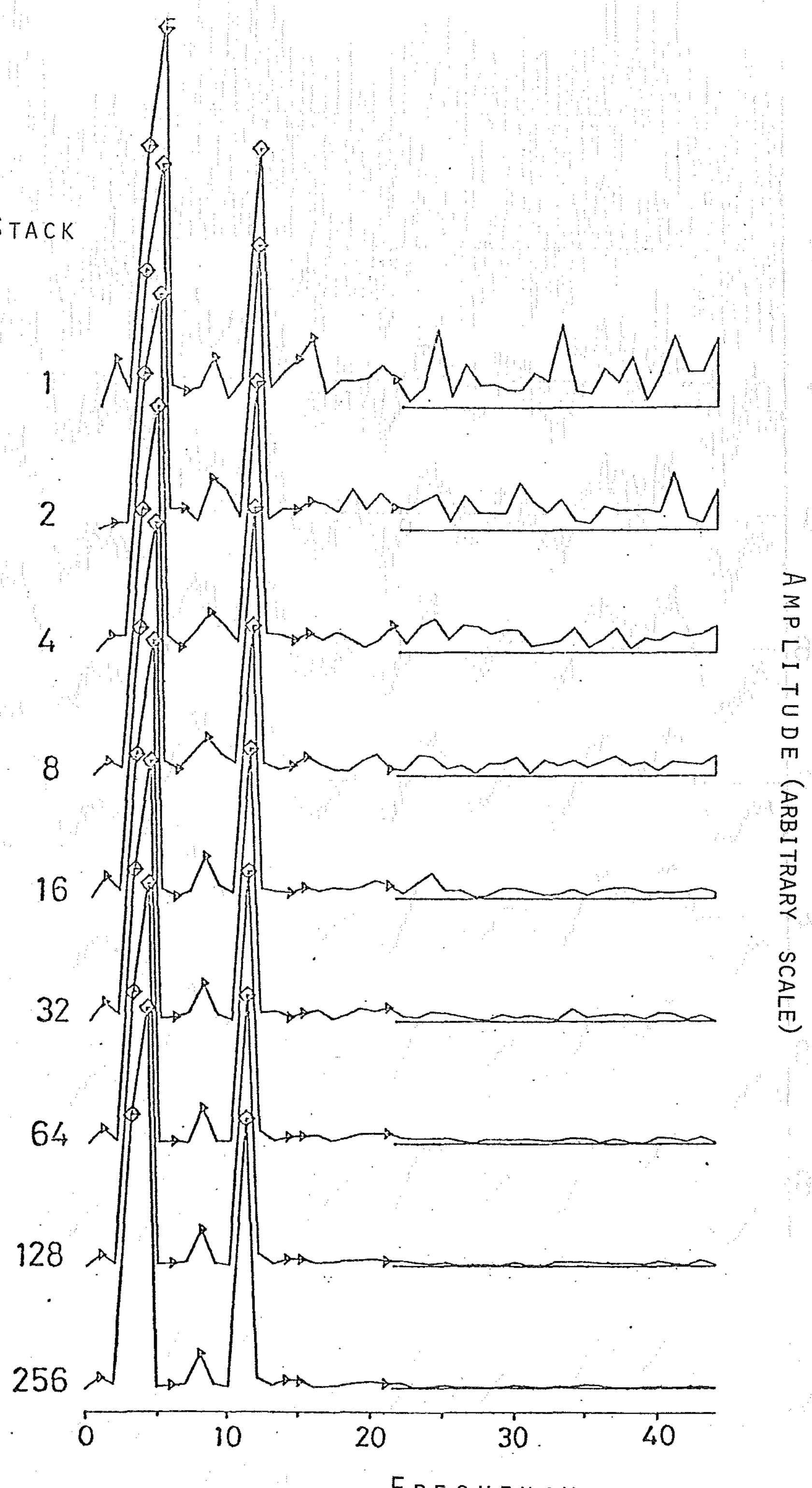


Fig. 4. Amplitude spectra (first 45 terms) of the signals of Fig. 5 obtained by FFT technique. Horizontal bars indicate zero level for individual stacking.

## 4. Discussion

As a versatile measuring instrument, spinner magnetometers have importance in rock magnetism and paleomagnetism. Our effort in this study was devoted to develop a digitially controlled spinner, and we have succeeded to make a convenient system especially suited for magnetization of volcanic rocks ($1 \sim 10^2$ A/m).

Although the system at present is only a spinner magnetometer, we are now developing an alternating field (AF) demagnetizer which also is digitally controled. Because the samples need not be taken out and reoriented as in the conventional spinner measurements, and because the samples are rotated around two orthogonal axes, it is possible to AF demagnetize the sample in situ in our system. An AF coil is placed to enclose the two-axis tumbler, and alternating current with a frequency of about 500 Hz is supplied to the coil by a dipolar operational power supply similar to the one used in the Schonstedt demagnetizer. The maximum field as well as the rate of increase/decrease is controled by the microcomputer. One of the problems of including an AF demagnetizer in the system is that unwanted voltages are induced in the windings of fluxgate sensor with the hazardons consequence of heating and vibration. Such voltages are minimized by making the AF axis perpendicular to the fluxgate sensor. No damage is done if the field is not too strong ($\lesssim$ 0.06T), but if a larger field is to be generated the sensor needs to be removed out of the influence of AF.

Although practically important, a particular choice of geometry is not essential in our magnetometer. For instance, different gear ratios can be chosen if they satisfy the requirements discussed in section 3.1. Also, the fluxgate probe may take different positions or directions. Our geometry is similar to a satellite with vertical component magnetometer circling the earth on a polar orbit. As is the case with MAGSAT satellite, oblique orbits or horizontal components also give satisfactory results provided that the directions near pole are adequately sampled and that the vertical components are also sampled to some extent. However, the calculation becomes more complicated for such cases, and the amplitude of the signal is reduced.

## References

Foster, J.H. (1966) Earth Planet. Sci. Lett., 1, 463.
Graham, J.W. (1955) J. Geophys. Res., 60, 329.
Johnson, E.A., T. Murphy, and O.W. Torreson (1948) Terr. Mag. Atmos. Elec. 53, 349.
Molyneux, L. (1971) Geophys. J.R. astr. Soc., 24, 429.

(Submitted to Geophys. J.R. astr. Soc.)

SHIPBOARD MEASUREMENT OF THREE COMPONENTS
OF GEOMAGNETIC FIELD

Nobuhiro ISEZAKI , Jun-ichi MATSUDA , Hiroo INOKUCHI
and Katsumi YASKAWA

Department of Earth Sciences, Faculty of Science
Kobe University, Nada, Kobe 657, JAPAN

## INTRODUCTION

The recent results of the deep sea drilling (DSDP-IPOD) has revealed the detail feature of magnetization of the sea floor which is more complicated than the ever assumed model of magneization, especially for the total intensity anomaly lineations which has been the basis of the seafloor spreading hypothesis. In order to reexamine and refine the model, we should observe not only the total intensity but also the complete set of the three components of the geomagnetic field because the geomagnetic field has a vector quality.

While three component measurement has been usual by an airplane the surveyed areas should be confined almost in the coastal areas. Therefore the development of the shipboard three component magnetometer (STCM) long has been desired. We started instrumentation of STCM during the Japanese Geodynamics Program (1972-1975) and in 1977 the vector measurement, i.e. the total intensity, the vertical intensity and the declination was carried out for the first time along a long track line in the Shikoku Basin by the R/V Ryofu-maru of the Japan Meteorological Agency, where declination measurement was not succesful.

In 1979 the three components (north, east and vertical components) were measured by use of the improved STCM on the Zenisu seamount by the R/V Tansei-maru of the Ocean Research Institute of the University of Tokyo and in 1980 the same survey by a microcomputer controled STCM with the total intensity measurement by a proton magnetometer followed in the area around the Nansei-shoto.

The STCM is a flux gate type and the sensors (ring core) are hung with an almost frictionless fulcrum. The measured values are processed to be the true three components of the geomagnetic field by eliminating from the magnetic field induced by a ship.

In this paper, first the important role of three component measurement for the analysis of lineations of geomagnetic anomalies is discussed and the measured results of three component anomalies are reported.

## GEOMAGNETIC ANOMALY LINEATIONS

For the analysis of geomagnetic anomaly lineations in terms of two dimensional source bodies, we introduce the following relatons;

$$t(\xi) = h(\xi)\cdot \cos I\cdot \sin(D-S) + z(\xi)\cdot \sin I \qquad (1)$$

$$h(\xi) = \sqrt{x(\xi)^2 + y(\xi)^2} \qquad (2)$$

$$z(k) = i\cdot H(k)\cdot \mathrm{sgn}(k) \qquad (i= -1) \qquad (3)$$

$$|T(k)| = |H(k)|\cdot\sqrt{\cos^2 I\cdot \sin^2(D-S) + \sin^2 I}$$
$$|Z(k)|\cdot\sqrt{\cos^2 I\cdot \sin^2(D-S) + \sin^2 I} \qquad (4)$$

$$\theta_H = \theta_T - I' \qquad (5)$$

$$\theta_Z = \theta_T - I' + \pi/2 \qquad (6)$$

$$\tan I' = \tan I/\sin(D-S) \qquad (7)$$

where

$t(\xi)$ : the total intensity anomaly
$h(\xi)$ : the horizontal intensity anomaly
$z(\xi)$ : the vertical intensity anomaly
$x(\xi)$ : the north component anomaly
$y(\xi)$ : the east component anomaly

$\xi$ : the abscissa, the positive direction is clockwise perpendicular to the strike of the lineation
I : inclination of the present geomagnetic field
D : declination of the present geomagnetic field
S : the strike of lineation measured clockwise from the geographycal north
T(k),H(k),Z(k) : the Fourier transforms of $t(\xi)$, $h(\xi)$ and $z(\xi)$ respectively
$\theta_T$, $\theta_H$, $\theta_Z$: the phase spectra of T(k), H(k) and Z(k) respectively
k : wave number

With above relations we can examine the geomagnetic anomaly lineations as follows,

1. Identification of lineations: Identification of the geomagnetic anomaly lineation is very important because it is the common way that the normally and reversally magnetized sourece is modelled after idendification of lineations, then the movement and the age of the seafloor are determined. In every ocean there are many lineations which are deformed and disturbed by the magnetic field (magnetic noise) produced by the three dimensional bodies (topography of the ocean floor, undulations of the basal basalt burried beneath the sediments, fracture zones etc.) which are found more often in the marginal basins, for instance, the Japan Sea (Isezaki and Uyeda,1973; Isezaki, 1975) and the Shikoku Basin (Tomoda et al., 1975; Watss and Weissel, 1975; Watss et al., 1977; Isezaki and Miki, 1979) where identification of lineations and correlation of geomagnetic anomaly profiles could not be done so easily. If we have the three component anomalies, as a matter of course, the correlation of geomagnetic anomaly profiles ought to be much easir because we have three independent anomaly profiles. Moreover, with the relation (3) we can examine the lineality. If the relation (3) holds well actually, anomalies are two dimensional, that are, lineated. If not, anomalies contain the magnetic noises produced by the three dimensional bodies. One method to eliminate such magnetic noises is to stack $z(\xi)$s and $h(\xi)$s obtained from many different profiles which are regarded as the crossings of the same lineations. By this method the magnetic field produced by the randomly distributed bodies is to be reduced. The other method is that proposed by Blakely et al. (1973). They calculated $t(\xi)$ from the measured three components on a single track and transformed $t(\xi)$ into $h(\xi)$ and $z(\xi)$ under assumption of the two dimensionality of the source body. By comparing the calculated $h(\xi)$ and $z(\xi)$ to the observed ones, they distinguished the anomalies due to the three dimentional bodies. As the result, they found two small peaks of anomalies, which were not regarded as the magnetic noises, and identified them with those due to short polarity events of the geomagnetic reversals and refined the time scale of the geomagnetic polarities of Heirtzler et al. (1968).

2. Magnetization : Sincee Talwani et al. (1971) reported the results of the survey on the Reykjanes Ridge, it has become common to assume the magnetized layer is about 500m thik. However, the basement rocks collected by DSDP-IPOD usually show the intensity of magnetization smaller than those required for explaining the amplitude of the total intensity anomalies caused by the magnetized layer of 500m thick (Lowrie, 1974, 1977; Harrison, 1976). Kent et al. (1978) showed that the samples dredged in the north Atlantic presented the smaller intensities of magnetization which would require the thicker and deeper magnetized layer, including Layer 2 and 3, for explaining the amplitude of the total intensity anomalies observed on the sea surface. The result of DSDP-IPOD has also revealed that magnetization of the upper part of

the basement did not coincide with the expected one from the observed total intensity anomalies on the sea surface in the several areas of the world oceans. For example, in the Shikoku Basin on Leg 58 at Site 443, the magnetic polarity of upper 50m of the basement is reversed and a succession of both normal and reversed magnetic polarities occurs at Site 442 and 444 (Scientific Staff Leg 58, 1978), which does not seem to accord with the rather simple magnetization model in this area which ever been thought for explaining the total intensity anomaly lineations. The three component anomalies will play an important role to solve these problems because by use of the three component anomalies we can determine much more precisely the intensity of the magnetizaton and the upper and lower depth of the magnetized layer than by use of only the total intensity anomalies.

The inclination of magnetization of seafloor (Im) is the direct information of the movement of the seafloor or the plate. The common method to get Im has been to deskew the observed total intensity anomalies $t(\xi)$ (e.g. Shouten, 1971; Larson and Chase, 1972; Shouten and Cande, 1976). A weak point of this method is that the judgement how completely a profile of $t(\xi)$ is deskewed has been done only by the inspection which would apt to suffer the inclined subjectivity of an inspector. From the relation (5), (6) and (7), we can easily get Im regardless of the inclined subjectivity because by use of the relation $\theta_T = Im' + I' - \pi$ (8) (Shouten, 1971), $\theta_H$ and $\theta_Z$ become to have the simple relation to Im as follows,

$$\theta_H = Im' - \pi \qquad (9)$$

$$\theta_Z = Im' - \pi/2 \qquad (10)$$

$$\tan Im' = \tan Im/\sin(Dm-S) \qquad (11)$$

where Dm is the declination of magnetization. The relations (9) and (10) mean that $h(\xi)$ and $z(\xi)$ are not skewed by the present geomagnetic field, $I'$. In other words, $h(\xi)$ and $z(\xi)$ have the same form (profile) at any places on the earth's surface if the source bodies have the same $Im'$ while $t(\xi)$ suffers from skewing by $I'$ as shown in (8). $\theta_H$ and $\theta_Z$ are obtained directly from observed $h(\xi)$ and $z(\xi)$ and Im is easily obtained by the relations (9), (10) and (11), if Dm is given. This is one of the most important characteristics of the three component anomalies.

## RESULTS OF MEASUREMENT OF THREE COMPONENTS

1. Shikoku Basin : In 1977, $t(\xi)$ and $z(\xi)$ were successfully measured in the Shikoku Basin on a single track (Fig. 1). $t(\xi)$ was measured by a proton magnetometer and $z(\xi)$ by a flux-gate magnetometer whose sensor was a rod coil. In this area several authors reported the total intensity anomaly lineations and there are much different identifications among the authors because of many offsets of lineations caused by faults or fracture zones and low amplitude anomalies (Tomoda et al., 1975; Watts and Weissel, 1975; Isezaki and Miki, 1979). As mentioned above the lineality check was done by calculating $z'(\xi)$ from observed $t(\xi)$ assuming the two dimensional source bodies and comparing $z'(\xi)$ to observed $z(\xi)$. Because the difference between $z'(\xi)$

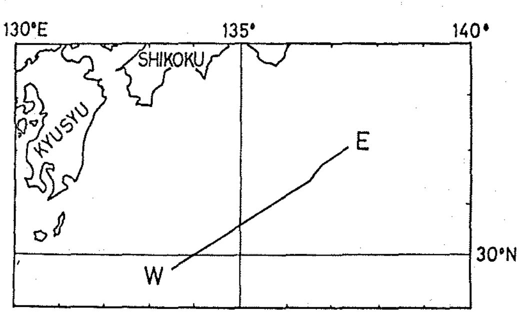

Fig. 1 : Track line in the Shikoku Basin, indicated by W-E. The strike of magnetic anomaly lineations is almost perpendicular to the track.

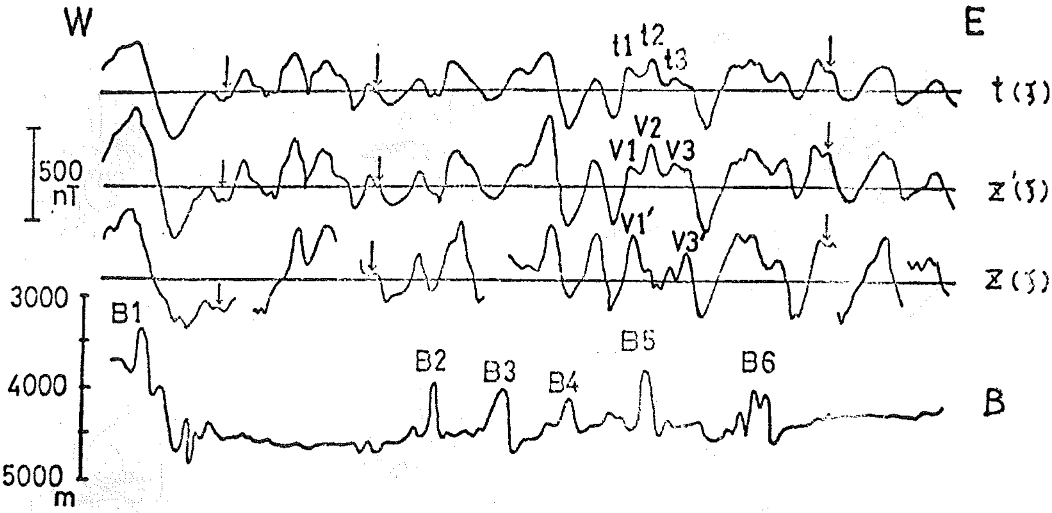


Fig. 2 : The observed total intensity anomalies $t(\xi)$, the calculated vertical anomalies $z'(\xi)$ from $t(\xi)$ and observed vertical anomalies $z(\xi)$. B is the bathymetric profile along the track.

and $z(\xi)$ may be caused by the three dimensional sources, the corresponding anomalies should not be regarded as lineated ones. As seen in Fig. 2 the large difference between $z(\xi)$ and $z'(\xi)$ occurs associated with the bathymetric uplift B5. V1 and V3 correspond to V1' and V3' respectively but V2 has no corresponding observed vertival anomaly. Then we can conclude that the total intensity anomalies t1 and t3 are lineated but t2 is not, in other words, the anomaly t2 does not belong to the anomaly lineations. The anomaly associated with B1 appears both in $z'(\xi)$ and $z(\xi)$, because B1, the Kyushu-Palau Ridge, is lineated NW-SE. The other bathymetric highs seem not to affect the geomagnetic lineations so much. Three small peaks indicated with the small arrows could be produced by short polarity events of the geomagnetic reversals because they appear both in $z'(\xi)$ and $z(\xi)$ as suggested by Blakely et al. (1973), but it should be concluded more confidently if we had $x(\xi)$ and $y(\xi)$ as well.

2. Zenisu seamount : In 1979, the three components, those are, the north, the east and the vertical components, were measured by the improved STCM whose sensors were ring cored coils, above a seamount on the Zenisu ridge located south to the Enshu-nada (Fig. 3). Magnetization of a seamount has usually been obtained by the inversion method from the total inensity anomalies, but sometimes it has been impossible to get the reliable solution only from the total intensity anomalies because the true shape of the magnetized body or the true distribution of magnetization inside a seamount are, in almost

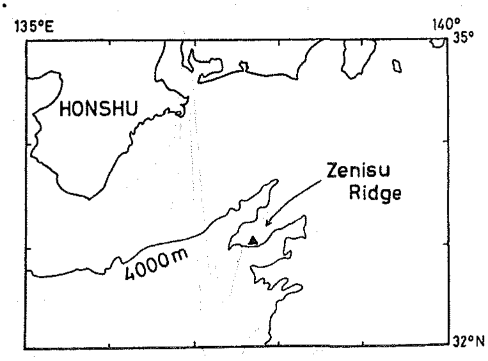


Fig. 3 : The location of the surveyed seamount on the Zenisu ridge is indicated by ▲.

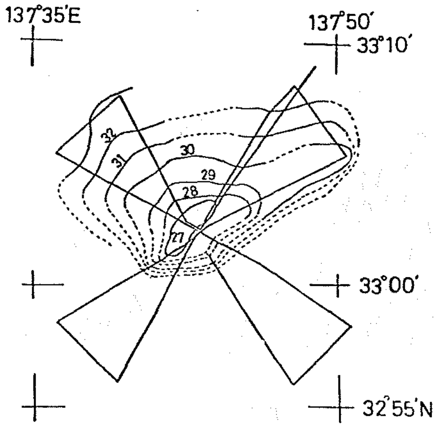


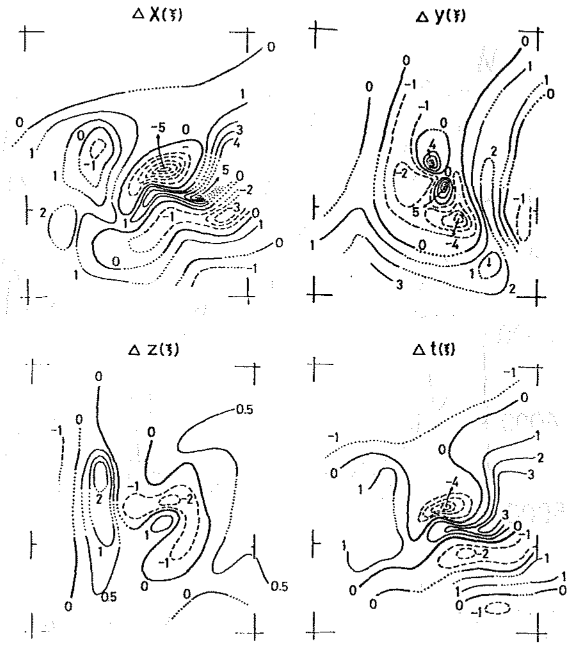


Fig. 4 : above; The track lines and the rough topographic contours of the seamount. Numerals are in unit of 100m. The detail feature of the southern part of the seamount is almost unknown at the present time. right; The north (Δx), the east (Δy), the vertical (Δz) and the total (Δt) intensity anomaly contours respectively. Unit is **100nT**. The total intensity anomalies are calculated from the three component anomalies.

all cases, kept unknown for us. However, the three component anomalies can help us greatly to attain the nearly unique solution, because they are the three independent informations. Fig. 4 shows the ship tracks, the observed three component anomalies and the total intensity anomalies synthesized from them. Because this seamount is not mapped on any bathymetric chart published by the Japan Hydrographic Board, and we could not measure the sea depth by echo-sounding along all tracks, we show only rough topographic contours of the seamount in Fig. 4. Although the information of the topography is rather poor and the ship tracks are very sparce, we are going to analyze these anomalies and the result will be reported soon.

3. Nanei-Shoto : In order to determine the accuracy of our measurement, the three components of geomagnetic field were measured in 1980 by M/V Keiten-maru of Kagoshima University around the Nansei-shoto. The improved STCM was

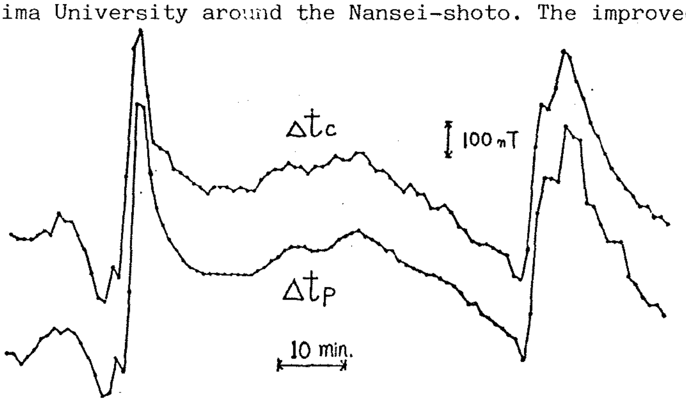


Fig. 5 : Synthesized total intensity anomalies $\Delta t_c$ and observed ones by a proton magnetometer $\Delta t_p$. The base lines of two profiles are shifted for comparing.

controlled by a microcomputer and the processed results were stored in the mini-floppy disk. The accuracy of measurement was checked by comparing the calculated total intensity, $t_c$ , from the observed three components to the observed total intensity, $t_p$, measured simultaneously by a proton magnetometer (Fig. 5). The standard deviation between $t_c$ and $t_p$ is about 15nT which is small enough for analysis of the geomagnetic anomalies in the normal ocean basins. The coincidence between $t_c$ and $t_p$ is not a necessary and sufficient condition for concluding that the three components were measured rightly, however, it should give strong support to conclude that. The accuracy could be less than 10nT with the additional measurement of roll and pitch angles of a ship. The detailed description of the data processing and the instrument is done by the authors (Isezaki et al., 1980).

SUMMARY

By measuring the three components of the geomagnetic field on the sea, the followings are immediately expected.

1. The geomagnetic anomalies which are not lineated are eliminated even by a single track and the true lineations can be easily identified.
2. The geomagnetic anomalies produced by the short polarity events of the geomagnetic reversals can be easily identified even by a single track and it will help to improve the time scale of the geomagnetic polarities.
3. The reliable inclination of magnetization of the magnetic source which produces the geomagnetic anomaly lineations is obtained because the three component anomalies are not skewed by the present geomagnetic field while the total intensity anomalies are skewed.
4. The seamount magnetization is obtained more accurately than by use of only the total intensity anomalies.

Funds for this research were mainly provided by the grant in aid for scientific research from Japan Ministry of Education, the project number 242015.

REFERENCES

Blakely, R. J., A. Cox and E. J. Iufer (1973) J. Geophys. Res., 78, 6977.
Harrison, C. G. A. (1976) Geophys. J. Roy. Astr. Soc., 47, 257.
Heirtzler, J. R., G. O. Dickson, E. M. Herron, W. C. Pitman and X. Le Pichon (1968) J. Geophys. Res., 73, 2119.
Isezaki, N. and S. Uyeda (1973) Marine Geophys. Res., 2, 51.
Isezaki, N. (1975) Marine Geophys. Res., 2, 53.
Isezaki, N. and H. Miki (1979) J. Phys. Earth, 26, 403.
Kent, D. U., B. M. Honnorez, N. D. Opdyke and P. J. Fox (1978) Geophys. J. Roy. Astr. Soc., 55, 513.
Larson, R. L. and C. G. Chase (1972) Geol. Soc. Am. Bull., 83, 3645.
Lowrie, W. (1974) J. Geophys. Res., 79, 2686.
-------- (1977) J. Geol. Soc. London, 133, 61.
Scientific Staff Leg 58 (1978) Geotimes, 23, 23.
Shouten, J. A. (1971) Marine Geophys. Res., 1, 111.
Shouten, J. A. and S. C. Cande (1976) Geophys. J. Astr. Soc., 44, 567.
Talwani, M., C. C. Windish and M. G. Langseth (1971) J. Geophys. Res., 76, 473.
Tomoda, Y., K. Kobayashi, J. Segawa, N. Nomura, K. Kimura and T. Saki (1975) J. Geomag. Geoelectr., 28, 47.
Watts, A. B. and J. K. Weissel (1975) Earth Planet. Sci. Lett., 25, 239.
Watts, A. B., J. K. Weissel and R. L. Larson (1977) Tectonophysics, 37, 167.

(Submitted to J. Geomag. Geoelectr.)

PRELIMINARY REPORT ON THE MAGNETIC SURVEY IN NIUE ISLAND

Masayuki HYODO, Toshiki ISHIZAWA, Yasushi HASE, Hiroo INOKUCHI
Nobuhiro ISEZAKI and Katsumi YASKAWA

Department of Earth Sciences
Faculty of Science
Kobe University, Nada, Kobe 657, Japan

## Introduction

Magnetic surveys were made in the Niue island. It is the uplifted atoll situated at the south-western most edge of the Pacific plate and it is subsiding beneath the Tonga-Kermadic trench. Its latitude and longitude are 19.1 S and 169.9 W. Although the three seamount chains in the Pacific have been interpreted by the hot spot hypothesis (Morgan, 1972), it does not belong to these chains. Many isolated islands such as Niue have been scarcely discussed yet. Our purpose in this paper is to report the results of calculation of the magnetization of the volcanic body beneath the coral and paleoposition of the island.

## Survey and data

Magnetic measurements were carried out on the uniformly distributed 182 sites for the total field and 97 sites for the vertical field. The daily variation of the total field was observed at the same time for the correction. Figure 1 contains the total field map after the correction of daily variation and the vertical field map without correction. The observed vertical field is relative one to some fixed field.

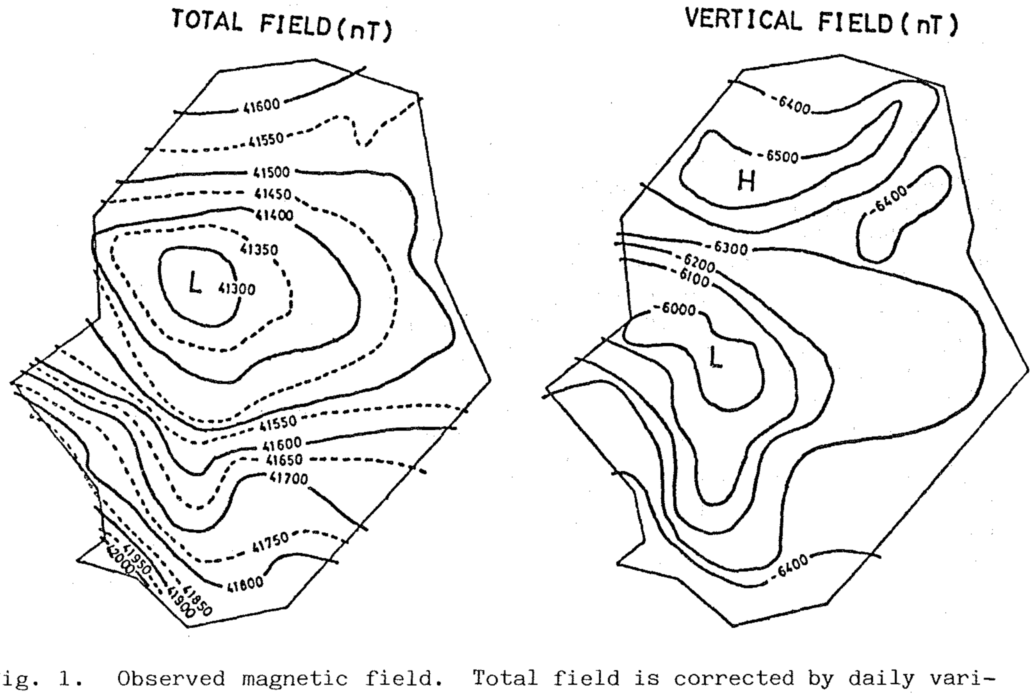


Fig. 1. Observed magnetic field. Total field is corrected by daily variation. The values of vertical field are biassed.

Some informations were obtained in addition to our magnetic data. They are for example the bathymetry around Niue, the gravity map, the report of drilling and so on. These data were referred when the pyramid model was formed. Because the result of drilling was that every hole did not reach the basement, it did not play an important role in modeling.

Analysis

Since some anomalous peaks are recognized in the observed data, it is reasonable to imagine that the observed magnetic field is composed of regional field and the anomalous field generated by the magnetic body beneath the coral. Suppose the regional field is represented by one-dimensional plane, the observed field is expressed as

$$Foi = Fai + Fri \qquad ( Fri = a\,Xi + b\,Yi + c )$$

where Foi, Fai and Fri are the observed field, the anomalous field and the regional field at the i-th site, Xi and Yi are the North co-ordinates and the East co-ordinates, and a, b and c are the N gradient, the E gradient and the constant of regional field, respectively. In this paper the regional field was decided by approximating the IGRF. For the calculation of magnetic anomaly we took a method that the volcanic body was approximated by a pyramid and the shape factor was calculated by the Talwani's method (Talwani,1965). In practice the magnetization was computed by the inversion using the least-square method (Uyeda and Richard, 1965).

The pyramid model was constructed with reference to the bathymetric data and the gravity data (Figure 2). The dotted line represents the costline. The position of the top plane is in accordance with that of high peak of the gravity. The confirmed information about the depth of the

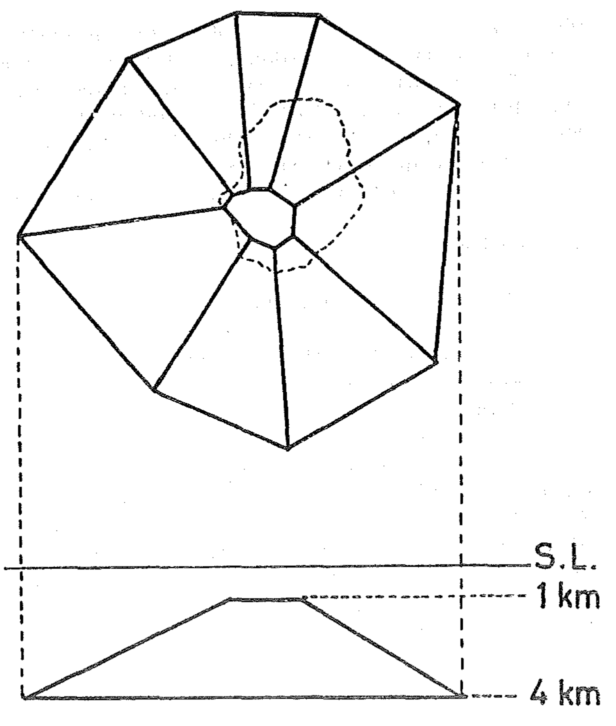


Fig. 2. Pyramid model for the volcanic body beneath the coral. Top view (top) and sectional view (bottom). Dotted line is the cost line.

| Site | LAT. 19.1°S | Present | INC. -37.6° |
|---|---|---|---|
| | LON. 169.9°W | field | DEC. 13.1° |

| Data | Depth of top plane (Km) | Constant regional (nT) | Magnetization DEC. ( ° ) | INC. ( ° ) | J (A/m) | Goodness of fit ratio | C.C. |
|---|---|---|---|---|---|---|---|
| Total field | 0.8 | 41840 | 229. | 55. | 2.80 | 3.47 | 0.985 |
| | 1.0 | 41840 | 229. | 56. | 3.04 | 3.41 | 0.984 |
| | 1.2 | 41840 | 228. | 56. | 3.30 | 3.35 | 0.984 |
| Vertical field | 1.0 | -6828 | 219. | 61. | 4.14 | 5.94 | 0.788 |
| | 1.0 | -6889 | 220. | 59. | 4.68 | 6.80 | 0.789 |

Table 1. Results of analyses.

basement was very poor, then referred to the results of seismic refraction measurement at the Bikini atoll (Dobrin and Perkins, 1954) and drilling at the Eniwetok atoll (Ladd and Schlanger, 1960), the value of 1 Km was employed for the top depth.

We have two kinds of data, the total field and the vertical field. It is possible to calculate magnetization from each data independently, and the two results must theoretically coinside. It is interesting to examine how it dose in practice.

The degree to which the observed anomalies are approximated by the calculated anomalies is estimated by the correlation coefficient and the " goodness of fit " ratio (Richards et al.,1967):

$$r = \sum_{i=1}^{n} |\Delta Fi| \Big/ \sum_{i=1}^{n} |Ri|$$

where $\Delta Fi$ (= Foi-Fri) is observed anomaly, Ri (=observed anomaly - calculated anomaly) is residual, and n is the number of observations.

The results of analyses are shown in table 1. The calculations with the data of total field were undertaken with respect to several depths of the top plane. On the other hand the constant regional field was shifted in calculating with the data of vertical field since the observed values of vertical field were not absolute but biassed.

## Discussion

The calculations about different depths of the top plane resulted in that the direction of magnetization did not vary nevertheless the intensity did. Consequently the top depth was fixed to 1 Km when the vertical field data were analyzed.

Comparing the magnetizations computed from each data, it is found that the directions are almost identical. We interpreted the analyses to be reliable. The magnetization has the declination of 220°~230° and the inclination of 55°~60°. Considering that the direction of the present field in Niue is of the declination of 13.1° and the inclination of -37.6°, it implies that the volcanic body was magnetized in a reversal epock or event. Using the inclination of 56° the paleolatitude turns out to be 36.5°S. This does not conflict with the result deduced from the rotation of the Pacific plate.

## References

Dobrin,M.B., and B.Jr. Perkins (1954) Geological Survey Professional Paper.
Ladd, H.S., and S.O. Schlanger (1960) Geological Survey Professional Paper.
Morgan, G.A. (1972) Amer. Ass. Petrol. Geol. Bull., v.56, p. 203-213.
Richards, M.L. et al. (1967) Geophysics, v.32, No.4, p. 678-707.
Talwani, M. (1965), Geophysics, v.30, No.5, p. 797-817.
Uyeda,S. and M. Richard (1965) Bull. Earthq. Res. Inst., v.44, p. 179-213.

# NOTE ON EFFECTS OF DRYING ON POST DEPOSITIONAL REMANENT MAGNETIZATION OF SEDIMENTS

Yo-ichiro OTOFUJI, Ikuo KATSURA

and

Sadao SASAJIMA

*Department of Geology and Mineralogy, Faculty of Science, Kyoto University, Kyoto 606, Japan*

## Introduction

Changes in remanent magnetization within a drying sediments have been perceived since the initial investigations of natural remanent magnetization (NRM) of sediments exposed on land (Clegg et al., 1954; Graner, 1958). Recently the magnetic effects associated with drying were also reported in deep-sea core (Johnson et al., 1975) and lake sediments (Shuey et al., 1977; Stober and Thompson, 1979). The effects of drying under presence of a magnetic field are (1) reduction in NRM in intensity and (2) an acquisition of a magnetization parallel to the applied magnetic field (Johnson et al.,1975). Only reduction is observed when sediments are allowed to dry in a nonmagnetic field.

Several investigators tried to obtain a geomagnetic paleointensity from continuous deposited sediments (Opdyke et al., 1973; Levi and Banerjee, 1976; Kawai et al., 1976). They paid no attentions unfortunately to the effects of drying that original intensity of NRM is not necessarily preserved in sediments until the time when the remanent magnetization is measured at a laboratory. In order to more accurately assess the paleointensity from the sediments, further quantitative understandings on the effects of drying are clearly required.

Sediments with the post-depositional remanent magnetization (post-DRM) with different remanent intensity and water content can be produced at our will by the centrifuge method (Otofuji and Sasajima, 1980). These sediments are well-suited to study quantitatively on the effects of drying on post-DRM. This article reports quantitative experiments of effects of drying in the nonmagnetic field.

## Experimental procedure

Two types of sediments were used; lake sediments dredged from Lake Biwa, central Japan and pelagic sediments (GH 76-2 D148) from an abyssal plain of the North Pacific Ocean (Honza, 1977).

Sediments with post-DRM were produced by the centrifuge method under a moderate acceleration. The apparatus and the experimental procedure were the same as those described by Otofuji and Sasajima (1980). The densities of suspensions before centrifuging were 1.12 g/cm$^3$ and 1.21 g/cm$^3$ for the lake and the pelagic sediments, respectively.

The compacted sediments in a specimen holder (25 mm both in diameter and length) were allowed to dry in a room temperature within a space of 53 x 56 x 59 cm$^3$ where the geomagnetic field was reduced to less than 200 gamma by a double-shield of $\mu$-metal. The remanent magnetization of the sediments in the holder was measured at intervals on the Schonstedt spinner magnetometer (SSM-1A) before complete dryness. The water content was obtained by weighing the specimen. The water content as used here is percent content. The bulk density was calculated from the water content by the assumption that the density of the solid in sediments was 2.60 g/cm$^3$.

### The sense of effects of drying in nonmagnetic field

The lake sediments were compacted into a specimen whose water content (density) and the remanent intensity were 166.8 % (1.30 g/cm$^3$) and 7.89 x10$^{-5}$ emu/g. While the water of 28.2 % in the specimen evaporated for 6,384 min, the reduction of 11.4 % in intensity of remanence (0.90 x 10$^{-5}$ emu/g) was observed without any corresponding directional changes. As shown in Fig. 1, the linear relation was not established between the change in remanent magnetization and the logarithm of time. The reduction curve of remanent magnetization was concave upwards. Five specimens produced later also deviated from a logarithmic dependence of time.

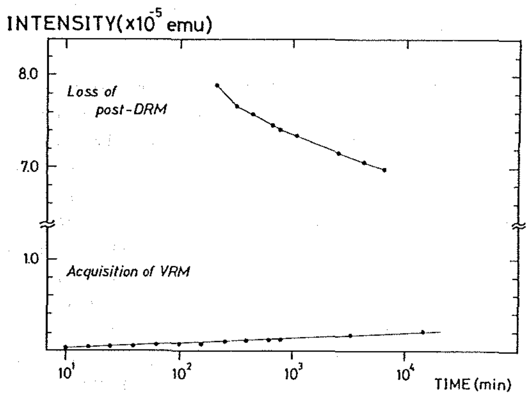


Fig. 1. Decay of the post-DRM in the wet sediment specimen and remanence grown in the dry sediment specimen as a function of time (logarithmic scale).

The specimen was subsequently placed in a geomagnetic field (0.45 Oe), after complete desiccation in the oven and a subsequent alternative field (AF) demagnetization up to 400 Oe. The acquisition of viscous remanent magnetization (VRM) by the dry sediments is plotted as a function of the logarithm of time in Fig. 1. The specimen acquired an increasing VRM whose viscous coefficient was 5.47 x 10$^{-7}$emu/g in room temperature. As viscosity coefficient in time

TABLE 1. Experimental results for effects of drying (1)

| Sample | water content (%) | density (gr/cm$^3$) | Intensity before (x 10$^{-5}$emu/gr) | Intensity after (x 10$^{-5}$emu/gr) | loss of remanence (%) |
|---|---|---|---|---|---|
| 9/29/4 | 146.8 | 1.332 | 1.51 | 0.85 | 43.9 |
| 9/29/4' | 143.0 | 1.339 | 1.65 | 0.84 | 50.1 |
| 9/28/3 | 145.4 | 1.335 | 2.82 | 1.64 | 42.3 |
| 9/28/3' | 144.2 | 1.337 | 2.96 | 1.64 | 44.8 |
| 9/28/2 | 142.4 | 1.340 | 5.22 | 2.81 | 46.1 |
| 9/28/2' | 138.2 | 1.348 | 5.11 | 2.85 | 45.8 |
| 9/28/1 | 145.9 | 1.334 | 6.78 | 3.66 | 46.7 |
| 9/28/1' | 148.4 | 1.329 | 7.06 | 3.95 | 44.1 |
| 9/29/5 | 150.9 | 1.325 | 12.6 | 6.78 | 46.5 |
| 9/29/5' | 138.2 | 1.348 | 12.7 | 6.96 | 45.3 |
| 9/29/6 | 150.2 | 1.326 | 16.6 | 8.86 | 46.5 |
| 9/29/6' | 147.2 | 1.331 | 16.5 | 9.21 | 44.3 |
| 9/29/7 | 149.2 | 1.328 | 19.7 | 11.1 | 43.5 |
| 9/29/7' | 149.5 | 1.327 | 19.6 | 11.2 | 43.0 |
| 9/30/8 | 144.3 | 1.337 | 20.3 | 11.2 | 44.9 |
| 9/30/8' | 149.3 | 1.328 | 20.3 | 11.4 | 44.0 |
| 9/30/9 | 149.4 | 1.327 | 20.8 | 12.1 | 41.6 |
| 9/30/9' | 154.0 | 1.320 | 20.2 | 11.8 | 41.7 |
| 9/30/10 | 149.1 | 1.331 | 28.7 | 16.3 | 42.5 |
| 9/30/10' | 147.7 | 1.328 | 28.3 | 16.7 | 42.1 |

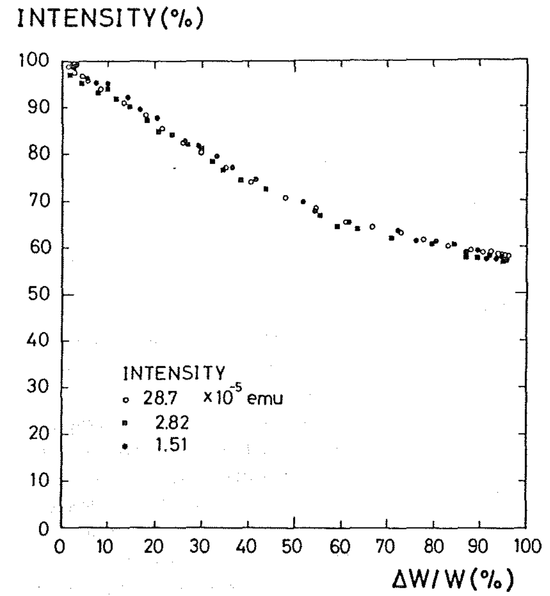


Fig. 2. Relative intensity changes, during desiccation, of specimens with different remanent intensities. The abscissa shows the drying stage which is expressed by the ratio of the weight of the evaporation loss, ΔW, and the weight of water before desiccation, W.

decay of isothermal remanent magnetization (IRM) in non-magnetic space is nearly half of that in acquisition of VRM (Shimizu, 1960), the result shows that the reduction during desiccation is about an order of magnitude larger than the time decay of IRM.

A loss of remanence in the non-magnetic field seems to be caused by both the reduction due to the drying on post-DRM and time decay of IRM. Since the time decay forms only a small percentage of the reduction (about 10 %) within the drying sediments, the observed loss of remanence mainly represents the feature of the reduction due to effects of drying. In contrast to the decay of IRM with a logarithmic dependence on time, the loss of post-DRM due to the effect of drying seems to be dependent on the evaporation of water from sediments. A linear relationship to the logarithm of time reported by Stober and Thompson (1979) may be a pretended dependence of time.

The influence of the self demagnetization

Twenty specimens were produced carefully to have the same water content from the lake sediments. Their remanent intensity varied from a minimum 1.51 x $10^{-5}$ to 28.7 x $10^{-5}$ emu/g. Specimens were dried with the aid of fun for about 7,000 minutes until the time when about 96 % of water evaporated from specimens. The remanence decreased gradually and tended to level off at some value. The remanent intensities before and after dryness are listed in Table 1 together with the percentage of the loss of remanence.

The loss of intensity is almost constant throughout all specimens excepting both specimens of 9/30/9 and 9/30/9' in which a few pieces of algae were found. These

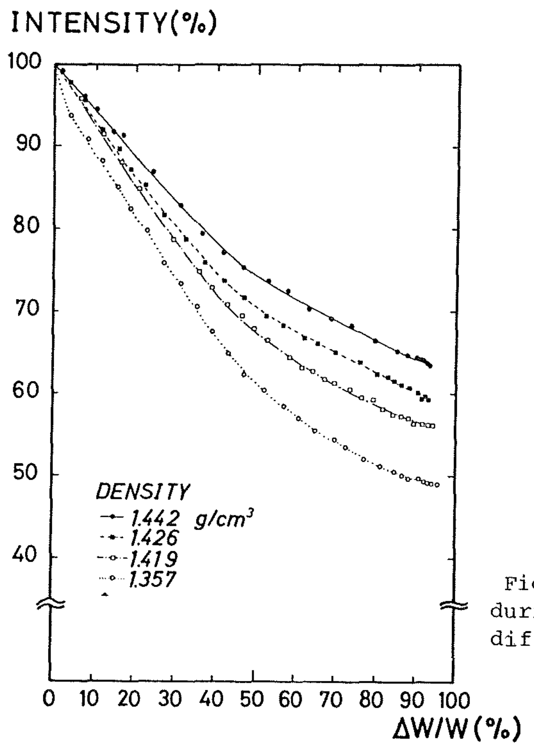


Fig. 3. Relative intensity change, during desiccation, of specimens with different bulk density.

TABLE 2. Experimental results for effects of drying (2)

| Sample | Water content (%) | density ($gr/cm^3$) | Intensity before ($\times 10^{-5}$ emu/gr) | Intensity after ($\times 10^{-5}$ emu/gr) | loss of remanence (%) |
|---|---|---|---|---|---|
| 8/22/2' | 133.7 | 1.357 | 11.1 | 5.45 | 50.9 |
| 8/22/4' | 126.0 | 1.374 | 8.58 | 4.39 | 48.8 |
| 8/22/5 | 110.7 | 1.412 | 9.60 | 5.13 | 46.6 |
| 8/23/6 | 109.2 | 1.416 | 9.14 | 5.03 | 45.0 |
| 8/23/6' | 108.4 | 1.419 | 9.06 | 5.07 | 44.0 |
| 8/24/8 | 105.9 | 1.426 | 8.61 | 4.87 | 40.9 |
| 8/27/10' | 102.9 | 1.435 | 9.24 | 6.08 | 34.2 |
| 8/25/9' | 100.6 | 1.442 | 8.38 | 5.32 | 36.5 |

contaminations may prevent magnetic particles from rotational motions in sediments or disturb an ordinary shrinkage of sediments during desiccation. We can safely conclude that the reduction does not depend on the magnitude of the remanent intensity. This conclusion is supported by the result of the relation between the relative intensity change and the evaporation of water (Fig. 2). The variance in reduction cannot be distinguished among specimens with different magnitude of remanent intensity. Self demagnetization mechanism proposed by Barton et al. (1980) may not operate to reduce the remanence during desiccation in sediments.

It is noted from the paleomagnetic viewpoint that the relative paleointensity change in the moist sediments core are well preserved after complete dryness if the sediments have the same water content throughout the core.

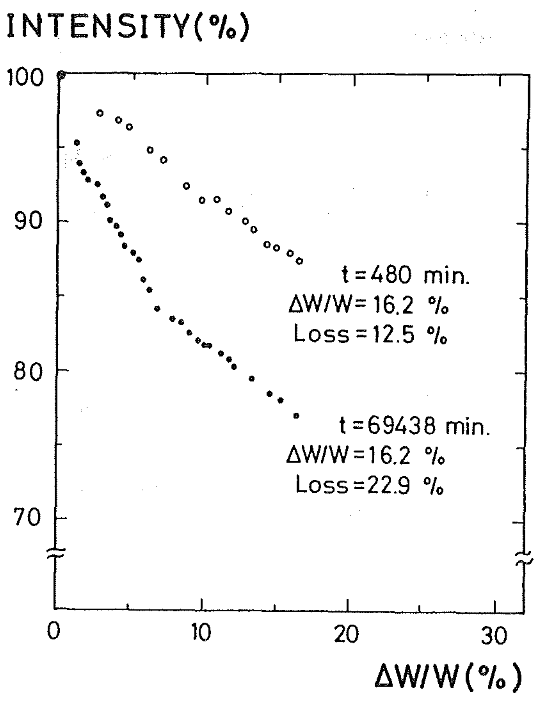


Fig. 4. Relative intensity changes of specimens dried under a condition of the different evaporation rate. The time 't' shows the drying duration until the specimen attained to the drying stage of 16.2%. The losses of remanence are also shown.

## The influence of the water content

Eight specimens with different water contents were produced from the lake sediments by changing the centrifugal force and the length of rotation of the centrifuge. The remanent intensities before and after dryness are listed in Table 2. Examples of the reduction of remanence are shown in Fig. 3. The result indicates clearly that the loss of remanence is highly dependence on the water content. The reduction may be associated with the amount of evaporation of water or the amount of volume change of sediments due to shrinkage.

It should be noted from the paleomagnetic viewpoint that the water content greatly controls the reduction in remanent intensity. Specimens with low water content shows apparently more than 20 percent larger magnitude of remanence than that with higher content after complete dryness, even if the remanent intensities are comparable each other before desiccation (cf. specimens of 8/22/4' and 8/25/9' in Table 2). A conservative estimate may be made for the remanent intensity of specimen at the upper part of sediment core after dryness.

## The influence of evaporation rate

Eight specimens with the nearly same water content and remanent intensity were produced from the lake sediments. Four specimens of them were dried fast in a room temperature with the aid of fun. The evaporation rate was about $9 \times 10^{-2}$ g/hr. Others were protected from desiccation by allowing to settlé in a moist space. Their evaporation rate decreased to less than two order of magnitude ($5 \sim 9 \times 10^{-4}$ g/hr) compared with that of the former. As shown in Fig. 4, the reductions in remanence for slow and fast evaporation have been plotted as closed and open circles, respectively. As the evaporation rate decreases, the amount of reduction in intensity increases. The loss of intensity in slowly evaporated specimens is about twice as large as that of fast evaporated specimens. The reduction of intensity seems to depend on the evaporation rate. The result indicates that the core must be placed under the condition of the same evaporation rate during desiccation for study of the relative paleointensity.

## Demagnetization curves

A total twenty specimens with almost similar water content and remanent intensity were produced from deep-sea sediments. They were demagnetized by

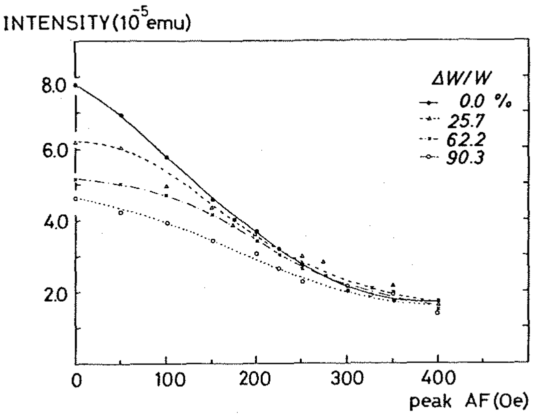


Fig. 5. Variation in the intensity of the remanence upon progressive AF demagnetization for several specimens of different drying stage. All specimens have the same remanent intensity of $7.81 \times 10^{-5}$ emu/g before desiccation.

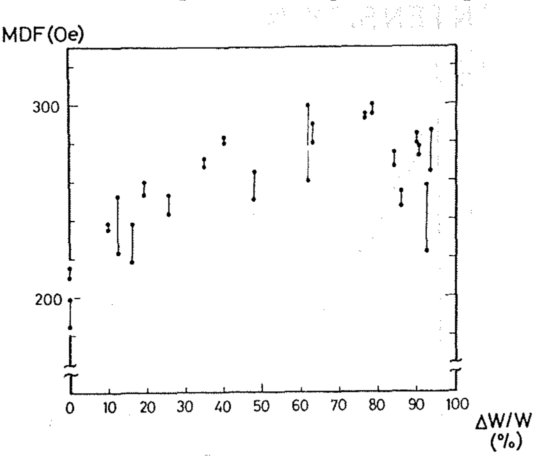


Fig. 6. Median destructive field (MDF) of AF demagnetization for several specimens of different density stage.

alternating field (AF) in increasing steps when the required amount of water evaporated from specimen in the nonmagnetic space. The demagnetized magnetic directions of each specimen form an extremely tight cluster ( $\alpha_{95}$ < 4.0°) for AF between 0 Oe to 400 Oe. As shown in Fig. 5, there is a fundamental difference among demagnetization curves: The wetter specimen has a lower stability in response to AF demagnetization. This property is clearly indicated by median destructive fields (MDF) against the drying stage (Fig. 6). The MDF increases from 192 Oe to 297 Oe during desiccation. A fairly high stability of remanence of deep-sea and lake sediment cores (Opdyke and Foster, 1970; Yaskawa et al., 1973; Kent and Opdyke, 1977) may be due to this effect.

It should be noted that each curve converges at about 300 Oe of demagnetization field (see Fig. 5). The fact infers that the reduction of remanence during desiccation is caused by the misalignment of magnetic particles which are randomized by demagnetization field of less than 300 Oe.

## Summary and conclusions

Although no clear mechanism of the reduction within the drying sediments under the nonmagnetic space has been found, some further properties have been accumulated:

(i) There appears no evidence to suggest that the reduction of remanence is caused by the self demagnetization mechanism. The reduction of remanence is independent of its remanent intensity.

(ii) The specimen with high water content presents a large reduction in remanent intensity.

(iii) The reduction depends on the evaporation rate as well as the water content.

(iv) Demagnetization curves of various drying stages indicate that the highly dry specimen has apparent stable remanence.

## References


Barton, C. E., M. E. McElhinny and D. J. Edwards (1980) Geophys. J. R. astr. Soc., 61, 355-377.

Clegg, J. A., M. Almond and P. H. S. Stubbs (1954) Phil. Mag. ser 7, 45, 583-598.

Graner, L. (1958) Ark. Geofys., 3, 1-40.

Honza, E. (1977) Cruise Report No.7., ed. E. Honza, Geol. Surv. Japan, 1-9.

Johnson, H. P., H. Kinoshita and R. T. Merill (1975) Geol. Soc. Am. Bull., 86, 412-420.

Kawai, N. Y. Otofuji and K. Kobayashi (1976) J. Geomag. Geoelectr., 28, 395-412.

Kent, D. V. and N. D. Opdyke (1977) Nature, 266, 156-159.

Levi, S. and S. K. Banerjee (1976) Earth Planet. Sci. Lett., 29, 219-226.

Opdyke, N. D. and J. H. Foster (1970) Geol. Soc. Am. Bull., 126, 83-119.

Opdyke, N. D., D. V. Kent and W. Lowrie (1973) Earth Planet. Sci. Lett., 20, 315-324.

Otofuji, Y. and S. Sasajima (1980) Geophys. J. R. astr. Soc. (in press).

Shimizu, Y. (1960) J. Geomag. Geoelectr., 11, 125-138.

Shuey, R. T., R. O. Ugland and C. R. Schmit (1977) J. Geophys. Res., 82, 3739-3746.

Stober, J. C. and R. Thompson (1979) Geophys. J. R. astr. Soc., 57, 727-739.

Yaskawa, K., T. Nakajima, N. Kawai, M. Torii, N. Natsuhara and S. Horie (1973) J. Geomag. Geoelectr., 25, 447-474.

THERMOMAGNETIC PROPERTIES OF THE PLEISTOCENE PYROCLASTIC FALL DEPOSITS IN THE YATSUGATAKE VOLCANOES, CENTRAL JAPAN

Mitsuo YOSHIDA

Department of Geology & Mineralogy Faculty of Science,
Hokkaido University Sapporo, 060

Pyroclastic fall deposit is one of the most reliable horizon marker in lithostratigraphic correlation. Momose et al.(1968) proposed an application of a variation of Curie temperatures of ferromagnetic minerals for idetification of pumice fall deposits. Fujiwara et al.(1977), Aida(1978) and Okada(1979) reported that the Curie temperatures of the ferromagnetic minerals in sucessive pyroclastic layers gradually increase from lower to higher stratigraphic unit in one eruptive sucession. These reports empasize that the gradual change of the Curie temperatures may be due to slightly and constanly changing of chemical compositions of the ferromagnetic minerals of the pyroclastic products during a series of the volcanic activity. An analysis of thermomagnetic properties and also heavy mineral assemblages of the pyroclastic fall deposits developed around the eastern foot of the Yatsugatake volcanoes are briefly represented in this report.

Various type of tephra beds occur within lacustrine beds are widely distributed on the foot of the Yatsugatake volcanoes. A total of 80 samples were collected from various horizons of tephla beds. Thermomagnetic anlysis of them was made by using a vertical type automatic magnetic balance .

Obtained thermomagnetic curves may classify into three types based on a difference of the Curie temperature and a mode of thermomagnetic curve.

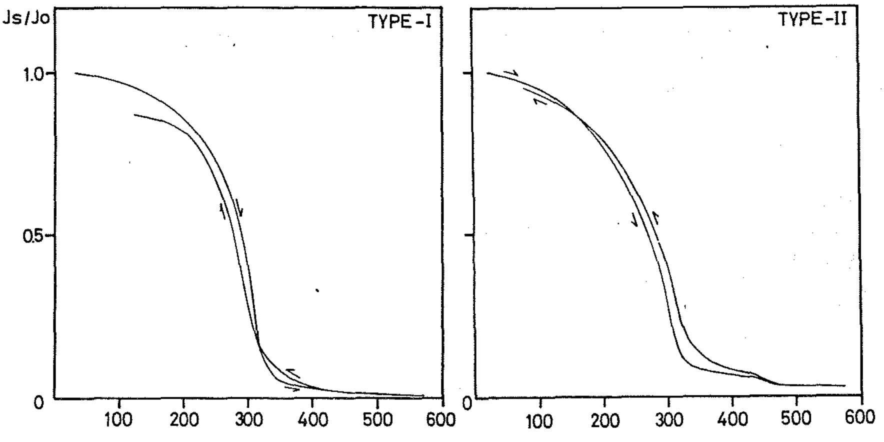


Fig.1-a Typical example of thermomagnetic curves classified into Type-I and Type II.

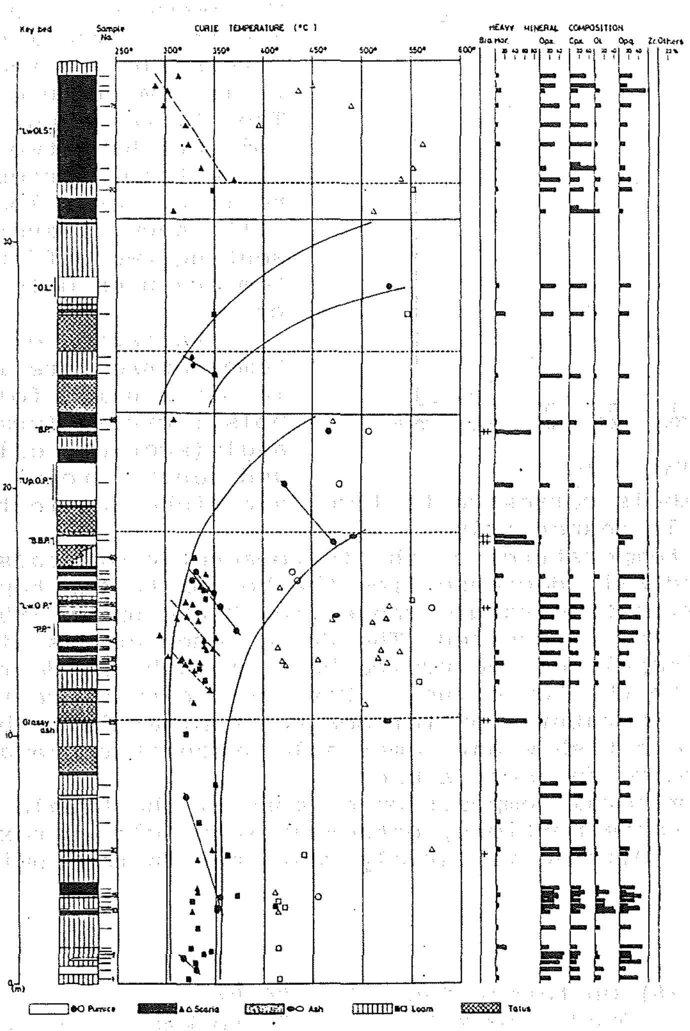


Fig.2 Variation of Curie temperatures of each pyroclatic fall unit and the heavy mineral composition of the tephla beds around the Yatsugatake volcanoes.

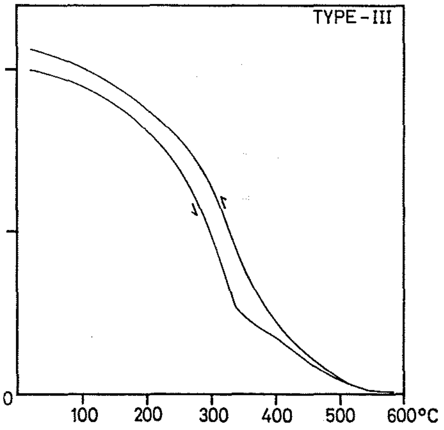


Fig.1-b

Thermomagnetic curves beolonging to to Type-I show nearly reversible and reprent a single Curie temperature. Curves of Type II represent also reversible but have two independent Curie temperatures. Thermomagnetic curves belonging to Type -III show irreversible representing two different Curie temperatures only in heating curve.

Variation of the Curie temperatures are illustrated in Fig.2 using following siymbols : circle (pumice), triangle(scoria), ellipse (ash), and square (roam). Open and closed symbols correspon to lower and higher Curie temperaure in one sample respectivly.

Curie temperatures of the ferromagnetic minerals in the scoria bed are gradually decrease from the bottom to the top in one fall unit with temperature range from 300°C up to 350°C. Four cyclic unit are recognized. The Curie temperatures of the ferromagnetic minerals of the pumice bed , meanwhile, decrease from the bottom to the top of unit. Five cyclic unit are recognized. The Curie temperatures of ferromagnetic minerals in both ash and roam beds do not show any remarkable systematic change as recognized in pumice and scoria beds.

Heavy mineral composition of most of the tephla beds mainly consist of three portions; ortho-pyroxene, clio-pyroxene and opaque mineral. Olivine is largely contained in the pumice and ash bed .

## REFERENCES

Aida,N. (1978) Quaternay Res. 17 2 86-94.

Fujiwara,Y.,S.Okada and N.Aida (1977) Rockmagnetism & Paleogeophys. 4 14-17.

Momose,K. et al. (1968) Bull.Earthq.Res Inst. 46 1275-1292

Okada,S. (1979) Jour.Fac.Eduction Tottori Univ. 29 2, 173-183

IDENTIFICATION OF PYROCLASTIC FLOW BY THERMOMAGNETIC AND NEUTRON ACTIVATION ANALYSIS

Yoshiki FUJIWARA, Sakae MUKOYAMA and Tatsuji KOSHIMIZU

Department of Geology & Mineralogy, Faculty of Science
Hokkaido University. Sapporo, 060

Identification of individual pyroclastic unit which is spread over a wide area is one of the important process for long distance correlation. For this purpose, many methods have been proposed by many investigators. Microscopic observation of thin sections, assemblage analysis of heavy minerals, reflactive index of volcanic glass and some chracteristics of certain rock forming minerals have been generally carried out. Furthermore, espcially for the strongly altered or weathered volcanic products such as pyroclastic fall and flow deposits, a mode of the Curie temperatures and also thermomagnetic curves of the ferromagnetic minerals in the pyroclastic deposits become useful tool for identification and correlation (Momose et al. 1968, 1972). We have also carried out thermomagnetic analysis of various type of both pyroclastic fall and flow deposits successively developed in Hokkaido, for an aid of their litho-stratigraphic correlation (Fujiwara, 1972 Fujiwara et al. 1977).

Recently, neutron activation analysis has widely been used to idetify the origin and/or location of the archeological and geological specimens. We have also undertaken neutron activation analysis of volcanic glass in sucessive pyroclastic flow units developed in central to western Hokkaido.

This short note provides distinct uniformity of the thermomagnetic properties and also the rare elements distributions of one pyroclastic flow unit.

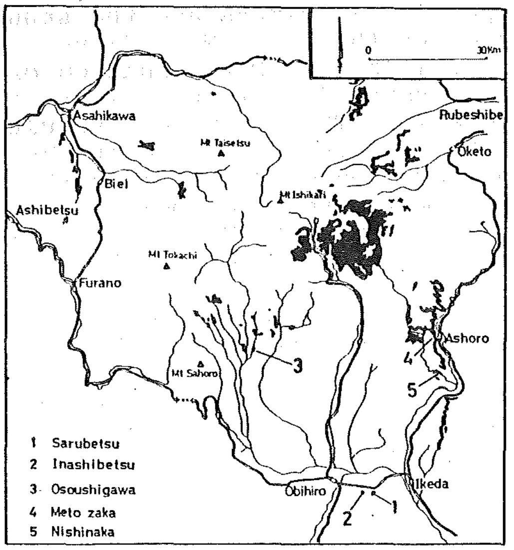


Fig.1 Distribution of the pyroclastic flow and delected sampling locations for the present note.

The pyroclastic flow deposit now in problem, is distribute widely in the northern Tokachi plain and around the central mountainous region in central-western Hokkaido. Because of varieties of lithologic occurences in many places, this pyroclastic flow unit has been differently named by many investigators. For instance, the Shimoaikappu welded tuff in eastern region, the Meto welded tuff in northern Tokachi plain, the Osoushi-gawa welded tuff in northwestern region, Nishinaka tuff, Kita-kyu-sen tuff and Sarubetsu tuff in southwestern region. For that reason, stratigraphic correlations among them have been somewhat misrepresented until present(Fig.1).

The results of the measurements of the thermomagnetic properties of the samples widely collected from various localities show distinct uniformity regardless of their locations. In Fig. 2, typical examples of the thermomagnetic curves are illustrated.

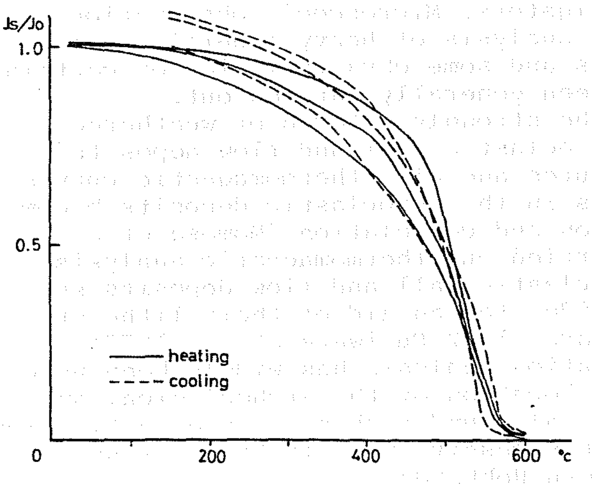


Fig.2 Typical examples of thermomagnetic curves of 3 samples which were collected from each individual locality.

8 samples were selected for the determination of neutron activation analysis. The analyzed specimens consit of only volcanic glass fragments of which impurities are removed by hand picking under a binocular micoscope. The specimens and the standards (G-2 and AGV-I) were irradiated at the Triga Mark II neuclear reacter at the Rikkyo University for 18 hours. Determination of the irradiated specimens was made by using Ge(Li)-puls hight analyzer after 8 days after the irradiation. The analytical results are listed in Table 1. As illustrated in Fig.3 , distributions of each rare elemnet show uniform concentration in certain ranges regardless of their locations while those of only no.8 are fallen slightly different ranges. Specimen no.8 which was collected from stratigraphically lower pyroclastic unit was analyzed for comparison.

Accordingly, it may be concluded that these samples collected from the pyroclastic unit at various localities probably belong to one wide spread pyroclastic flow unit.Thermomagnetic characteristics and rare elements distributions are unique for one flow unit and remarkably uniform throughout the horizotal extent regardless of their litho-facies variations.

Table1

Results of rare element (ppm) determinations of the pyroclastic flow deposits in central Hokkaido.

Satoshi KOSHIMIZU

| No | Sc | Co | Cs | La | Ce | Eu | Sm | Tb | Hf | Th |
|---|---|---|---|---|---|---|---|---|---|---|
| 1 | 4.52 | 0.43 | 6.49 | 30.7 | 45.9 | 0.37 | 4.51 | 0.14 | 2.74 | 13.4 |
| 2 | 4.25 | 0.49 | 6.44 | 28.7 | 44.8 | 0.33 | 4.35 | 0.41 | 2.59 | 13.1 |
| 3 | 4.31 | 0.42 | 6.15 | 29.2 | 48.1 | 0.4] | 4.53 | 0.26 | 3.00 | 12.4 |
| 4 | 4.31 | 0.43 | 6.19 | 29.9 | 45.0 | 0.37 | 4.35 | 0.32 | 2.31 | 12.4 |
| 5 | 4.43 | 0.46 | 9.01 | 33.6 | 56.9 | 0.54 | 5.98 | 0.61 | 2.98 | 17.8 |

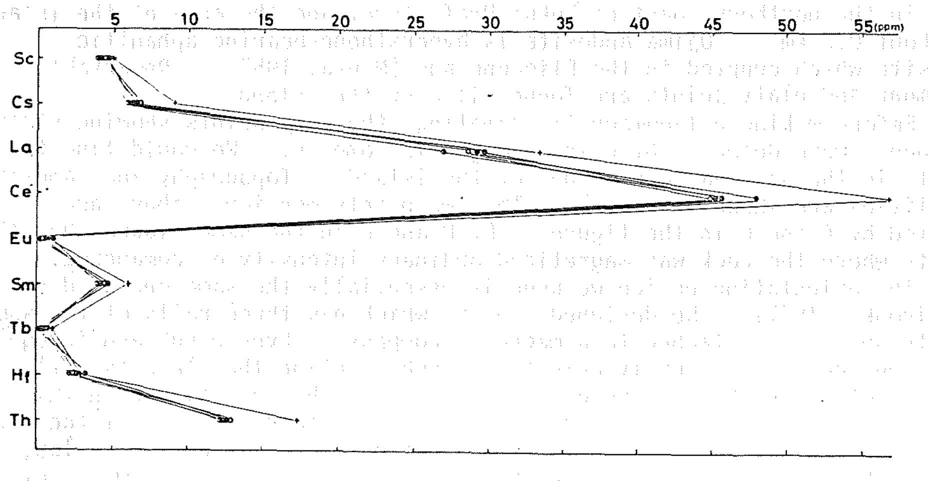


Fig.3 Rare elemnet variations of the pyroclastic flow samples. + : inffered from the data of no.8

## REFERENCES


Fujiwara,Y. (1972) Jour.Fac.Sci.Hokkaido Univ. SerIV.15 3,4
Fujiwara,Y.,S.Okada and N.Aida (1977) Rock Mag.& Paleogephys.4
Momose,K. et al.(1968) Bull.Earthq.Res.Inst. 46 1275-1292
Momose,K and K.Kobayashi (1972) J. Geomag.Geoelectr. 24 1

# ANOMALOUS REMANENT MAGNETIZATION CAUSED BY THUNDERBOLTS FOUND IN OJIMA ANDESITE, FUKUI PREFECTURE

Tadashi NAKAJIMA* and Kimio HIROOKA**

* Geological Laboratory, Faculty of Education, Fukui University, Fukui 910.
** Department of Earth Sciences, Faculty of Science, Toyama University, Toyama 930.

## Introdution

Anomalous strong remanent magnetization of andesite was reported by Sasajima (1954a, b) in a tiny island, Ojima in Fukui Prefecture. The whole island is constituted by andesite which is reversally magnetized. He found very strongly and anomalously magnetized parts in the northeastern corner of the island. It is very easy to find out the parts by using the magnetic compass of which needle rotates by large deflections from the geomagnetic north at the points. Sasajima suggested that this strong magnetization were caused by thunderbolts.

We made intense sampling again intending to make clear the origin and mechanism of the strong remanent magnetization.

## Sampling

Ojima island is located at 36°14'N and 136°07'E, 100 m off the shoreline in the northern coast of Fukui Prefecture, and the area of the island is about 0.2 $km^2$. Ojima Andesite is hypersthene-bearing aphanitic andesite which erupted in the Pliocene age (Miura, 1957). Remarkable columnar and platy joints are found all over the island.

Before making palaeomagnetic sampling, the very points showing strong remanence were detected by using a magnetic compass. We could find two points in the northeastern corner of the island. Topography and sampling localities are shown in Fig. 1. The two points mentioned above are denoted by A and C in the figure. B, D and E in the same figure show the points where the rock was magnetized ordinary intensity of remanence.

The orientating device we used is essentially the same one as described by Hirooka (1971). He designed a plate which has three nails of the same length and it is attached to a magnetic compass. Even rough and irregular surfaced rock can be surely oriented by substituting the plate as a flat surface of the rock. We reform the device for the special use in this study to escape from the influence of the strong magnetization of the rock. In connecting the compass and the three nailed plate, we applied a long arm so that the orientation of compass needle can be read 1 m away from the rock surface.

Together with the palaeomagnetic sampling, the present-day geomagnetic declination were determined by the sun azimuth observation by using a theodolite at the level of 1 m high from the ground surface. The 16 locations numbered in Fig. 1 indicate the sites where the sun observation was carried out. The isogonic map of the island illustrated in Fig. 2. In spite of a small area, the declination changes greatly. The explanation of this fact might be that the geomagnetic field is distorted by the field caused by the remanent magnetization of andesite body.

Fig. 1 Palaeomagnetic sampling sites (A - E) and localities of the observation of the present-day declination (1 - 16).

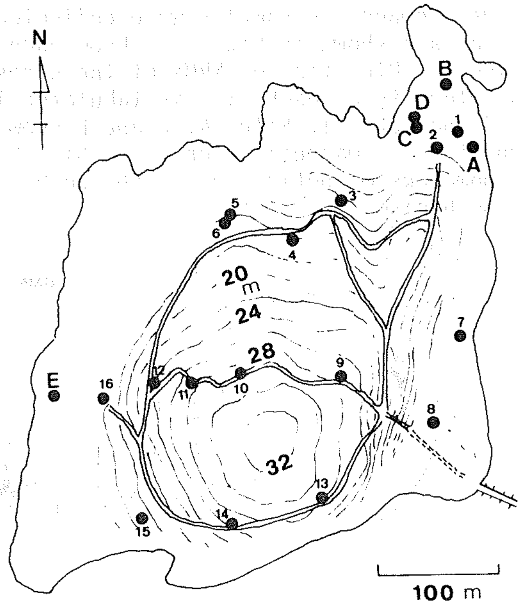


Fig. 2 Isogonic map at Ojima.

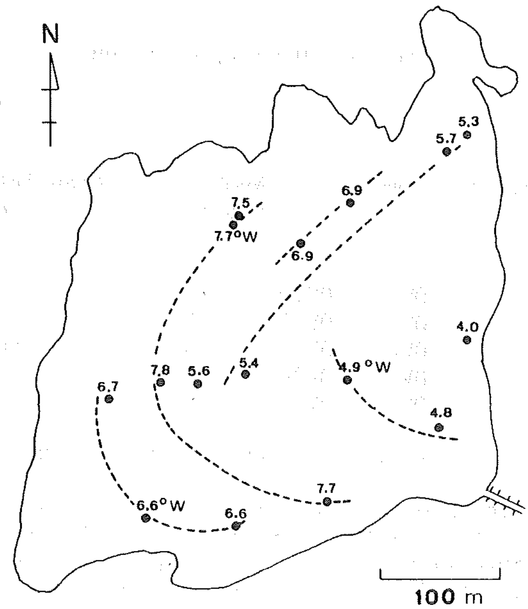

Results of measurement

Palaeomagnetic samples were collected from five sites of A, B, C, D and E as are shown in Fig. 1. From each site, 8 to 15 samples were obtained. Direction of NRMs of the sites is presented in Fig. 3, and mean intensity of each site is tabulated in Table 1. As are seen in Fig. 3 and Table 1, Sites A, C and D show anomalous directions and strong intensities of magnetization. As Site D is neighbouring to Site C, the the anomalous magnetization of the both sites seems to be acquired by the same mechanism.

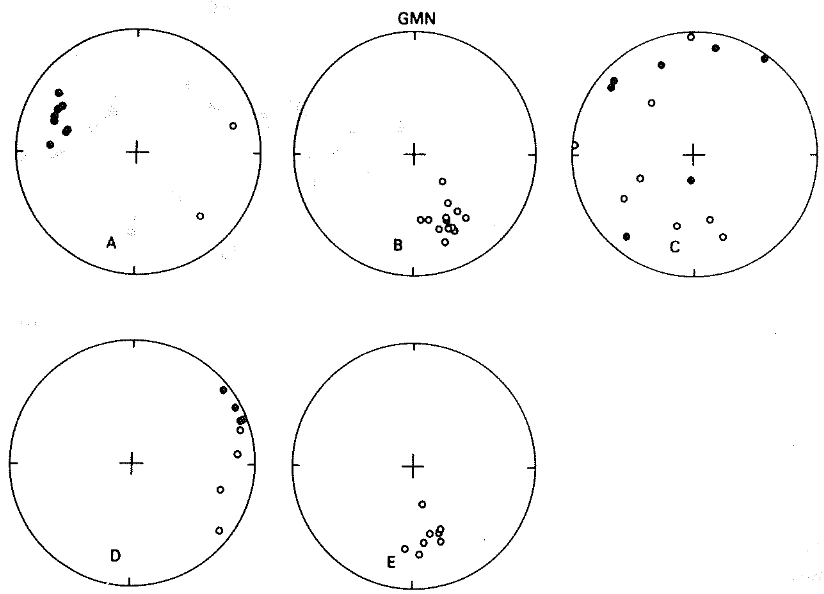


Fig. 3 Direction of NRMs.

| Sampling Site | Samples | Number of Samples | Mean Intensity ( x $10^{-4}$ CGSemu/g) |
|---|---|---|---|
| A | OV 1 - OV10 | 10 | 100.4 |
| B | OV11 - OV23 | 13 | 1.5 |
| C | OV24 - OV38 | 15 | 156.3 |
| D | OV39 - OV46 | 8 | 26.1 |
| E | OV51 - OV58 | 8 | 3.5 |

Table 1 Mean intensity of NRMs.

To know the properties of magnetization of samples obtained from these sites, alternating field (a.f.) demagnetization was applied. The intensity decay by the stepwise demagnetization is shown in Fig. 4. In Fig. 4, (1) and (2) represent the decay curves of samples of Site C, and Sites B and E, respectively. Not only the great difference of the value of intensity but also the pattern of the decay of both sites is distinctly different from each other.

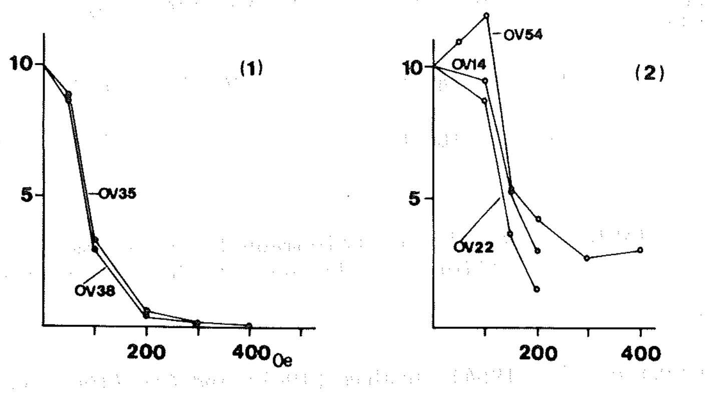


Fig. 4 A.f. demagnetization curves of NRMs.

Location of the individual sample in Sites C and D and its direction of declination are drawn in Fig. 5. The cross mark in the center of Site C indicates the point where the needle of a magnetic compass turned completely opposite direction to the geomagnetic north. The length of arrows in the figure is proportional to the intensity of NRM of samples.

As the palaeomagnetic data of Sites B and E, we adopted the mean declination and inclination after a.f. demagnetization by the step of 100 Oe. These sites are seemed to be representatives of the original magnetization of Ojima andesite body. The results are tabulated in table 2. Although the directions of NRM which were obtained before by Sasajima (1954a) show a big scattering, the mean declination and inclination are almost the same as those of Sites B and E.

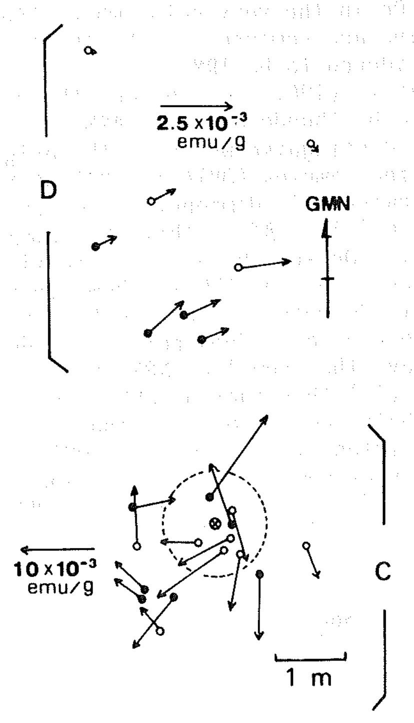


Fig. 5 Location of the individual sample in Sites C and D, and its direction of declination.

| Sampling Site | N | Declination | Inclination | $\alpha_{95}$ | k |
|---|---|---|---|---|---|
| B | 13 | 145.8° E | - 39.5° | 6.7° | 39.7 |
| E | 7 | 167.6° E | - 37.0° | 7.6° | 64.8 |

Table 2 Results of paleomagnetic measurement (after a.f. demagnetization at 100 Oe).

## Discussion

Matsuzaki et al. (1954), Graham (1961) and Cox (1961) reported on the anomalous and strong magnetization of volcanic rocks similar to our case. They concluded that the anomalous remanence was acquired by the strong magnetic field caused by the electric current of thuderbolt. As the strength of the current is $10^4$ - $10^5$ A, the magnetic field reached up to $10^3$ Oe in the very point where lightning strikes. Rocks struck by lightning are remagnetized by the field. The magnetization, therefore, is considered to be IRM.

Nagata (1961) pointed out the possibility that the magnetization produced by thunderbolts is ARM.

To distinguish which is the origin of our anomalous remanence, we magnetized samples (OV14 and 22) of Site B in the steady field of 1,000 Oe. The stepwise a.f. demagnetization curves of IRM of the samples were presented in Fig. 6 (1). After that, the sample OV14 was given ARM in the steady field of 1 Oe and the alternating field of 1,000 Oe. The a.f. demagnetization curve of the ARM is shown in Fig. 6 (2). The behaviours of the intensity decrease of IRM and ARM in Fig. 6 are clearly different. The patern of a.f. demagnetization decay curves (Fig. 4 (1)) of samples which have the anomalous NRM in Site C is more similar to those of IRM (Fig. 6 (1)) than that of ARM (Fig. 6 (2)). Moreover the IRM intensity of the both samples of OV14 and 22 is in the order of $10^{-2}$ emu/g while the ARM intensity of sample of OV14 is only $1.4 \times 10^{-3}$ emu/g. The NRM intensity of samples of Sites A and C is in the same order of IRM of OV14 and 22. From such a property of NRM of Site C, we can conclude that the magnetization is IRM.

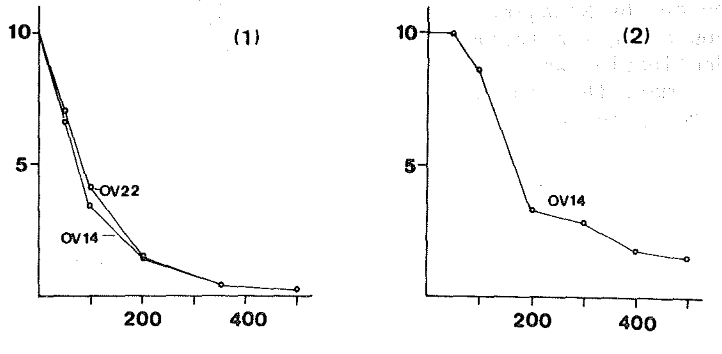


Fig. 6 A.f. demagnetization curves of IRMs and ARM.

If the remanent magnetization were assumed to be IRM originated by thunderbolts, we can reproduce the electric current direction from the direction of remanence. As are clearly seen in Fig. 5, declinations of Sites C and D show NRMs acquired under a circular magnetic field due to line electric current of lightning discharge. Since the declinations of the sites have the clockwise directions surrounding the cross mark in the figure, the current flowed from the cloud to the ground. Usually, at the time of lightning discharge, negative charges descend from the thundercloud. But the thunderstorms in Hokuriku District show unusual occurrence that a great number of lightnings is observed in winter time. More than 80 % of thunderbolts transport positive charges to the ground in the District (Takeuchi et al., 1976). The sense of electric current presumed in this paper agrees with the characteristic features of thunderstorms in Hokuriku.

Providing that a lightning struck the very point of cross mark in Fig. 5, the IRM must decrease its intensity as the distance from the point increases. NRM intensity is plotted against the distance from the point in Fig. 7. The intensity decreases excellently with the distance.

The samples in Site C were devided into two groups. 7 samples

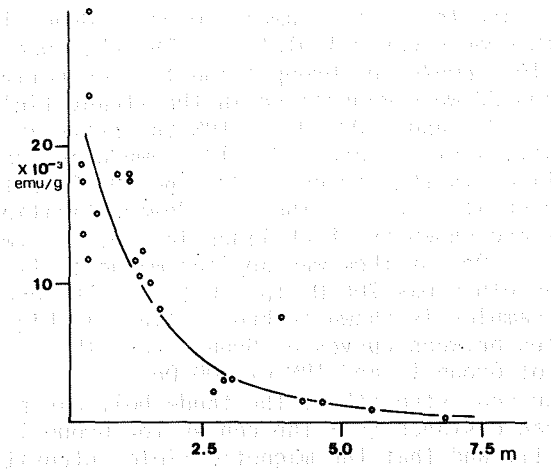


Fig. 7 Intensity of NRM of samples in Sites C and D against the distance from the cross mark in Fig. 5.

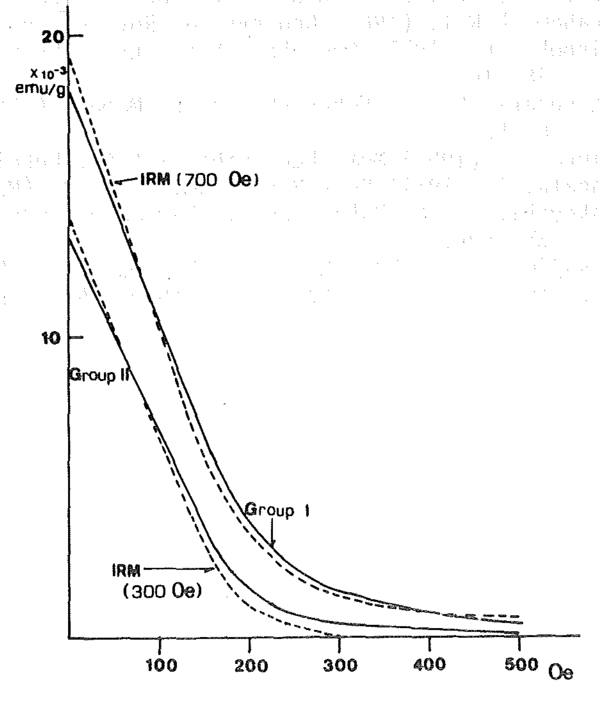


Fig. 8 A.f. demagnetization curves of NRMs and IRMs.

situating within the distance of 75 cm from the lightning center were in Group I and the rest 8 samples were in Group II. The mean NRM intensity of both groups was calculated. The obtained mean intensities are 1.8 and $1.3 \times 10^{-2}$ emu/g for Group I and II, respectively. The two samples of OV14 and 22 were magnetized in the steady field of 200, 400, 600, 800, 1,000, 2,000 and 3,000 Oe. IRM intensity at every steps was measured. Intensities of 1.8 and $1.3 \times 10^{-2}$ emu/g are corresponding to the intensity magnetized in the fields of 700 and 300 Oe estimated from the increasing IRM intensity curve. The a.f. demagnetization decay features of the both groups are shown in thick lines in Fig. 8. Two samples were taken from Site E. One of them was applied magnetic field of 300 Oe to get IRM and the other was 700 Oe for that. The decay of the IRM intensity of these samples is shown in broken lines in Fig. 8. Marvelous fittings are seen between curves of Group I and IRM of 700 Oe and also between those of Group II and IRM of 300 Oe.

Current strength of the thuderbolt can be calculated assuming that the mean distance from the center for Group I is 40 cm and 110 cm for Group II, and that the magnetic field intensity is 700 and 300 Oe at respective distances. From the results of the calculation, the electric current strength is 140 kA for Group I and 165 kA for Group II. The current of this thunderbolt is considered to be about 150 kA. As the mean lightning discharge current in Japan is 26 kA and the maximum is 240 kA, 150 kA is a very reasonable value.

## References


Cox, A. (1961) U. S. Geol. Surv. Bull., 1083-E, 131.

Graham, K.W.T. (1961) Geophys. J. Roy. Astron. Soc., 6, 85.

Hirooka, K. (1971) Mem. Fac. Sci., Kyoto Univ., Ser. Geol. & Mineral., 38, 167.

Matsuzaki, H., K. Kobayashi and K. Momose (1954) J. Geomag. Geoelectr., 6, 53.

Miura, S. (1957) Mem. Fac. Liberal Arts, Fukui Univ., Ser. 2, no. 7, 149.

Nagata, T. (1961) Rock Magnetism, 2 nd ed. (Maruzen, Tokyo), p 144.

Takeuchi, T., M. Nakano and Y. Yamamoto (1976) J. Meteorol. Soc. Japan, 54, 436.

Sasajima, S. (1954a) Mem. Fac. Liberal Arts, Fukui Univ., Ser. 2, no. 3, 79.

Sasajima, S. (1954b) Mem. Fac. Liberal Arts, Fukui Univ., Ser. 2, no. 4, 11.

# CHEMICAL AND ALTERNATIVE MAGNETIC FIELD CLEANING OF HOLOCENE BASALT FROM KASA-YAMA, YAMAGUCHI, JAPAN.

Haruo DOMEN

Institute of Physical Sciences, Faculty of Education, Yamaguchi University, Yamaguchi City, 753 Japan

In the previous paper (Domen, 1978), the present author reported on the natural remanent magnetization (NRM) direction of Holocene basalt come from Kasa-Yama, which stands on the coast of the Sea of Japan at the eastern end of Hagi City, Yamaguchi Prefecture, west Japan. Those NRM data reviewed as follows;

| N | D(E) | I(D) | K | $\alpha_{95\%}$ |
|---|---|---|---|---|
| 14 | -8.7° | +54.1° | 84 | 4° |

Thereafter, not a few of the samples have been collected from the same site and also its vicinity and these NRM have now been under measurement by means of an astatic and a spinner magnetometers successively. Some of them are submitted to the chemical and alternating magnetic field (AF) cleaning.

In this report, a sketch on the experimental study of the cleaning mentioned above is shown.

1) Chemical demagnetization.

The present author previously reported (Domen, 1966, 1967, 1969) on the chemical demagnetization technique performed on a set of three thin plate specimens which were cut out mutually perpendicular to each other from one sample.

In the present study, however, the columnar specimen with 25 mm in both diameter and height cut out from the bulk rock sampl is mostly employed. The previous demagnetization was performed by conc-HCl (12N) as the acidic reagent. And this time, not only conc-HCl but also diluted ones; 6N and 3N either, have been used as the chemical agent.

So far as the obtained results were concerned, the slope of the disintegration of the NRM intensity increased with the increase of the concentration of the reagent. But not so much the change in the NRM direction was recognized even after 10,000 min of chemical etching. Moreover it seems that the conc-HCl is preferable as the concentration of the acidic reagent as well as the previous test.

2) AF demagnetization.

Three different ways of treatments of the AF demagnetization were provided such that;

(1) successive demagnetizations of the same specimen were repeated from low AF intensity up to higher field stepwisely.

(2) several separate specimens come from the single sample were cleaned by the specified peak intensity of the demagnetizing field one by one. Then the RM intensity of each specimen partly cleaned by different AF intensity was normalized by the original NRM intensity and arranged according to the AF intensity.

(3) Performance with different time durations of AF demagnetization.

Every cases of the above-mentioned treatment showed not so much difference each other in the decay mode of NRM intensity so far as AF intensity increased up to 400 Oe in peak value. The directional changes of RM vectors thus demagnetized were rather small. The mean AF intensity for the half decayed of NRM intensity of the test specimens was around 200 Oe. And it seems that the submitted samples were mostly destroyed of their soft component of NRM by the initial stroke of AF, say less than few minutes.

As far as the obtained results mentioned above, by this time are concerned, it seems that the Kasa-Yama Holocene basalt hold rather stable NRM (normally magnetized) and may be used as the paleogeomagnetic fossil.

References.

Domen, H. (1966) Abst. of papers, Rev. Meeting on paleomag. study of circum-Pacific area, U.S.-Japan Sci. Coop., 70.

Domen, H. (1967) Bul. Fac. Educ., Yamaguchi Univ., 16 (Part 2), 25.

Domen, H. (1969) ibid., 18 (Part 2), Special No., 1.

Domen, H. (1978) Rock Mag. Paleogeophys., 5, 47.

# VARIATION OF THE GEOMAGNETIC FIELD INTENSITY DEDUCED FROM ARCHAEOLOGICAL OBJECTS

Hideo SAKAI

Department of Earth Sciences, Faculty of Science, Toyama University, Toyama 930

## 1. Introduction

Thelliers' method has been undertaken on samples from various sites in the world such as France, Czechoslovakia, Bulgaria, U.S.A., Peru, U.S.S.R., and Japan. The variation of the geomagnetic field intensity in archaeological time has thus become gradually clearer.

In this study, the variation of the geomagnetic field intensity was measured by using Thelliers' method. From archaeologicl materials( potteries, tiles, and baked earth), the variation of the geomagnetic field intensity was studied during the last 7,000 years in Japan and in a period from 6,000 B.C. to 0 A.D. in the Middle East.

## 2. Samples

Studies were made on materials collected from Japan and Middle East.

(a) Pottery, baked earths, kamadogu and tiles collected from various parts in Japan.

(b) Pottery collected from the Middle East, mainly from Iran and Iraq.

The ages of the archaeological samples were determined primaly by the archaeological methods. The radiocarbon method and thermolumi-nesence method were also applied.

Table 1 and 2 give the age, collected site and material of the archaeological samples.

## 3. Experimental Apparatus

The apparatus for heating experiment consists of two parts, namely, heating system and shielding sytem of the geomagnetic field. Heating was undertaken in an atmosphere of nitrogen for most samples. Some of the samples were heated in an air. Shielding of the magnetic field was provided by the Helmholtz coiles and $\mu$-metals, so that the magnetic field at the sample position could be shielded near to 50$\gamma$ (equivalent to approximately 1/90 of the geomagnetic field in the labolatory).

## 4. Rejection of insufficiently fired sample

### (a) Application of X-ray analysis

Some of archaeological samples have not experienced high temperatures exceeding the Curie temperatures at their formation. When the samples were not heated adequately by original firing, they usually contained some nonheated part so that the result of Theliers' method becomes considerably erroneous. It is desirable that these samples be rejected prior to the intensity measurements.

There has been no established method to see whether TRM is partial or not. In case of Sue pottery which is believed to have been heated to above 1000°C, X-ray analysis reveals that the samples with unsuccessful results for Thelliers' method contained neither tridymite nor cristobarite. These phases should appear in samples heated above 700°C. (Mitsuji et al., 1976; Sakai., 1978)

(b) Utilization of TRM/ARM (NRM/ARM) ratios

Anhysteric remanent magnetization (ARM) is, similar to TRM, stable against progresive heating (Rimbert, 1945). As the thermal characteristics of ARM are similar to TRM, ARM has been studied in intensity measurements (Banerjee et al.,1974; Stephanson et al., 1974; Shaw, 1974). Stephanson (1974) referred first the f value given by

$$f = arm/trm,$$

where arm and trm are the remanence induced in a unit direct field, respectively.

The f value were calculated from the potteries and tiles of Kinki district. The trm was obtained by diving TRM with the field intensity, which in turn had been determined by Theliers method. Figure 1 shows by the frequency histogram, the f values obtained from the samples on which the intensity measurements were succeeded. The f values of the potteries are in a range 1.5 to 2.0 while those of the tiles are near to 3.0. The f value has been connected to the size of relevant magnetic particles (Levi and Merrill, 1976). In this work, samples which exhibit deviations from straight Jn-Jt line at high temperatures yield f values apart from the above value. The larger value is probably due to the growth of the magnetic particles upon heating in the laboratory from which follows a decreae of TRM. The smaller value is probably caused by the nonheated part of the sample.

The values NRM/ARM of the potteries are similar if the time of the formation of the samples was close, giving a similar value to the geomagnetic field intensities.

Once the f value is determined on a certain sample, this could be applied to other samples formed in a similar condition (basic materials, heating environment, etc.). Samples which were heated insufficiently or attacked by physico-chemical change in laboratory, have f values different from those of satisfactory condition. Therefore, the ratio (TRM/ARM or NRM/ARM) would be a measure for selecting samples for use in Thelliers' method.

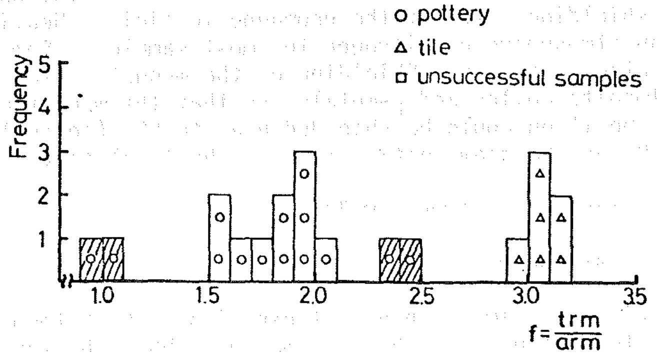


Fig.1. Frequency spectrum of the ratio f obtained from pottery and tile of Kinki district.

## 5. Variation of the Geomagnetic Field Intensity during the Archeological Time

More than 300 samples were submitted to Jn-Jt analysis. Figures 2 and 3 show some typical examples of Jn-Jt diagram. As seen in potteries Sue, fairly straight lines are displayed in the diagram by the samples which are believed to have been formed during the last 2,,000 years. For older potteries such as Jomon and from the Middle East, there appears a slight deviation from the straight line at low temperature region in the diagram.

The geomagnetic field intensities were obtained from the slopes of the straight part of the Jn-Jt diagrams. Data approximately 200 in number were succesfully obtained in this study. Tables 1 and 2 give the intensities for the present samples.

The obtained geomagnetic field intensity for the last 2,000 years is shown in Fig. 4. The results reported by Nagata et al.(1963) and by Sasajima et al. (1966) are also plotted on the same diagram. Although the periodical changes show less agreement, a similar trend in the results between the present work and that of Nagata et al. is found in the change from 1,000 to 1,500 A.D. These diagrams also suggest that the geomagnetic fiel intensities were stronger than that of the present by a factor of 1.3 to 1.5 in Japan.

In Fig.5 , the variations of the field intensity obtained in this study are shown. The geomagnetic field intensity in Japan from 6,000 to 1,000 B.C. was lower than the present value by a factor of about 0.8, excep for that(1.3 times) around 2,000 B.C.. The intensity increased after 1,00 B.C. up to about 1.3 times that of the present around 0 A.D.

The archaeomagnetic field intensity in the Middle East has been scarcely studied. Fig.5 suggests that the field intensity in the Middle East from 6,000 B.C. to 0 A.D. was similar to that in Japan.

## References

Banerjee, S.K. and J.P. Mellema (1974) Earth Planet. Sci. Lett., 23, 177.
Levi, S. and R.T. Merrill (1976) Earth Planet. Sci. Lett., 32, 171.
Mitsuzi, T., S. Hiraga (1976) Suemura I (Report on the Research of the Cultural Properties in Osaka Prefecture), (In Japanese).
Nagata, T., Y. Arai and K. Momose (1963) J. Geomag. Geoelectr., 98, 5277.
Rimbert, K., (1945) Thesis, University of Paris.
Sakai, H., (1978) Suemura III (Report on the Research of the Cultural Properties in Osaka Prefecture), (In Japanese).
Sasajima, S. and K. Maenaka (1966) Mem. Coll. Sci. Univ. Kyoto, 33, 53.
Stephanson, A. and P.W. Collinson (1974) Earth Planet. Sci. Lett., 23, 220.

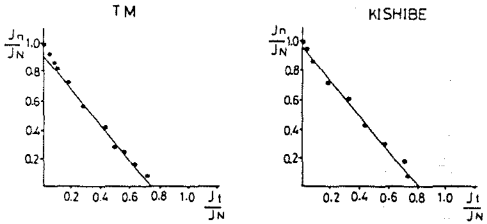


Fig.2. Jn-Jt diagram of the potteries Sue.

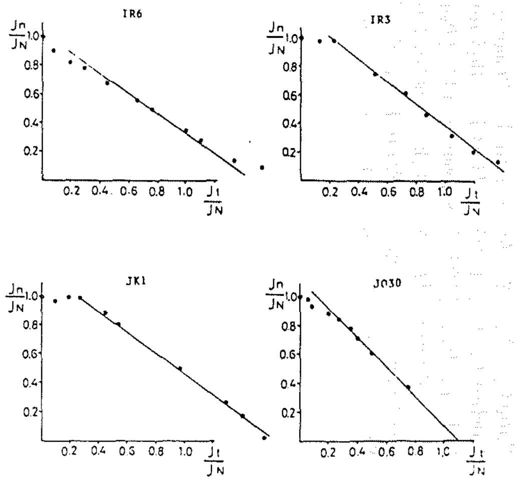


Fig.3. Jn-Jt diagrams of the older samples; upper two are from Iraq potteries and lower two from potteries Jomon.

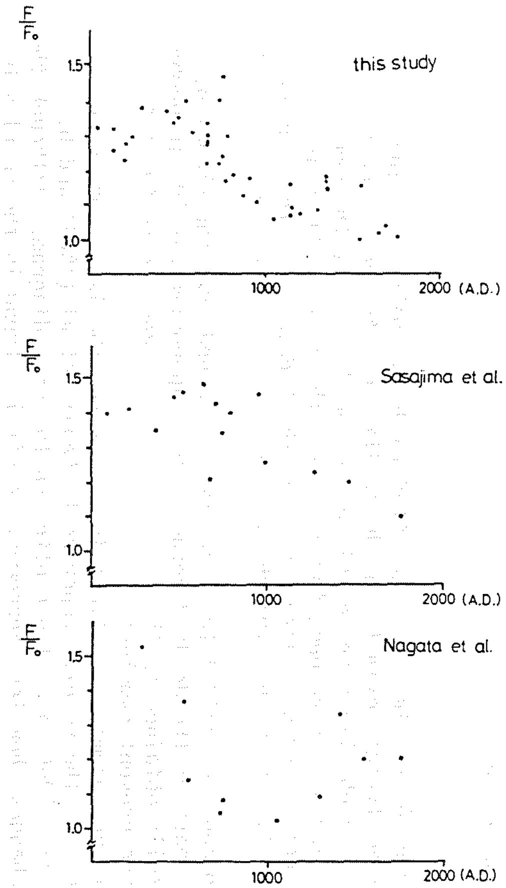


Fig.4. Variation of the geomagnetic field intensity during the last 2,000 years obtained in Japan.

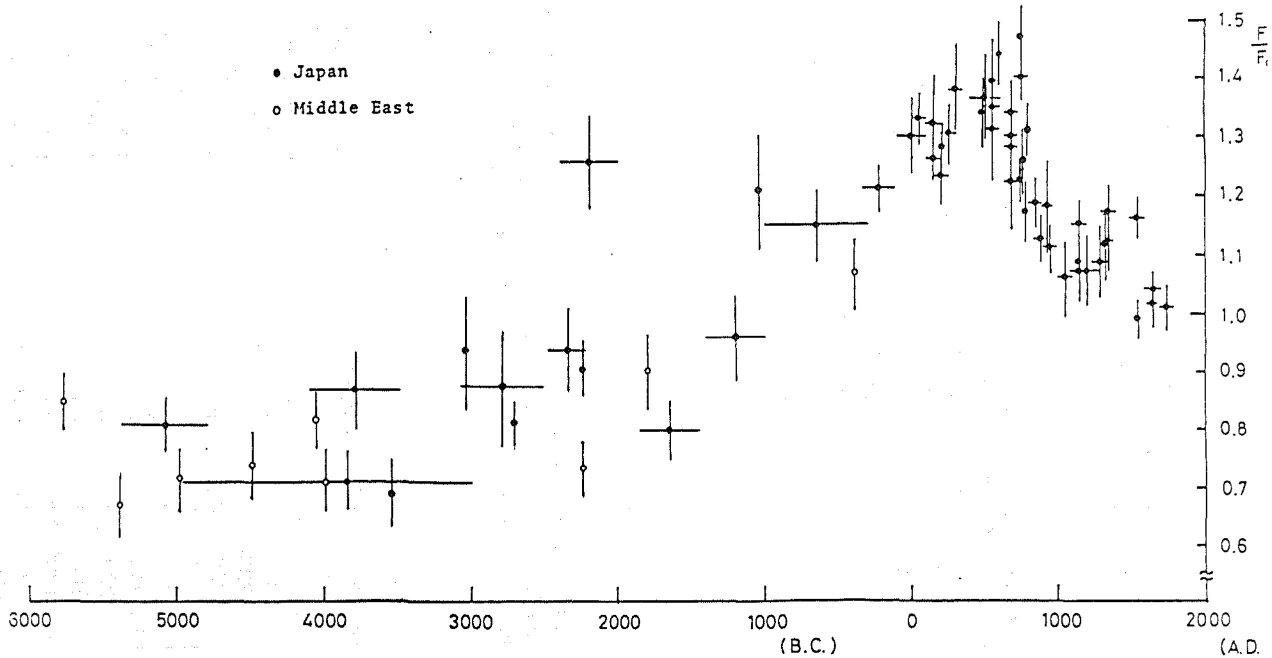


Fig.5. Variation of the geomagnetic field intensity obtained from this study.

Table.1. Data of samples including the estimated age, material, the ancient geomagnetic field intensity and its ratio to that at present; samples collected from Middle East.

| Sample | Locality | Age(B.C.) | Material | Sample No. | F(Oe) | F/Fo |
|---|---|---|---|---|---|---|
| IR5 | IRAN | 5800±600 | pottery | 4 | 0.410±0.027 | 0.921 |
| IR1 | IRAQ | 5410±100 | pottery | 4 | 0.322±0.031 | 0.724 |
| IR6 | IRAQ | 5000 | pottery | 3 | 0.346±0.030 | 0.776 |
| IR7 | IRAQ | 4500 | pottery | 3 | 0.317±0.025 | 0.713 |
| SY | SYLIA | 4000±1000 | pottery | 4 | 0.353±0.024 | 0.794 |
| IR4 | IRAQ | 2250±90 | pottery | 4 | 0.394±0.024 | 0.885 |
| IR8 | IRAQ | 1800 | pottery | 2 | 0.430±0.035 | 0.966 |
| IR9 | IRAQ | 200 | pottery | 2 | 0.507±0.028 | 1.134 |

Table.2. Data of samples including the estimated age, material, the ancient geomagnetic field intensity and its ratio to that at present; samples collected from Japan.

| Sample | Locality | Age(B.C.) | Material | Sample No. | F(Oe) | F/Fo |
|---|---|---|---|---|---|---|
| JO4 | Saitama | 5100±300 | pottery | 2 | 0.373±0.020 | 0.810 |
| JK1 | Tokyo | 3900±300 | pottery | 2 | 0.398±0.020 | 0.865 |
| JY1 | Hiroshima | 3850±115 | pottery | 3 | 0.336±0.022 | 0.715 |
| JK2 | Tokyo | 3550 | pottery | 3 | 0.317±0.026 | 0.690 |
| JO14 | Tokyo | 3050 | pottery | 2 | 0.432±0.045 | 0.939 |
| JO17 | Tokyo | 2800±300 | pottery | 2 | 0.413±0.052 | 0.898 |
| JY2 | Hiroshima | 2710±210 | pottery | 2 | 0.383±0.017 | 0.815 |
| JY3 | Hiroshima | 2350±130 | pottery | 3 | 0.441±0.032 | 0.938 |
| JO23 | Hiroshima | 2350±130 | pottery | 3 | 0.416±0.023 | 0.905 |
| JS1 | Tokyo | 2200±200 | pottery | 4 | 0.580±0.030 | 1.260 |
| JS2 | Tokyo | 1600±200 | pottery | 2 | 0.373±0.026 | 0.798 |
| JO28 | Saitama | 1200±200 | pottery | 2 | 0.452±0.036 | 0.968 |
| JO30 | Tokyo | 1040±130 | pottery | 5 | 0.557±0.058 | 1.210 |
| JN | Nara | 650±350 | pottery | 3 | 0.538±0.029 | 1.151 |
| JY4 | Hiroshima | 230±10 | pottery | 3 | 0.567±0.019 | 1.207 |
| JM | Osaka | 50±50 | pottery | 3 | 0.607±0.032 | 1.299 |

Table.2. continued.

| Sample | Locality | Age(A.D.) | Material | Sample No. | F(Oe) | F/Fo |
|---|---|---|---|---|---|---|
| KM1 | Osaka | 1c | pottery | 3 | 0.623±0.021 | 1.334 |
| KF | Osaka | 2c | pottery | 3 | 0.616±0.004 | 1.320 |
| NK1 | Nara | 2c | pottery | 2 | 0.589±0.020 | 1.260 |
| KM2 | Osaka | 2c | pottery | 2 | 0.577±0.023 | 1.234 |
| YS1 | Hiroshima | 210 | pottery | 3 | 0.598±0.021 | 1.280 |
| NK2 | Nara | 3c | pottery | 4 | 0.609±0.025 | 1.304 |
| KM4 | Osaka | Late 3c | pottery | 2 | 0.577±0.023 | 1.234 |
| AM | Osaka | 300±35 | pottery | 4 | 0.643±0.037 | 1.380 |
| MT84 | Osaka | 490±10 | pottery | 2 | 0.626±0.028 | 1.340 |
| WT | Wakayama | 5c | tile | 3 | 0.640±0.035 | 1.367 |
| SRIV-2A | Wakayama | Early 6C | baked earth | 2 | 0.630±0.026 | 1.350 |
| TM | Osaka | 6c | pottery | 3 | 0.652±0.031 | 1.397 |
| SR-III | Wakayama | Late 6c | baked earth | 3 | 0.614±0.041 | 1.313 |
| KM3 | Osaka | 610±10 | pottery | 3 | 0.678±0.030 | 1.440 |
| TH | Nara | Late 7c | tile | 4 | 0.568±0.035 | 1.220 |
| NM1 | Nara | Late 7c | tile | 2 | 0.607±0.020 | 1.300 |
| NK2 | Nara | Lata 7C | tile | 3 | 0.599±0.019 | 1,280 |
| NK4 | Nara | Late 7c | tile | 2 | 0.587±0.035 | 1.151 |
| NY | Nara | Late 7c | tile | 4 | 0.625±0.025 | 1.340 |
| NM2 | Osaka | 8c | tile | 3 | 0.572±0.017 | 1.224 |
| TK230 | Osaka | 8c | pottery | 2 | 0.654±0.019 | 1.400 |
| TK57 | Osaka | 760±10 | pottery | 3 | 0.589±0.026 | 1.260 |
| KM38-II | Osaka | 770±10 | pottery | 4 | 0.686±0.023 | 1.471 |
| KM22 | Osaka | 780±10 | pottery | 3 | 0.546±0.023 | 1.172 |
| KISHIBE | Osaka | 790±10 | pottery | 2 | 0.613±0.030 | 1.315 |
| SR56 | Wakayama | Early 9c | baked earth | 3 | 0.555±0.017 | 1.189 |
| MT200-I | Osaka | 875±25 | pottery | 4 | 0.526±0.020 | 1.126 |
| TK314 | Osaka | 925±25 | pottery | 3 | 0.551±0.037 | 1.180 |
| NH3 | Osaka | 10c | pottery | 3 | 0.517±0.018 | 1,107 |
| NH5 | Osaka | 11c | pottery | 3 | 0.494±0.029 | 1.058 |
| MK3 | Osaka | 12c | pottery | 2 | 0.542±0.021 | 1.160 |
| NH4 | Osaka | 12c | pottery | 3 | 0.498±0.026 | 1.067 |
| NH7 | Osaka | 12c | pottery | 3 | 0.508±0.017 | 1.090 |
| NH1 | Osaka | 1200±100 | pottery | 4 | 0.501±0.028 | 1.072 |
| IW | Nara | 1300±50 | pottery | 3 | 0.506±0.029 | 1.084 |
| NH2 | Osaka | 14c | pottery | 3 | 0.522±0.022 | 1.118 |
| MOZU | Osaka | 1350±50 | pottery | 3 | 0.548±0.024 | 1.173 |
| BI3 | Osaka | 14c | baked earth | 4 | 0.521±0.027 | 1.115 |
| JR3 | Gifu | 1550±30 | baked earth | 3 | 0.462±0.017 | 0.990 |
| TK3 | Osaka | 16c | tile | 2 | 0.542±0.016 | 1.160 |
| HA | Yamaguchi | Late 17c | kamadogu | 3 | 0.487±0.014 | 1.037 |
| SU | Saga | Late 17c | kamadogu | 3 | 0.478±0.019 | 1.016 |
| KN | Gifu | 1760±50 | baked earth | 3 | 0.470±0.017 | 1.010 |

PALEOMAGNETISM OF FLOWSTONE COLLECTED AT GUJO-HACHIMAN

Hiroo INOKUCHI, Hayao MORINAGA and Katsumi YASKAWA

Department of Earth Sciences, Faculty of Science,
Kobe University, Nada, Kobe 657 (Japan)

## Introduction

It is well-known fact that usually there exist net works of innumerable caves developed or still being developed by underground streams in the area widely covered by massive limestone. Most enterable caves, however, seamed to grow larger because of the lowering of the water table, and instead they are suffering decrease in size from the secondary deposition of calcium carbonate in the form of stalactites on the ceiling, draperies and curtains on the walls and stalagmite on the floor. The stalagmites growing broader, flatter cones on a cave floor which generally grade outward into a sheet of secondary limestone are known as cave travertine or more specially as flowstone. The growing rate of these cave deposits of secondary lime are different by the circumstancial condition i.e. somewhat between 0.1 mm/yr and 0.01 mm/yr.

Recently we found that some of these secondary deposits of lime is carrying weak but considerably stable remanent magnetization of the order of $10^{-6}$ to $10^{-7}$ emu/cc. Since these cave deposits are gradually growing year by year, the past geomagnetic field variation must be recorded continuously in the sequence of thin films of secondary lime from inner side to outer side, although the magnetic minerals have not been analysed yet because their quantities are too little and their size seems too small to separate them from calsite. The purpose of this paper is to show the result of paleomagnetic measurement of a piece of flowstone collected from a cave at Gujo-Hachiman, Gifu, Central Japan.

## Measurements

The sample used in the paleomagnetic study was quarried out perpendicularly to a flowstone layers in the shape of square prism having a side of about 3 cm and a length of about 18 cm in an attempt at analysis of carbon isotope by N. Nakai and his colleagues of Nagoya University.

All the measurements of natural remanent magnetization (NRM) were carried out using a SCT superconducting rock magnetometer. At first, as shown in the right of Fig. 1, we measured the NRM of specimens of the flowstone in the shape of thin disk of 1/2" diameter and about 5 mm thick. They were cored from the thin sections sliced perpendic-

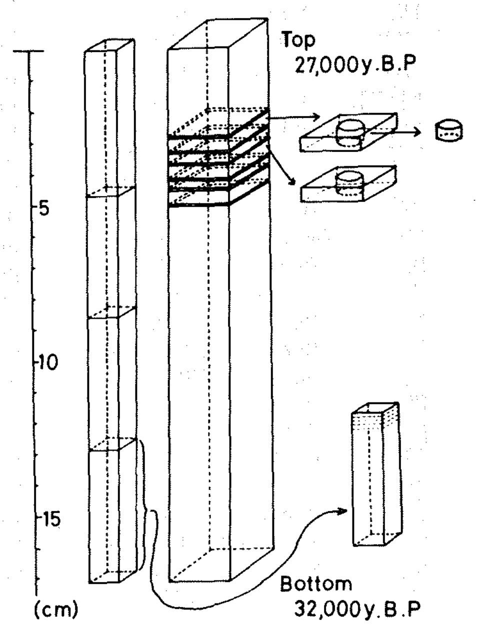


Fig. 1. Schematic view of specimens, the right shows those for "off-and-on" measurement and the left those for "continuous" measurement.

ularly to the axis of the right square prism of the flowstone sample mentioned above. These results are plotted in Fig. 2. The measurement of this kind of specimen, however, has fatal defect that the considerable quantity of flowstone materials is always wasted between adjacent specimens by the thickness of diamond brade. In our case this was about 2 mm or more, corresponding to several hundred years.

In order to avoid wasting the sample material and making time gaps, we also tried a different method of measurement from that mentioned above. The measurements of NRM of each layer in this case were carried out in following way : Four right square prisms of 1 $cm^2$ and 4.5 cm long were made of the original flowstone sample (the left in Fig. 1). Their axis are perpendicular to the flowstone layers and all the layers in the flowstone sample are covered with these four prisms except for three gaps between the lower and the upper ends of adjacent prisms. The reason why we did not use a single right square prism of 18 cm long or why we divided it into four pieces of 4.5 cm long is that uniform sensitivity-limit of the sensor coil in our cryogenic magnetometer is 5 cm. After measuring three components of NRM of the prism, it was scraped off by 1 mm at the top and the three components of its NRM were remeasured. The subtraction vector of the latter from the former is to be the NRM of the layer scraped off from the specimen. Repeating this operation until there remained a thin bottom layer of only 1 mm thick in the prism specimen, we could obtaine the NRM informations over whole sequence of layers in the prism without any time

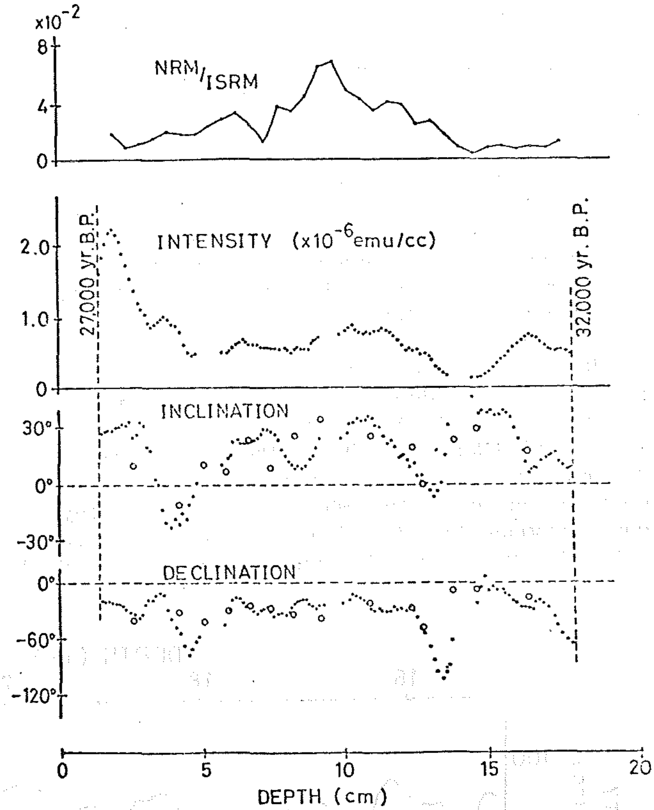


Fig. 2. Intensity and direction of magnetization as functions of depth from the surface of flowstone-sample. Each dot shows seven-points moving average of the virginal values of the magnetic measurements in the direction perpendicular to the flowstone surface. The depth variation of the intensity of natural remanent magnetization (NRM) v.s. that of saturation remanent magnetization (ISRM) is also shown. Each open circle shows the virginal value from "off-and-on" magnetic measurement. The values of inclination were given as the angle between magntization and the surface of flowstone sample, so that zero in the figure does not mean the horizontal surface. The declination in the figure is the relative value between each point, so that zero does not have any meaning at all.

gaps. In the same way as in the measurment of NRM, the values of SIRM intensity were also determined. Spacimens were placed in the uniform field of $3x10^3$ Oe to acquier SIRM and the intensity ratio of NRM to SIRM was calculated for each layer.

## Results and Discussions

All the results are shown in Fig. 2. It is clearly shown in this Figure that the results in both cases mentioned in the preceding section coincide each other. The original sample was collected with the purpose of carbon isotope analysis as mentioned already, and therefore it was oriented neither azimuthally nor zenithally in situ. Considering the fact that usually the layers in flowstone are not horizontal but rather parallel to its basal surface, it is clear that the declination and inclination of NRM do not correspond directly to those of geomagnetic field in the period of the deposition of this sample. The period is determined by $^{14}C$ method as 27,000 yr B.P. for the upper end and 32,000 yr B.P. for the lower end (Nakai, 1979). Thus, both the declination and the inclination of magnetization of this sample shoud be required certain uniform corrections over the whole sequence of layers of the sample to infer the past geomagnetic field variation. In order to know whether the result actually reflects the past geomagnetic field variation, the following

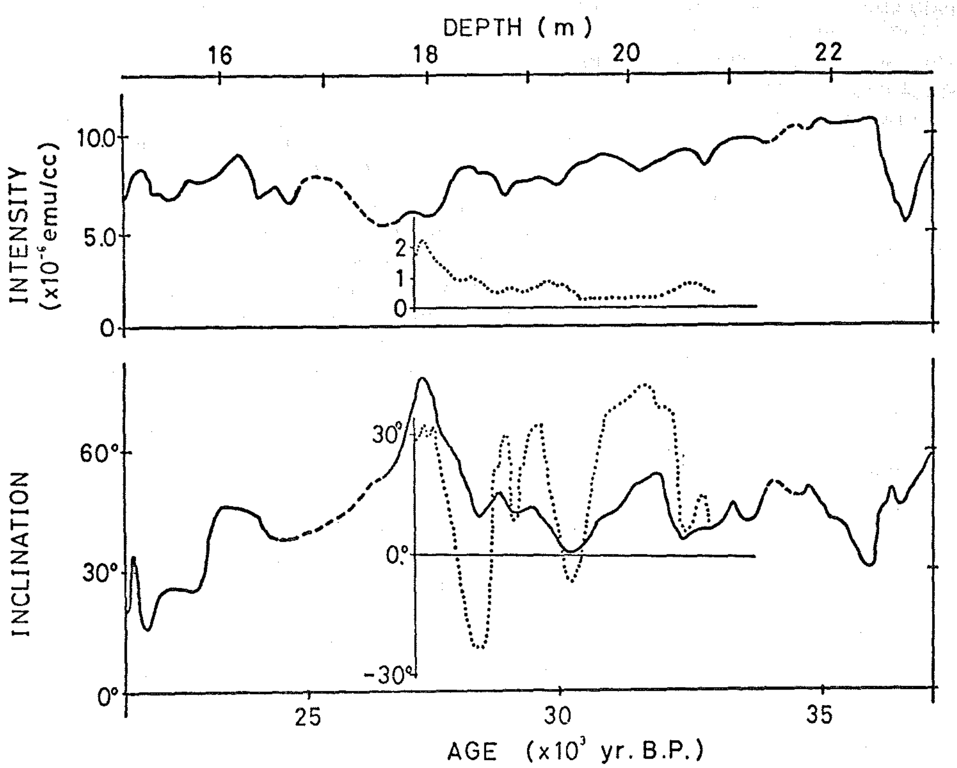


Fig. 3. Intensity and inclination v.s. age relations in the 200 m core sample from Lake Biwa (after Yaskawa et al., 1973) in which those in the cave deposit are also plotted in consideration of the errors in both datations of the core and the cave deposit. The ages of the core were determined by $^{14}C$ and fission track method and those of the cave deposit were by $^{14}C$ method.

comparison was taken place. Fig. 3 shows the inclination- and intensity-variation of NRM of sediments cored from the bottom of Lake Biwa (Yaskawa et al., 1973). The datation of this sediments was given by $^{14}C$ for the upper 10 m and for the rest by fission track method using zircons separated from several tuff layers lying in the sediments. The results of present study are also plotted in Fig. 3 in consideration of the errors in both datations of the lime and the core and the ignorance about tilting angle of the flowstone layers. The curves from the core and the lime seem to be neither excellent nor bad in fitting each other. However, preliminarily it looks enough to say that the secondary deposits of limestone keep the record of the past geomagnetic field variation.

Taking the fact into consideration that the age determination by $^{14}C$ method is rather easy at any parts of the secondary deposit of calcium cabonate in the limstone cave, the magnetic investgation of these secondary cave deposits, i.e. stalactite, stalagmite or flowstone, may become important to know the geomagnetic secular variation during the past several ten-thousands of years and also in the remote-past duration covered over several ten-thousand years, considering the fact that there are various secondary deposits of lime, e.g. stalactite etc., in the world, i.e. some had already finished its growth more than a hundred-thousand years before but some are still growing. The investigation concerning magnetic minerals carrying NRM of the stalactite etc. and the further investigation with the samples orientated correctly in the cave by ourselves are now in progress.

## References

Nakai, N. (1979) personal communication.

Yaskawa, K., T. Nakajima, N. Kawai, M. Torii, N. Natsuhara and S. Horie (1973) J. Geomag. Geoelectr., 25, 447.

(Submitted to J. Geomag. Geoelectr.)

PALEOMAGNETIC STUDY OF SECULAR VARIATION IN JAPAN
DURING THE LAST 40,000 YEARS

Kohsuke HEKI

Geophysical Institute, University of Tokyo
Bunkyo-ku, Tokyo 113.

## 1. Introduction

The variation of geomagnetic field has a spectrum ranging from seconds to millions of years. What we call secular variation is a slow change in intensity and/or direction of the field with periods between 10 and $10^4$ years. It is worth while investigating ancient geomagnetic secular variation (paleosecular variation, PSV) with a purpose of understanding the character or the source mechanism of the geomagnetic field.

In order to measure PSV with paleomagnetic methods, first, we obtain a set of spot readings of ancient geomagnetic field which has the time span long enough to cover the maximum period of secular variation but not too long to be disturbed by the effects of tectonic movements. For example, we usually use the natural remanent magnetization (NRM) of successive lava flows of a stratovolcano such as the volcanoes in Hawaii Islands. To get statistical reliability, it is said that more than a certain number of the measurements of independent flows are needed, that is, 10 should be the minimum number of flows (Creer and Sanver, 1970; Brock, 1971; Bringham and Stone, 1972) or 15 flows are needed (Watkins et al., 1972). Baag and Helsley (1974) state that 30 flows are necessary if we analyze the shape of direction data set.

After collecting these field direction data, we commonly transform them into the virtual geomagnetic poles (VGP) assuming that the source of the geomagnetic field is an axial geocentric dipole. When we have a number of VGPs, the angular variance around the mean VGP is calculated as follows; let $D_i$ be the angle between the mean VGP and the ith VGP, and let N be the total number of VGPs, then the best estimate of the angular variance of the VGPs is

$$S^2 = (N - 1)^{-1} \sum_i D_i^2 \qquad (1)$$

According to the geocentric axial dipole hypothesis, if the time span is relevant and the number of data points are sufficiently large, the mean VGP falls in the close vicinity of the geographic pole. So if we use $\Delta_i$ which is the angle between the geographic pole and the ith VGP, instead of $D_i$, the angular variance is

$$S^2 = N^{-1} \sum_i \Delta_i^2 \qquad (2)$$

The angular standard deviation is the square root of the angular variance.

Several models about the origin of the PSV have been presented. Today, it is most commonly believed that the cause of PSV lies both in the drifting and/or fluctuation of the non-dipole field and in the random wobbling motion of the dipole (Cox, 1962, 1970). This model predicts a certain latitude dependence of the angular standard deviation of VGPs. The angular standard deviation calculated using equation (2) from the paleomagnetic data obtained in different sites over the world show a

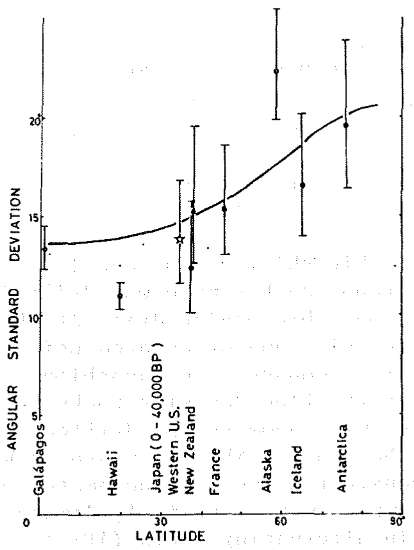


Fig. 1. Angular standard deviation of VGPs from the geographic pole. Error bars show 95% confidence intervals. Except the Japanese data, the figure is redrawn from Doell & Cox (1972). Solid curve is the total angular standard deviation.

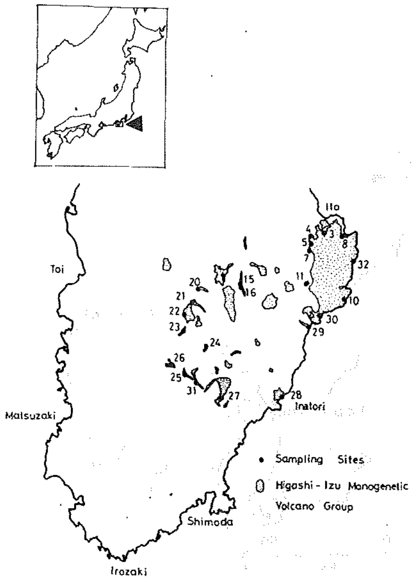


Fig. 2. Sampling sites in Higashi-Izu monogenetic volcano group. The names of these volcanoes are shown in Table 1.

latitude dependence consistent with this model (Fig. 1). As may be recognized at a glance, the angular standard deviation in Hawaii is anomalously small. Doell and Cox (1972) hypothesized that in the Central Pacific region, non-dipole field may be subdued due to some unclarified mechanisms (Pacific dipole window hypothesis). For Japanese region, Ozima and Aoki (1971) also reported a very small angular standard deviation obtained from the archeomagnetic data of the last 9,500 years compiled by Kinoshita (1970). The interpretation of this quiet secular variation data in Japan and the re-calculation of PSV using the new paleomagnetic data is the principal aim of this research.

## 2. Sampling sites

Sampling sites are divided into two regions, one the Higahsi-Izu monogenetic volcano group in Izu Peninsula and the other pyroclastic flow deposits around Kagoshima Bay. Both formations are of Holocene and latest Pleistocene ages, and the geology and the stratigraphy of these rocks are well investigated by Aramaki and Hamuro (1977), Hamuro (1978), Aramaki (1969), and others. Higashi-Izu monogenetic volcano group consists of about 70 monogenetic volcanoes scattered over an area of more than 400 $km^2$ in the middle and eastern part of Izu Peninsula, from which 22 lava flows were sampled (Fig. 2). From Kagoshima pyroclastic flow deposits, 5 pyroclastic flows and 1 lava flow were sampled (Fig. 3). The ages of these

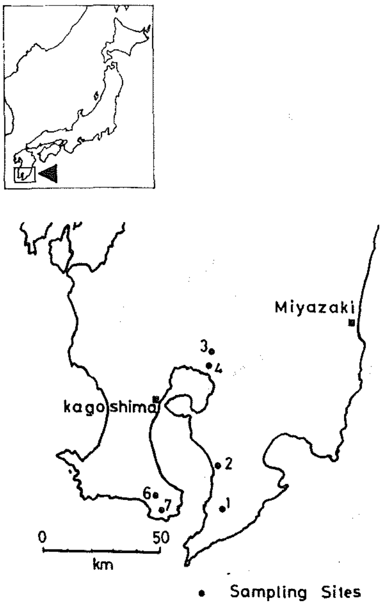


Fig. 3. Sampling sites in Kagoshima pyroclastic flow deposits. The names of these flows are shown in Table 1.

rocks are not determined radiometrically but from geological and stratigraphical study, they are considered to have erupted during the last 40,000 years. The names of these volcanoes and pyroclastic flows are tabulated in Table 1.

3. Experimental procedure and paleomagnetic results

In Higashi-Izu monogenetic volcano group, each sample was drilled with a portable engine drill at the sampling site and orientated using a Brunton compass. In Kagoshima pyroclastic flow deposits rocks were sampled with hammers and drilled at the laboratory. NRM was measured with a Schonstedt spinner magnetometer and all samples were stepwisely demagnetized in alternating field (AF). These samples showed good within-site precision parameter (Fisher, 1953), and the direction of remanent magnetization was very stable against AF-demagnetization. Ancient geomagnetic field direction was taken to be the same as the remanent magnetization which had the maximum precision

Table 1. The names of volcanoes and pyroclastic flows.

| site | name | site | name |
|---|---|---|---|
| HI- 3 | Joboshi | HI-25 | Numanokawa-1 |
| HI- 4 | Kadono-1 | HI-26 | Numanokawa-2 |
| HI- 5 | Kadono-2 | HI-27 | Hachiyama |
| HI- 7 | Omuroyama-1 | HI-28 | Inatori-2 |
| HI- 8 | Komuroyama | HI-29 | Akakubo |
| HI-10 | Omuroyama-2 | HI-30 | Iyuzan |
| HI-11 | Dainoyama | HI-31 | Noboriominami |
| HI-15 | Jizodo-3 | HI-32 | Chikubo-gairinzan |
| HI-16 | Jizodo-2 | KS- 1 | Tashiro |
| HI-20 | Nagano | KS- 2 | Ata |
| HI-21 | Yoichizaka | KS- 3 | Ito |
| HI-22 | Hachikuboyama | KS- 4 | Iwato |
| HI-23 | Hontanigawa-shiryu | KS- 6 | Ikeda |
| HI-24 | Haccho-rindo | KS- 7 | no name |

Table 2. Results of paleomagnetic measurements

| Site | N | Incl. | Decl. | k | VGP lat. | VGP long. | ODF |
|---|---|---|---|---|---|---|---|
| HI- 3 | 7 | 52.7° | -12.9° | 520 | 79.2° | 43.9° | 25oe |
| HI- 4 | 7 | 73.2 | 41.8 | 240 | 53.7 | 174.7 | 150 |
| HI- 5 | 7 | 68.5 | 28.6 | 370 | 63.5 | 180.7 | 150 |
| HI- 7 | 6 | 44.3 | 7.5 | 382 | 79.0 | 281.2 | 400 |
| HI- 8 | 7 | 67.9 | 19.3 | 709 | 68.8 | 174.3 | 150 |
| HI-10 | 7 | 48.2 | 0.7 | 3127 | 84.3 | 313.0 | 0 |
| HI-11 | 6 | 65.8 | 23.9 | 461 | 67.9 | 185.2 | 100 |
| HI-15 | 7 | 35.4 | -3.3 | 278 | 74.4 | 330.6 | 50 |
| HI-16 | 7 | 33.2 | -3.5 | 519 | 73.0 | 330.4 | 150 |
| HI-20 | 7 | 55.6 | 11.3 | 168 | 80.7 | 217.9 | 50 |
| HI-21 | 7 | 60.2 | 16.8 | 163 | 75.4 | 198.6 | 400 |
| HI-22 | 7 | 53.4 | 0.0 | 218 | 89.1 | 318.9 | 100 |
| HI-23 | 6 | 53.5 | -2.6 | 467 | 87.7 | 29.6 | 100 |
| HI-24 | 7 | 55.8 | -1.2 | 291 | 88.2 | 106.7 | 50 |
| HI-25 | 7 | 56.5 | -0.3 | 2164 | 87.7 | 132.9 | 100 |
| HI-26 | 7 | 59.5 | -17.7 | 396 | 75.0 | 75.6 | 100 |
| HI-27 | 7 | 55.9 | 0.5 | 768 | 88.3 | 152.5 | 100 |
| HI-28 | 6 | 55.6 | 16.5 | 737 | 76.5 | 218.5 | 100 |
| HI-29 | 7 | 57.0 | 18.3 | 261 | 75.0 | 213.2 | 150 |
| HI-30 | 7 | 39.2 | -8.3 | 800 | 75.4 | 351.1 | 100 |
| HI-31 | 7 | 48.9 | -9.0 | 181 | 80.9 | 18.2 | 0 |
| HI-32 | 7 | 60.0 | 10.0 | 501 | 80.1 | 189.1 | 150 |
| | | | | | | | |
| KS- 1 | 7 | 34.1 | -7.2 | 292 | 75.9 | 340.0 | 50 |
| KS- 2 | 7 | 31.8 | -1.6 | 861 | 75.8 | 317.1 | 100 |
| KS- 3 | 7 | 43.5 | 4.8 | 100 | 82.3 | 276.2 | 100 |
| KS- 4 | 4 | 49.6 | 0.0 | 98.5 | 88.7 | 306.8 | 10 |
| KS- 6 | 6 | 51.5 | -3.3 | 94.1 | 87.0 | 60.1 | 400 |
| KS- 7 | 7 | 53.8 | 6.0 | 210 | 84.1 | 187.1 | 600 |

N: Number of samples, Incl.: inclination, Decl.: declination, k: Fisher's precision parameter, VGP lat.: VGP latitude, VGP long.: VGP longitude, ODF: optimum demagnetizing field.

parameter in the process of stepwise AF-demagnetization. All the results are tabulated in Table 2.

Site mean directions projected on the Schmidt net (Fig. 4) show a rather wide spread around the axial dipole field direction with a slight elongation in the north-south direction. This direction data set was

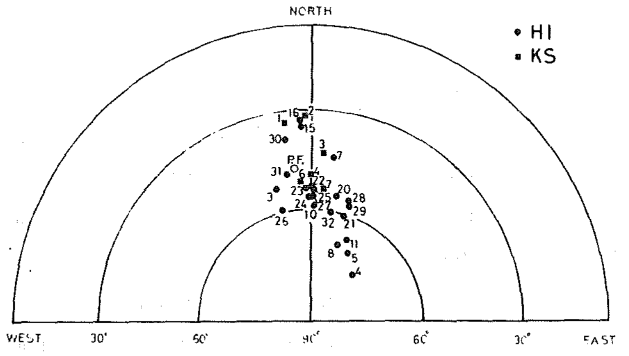


Fig. 4. Average direction of remanent magnetization for each site. The open circle shows the direction of present field direction at the sampling site. Solid circles and squares show Higashi-Izu monogenetic volcano group and Kagoshima pyroclastic flow deposits respectively.

converted to a set of virtual geomagnetic poles (Fig. 5), and the angular standard deviation was calculated using equation (2). Let the total angular standard deviation be $S_t$, then

$$S_t^2 = S_b^2 + S_w^2/N \qquad (3)$$

where $S_b$ is the between-site dispersion which is the real angular standard deviation of paleomagnetic poles and $S_w$ is the within-site dispersion which is noise for the purpose of this study. N is the number of samples measured in one site. As shown in Table 2, Fisher's precision parameter is large for almost the all sites, making corresponding within-site dispersion ($S_w = 81/\sqrt{k}$ degrees) very small. Therefore the second term in equation (3) is small and the total angular standard deviation does not change markedly after this correction. 95% confidence limit of angular standard deviation was calculated by interpolation from the table presented by Cox (1969). Statistical results are tabulated in Table 3.

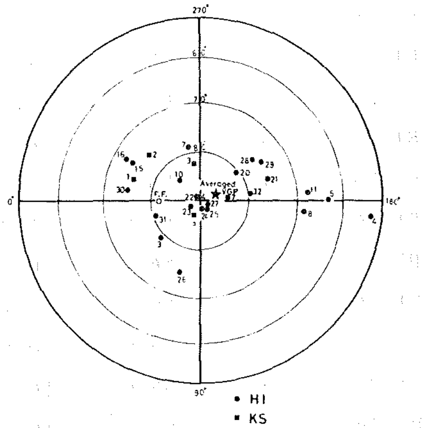


Fig. 5. Calculated VGP for each site. The asterisk indicates the position of the average VGP, and the open circle is the VGP corresponding to the present field direction. Solid circles and the squares are the VGPs from Higashi-Izu monogenetic volcano group and Kagoshima pyroclastic flow deposits respectively.

Table 3. Statistical results of VGPs

| av.VGP lat. | av.VGP long. | N | k | $S_b$ | $S_u$ | $S_l$ |
|---|---|---|---|---|---|---|
| 87.3° | 220.4° | 29 | 34.2 | 13.9° | 16.9° | 11.7° |

av.VGP lat.: averaged VGP latitude, av.VGP long.: averaged VGP longitude, N: Number of VGPs, k: Fisher's precision parameter, $S_b$: between-site angular standard deviation, $S_u$: upper limit of 95% confidence interval of $S_b$, $S_l$: lower limit of 95% confidence interval of $S_b$.

## 4. Discussion

In a former PSV study in Japan, Ozima and Aoki (1972) obtained an angular standard deviation of 10.3° with a 95% confidence interval of 12.6° to 8.7° from 28 VGPs between 0 and 9,500 y.B.P., indicating that secular variation was fairly quiet in Japan during that period. Whether this phenomenon is an areal feature as is hypothesized in the Central Pacific region or long term time characteristic remains a most interesting problem.

Later, Baag (1974) criticized that this small angular standard deviation might be due only to the insufficiency of the total time span. He pointed out from the results of the shape analysis of Japanese archeomagnetic data that the time span of 9,500 years is less than the period of dipole wobble and too short to provide an adequate estimate of total secular variation. The time span of 40,000 years in this research is four times longer than Japanese archeomagnetic data, and seems to be enough to cover the period of dipole wobble. This is inferred from the position of the average VGP which deviates from the present geographic pole by only 2.7 degrees (Table 3). Angular standard deviation of 13.9° with confidence limits of 16.9° and 11.7° is quite consistent with the worldwide trend summerized by Doell and Cox (1972)(Fig. 1). Solid curve in Fig. 1 is the total angular standard deviation supposing that the amplitude of dipole wobble is 11.5° and the non-dipole field was estimated from IGRF 1965. The angular standard deviation of 13.9° obtained from the present study indicates that the quiet secular variation reported by Ozima and Aoki (1972) is not due to spacial characteristics nor the world-wide time characteristics which last more than a few ten thousands of years, but rather due to the insufficiency of the time span covered by archeomagnetic samples.

## References


Aramaki, S. (1969) J. Geol. Soc. Japan, 75, 425 (in Japanese).

Aramaki, S. and K. Hamuro (1977) Bull. Earthq. Res. Inst., 52, 235 (in Japanese).

Baag, C. (1974) J. Geomag. Geoelectr., 26, 83.

Baag, C. and C.B. Helsley (1974) J. Geophys. Res., 79, 4923.

Bringham, D.K. and D.B. Stone (1972) Geophys. J. R. astr. Soc., 28, 337.

Brock, A. (1971) Geophys. J. R. astr. Soc., 24, 303.

Cox, A. (1962) J. Geomag. Geoelectr., 13, 101.

Cox, A. (1969) Geophys. J. R. astr. Soc., 18, 545.

Cox, A. (1970) Geophys. J. R. astr. Soc., 20, 253.

Creer, K.M. and M. Sanver (1970) Paleogeophysics, edited by S.K. Runcorn, (Academic, New York) p. 91.

Doell, R.R. and A. Cox (1972) Nature of the Solid Earth (McGraw-Hill, New York) p. 245.

Fisher, R.A. (1953) Proc. R. Soc. London, Ser. A, 217, 295.

Hamuro, K. (1978) J. Geol. Soc. Japan, 84, 433 (in Japanese).

Kinoshita, H. (1970) J. Geomag. Geoelectr., 22, 507.

Ozima, M. and Y. Aoki (1972) J. Geomag. Geoelectr., 24, 471.

Watkins, N.D., A. Hajash and C.E. Abranson (1972) Geophys. J. R. astr. Soc., 28, 1.

## PALAEOMAGNETIC CORRELATION OF THE LATE PLEISTOCENE TEPHRA SEDIMENTS IN JAPAN

Kimio HIROOKA

Department of Earth Sciences, Faculty of Science,
Toyama University, Toyama 930.

### Introduction

Two geomagnetic excursions successively occurred were found in the late Pleistocene by the palaeomagnetic studies on Ontake Tephra Formation in Ina City, Central Japan (Hiroka, 1977a; Hirooka et al., 1977 & 1978). The Younger and the older excursions were named Ina I and Ina II, respectively. Ina II excursion began at Pm-I Pumice Bed and lasted untill Pm-II Bed. Intercalating a normally magnetized loam layer, Ina I excurtion started and ended at Pm-III Bed. Fission-track age of Pm-I is about 80 thousand years B.P. (Machida and Suzuki, 1971). The $^{14}$C age of Pm-III is 35,000 $\pm$ 1,400 years B.P. (Kobayashi, 1970).

Although the precise ages of the excursions are not yet so clear, Ina I geomagnetic excursion is considered to have occurred during 60 to 35 x $10^3$ years ago, and Ina II is 85 - 70 x $10^3$ years ago. Since there are many tephra formations which are supposed to be the same age of Ontake Tephra in Japan, the present author intended to find the evidence of these geomagnetic excursions in the another late Pleistocene tephra formations.

### Geomagnetic excursions of the late Pleistocene

There are several reports on the anomalous remanent directions which are seemed to correspond to Ina I and Ina II geomagnetic excursions. In cored samples of Lake Biwa sediment, Yaskawa et al. (1973) found a horizon showing very rapid and drastic direction changes. The age is estimated to be 49 thousand years from the rate of sedimentation. Hirooka (1977b) reported about the anomalous remanent direction of the "Older Sand Dune" sediments of Awara which distribute along the northern coast line in Hokuriku District. The sand dune sediments were covered by a tephra bed which is correlated to Daisen-Kurayoshi Pumice by Miura and Fujita (1967). The pumice is dated by $^{14}$C method to be 30,200 $\pm$ 3,500 years B.P. (San'in Quaternary Research Group, 1969). Recently, Machida and Arai (1979) proposed that the age of this thin pumice bed to be 45 - 47 x $10^3$ years from the thephrochronological point of view. On the eastern flank of Mt.Yatsugatake in Central Japan, Aida (1978) detected a big deflection in NRM direction. The anomalous direction began at Pm-I Pumice of Mt.Ontake origin and ended at YPm-I of Yatsugatake Tephra. In Saruuchi Formation of Tohoku District are noticed intermediately and reversally magnetized horizons by Manabe (1980). The age of horizons are 30 - 35 x $10^3$years B.P. Such reports suggest that at least two geomagnetic excursions occurred during 80 x 30 thousand years ago in Japan.

### Sampling

To get the new evidences of Ina-I and Ina II excursions more widely in Japan, sampling were carried out at the two localities, the one is Hirose in Shimane Prefecture and the other is Bibi in Chitose City, Hokkaido Island. At Hirose, Kisugi Pumice Bed (SK) which derived from Mt. Sambe directly covers Daisen-Matsue Pumice Bed (DMP) from Mt. Daisen. Daisen-Matsue Pumice is considered to be older than Daisen-Kurayoshi Pumice.

Palaeomagnetic samples were collected from 3 horizons in Daisen-Matsue Pumice and 2 horizons in Kisugi Pumice. The horizons are denoted DL 1, 2, 3, 4 and 5 as ascending order respectively. The uppermost sampling horizon of Daisen-Matsue Pumice (DL 3) is in the part where soil was formed. Samples were obtained from 5 horizons of HL 1, 2, 3, 4 and 5 at Bibi site. Their stratified six pumice beds which were derived from Shikotsu Caldera and its parasitic volcanoes such as Mt. Tarumae and Mt. Eniwa. The lowermost bed, Shikotsu Pumice Flow Deposit (Spfl) was distributed at the volcanic activity which formed Shikotsu Caldera. $^{14}$C age of the activity is 31,900 ± 1,700 years B.P. The second lowest pumice bed was formed at the time of eruption of Mt. Eniwa. This bed is usually denoted as Ea. The upper pumice beds were derived by the eruptions of Mt. Tarumae. From the upper to the lower, the beds were named a, b, c and d Pumice Beds and Ta, Tb, Tc and Td are used as abbreviations for the beds respectively. Tb Bed was formed by the eruptions in 1,667 A.D. and Ta was in 1,739 A.D. Horizon HL 1 is in Spfl. HL 2 horizon is in the loam under Ea Pamice Bed. Palaeolithic arrowheads made of obsidian were excavated from this horizon. The age of the horizon, 18,500 ± 1,000 B.P. was determined by obsidian hydration method (Katsui and Nemoto, 1979). HL 3 is in Td Bed whose age is estimated to be around 9 thousand years ago. HL 4 and HL 5 are Tc and Ta Pumice Beds, respectively.

## Results of measurement and Discussion

Results of NRM measurements of sites of Hirose and Bibi are tabulated in Table 1. As are seen in the table, remanent direction of horizon DL 1, 2 and 5 in Hirose site are intermediate ones while all of the horizons exept HL 3 show normal NRM directionin Bibi site. The NRM intensity of Horizon HL 3 is very weak. The direction of remanence of it is also very much scatterd as shown in Fig. 1. As the Tarumae d Pumice is very large grained and loosely packed bed, this large magnetic scattering is a matter of course. During the time of the late Pleistocene excursions, the geomagnetic field seems to have change its direction greatly and rapidly so that many intermediate directions of the geomagnetic field were recorded in tephra sediments. Since geomagnetic excursions of Ina I and II are very good time markers,

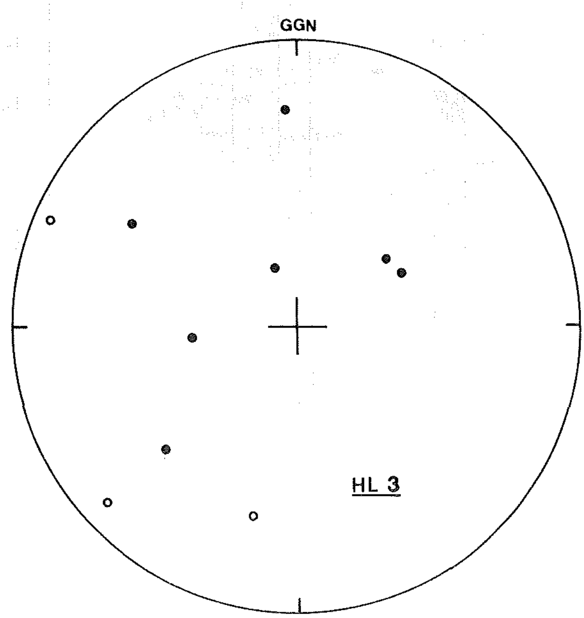


Fig. 1 NRM direction of Horizon HL 3 in Bibi site.

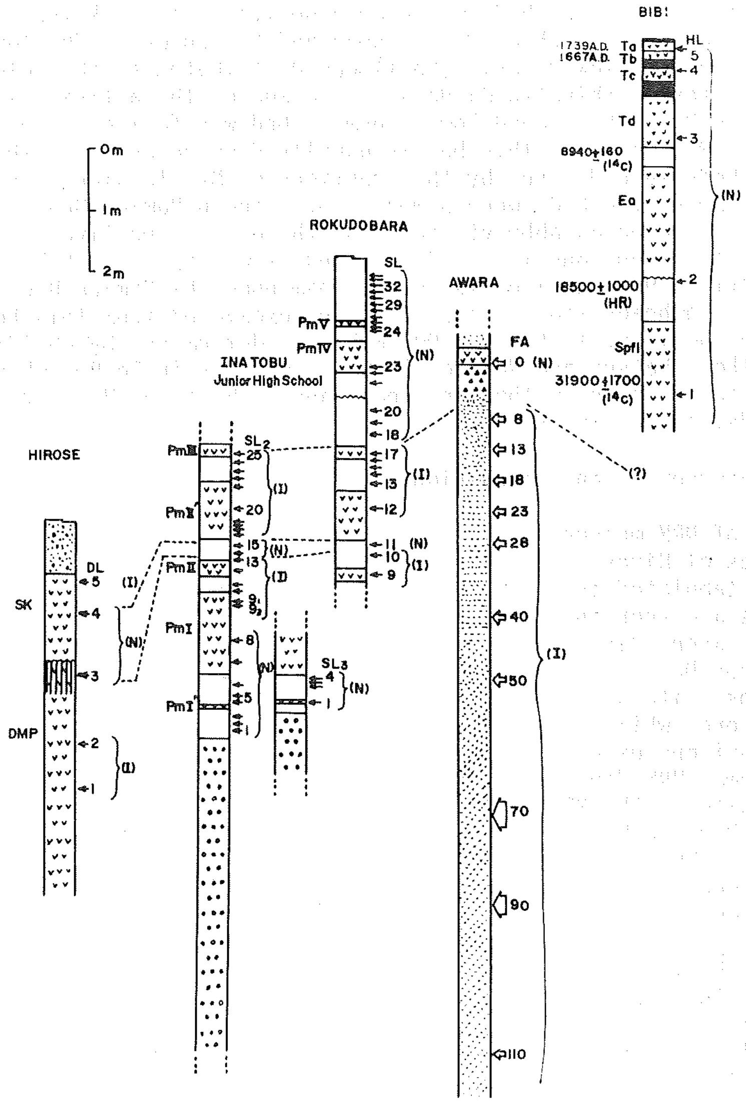

Fig. 2  Geological columns and magnetostratigraphic correlation of the late Pleistocene tephra formations.

we can correlate the late Pleistocene tephra formations palaeomagnetically by using the horizons of intermediate remanent magnetization as key beds.

Sampling horizons and their polarities are written in geological columns of the sites in Fig. 2. Palaeomagnetic results of sites such as Rokudobara (Hirooka et al., 1977), Ina Tobu Junior High School (Hirooka et al., 1978) and Awara (Hirooka, 1977b) were also presented in the figure. It is obvious that the intermediate remanent magnetizations are correlated with each other as shown in broken lines. There is no geological and tephrochronological problems in this correlation. Palaeomagnetic study is found to be a very useful means to correlate the late Pleistocene tephra formations of different regions.

| Sampling Horizon | N | Declination ( °E) | Inclination ( °) | $\alpha_{95}$ ( °) | K |
|---|---|---|---|---|---|
| Hirose | | | | | |
| DL 5 | 9 | 9.1 | 57.4 | 6.7 | 59.2 |
| DL 4 | 9 | 35.4 | 53.1 | 12.7 | 17.3 |
| DL 3 | 9 | 64.8 | 57.8 | 8.0 | 42.6 |
| DL 2 | 9 | 76.1 | 27.9 | 30.8 | 3.7 |
| DL 1 | 6 | 176.6 | 69.3 | 17.0 | 16.4 |
| Bibi | | | | | |
| HL 5 | 7 | 15.5 | 65.5 | 8.7 | 49.3 |
| HL 4 | 8 | 1.4 | 60.2 | 15.0 | 14.5 |
| HL 3 | - | - | - | - | - |
| HL 2 | 10 | 11.2 | 59.2 | 4.9 | 99.9 |
| HL 1 | 11 | - 3.8 | 61.4 | 2.1 | 472.3 |

Table 1 Direction of NRM.

## References


Aida, N. (1978) Quaternary Res., 17, 86.
Hirooka, K. (1977a) Quaternary Res., 16, 105.
Hirooka, K. (1977b) Paleolimnol. Lake Biwa Japanese Pleistocene, 5, 102.
Hirooka, K., C. Tobita, T. Yokoyama and S. Nakaya (1977) Rock Mag. Paleogeophys., 4, 81.
Hirooka, K., E. Hasegawa, T. Hirota, S. Nakaya and T. Yokoyama (1978) Paleolimnol. Lake Biwa Japanese Pleistocene, 6, 101.
Katsui, Y. and S. Nemoto (1979) Remains in the Basin of the River Misawa, III, 519 (in Japanese).
Kobayashi, K. (1970) Kagaku, 40, 74.
Machida, H. and F. Arai (1979) J. Geograph., 88, 33.
Machida, H. and M. Suzuki (1971) Kagaku, 41, 263 (in Japanese).
Manabe, K. (1980) Quaternary Res., 19, 225 (in Japanese).
Miura, S. and S. Fujita (1967) Mem. Fac. Educ., Fukui Univ., Ser. 2, no.17, 93.
San'in Quaternary Research Group (1969) In "Nihon no Daiyonki",335 .

MAGNETIC PROPERTIES OF THE OLD SOMMA LAVAS OF HAKONE VOLCANO

Jun FURUYA*, Hiroshi AKAI* and Toshio FURUTA**

* Depertment Geology, Chiba University, Yayoi-cho Chiba 260
**Ocean Research Institute, University of Tokyo, Nakano, Tokyo

## Introduction

This report presents the preliminary results of magnetic properties of the Hakone Volcano. The detailed petrology of this area was studied by Kuno(1950,1951). The samples for this study were the andesitic lavas which were called $OS_2$ and $OS_5$. The sampling sites are indicated in Figure 1. We studied paleomagnetic and rockmagnetic properties of these samples. Some interesting results are clarified for thermomagnetic and chemical composition of titanomagnetites in studied samples.

## Results

### Thermomagnetics

Thermomagnetic measurement was carried out on 43 samples. First we picked up sample into a small chip (approx. 100 mg). The small chip was heated to 640 °C and cooled to room temperature at 6 °C/min in a vacuum of $10^{-4}$ torr. The cycle of heating and cooling was accomplished in a magnetic field of 4.5 kOe. Since thermomagnetic curves for each sample were drawn, these thermomagnetic curves were mainly classified in three types(Fig. 2). Type I shows a reversible curve which is observed in non-oxidized samples. Four samples of type I were obtained from 43 samples(approx.10% of all samples). Type II shows the curve which is due to high temperature oxidation resulting to exsolve ilmenite lamellae. This curve obtained 11 from 43 samples(approx.25% of all samples). Type III shows a typical low temperature oxidation curve which is commonly observed among submarine basalts. This curve obtained 27 from 43 samples(approx.60% of all samples). Under a reflected-light microscope, ilmenite exsolusion lamellae were distinguished in the titanomagnetite whose samples shows type II. Titanomagnetites suffered from low temperature oxidation

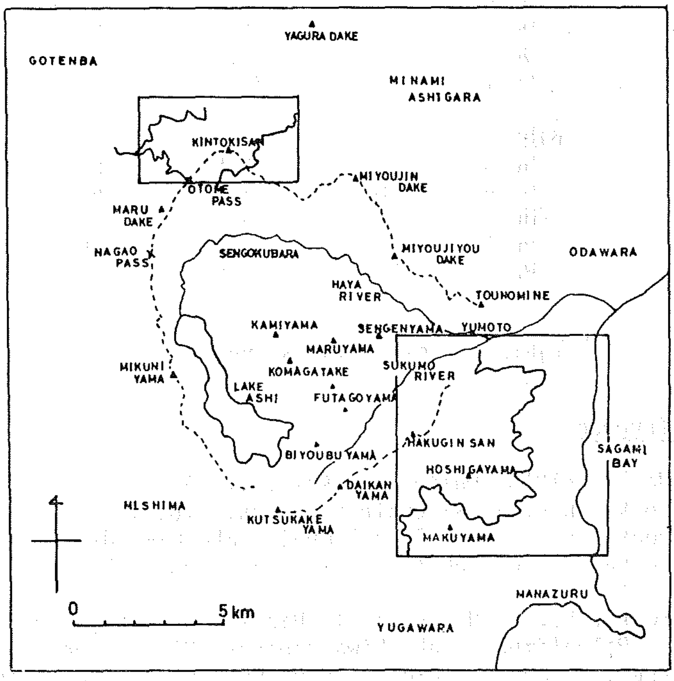

Figure 1. Locality map of the Hakone Volcano. Squares are denoted the sampling sites.

show type III and a part of titanomagnetite in these samples was observed as titanomaghemite. Ilmenite lamellae and titanomaghemites were sometimes observed in the same titanomagnetite grain. A titanomagnetite suffered from both high and low temperature oxidation is recognized in some samples. From these results, non-oxidized titanomagnetites in these andesitic lavas are a little. The old somma lavas of the Hakone Volcano whose age is estimated younger than 0.5m.y. could be rather than oxidized at low temperature.

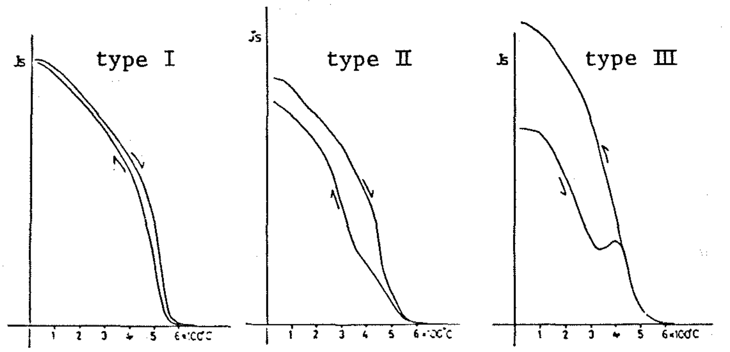


**Figure 2. Typical thermomagnetic curves of samples from studied area.**

Opaque mineralogical properties

We will discuss here the crystalization stage of titanomagnetite and its chemical composition and minor elements in titanomagnetite. Chemical composition of titanomagnetite was determined by an electron probe microanalyzer (JXA-5). Twelve polished thin sections were measured FeO* (throughout this paper, FeO* means total iron as FeO), $TiO_2$, $Al_2O_3$. Selected several grains of inclusion,phenocryst, and groundmass titanomagnetite were measured for individual thin sections. One thin section of these samples was analyzed on 6 elements as FeO*, $TiO_2$, $Al_2O_3$, MnO, MgO and $V_2O_3$. To test zoning, some grains were measured by scanning or point analysis on the core and the rim of titanomagnetite, these grains were almost homogenious in composition. The most inclusion titanomagnetites were enclosed in orthopyroxene minerals and could not be found in plagioclase or olivine.

Table 1. Ti/Fe mol ratio, x-value and content of $Al_2O_3$ of titanomagnetite for selected samples.

| | Ti/Fe mol ratio | | | x-value | | | $Al_2O_3$ | | | Thermo-magnetic type |
|---|---|---|---|---|---|---|---|---|---|---|
| | Inclusion | Phenocryst | Groundmass | Inclusion | Phenocryst | Groundmass | Inclusion | Phenocryst | Groundmass | |
| HK 00-50 | - | 0.207 | 0.250 | - | 0.51 | 0.60 | - | 1.5 | 0.9 | III |
| HK 025-01 | 0.094 | 0.132 | 0.186 | 0.26 | 0.35 | 0.47 | 4.3 | 3.9 | 2.2 | II |
| HK 06-52 | - | 0.172 | 0.200 | - | 0.44 | 0.50 | - | 2.2 | 1.9 | II |
| HK 08-53 | - | 0.167 | 0.200 | - | 0.43 | 0.50 | - | 3.5 | 2.4 | III |
| HK 21-51 | 0.124 | 0.154 | 0.200 | 0.33 | 0.40 | 0.50 | 4.0 | 2.8 | 1.6 | I |
| HK 25-54 | - | 0.163 | 0.224 | - | 0.42 | 0.55 | - | 1.4 | 1.5 | ? |
| HK 26-51 | 0.141 | 0.190 | 0.224 | 0.37 | 0.48 | 0.55 | 1.6 | 2.5 | 1.8 | I |
| HK 28-52 | - | - | 0.176? | - | - | 0.45? | - | - | 1.5? | II |
| HD 13-60 | 0.111 | 0.119 | 0.163 | 0.30 | 0.32 | 0.42 | 4.1 | 1.7 | 1.8 | II |
| HD 14-61 | 0.145 | 0.145 | 0.195 | 0.38 | 0.38 | 0.49 | 1.9 | 2.8 | 1.8 | III |
| HD 23-02 | 0.136 | 0.149 | 0.181 | 0.36 | 0.39 | 0.46 | 3.0 | 2.5 | 1.0 | ? |
| HD 27-57 | 0.103 | 0.119 | 0.158 | 0.28 | 0.32 | 0.41 | 3.8 | 2.4 | 1.5 | III |

These results are listed in Table 1 and Figure 3. Table 1 shows the Ti/Fe mol ratios, x-values and the contents of $Al_2O_3$. Ti/Fe mol ratio shows the decrease from inclusion grains to groundmass grains. On the contrary, the content of $Al_2O_3$ decreases from inclusion grains to groundmass grains. This fact suggests that crystalization of titanomagnetite is wide range in magma. The component of ulvospinel increases and spinel decreases in order to this crystalization. The host minerals of inclusion titanomagnetites are all of orthopyroxene, so that the first stage of titanomagnetite may be after the crystalization of plagioclase or olivine before that of orthopyroxene.

Mean x-value and grain distribution are shown in Figure 3. From this Figure, the x-value shows a relatively wide variation for each sample. Moreover, the averaged x-values for individual samples indicate their own values.

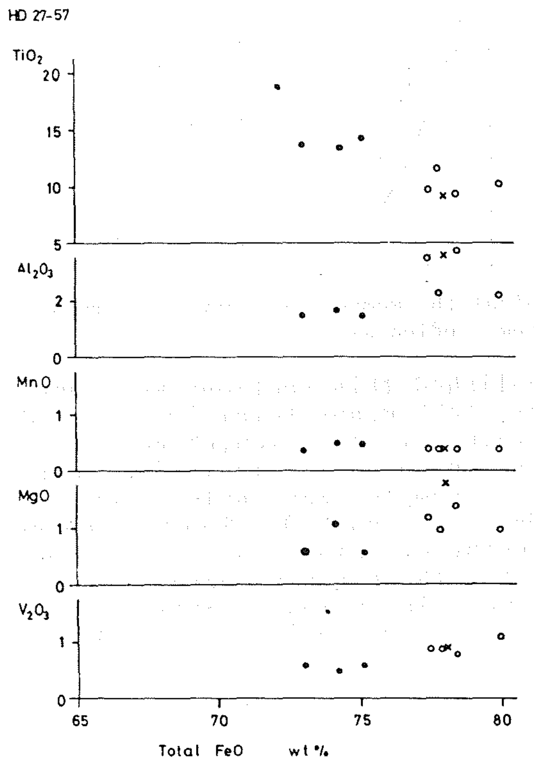


Figure 4. Plot of the chemical compositions of titanomagnetite(in wt %).
cross: inclusion,
open circle: phenocryst,
hold circle: groundmass.

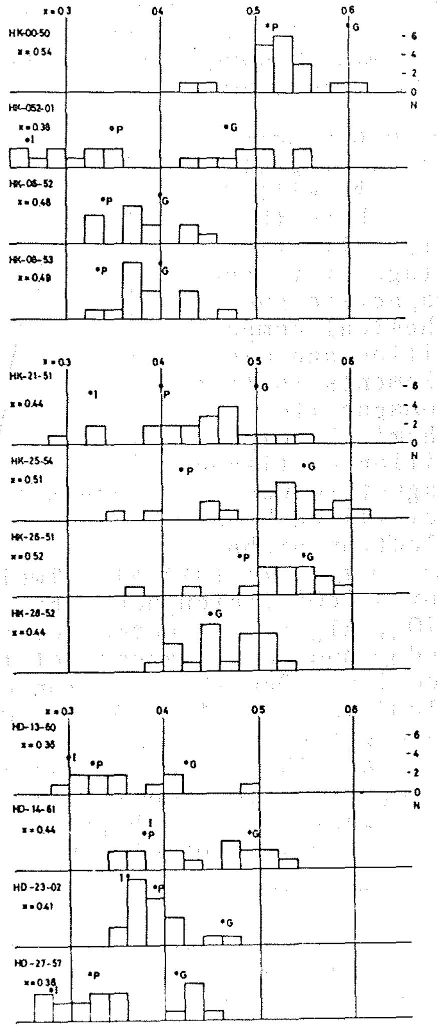


Figure 3. Histogram of titanomagnetite composition.
I: inclusion, P: phenocryst,
G: groundmass.

Patterns of grain distribution show also a wide range or Gaussian's, so that these patterns may suggest the different physical environment during crystalization in magma. Correlation between FeO* and other elements are shown in Figure 4. As shown in Figure 4, the contents of FeO* increases in order to decrease of $TiO_2$, and to increase of MgO and $V_2O_3$. These tendencies are commonly recognized in titanomagnetite from igneous rocks(Oshima,1975).

References


Kuno,H.(1950) J. Fac. Sci. Univ. Tokyo, Sec. II, v.7, 257.
Kuno,H.(1951) J. Fac. Sci. Univ. Tokyo, Sec. II, v.7, 351.
Oshima,O.(1975) Bull. Volcanol. Soc. Japan, v.20, 275.

# CONFIRMATION OF A MAGNETIC POLARITY EPISODE IN THE BRUNHES NORMAL EPOCH: A PRELIMINARY REPORT

Akira HAYASHIDA

Department of Geology and Mineralogy, Kyoto University, Kyoto 606

The occurrence of geomagnetic polarity excursions or short-term events during the Brunhes normal epoch has been proposed as an interpretation for anomalous directions of natural remanent magnetization(NRM) in some materials of the late Pleistocene(Verosub and Banerjee, 1977). If these fluctuations of NRM are real records of geomagnetic variation, they can usefully adopted as chronostratigraphic keys for geologic correlation, and also they are expected to provide important informations on nature of the source of geomagnetism. However the evidence of proposed excursions and events are not still adequate to establish the magnetic history within the Brunhes epoch in world-wide scale. This is probably due to the lack of appropriate materials for paleomagnetic study with continuous performance and high resolution, for example a long, continuous section of fine sediments with such a high accumulation rate as allows of recording geomagnetic feature shorter than $10^4$ years. When the record of a short polarity episode is detected by chance, the data often contains some weakness. For instance, the paleomagnetic data for polarity episodes appears mostly in samples collected by coring underwater or underground sediments. In such cases, samples may be subjected to a risk of distortion by the coring operation. Natural deformation of sediments by slides or slumps are also difficult to evaluate for recovered core samples. Therefore, the necessary procedure to realize a short-term episode of geomagnetic field is suggested to produce the consistent data repeatedly within each core site or outcrop and further from a wide region on the earth.

The Biwa I event is one of candidates for short-term polarity episodes in the late Brunhes epoch. A record of this event was discovered in a 200-m-long core sediment from Lake Biwa, Central Japan, and dated between 176,000 and 186,000 years B.P.(Kawai *et al.*, 1972). The 200-m core was taken from the lake bottom at the water depth of 65 m(Fig. 1). The sediment consisted of lacustrine clay with numbers of volcanic ashes which was estimated covering the last 0.5 m.y.(Yokoyama and Horie, 1972). Upward inclinations of NRM were found at five horizons in the core and three of them were suggested to accompany declination changes of almost 180 degrees, that is, those were claimed to be the polarity events. One at 55 m in depth from the lake bottom was correlated to the Blake event (Smith and Foster, 1969) of about 100,000 years B.P. The other two at 85 m and 130 m were supposed newly discovered events, which were named Biwa I and Biwa II events. Radiometric ages of zircons in some volcanic ashes in the core were determined by fission track method(Nishimura and Yokoyama, 1973), the results of which were concordant with the estimated ages for the magnetic events.

On the other hand, the Plio-Pleistocene strata of lacustrine origin are distributed in hilly areas around Lake Biwa and called as the Kobiwako Group. The Kobiwako Group is regarded the sediment of the ancient Lake Biwa which were exposed on land(Ikebe and Yokoyama, 1976). The uppermost part of the Kobiwako Group is the Takashima Formation distributed in Aibano Hills on the northwest coast of Lake Biwa(Fig. 1). The age of the Takashima Formation was assigned to be in the Brunhes epoch based on normal magnetic polarity of some volcanic ashes and the evidence

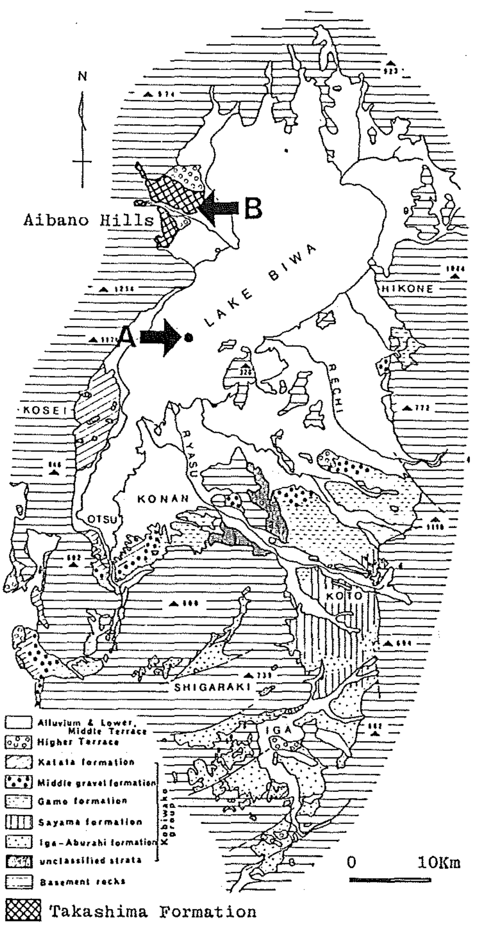


Fig. 1 Map showing the site of the 200-m core from Lake Biwa(A) and the sampling location of the Takashima Formation, the uppermost Kobiwako Group(B). Base map from Ikebe and Yokoyama(1976).

of plant remains(Yokoyama *et al.*, 1977; 1979). Recently two volcanic ash layers, the Akatsuki and Taihoji volcanic ashes, were identified in the upper sandy facies of the Takashima Formation and they were correlated to the volcanic ashes in the 200-m core(Yokoyama *et al.*, 1980; Hayashida and Takemura, 1980). These volcanic ashes are those called as BB195 and BB207 situated at 82.3 m and at 88.2 m deep in the core, respectively, where the Biwa I event was found to be recorded. While these volcanic ashes are intercalated in clay at interval of 5.9 m in the 200-m core, the Akatsuki and Taihoji volcanic ash layers are observed with a space about 2 m in sand and mud layers of the upper Takashima Formation (Hayashida and Takemura, 1980). This implies that the upper part of the Takashima Formation was deposited in a marginal environment of the lake. Thus it becomes possible to confirm the occurrence of the Biwa I polarity episode using the land section which was reliably shown synchronous with the original core sediment and which was formed in a different sedimentary environment.

Samples for magnetic measurements were collected mainly from the two outcrops, the northeast outcrop and southeast one which are situated about 60 m apart at the location shown in Fig. 1. The samples were taken from sporadically distributed horizons of mud and volcanic ashes avoiding sand and granule layers. Each sample, which represented one horizon of the section, comprised five or six specimens. Remanent magnetization of specimens were measured on a Schonstedt spinner magnetometer(Type SSM-1A). One or two specimens were chosen from each horizon for progressive alternating field(AF) demagnetization tests. Although NRM of most specimens seemed to be stable in responce to AF demagnetization, some specimens showed significant changes in remanent directions. In these cases, magnetic directions of most specimens tended to concentrate toward the reversed polarity. This could be interpreted because secondary overprints in a soft magnetic component, which was probably originated from viscous remanent magnetization, were erased by AF demagnetization. Magnetization of a few specimens showed rather noisy wiggles in direction changes, which were possibly caused by so weak magnetization as the noise level of our measuring instrumentation or by intrinsic unstability of sample's magnetization. Remanent magnetization

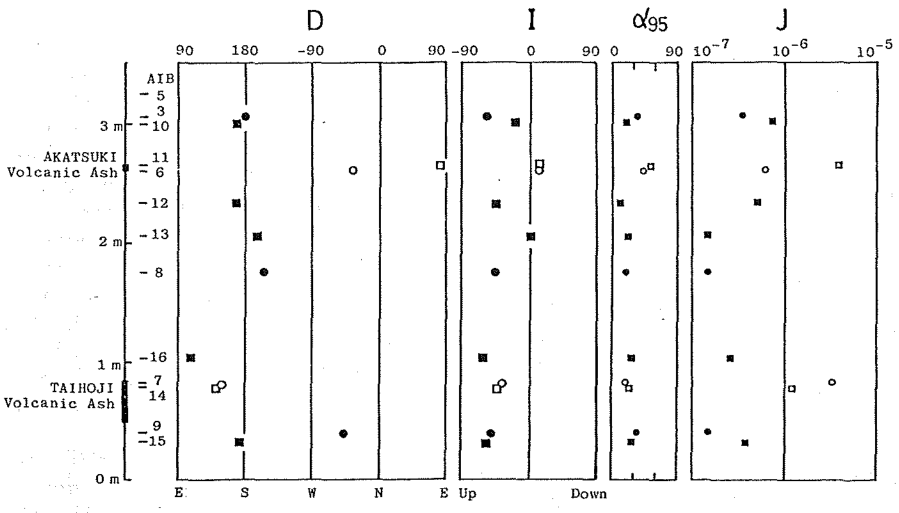


Fig. 2 Remanent magnetization of two outcrops of the upper Takashima Formation plotted as a function of the stratigraphic level. D and I: site mean declination and inclination in degrees east and downward, respectively. $\alpha_{95}$ : 95% confidence circle radius in degrees. J: mean intensity of magnetization in emu/cc. Circles and squares show the data from the north-east and southwest outcrops, respectively. Open symbols indicate volcanic ash samples.

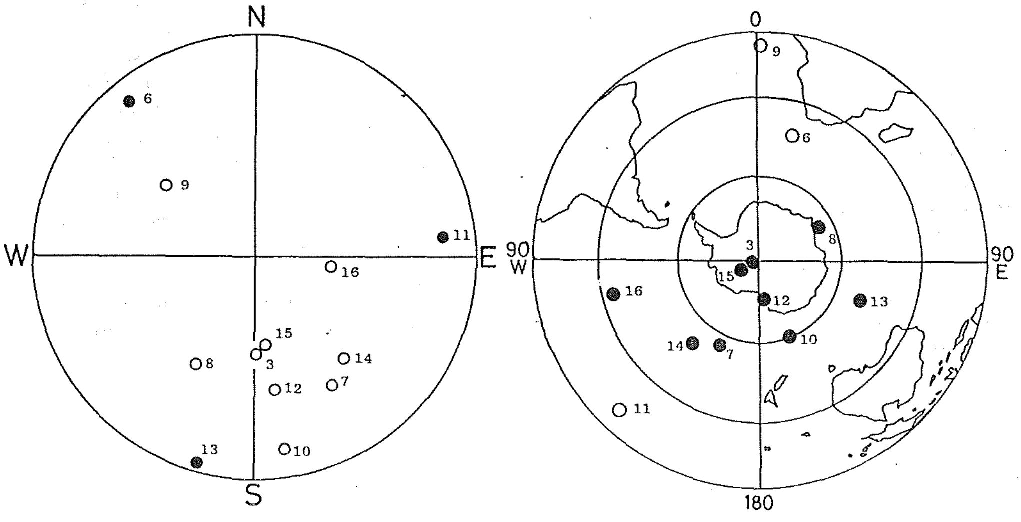


Fig. 3 Equal-area projection of paleomagnetic directions (left) and positions of VGP's(right). Closed and open circles are on the lower(southern) and upper(northern) hemispheres in the left(right) diagram, respectively. Numbers correspond to sample identifications in Fig. 2.

of other specimens were routinely measured after AF demagnetization in peak fields of 100 Oe and 200 Oe, and mean directions and precision parameters were calculated for each sample. The more clustered direction data was chosen between the two mean directions of 100 Oe and 200 Oe treatments as a site mean direction for each horizon. The resulted paleomagnetic data is shown in Fig. 2 for both of the northeast and southwest sections, except for several samples whose remanent directions were highly scattered. Fig. 3 shows the equal-area projection of paleomagnetic directions and the position of their corresponding virtual geomagnetic poles(VGP's). As shown in these figures, none of the present samples were magnetized in the normal polarity, while the entire section is suggested in the Brunhes age. A few samples including the Akatsuki volcanic ash seem magnetized in anomalous directions. Although it might be infered that these intermediate directions are of the original record of the past geomagnetic field, the interpretation that these were caused by unsuccessful cleaning of the secondary magnetism is supposed preferable. In fact, the Akatsuki volcanic ash was revealed to have inconsistent NRM directions between two samples from the separated outcrops. Both samples showed larger dispersions in magnetic direction than the others, also within samples. Most samples had remanent magnetizations of reversed polarity, from which the VGP's were calculated as situated in the higher south latitudes than 45°S.

This result is supposed to confirm the occurrence of a reversed polarity episode about 180,000 years B.P., because the present section is tightly correlated with the horizon in the 200-m core where the Biwa I event was previously proposed to occur. The studied strata are located about 16 Km apart from the site of the 200-m core(Fig. 1), and the sedimentary environment of each site was also suggested to be different. So the possibility that the original record of the Biwa I event in the 200-m core might be originated by natural deformation of sediment or sample distotion during the coring procedure is clearly precluded. It was also ensured that the Biwa I episode is characterized by the full reversal of magnetic field at least in the vicinity of Lake Biwa. The present data, however, is not sufficient to describe the whole of the Biwa I episode in detail. The duration of this episode is uncertain and the fine structure of the polarity transitions are left unknown, as the upper and lower boundaries of the Biwa I magnetozone have not been identified in the Takashima Formation. It is hoped that the more concentrated data is acquired from multiple sections which are reliably correlated and distributed in a wide region. Fortunately, the Biwa I episode was shown to be recorded about the horizon of the outstanding volcanic ash layers. These volcanic ashes are expected to aid the setting of parallel sections in Central Japan, where the validity of a magnetic polarity episode as a stratigraphic time marker could be also examined in relation to tephrostratigraphic keys.

## REFERENCES

Hayashida, A. and K. Takemura(1980): In preparation.

Kawai, N., K. Yaskawa, T. Nakajima, M. Torii and S. Horie(1972): Proc. Japan Acad., 48, 186-190.

Nishimura, S. and T. Yokoyama(1973): *ibid.*, 49, 615-618.

Smith, J. D. and J. H. Foster(1969): Science, 163, 565-567.

Verosub, K. L. and S. K. Banerjee(1977): Rev. Geophys. Space Phys., 15, 145-155.

Yokoyama, T. and S. Horie(1974): Paleolim. Lake Biwa Japanese Pleist., 2, 31-37.

Yokoyama, T., Y. Nakagawa, K. Takemura and A. Hayashida(1980): Quaternary Res., 19, 185-201.
Yokoyama, T., Y. Nakagawa, K. Takemura, S. Mori, T. Makinouchi, A. Hayashida, Y. Iida and K. Matsuoka(1979): Paleolim. Lake Biwa Japanese Pleist., 7, in press.
Yokoyama, T., K. Takemura and K. Matsuoka(1977): *ibid*., 5, 54-64.

STUDIES ON THE BLAKE EPISODE WITH SPECIAL EMPHASIS TO EAST ASIAN RESULTS OBTAINED

Sadao SASAJIMA*, Susumu NISHIMURA* and Kimio HIROOKA**

* Department of Geology and Mineralogy, Kyoto University, Sakyo, Kyoto 606
** Institute of Earth Science, Toyama University, Gofuku, Toyama 930

## 1. Introduction

Denham (1976; Denham et al., 1977) has made detailed examination of the Blake event (Smith and Foster, 1969) in several giant cores recovered from the Greater Antilles Outer Ridge. On the basis of rigorous check on magnetostratigraphic and radiometric results and of some possible Blake events published by other scientists, he has reached a conclusion that the Blake event might not have been a global polarity reversal but only a locally reversed geomagnetic feature covered a relatively small area of the western North Atlantic region ($\approx$67°W, 22°N). In their summary list of candidates for the Blake episode (Table 1 of Denham et al., 1977) an indefinite status of the reversed magnetozone in the Inuzako pyroclastic flow (Sasajima, 1973) was mentioned. Then, the senior author (S. S.) has undertaken a paleomagnetic reexamination on the Kagoshima area, South Kyushu, therein a short-lived Inuzako reversed episode was previously reported as correlatable with the Blake event (Sasajima, 1973). The result obtained will be described in the next section. The other possible Blake episodes reported from the Honshu, main island of Japan, come from sediments core of Lake Biwa (Kawai et al., 1972) and from a silty sequence of the marine terrace in Fukushima, Northeast Honshu (Manabe, 1977).

On the other hand, in the course of the paleomagnetic survey in Sumatra, Indonesia, the present authors have had a chance to find out a short-lived reversed magnetozone in the upper layer of Toba ignimbrite cropped out near Asahan (Sigulagura) to the southeast of Lake Toba. Zircon crystals separated from the ignimbrite sample were dated as 0.10 m.y. by the fission track technique. It seems safer to correlate the reversed episode with the Blake episode. Taking into account of the successful magnetostratigraphic correlation of loess sequences in North China (Wang et al., 1980), the present authors discuss about the problem that the Blake episode is assigned to either the local reversal origin or the global reversed event.

## 2. Result and discussion

The improved paleomagnetostratigraphic results from the Kagoshima area are summarized in the schematic illustration (Fig. 1) which include fission track ages and the standard sea-level change found in the Kanto district (Machida, 1975), as a reference of the Pleistocene glacial/interglacial changes. As shown in the diagram it has been confirmed that the short polarity reversed interval in Keno and Kogashira pyroclastic flows is correlatable with the Blake episode in place of the previous Inuzako pyroclastic flow. The paleomagnetic data of the former two are shown in Table 1. Both inclinations seem, more or less, lower than the expected inclination 52.6° for the axial dipole field, however, their virtual pole positions are almost enclosed within the range of secular variation. Fission track age data of zircons extracted from the Keno welded tuff are listed in Table 2. The grain-by-grain ages of zircons seem to exhibit a rough bimodal frequency, which is more or less common feature for water-laid tuffs and pyroclastic flows (Tamanyu, 1975; Okaguchi and Otsuka, 1980). Judging from the genetic nature of such rocks, it is usual to regard the youngest peak

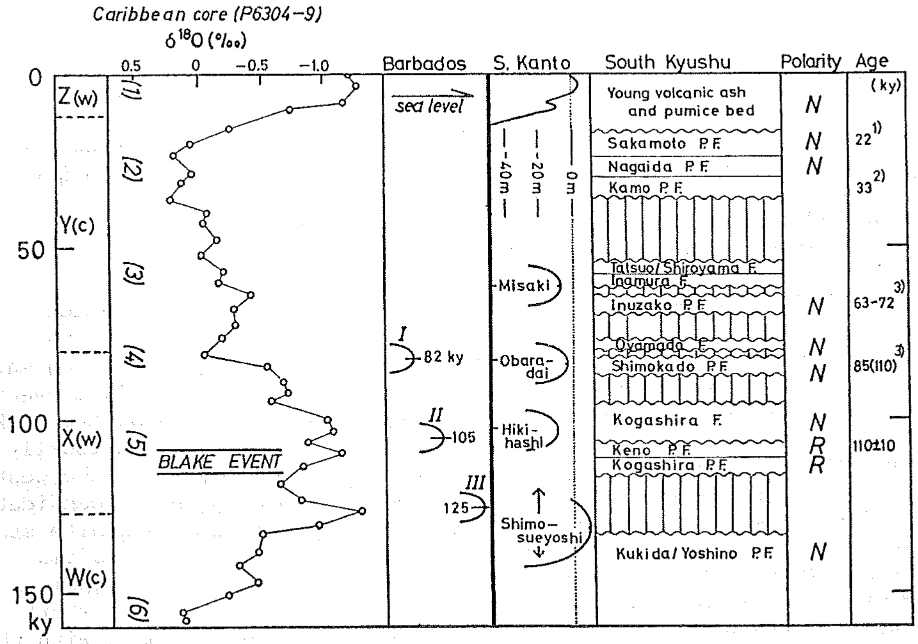


Fig. 1 A tentative chronostratigraphic comparison of the upper Pleistocene series investigated with the other reference paleoclimatic records due possibly to glacial-interglacial changed: the $\delta^{18}O$ stratigraphy of Caribbean core P6304-9 (SHACKLETON and MATTHEWS, 1977) and a representative sea level change estimated in South Kanto region (MACHIDA, 1975). W, X, ··· : Faunal zone after ERICSON *et al.* (1961), 1) : KIGOSHI *et al.* (1972) ; YOKOYAMA (1971), 2) : ISHIKAWA *et al.* (1972), 3) : NISHIMURA and MIYACHI (1973). N : Normal remanent magnetization, R : Reversed reamanent magnetization, (W) : Warm water temperature, (C) : Cold water temperature, (1), (2), ······ : Emiliani's no.

Table 1. Paleomagnetic result suggesting possible correlation with the Blake Event.

| locality | Long. | Lat. (N) | N | D | I | $\alpha_{95}$ | Long. | Lat. | Age (m.y.) | AF-field |
|---|---|---|---|---|---|---|---|---|---|---|
| Keno | 130°31' | 31°39' | 9 | 180.1 | -24.4 | 5.6 | 130.2E | -71.2 | {0.10 0.13 | 160 |
| Kogashira | 130°30' | 31°39' | 11 | 163.3 | -34.9 | 12.7 | 185.0 | -70.5 | — | 50 |
| Sigulagura | 99°20' | 2°16' | 10 | 191.7 | - 0.3 | 3.6 | 15.7 | -77.4 | 0.10 | 200 |

value as the fission track age of the rock. The age distribution in Table 2 is not enough for such a statistical analysis, therefore, the age of the Keno welded tuff may be estimated at between 0.13 to 0.10 m.y.

It should be noted that the period covered by the short reversed polarity is limited within a relatively higher sea-level interval, that is, the Latest Interglacial Age. Consequently, the short-lived reversed episode of Keno and Kogashira layers is safely comparable with any of subdivided three polarity reversals of the rigorous Blake episode (Denham, 1976).

On the other hand, the age data of individual zircons separated from the rhyolitic tuff in Sigulagura, North Sumatra, excellently converge to the mean value, 0.10±0.02 m.y. as listed in Table 3; the standard deviation ($1\sigma$) of the mean is represented. Paleomagnetic properties of the reversed magnetozone in ignimbrites obtained from Sigulagura, Sumatra are shown also in Table 1. The virtual pole position seems slightly separate from the south pole of the axial dipole field, suggesting insufficient average out of secular variations. Combining with the age estimation mentioned above, this reversed magnetozone can safely be correlated with the Blake episode. To the best of our knowledge, these are the first results in which the Blake episodes have been observed by continental rocks with igneous nature.

Recently the other possible Blake magnetozones have been found in loess sequences widely developed in North China, especially in the northern region of Xian (110°E, 35°N), (Wang et al., 1980). The short-lived polarity reversals which are correlated by the original authors with the Blake event may be somewhat premature until they are established, however, positive indications supporting the existence of the Blake episode are encouraging to resolve the problem whether the Blake episode is due to the global geomagnetic polarity reversal or not.

Very recently, Creer et al. (1980) have reported a presumable Blake event recorded in an unoriented clayey core from Calabria, Italy (16°E, 38°N). The reversed polarity zone is characterized by a rather long duration of about 50,000 yr from the most reliable sedimentation rate of the core, although the magnetozone is split into two by a short sequence of normal inclinations with estimated duration 10,000 yr in the middle. This fact is not consistent with the result that the inferred Blake magnetozone from the Greater Antilles region (KN 25-4) is split into three subzones by two excursions (Deham, 1976). Unfortunately, such fine structures were not able to identify by the preseent authors' study.

After a rigorous identification of a number of "the Blake events" reported by several authors from ocean sediments cores, Denham (1976) and Denham et al. (1977) tend to support an idea that in the strict sense of the definitions, the Blake magnetozones which are found in a limited region of the Caribbean Sea and the Greater Antilles are assigned to the local reversal feature resulted from a small auxiliary dipole which is positioned at the core/mantle boundary under the region; the direction of the off-centered dipole is antiparallel to that of the centered dipole.

Table 2 Fission Track Age of the Keno Welded Tuff, Kagoshima Prefecture

| No. | $\rho_s$ | Counts | $\rho_I$ | Counts | $\phi$ | T(m.y.) |
|---|---|---|---|---|---|---|
| #1 | $2.3\times10^4$ | 12 | $1.4\times10^7$ | 730 | $1.05\times10^{16}$ | 0.11 |
| 2 | $2.4\times10^4$ | 15 | $1.5\times10^7$ | 938 | | 0.10 |
| 3 | $1.8\times10^4$ | 9 | $1.2\times10^7$ | 598 | | 0.13 |
| 4 | $1.1\times10^5$ | 45 | $4.0\times10^7$ | 327 | $1.05\times10^{15}$ | 1.8 |
| 5 | $2.6\times10^5$ | 101 | $1.4\times10^7$ | 109 | | 1.1 |
| 6 | $2.4\times10^5$ | 98 | $1.2\times10^7$ | 245 | | 1.4 |
| 7 | $2.7\times10^5$ | 129 | $1.5\times10^7$ | 287 | | 1.2 |
| 8 | $4.5\times10^4$ | 33 | $3.0\times10^6$ | 110 | | 0.96 |

Fission track age of Keno Pyroclastic flow obtained by the individual grain method (specimen : Zircon). $\rho_s$ : Spontaneous fission track density ($cm^{-2}$), $\rho_I$ : Induced fission track density ($cm^{-2}$), $\phi$ : Thermal neutron dose per $cm^2$.

Table 3. Fission track ages of zircons from Sigulagura, North Sumatra.

| Specimen | $\rho_s$ | $\rho_i$ | T (m.y.) |
|---|---|---|---|
| 1 | $3.2 \times 10^5$ | $8.05 \times 10^7$ | 0.12 |
| 2 | 3.0 | 8.23 | 0.11 |
| 3 | 2.2 | 7.58 | 0.09 |
| 4 | 1.4 | 6.23 | 0.07 |
| 5 | 1.9 | 6.56 | 0.09 |
| 6 | 3.3 | 8.34 | 0.12 |
| 7 | 3.4 | 8.08 | 0.13 |
| | Neutron dose = $o.50 \times 10^{15} (cm^{-2})$ | | $0.10 \pm 0.02$ |

Sample No: C-133 7608068-1 (Rhyolitic tuff) Sigulagura, Symbols are the same as for Table 2.

The longitudinal difference between the Kagoshima and Xian is only about 20°. If we apply to these sites the local pseud reversal model which is due to a small auxiliary dipole positioned at the core surface directly under the area, anomalous fields due to two small dipoles extend over the Japan-Korean Peninsula-China-Indochina region although in the marginal area the polarity reversal is not achieved (Harrison and Ramirez, 1975). In this inference, a partial superposition of the anomalous fields originated from a small reversed dipole underlying the Asahan site to the above region should indispensably be considered. If this is the case, much more complicate geomagnetic behaviors such as excursions may be expected in the Southeast Asian area surrounded by the three sites.

By making extension of the similar ways to the recently increased knowledge of the inferred Blake feature, it may be tolerable to say that the Blake episode, in the broad sense, might have covered almost whole area of Eurasia. It is very difficult, though not impossible, to assess paleomagnetically the global existence of the Blake polarity reversal (Kukla and Nakagawa, 1977), however, these inferred Blake episodes from Caribbean/ Greater Antilles, South Italy, North Sumatra, North China and Southwest Japan are supposed to have simultaneously occurred, suggesting a positive confession of the global geomagnetic reversed polarity of the Blake episode. The balance of evidence seems in favor of the view that the Blake reversal is a global geomagnetic event. It implies at least that a limited use of the Blake episode for the correlation purpose is actually effective at first approximation, on the one hand, and on the other hand, much more precise clarification is necessary to substantiate the geomagnetic feature concerning the Blake event. Further investigation on the Blake episode is necessary not only in the shallow-sea area but in the continental area.

## Reference


Creer, K., P. W. Readman and A. M. Jacobs (1980) Earth Planet Sci. Lett. 50, 289.

Denham, C. (1976) Earth Planet. Sci. Lett., 29, 422.

Denham, C., R. F. Anderson and M. P. Bacon (1977) Earth Planet. Sci. Lett. 35, 384.

Ericson, D. B., M. Ewing, G. A. Wollin and B. C. Heezen (1961) Geol. Soc. Am. Bull., 72, 193.

Harrison, C. G. A. and E. Ramirez (1975) J. Geomag. Geoelectr., 27, 139.

Ishikawa, H., S. Higo, Y. Tomari, K. Ohki and K. Hamazaki (1972) J. Geol. Soc. Japan, 78, 563.

Kawai, N., K. Yaskawa, T. Nakajima, M. Torii and S. Horie (1972) Proc. Japan Acad., 48, 186.

Kigoshi, K., T. Fukuoka and K. Yokoyama (1972) Bull. Volcnol. Soc. Japan, 17, 1.

Kukla, G. and H. Nakagawa (1977) Quat. Res., 7, 283.

Machida, H. (1975) Quat. Studi., Roy. Soc. N. Z. Bull., 13, 215.

Manabe, K. (1977) Quat. Res., 7, 372.

Nishimura, S. and M. Miyachi (1973) J. Jap. Assoc. Min. Petro. Econ. Geol., 68, 225.

Nishimura, S. (1975) Tsukumo Chigaku (Mem. Fac. Lib. Arts, Kyoto Univ.), 10, 1.

Okaguchi, M. and H. Otsuka (1980) Quat. Res. Japan

Sasajima, S. (1973) Rock Mag. and Paleogeophys., 1, 47.

Shackleton, N. J. and R. K. Matthews (1977) Nature, 268, 618.

Smith, J. D. and J. H. Foster (1969) Science, 163, 565.

Tamanyu, S. (1975) J. Geol. Soc. Japan, 81, 233.

Wang, Y., L. Yue, T. Wu, X. Chen and W. Tuan (1980) Geol. Rev. (China), 26, 141.

# ON THE EXISTENCE OF PRE-JARAMILLO EVENT IN MATUYAMA EPOCH

Kazuaki MAENAKA

Hanazono College, Nishinokyo-Tsubonouchi, Nakagyo-ku, Kyoto 616

## INTRODUCTION

The writer with his collaborators has engaged in establishing the paleomagnetic stratigraphy in Plio-Pleistocene Series in Kinki and Tokai districts. Ishida et al. (1969) collected the volcanic ash specimens from each of 156 sites in Kinki and Tokai districts, and measured their NRMs. The result showed that the deposits of Osaka, Kobiwako and Tokai Groups were formed during the Gauss Normal, Matuyama Reversed, and Brunhes Normal Epochs. Torii et al. (1974) reported the paleomagnetic result on the water-laid volcanic ash layers in the Osaka Group, Sennan and Senpoku hills in Osaka Prefecture. Their result agreed well with ours. Maenaka et al. (1977) presented the newly constructed paleomagnetic stratigraphy adopting the data of fission track ages on some volcanic ash layers (Nishimura and Sasajima 1970, Nishimura and Yokoyama 1975). In the report, the writers pointed out the possibility of the existence of two event in late Matuyama Epoch; that is, short normal intervals of the Kamikatsura horizon and the Komyoike to Pink horizons. The writers correlated the Kami-Katsura horizon which occurs at a horizon between Ma (marine clay bed as important key layers of Osaka Group) 2 and Ma 3 to the Jaramillo event, and considered the Komyoike-Pink horizon between Ma 1 and Ma 2 to be possibly unknown event. For the fission track age of Komyoike volcanic ash determined by Nishimura and Sasajima (1970) was considered to be a reasonable one based on geological grounds, and the event corresponding to the normal polarity interval at the age of the Komyoike ash (1.1 MY) was not so far reported.

Recently, Iida (1980) established a magnetic stratigraphy basing on the data from 29 sites in the Tsuda River section, a stratotype of the Osaka Group in Sennan Hills. He insisted that the normal polarity of the Kamikatsura horizon was thought to be very short normal episode because it was represented by only one layer, and that the normal polarity zone intercalating the Komyoike and Pink ash layers is more than 10 m thick. So, Iida (1980) correlated the Komyoike-Pink horizon to the Jaramillo event.

In this short paper, the possibility of the existence of pre-Jaramillo event at 1.1 MY is discussed.

## THE PALEOMAGNETIC STRATIGRAPHY OF OSAKA GROUP

The results of paleomagnetic polarities with the fission trach ages of volcanic ash layers in Osaka Group are summarized as follows (Nishimura and Sasajima 1970, Torii et al. 1974, Maenaka et al. 1977, Yokoyama 1979, Iida 1980).

| | | |
|---|---|---|
| Handa | N | |
| Wada | N | Brunhes |
| Kasuri (0.37 or 0.38 MY) | N | |
| Neya | N | |
| Sakura | N | Normal |
| Toga | N | |
| Hacchoike | N | |
| Imakuma | N | Epoch |
| Fukakusa | N | |
| Sayama | R | |
| Azuki (0.87 MY) | R | |
| Kamikatsura | N | |
| Yamada | R | Matuyama |
| Komyoike (1.1 MY) | N | |
| Pink | N | |
| Tatsugaike | R | |
| Yellow | R | |
| Grey (1.2 or 1.5 MY) | R | Reversed |
| unconformity | | |
| Kamimura | R | |
| Senriyama | R | Epoch |
| Pumice (2.2 MY) | R | |
| Mitsumatsu | N | |
| Shimakumayama (2.3 or 2.4 MY) | R | |
| Asashiro | N | |
| Habutaki | N | Gauss |
| Tsuchimaru | N | Normal |
| Misaki | N | Epoch |

In Matuyama Reversed Epoch, three normal polarity zones are recognized. The normal polarity of Kamikatsura volcanic ash is stable in spite of its shallow inclination (Maenaka et al. 1977, Yokoyama and Hayashida 1980). The Kamikatsura ash is situated a few meters above Ma 2. The fission track age of the Azuki ash, intercalated in Ma 3, is 0.87 MY. Maenaka et al. (1977) suggested that the normal polarity of the Kamikatsura horizon was correlated to the Jaramillo event and the normal polarity polarity of Komyoike-Pink horizon was considered to be unknown event. Iida (1980) opposed this view. He correlated the Komyoike-Pink horizon to the Jaramillo event.

In Fig. 1, both views are compared. In this figure, the axis of the abscissa represents the paleomagnetic polarity time scale presented by Mankinen and Dalrymple (1979) and the axis of the ordinate represents the stratigraphic relation between marine clays and volcanic ash layers in the Osaka Group shown by Iida (1980). The solid line and the dotted line show respectively the writer's view and Iida's one. Iida (1980) considered that the Brunhes-Matuyama boundary was at the base of Ma 4 which occurs between Fukakusa volcanic ash layer and Sayama volcanic ash layer, and that the beginning of the Jaramillo event was at the base of Ma 1. On the other hand, the writer considers that the Jaramillo event is correlated to the horizon of the Kamikatsura ash. In the figure, the data of the polarities and the fission track ages on Kasuri, Azuki, Komyoike and Grey volcanic ash layers are also given. It is shown that they are closer to the solid line than the dotted

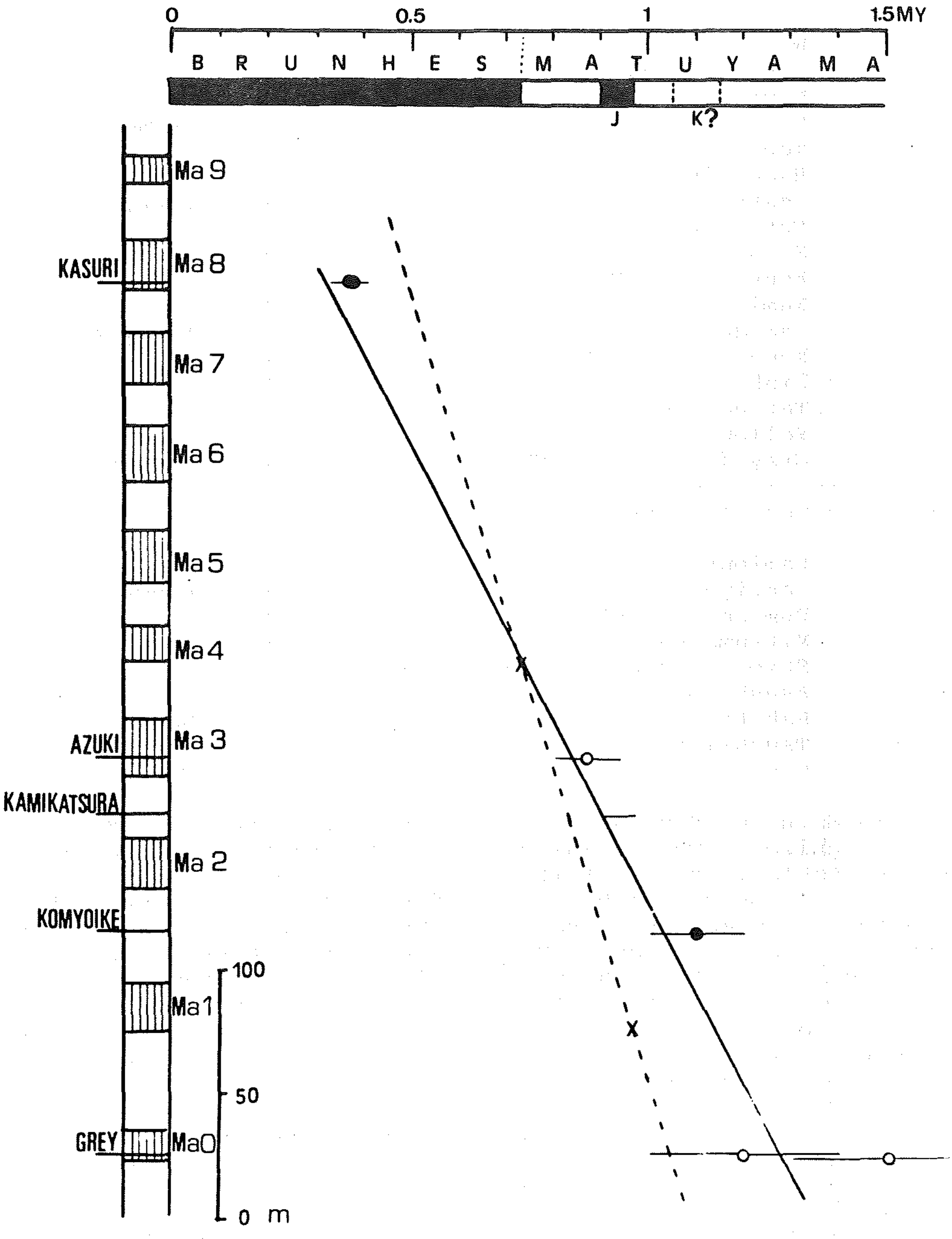


Fig. 1 The relation between the thickness of the upper Osaka Group sediments and the polarity time scale

line. The assumption of the constant rate of deposit in upper Osaka Group is more appropriate for the solid line.

THE SUPPOSITION OF PRE-JARAMILLO EVENT

The geomagnetic polarity time scale for the last 4 MY has been developed by combining paleomagnetic polarity and K-Ar age data from subareal volcanic rocks. Cox et al. (1964) compiled all available results and emphasized that during the last 3.5 MY, changes in the polarity of the geomagnetic field had taken place at irregular intervals, and that within intervals of predominantly one polarity (Brunhes Normal, Matuyama Reversed and Gauss Normal Epochs) shorter intervals of opposite polarity (Olduvai Normal Event in Matuyama Epoch and Mammoth Reversed Event in Gauss Epoch), about 0.1 MY in duration, were recognized. Jaramillo event was provided by Doell and Dalrymple (1966). Since 1966 there have been numerous studies published concerned with refinement and better definition of the polarity time scale for the last 4 MY. Fig. 2-A is cited from the report of Cox et al. (1968), whose ages are corrected by a change in the constants used K-Ar dating (Mankinen and Dalrymple 1979). In the time table shown in Fig. 2-A, normal events of Jaramillo, Olduvai and Reunion are recognized in Matuyama Reversed Epoch. Fig. 2-B shows the revised geomagnetic polarity time scale presented by Mankinen and Dalrymple (1979). This time table is not changed essentially from that of Fig. 2-A. However, recent data (Fig. 2-C), obtained by subtraction Fig. 2-A from Fig. 2-B, shows a increase in normal polarity data at about 1.1 MY.

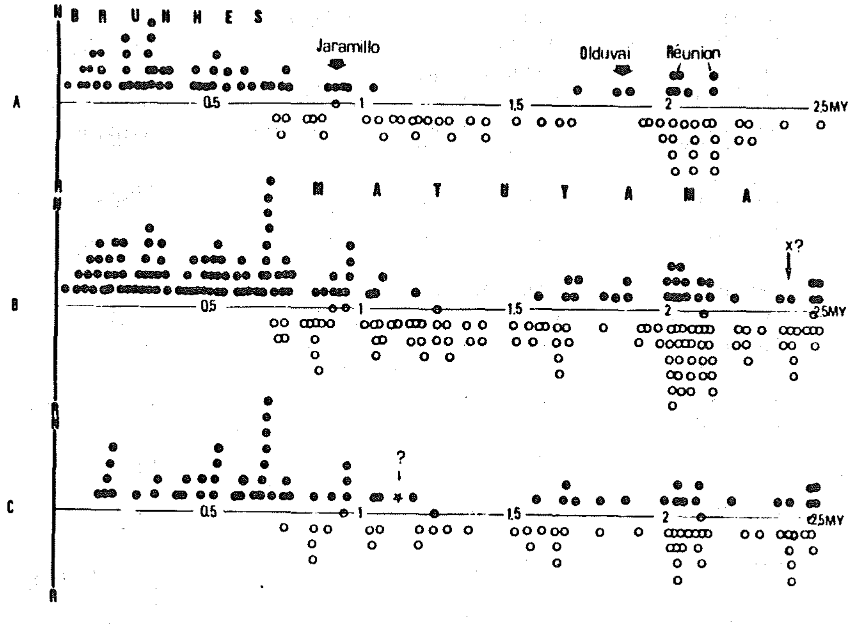


Fig. 2 The paleomagnetic polarity and K-Ar age data from subareal volcanic rocks for the last 2.5 MY. (A) after Cox et al. (1968) (B) after Mankinen and Dalrymple (1979) (C) after (B)-(A)

Mankinen et al. (1978) argued that a brief normal polarity event within the Matuyama Reversed Epoch was recorded by the rhylite units exposed on Cobb Mountain in northern California. They showed that these rocks had an age of 1.12 MY by K-Ar age determinations (star mark in Fig. 2-C), and concluded that this event clearly preceded to the Jaramillo event.

Sheriff et al. (1979) summarized paleomagnetic results for 37 sites, in lava flows and plug domes, in Leucite hills volcanic field (1.1 ± 0.4 MY), southwest Wyoming. They reported that about 90% of the sites are reversely magnetized, but that the two buttes (four sites) which lie at opposite ends of the field are normally magnetized.

The geomagnetic time scale has been especially useful dating sediments recovered from the ocean basins (Harrison 1966 and others). Ages within cores can be estimated from the known depth of the layers to be dated, and the known rate of deposition of accurately dated layers of identical types occurring higher up in the sequence. In an undisturbed sequence, the uppermost sediments will be of normal polarity, and the boundary between normal and reversed magnetized sediments is dated at 0.73 MY. An age of any normal polarity segments in late Matuyama Epoch of the ocean bottom sediments is given by the extrapolation of the sedimentation rate inferred from the thickness of the Brunhes Epoch sediments. Table 1 suggests that some data obtained from the ocean bottom sediments show an existence of unknown event preceded to the Jaramillo event.

Table 1 The estimated ages of pre-Jaramillo event supposing the constant sedimentation rate

| Core No. | Depth(Age) of B-M boundary | Depth(Age) of Jaramillo | Depth(Age) of Pre-Jaramillo | Reference |
|---|---|---|---|---|
| MSN12G | 91 cm (0.73 MY) | 118-128 cm (0.96-1.03 MY) | 135-140 cm (1.08-1.12 MY) | Harrison (1966) |
| V20-107 | 530 cm (0.73 MY) | 675-715 cm (0.93-0.98 MY) | 780-785 cm (1.07-1.08 MY) | Ninkovich et al. (1966) |
| E13-17 | 600 cm (0.73 MY) | 725-745 cm (0.88-0.91 MY) | 980-1020 cm (1.19-1.22 MY) | Hays and Opdyke (1967) |
| T13-224 | 105 cm (0.73 MY) | 130-150 cm (0.90-1.04 MY) | 185-190 cm (1.29-1.32 MY) | Steuerwald et al. (1968) |
| E14-14 | 545 cm (0.73 MY) | 650-745 cm (0.87-1.00 MY) | 855-880 cm (1.15-1.18 MY) | Watkins (1968) |
| V24-58 | 560 cm (0.73 MY) | 670-715 cm (0.87-0.93 MY) | 985-1015 cm (1.28-1.32 MY) | Hays et al. (1969) |
| V24-59 | 365 cm (0.73 MY) | 420-445 cm (0.84-0.89 MY) | 540-565 cm (1.08-1.13 MY) | Hays et al. (1969) |
| RC9-143 | 355 cm (0.73 MY) | 475-510 cm (0.98-1.05 MY) | 595-610 cm (1.22-1.25 MY) | Opdyke and Glass (1969) |
| V16-75 | 430 cm (0.73 MY) | 515-550 cm (0.87-0.93 MY) | 745-800 cm (1.26-1.36 MY) | Opdyke and Glass (1969) |
| RC12-66 | 415 cm (0.73 MY) | 475-510 cm (0.84-0.90 MY) | 640-680 cm (1.13-1.20 MY) | Foster and Opdyke (1970) |
| V21-148 | 380 cm (0.73 MY) | 425-455 cm (0.82-0.87 MY) | 605-640 cm (1.16-1.23 MY) | Opdyke and Foster (1970) |
| B32-47 | 485 cm (0.73 MY) | 645-680 cm (0.97-1.03 MY) | 765-785 cm (1.15-1.18 MY) | Watkins and Kennett (1972) |

## REFERENCES


Cox, A., R.R. Doell and G.B. Dalrymple (1964) Science, 144, 1537.

Cox, A., R.R. Doell and G.B. Dalrymple (1968) Quart. J. Geol. Soc. London, 124, 53.

Doell, R.R. and G.B. Dalrymple (1966) Science, 152, 1060.

Foster, J.H. and N.D. Opdyke (1970) Earth Planet Sci. Lett., 1, 463.

Harrison, C.G.A. (1966) J. Geophys. Res., 71, 3033.

Hays, J.D. and N.D. Opdyke (1967) Science, 158, 1001.

Hays, J.D., T. Saito, N.D. Opdyke and L.H. Burckle (1969) Geol. Soc. Amer. Bull., 80, 1481.

Iida, Y. (1980) Master Thesis of Kyoto Univ., p.79.

Ishida, S., K. Maenaka and T. Yokoyama (1969) J. Geol. Soc. Japan, 75, 183.

Maenaka, K., T. Yokoyama and S. Ishida (1977) Quart. Res., 7, 341.

Mankinen, E.A. and G.B. Dalrymple (1979) J. Geophys. Res., 84, 615.

Mankinen, E.A., J.M. Donnelly and C.S. Gromme (1978) Geology, 6, 653.

Ninkovich, D., N.D. Opdyke, B.C. Heezen and J.H. Foster (1966) Earth Planet. Sci. Lett., 1, 476.

Nishimura, S. and S. Sasajima (1970) Earth Science, 24, 222.

Nishimura, S. and T. Yokoyama (1975) Paleolim. Lake Biwa and Japanese Pleistocene, 3, 138.

Opdyke, N.D. and J.H. Foster (1970) Geol. Soc. Amer. Mem., 126, 83.

Opdyke, N.D. and B.P. Glass (1969) Deep Sea Res., 16, 249.

Sheriff, S., P.N. Shive and P. Ogden (1979) EOS Trans. AGU, 60, 244.

Steuerwald, B.A., D.L. Clark and J.A. Andrew (1968) Earth Planet. Sci. Lett., 5, 79.

Torii, M., S. Yoshikawa and M. Itihara (1974) Rock Magnetism and Paleogeophysics, 2, 34.

Watkins, N.D. (1968) Earth Planet. Sci. Lett., 4, 341.

Watkins, N.D. and J.P. Kennett (1972) Science, 173, 813.

Yokoyama, T. (1979) Tsukumo-chigaku, no. 14, 32.

Yokoyama, T. and A. Hayashida (1980) Tsukumo-chigaku, in press

PLEISTOCENE VOLCANIC ACTIVITY IN THE FOSSA MAGNA REGION, CENTRAL JAPAN
— K-Ar AGE STUDIES OF YATSUGATAKE VOLCANOES —


Ichiro KANEOKA[1,2], Harald MEHNERT[2], Shigeo ZASHU[1] and Shimpei KAWACHI[3]

1. Geophysical Institute, Faculty of Science, University of Tokyo, Bunkyo-ku, Tokyo 113, Japan.
2. Branch of Isotope Geology, U. S. Geological Survey, Federal Center, Denver, Colorado 80225, U. S. A.
3. Department of Geology, College of Arts and Sciences, Hokkaido University, N17 W8, Kita-ku, Sapporo 060, Japan.


## 1. Introduction

The Yatsugatake volcanic chain, one of the major volcanic massifs in central Japan, is located near the junction of the northeast and southwest Japan (Fig. 1a). It includes more than twenty centers of volcanic activities which are regarded to have been active since middle Pleistocene (Kawachi, 1974-75, 1977). It is noteworthy that the Yatsugatake volcanic chain erupted along the western side of the Fossa Magna region, dividing the southern Fossa Magna region and the northern Fossa Magna region (Fig. 1b). Based on the regional differences, the Yatsugatake volcanic chain can be subdivided into the southern and the northern area at the Natsuzawa Pass (Fig. 1b). From the sequence of lava flows in the Yatsugatake volcanic area, they are grouped into the Older (middle Pleistocene) and the Younger (post middle Pleistocene to Recent) periods separated by an erosional hiatus (Kawachi, 1979).

Due to its characteristic geographic-geological position, it is conjectured that its volcanic activity might have been related to some tectonic effects on this region. To elucidate the volcanic activity from the viewpoint of geochronology, it is inevitable to know the age of the initiation of the volcanism. Furthermore, the information on the period of relatively active volcanism in this region is very significant. For these purposes, K-Ar dating method was applied on rocks of the Yatsugatake volcanic chain of mostly the Older period.

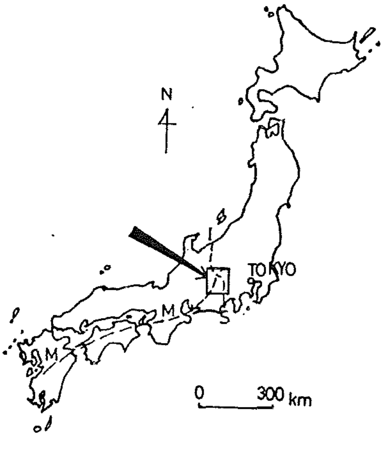


Fig. 1a. Locality of Yatsugatake Volcanoes in central Japan.

I-S : Itoigawa-Shizuoka tectonic line.
M : Median tectonic line.

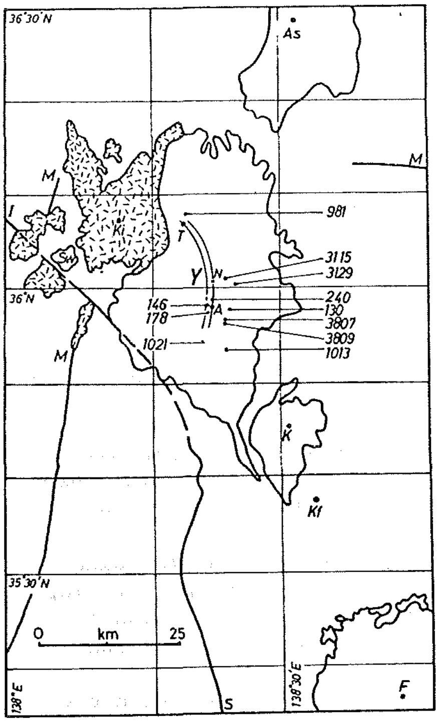


Fig. 1b. Sampling localities in the Yatsugatake area. Each number corresponds to each sample No.

Y : Yatsugatake Volcanoes. (T : Tateshina-yama, A : Akadake, N : Natsuzawa Pass).
As : Asama Volcano.
Ki : Kirigamine Volcano. (Hatched area indicates the distribution of the Enrei formation).
K : Kurofuji Volcano.
F : Fuji Volcano.
Sw : Suwa Lake.
Kf : Kofu city.
I-S : Itoigawa-Shizuoka tectonic line.
M : Median tectonic line.

## 2. Samples

Eleven samples of seven different lava units were selected for K-Ar dating. Their sampling localities are shown in Fig. 1b. They were selected to include typical rocks of the Older period (Early to Middle Pleistocene) from both the southern and the northern area of Yatsugatake, though most of which are derived from the southern area.

Among them, porphyrites of Mt. Nakadake from the southern area (146, 178) are considered to have formed a part of "the root of the volcanoes" (Kawachi, 1977). An andesite of Kasuga volcanic rocks (981) from the northern area is also considered to be volcanic products of relatively early stage during their activity (Kawachi, 1979). Andesites of the Todaru-no-sawa lava (3115, 3129) and of the Shinkyoji-yama lava (130, 3807, 3809) are also regarded to belong to the Older period of the southern area. They are stratigraphically younger than those of Mt. Nakadake and Kasuga volcanic rocks (Kawachi, 1977). Andesites of the Kannon-daira lava (1021) and the Mitsugashira lava (1013) also belong to the Older period of the southern area, but they are stratigraphically younger than those mentioned previously.

On the other hand, an andesite of Mt. Akadake (240), which is considered to belong to the Younger period (Late Pleistocene and Holocene), was examined to test the detectability of a relatively young age by the K-Ar method.

## 3. Experimental

All volcanic rocks were analysed as bulk samples.

K was analysed by a flame photometer with a Li-internal standard. Ar gas was extracted from each sample (9∿19 g) by using an induction heater and purified with two Ti furnaces following conventional procedures.

Most Ar analyses were undertaken at the U.S. Geological Survey, Denver, where Ar isotopes were measured on a Nier type mass spectrometer (60°, 6 inch radius) with a Hall-probe monitoring system. A few Ar measurements were done on a quadru-pole type mass spectrometer at the Geophysical Institute, University of Tokyo.

## 4. Results and discussion

K-Ar age results are summarized with a stratigraphical sequence of present samples in Fig. 2. As a whole, K-Ar ages are concordant with the stratigraphical sequence.

For rocks of the Younger Yatsugatake period, a fission-track age of 0.014 Ma has been reported for a tuff which has been regarded to belong to one of the latest volcanic activities of Yatsugatake Volcanoes (Kawachi et al., 1978). Furthermore, the ages of the activities of acid rocks such as rhyolites which followed the stratovolcano formation such as Mt. Akadake were dated to be 0.098 to 0.13 Ma by the fission track method (Kawachi, 1974-75). These results together with the K-Ar result for the sample 240 of Mt. Akadake suggest that the volcanic activity of the Younger Yatsugatake period might have started around 0.20 ± 0.05 Ma ago.

On the other hand, most rocks of the Older Yatsugatake period show K-Ar ages of 0.25 ∿ 0.38 Ma, which probably correspond to the most active period to have formed the stratovolcanoes in the southern area. Hence, the age gap between the Older Yatsugatake period and the Younger Yatsugatake period may be 0.1 Ma at most.

Among present samples, no rocks show the K-Ar age from 0.4 to 0.9 Ma. One may argue that this simply reflects the sample choice. In effect, some lavas exist which should be stratigraphically older than the Shinkyo-ji yama lava and the Todaru-no-sawa lava. Compared with later volcanic activities, however, they seem to have been less intensive. Hence, an apparent lack in the K-Ar age between 0.4 and 0.9 Ma may reflect a relatively poor volcanic activity in the Yatsugatake area.

On the other hand, the relatively old K-Ar age of Kasuga volcanic rocks in the northern area may suggest that such volcanic activity might have some relationships with the adjacent volcanic activities such as those of the Enrei formation and the Kirigamine Volcano. K-Ar ages for

YATSUGATAKE VOLCANOES

| | PERIOD | SOUTHERN REGION | NORTHERN REGION |
|---|---|---|---|
| PLEISTOCENE | YOUNGER YATSUGATAKE PERIOD | AKADAKE LAVA (Andesite) 240 <0.27Ma | |
| | OLDER YATSUGATAKE PERIOD | MITSUGASHIRA LAVA (Andesite) 1013 0.25Ma<br>KANNON-DAIRA LAVA (Andesite) 1021 0.28Ma<br>SHINKYOJI-YAMA LAVA (Andesite) 130, 3807, 3809 0.25~0.38Ma<br>TODARU-NO-SAWA LAVA (Andesite) 3115, 3129 0.28~0.37Ma | |
| | | NAKADAKE (Porphyrite) 146, 178 1.3Ma | KASUGA VOLCANIC ROCKS (Andesite) 981 1.0Ma |

Fig. 2. Schematic diagram of the stratigraphical sequences of present samples together with K-Ar age results.

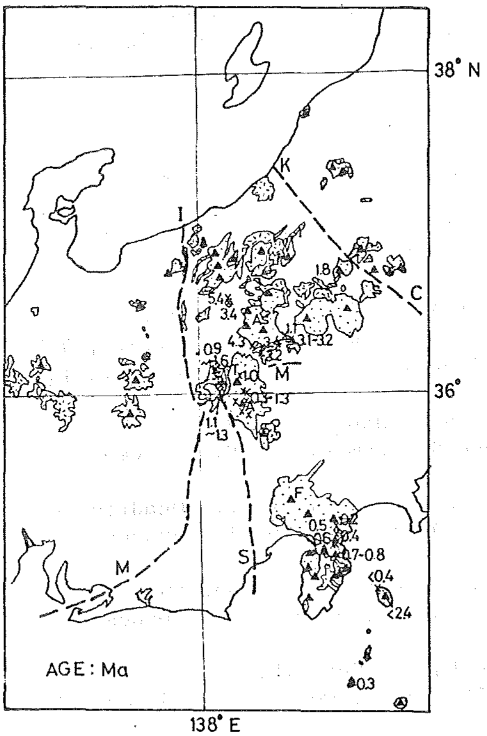


Fig. 3. Summary of radiometric ages of Pliocene and Pleistocene volcanic rocks in the Fossa Magna region.
K-C : Kashiwazaki-Choshi tectonic line.
I-S : Itoigawa-Shizuoka tectonic line.
M : Median tectonic line.

Data sources : Aoki et al. (1971), Kaneoka and Ozima (1970), Kaneoka and Suzuki (1970), Kaneoka et al. (1970a), Kaneoka et al. (1970b), Kaneoka et al. (1979), Momose et al. (1966), Morimoto et al. (1966), Ozima et al. (1968), Suzuki (1970).

andesites of the Enrei formation which extends to the west of the Yatsugatake volcanoes have been reported to be 1.2 ∿ 1.6 Ma (Momose et al., 1966; Kaneoka and Ozima, 1970). Both K-Ar and fission track ages on obsidians from the Kirigamine Volcano and the Wada Pass in the same area show the ages of 0.9 ∿ 1.3 Ma (Kaneoka and Suzuki, 1970). In this respect, the K-Ar age of 1.3 Ma of Mt. Nakadake, which is regarded to mark the initiation of volcanic activity in the Yatsugatake area, may also be related to these volcanic activities. These results imply that the Pleistocene volcanic activities around the area which is located at the junction of two great tectonic lines, the Median and the Itoigawa-Shizuoka tectonic lines, probably started around 1 ∿ 1.5 Ma ago. Furthermore, the similarities in these ages suggest that some tectonic effects might have affected the area to have triggered the volcanic activity.

In Fig. 3, radiometeric ages for volcanic rocks of Pliocene and Pleistocene ages in the Fossa Magna region are summarized. They include both K-Ar and fission track ages. In the Asama area, an andesite of the Hanamagari group was dated to be about 1.1 Ma, whereas andesites of the Kirizumi group, which directly underlies the former, show the K-Ar ages of about 3.1 Ma (Ozima et al., 1968). They are located about 50 Km to the northeast of the Yatsugatake Volcanoes. Some other volcanic rocks at the base of Mt. Asama area show K-Ar ages of 3 ∿ 4 Ma (Kaneoka et al., 1979). A dacite of Mt. Joshu-Hotaka indicates a K-Ar age of about 1.8 Ma (Aoki et al., 1971). These results suggest that the volcanic activity along the present volcanic front already occurred about 1.5 ∿ 2 Ma ago, at least in the Fossa Magna region. The Izu Peninsula, however, seems to have a different history of the volcanic activity based on the geochronological data so far obtained. This may imply that the southern Fossa Magna region has different volcanic activity from that of the northern Fossa Magna region which is separated by the Yatsugatake Volcanoes. Further works are desired to clarify finer structures of volcanic history in this region.

References


Aoki, Y., H. Kase, H. Kinoshita, and K. Ishibashi (1971) J. Geomag. Geoelectr., 23, 129.

Dalrymple, G.B., and M.A. Lanphere (1969) Potassium-Argon Dating, (W.H. Freeman and Company, San Francisco) p. 258.

Kaneoka, I. (1980) Earth Planet. Sci. Lett., 48, 284.

Kaneoka, I., N. Isshiki, and S. Zashu (1970a) Geochem. J., 4, 53.

Kaneoka, I., M. Ozima, and H. Kuno (1970b) J. Geomag. Geoelectr., 22, 559.

Kaneoka, I. and M. Ozima (1970) Bull. Volcanol. Soc. Japan, 2nd Ser., 15, 10 (in Japanese with English abstract).

Kaneoka, I. and M. Suzuki (1970) J. Geol. Soc. Japan, 76, 309.

Kaneoka, I., O. Matsubayashi, S. Zashu, and S. Aramaki (1979) J. Geol. Soc. Japan, 85, 547.

Kawachi, S. (1974-75) Geology of the Tateshinayama district. Quadrangle Series, scale 1 : 50,000, Geol. Surv. Japan, p. 119 (in Japanese with English abstract).

Kawachi, S. (1977) Geology of the Yatsugatake district. Quadrangle Series, scale 1 : 50,000, Geol. Surv. Japan, p. 92, (in Japanese with English agstract).

Kawachi, S. (1979) J. Fac. Sci., Hokkaido Univ., Ser. 19, 19.

Kawachi, S., S. Nakaya, and K. Muraki (1978) Bull. Geol. Surv. Japan, 29, 793.

Momose, K., K. Kobayashi, T. Yamada, M. Ozima and I. Kaneoka (1966) J. Fac. Sci. Shinshu Univ., 1, 93.

Morimoto, R., I. Murai, T. Matsuda, K. Nakamura, Y. Tsuneishi, and S. Yoshida (1966) Bull. Earthq. Res. Inst., Univ. Tokyo, 44, 230 (in Japanese).

Ozima, M., I. Kaneoka, M. Kono, H. Kinoshita, M. Ohnaka, T. Nagata and S. Aramaki (1968) J. Geomag. Geoelectr., 20, 101.

Suzuki, M. (1970) J. Anthrop. Soc. Nippon, 78, 50.


(To be submitted to Geochem. J.)

PALEOMAGNETIC STUDY OF THE SETOUCHI VOLCANIC BELT
PART 1. SHODO-SHIMA ISLAND (PRELIMINARY REPORT)

Masayuki TORII* and Yoshiyuki TATSUMI**

* Department of Geology and Mineralogy, Kyoto University, Kyoto 606
**Earthquake Research Institute, University of Tokyo, Tokyo 113

The Setouchi volcanic belt extends approximately 1,000 km parallel to the Japanese island arc from the western part of Kyushu to the Kanto district (Fig. 1). It includes many small volcano fields, and the predominant rocks are calc-alkaline andesite with subordinate basalt, dacite and rhyolite. Recently precise age determinations of the rocks were carried out by K-Ar method, revealing ages of the middle Miocene (Tatsumi and Yokoyama, 1978; Tatsumi and Ishizaka, 1978; Tatsumi and Ishizaka, 1979; Tatsumi et al., 1980 a,b). The linear arrangement and simultaneous activities of the volcanic rocks should have very close relationship to the plate motion at the time of its subduction. The fashion of the plate motion, possibly the motion of Philippine plate of the middle Miocene time, has not yet become clear. It is, therefore, interesting to study these rocks paleomagnetically to make a precise correlation of each volcano and to detect crustal movement since the time of emplacement of the rocks.

The Shodo-Shima Island is situated in the eastern part of the Seto-Inland Sea, southwestern Japan and is the typical locality for the Setouchi volcanic rocks. We firstly tried to establish a standard magnetostratigraphy of the Setouchi volcanics at this island. The volcanic rocks of the Shodo-Shima Island are divided into two groups, the Sakate and Kankakei volcanics in ascending order (Tatsumi, 1980). The former erupted directly on the basement, and are composed of dacites and rhyolites. The Kankakei volcanics overlies the Sakate volcanics and is composed of andesites and basalts. One of the authors (Y.T) has also divided the Sakate volcanics into six units and the Kankakei volcanics into twelve units. We have collected oriented hand samples at forty-three sites including most of the lavas and dykes.

In this report, we present only preliminary results of the magnetostratigraphy of these rock units. In Table 1, volcanostratigraphy, K-Ar ages, and paleomagnetic polarities of each volcanic unit are summarized. NRMs were measured on a spinner magnetometer after the experiments of the progressive alternating field demagnetization (AFD) for some pilot specimens to decide the optimum cleaning field for each site. Most of NRMs are very stable in response to AFD, and some of them show considerable scattering which are excluded from the further consideration.

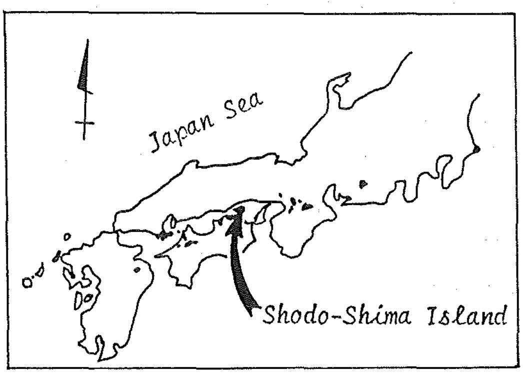


Fig. 1 Distribution of Setouchi volcanic rocks (shaded area) and location of Shodo-Shima Island.

As shown in Table 2, the Sakate volcanics erupted in the period of reversed polarity. Unconformity is recognized between Sakate and Kankakei volcanics. Lowermost volcanic rock of the Kankakei volcanics is Oto-Zan andesite lava which shows normal polarity. Overlying lava (Choshikei andesite, 11.6±0.6 Ma) shows intermediate polarity at several sites. Kiyotaki andesite, Dan-Yama andesite,

| Geologic age | Geologic Units | Polarity |
|---|---|---|
| Holcene | talus breccia, fanglomerates, alluvium | |
| Plio-Pleist. | Umagoe gravel | |
| Miocene | Kankakei volcanics | |
| | Shira-Hama basalt | N(7) |
| | Mito andesite (11.2±0.6 Ma) | N(1) |
| | Fuji-Toge sand and gravel | |
| | Seihou andesite (11.1±0.6 Ma) | ?(1) |
| | Hoshigajo andesite | ?(2) |
| | Kaerugo-Ike pyroclastics, andesite, basalt | R(2) |
| | Dan-Yama andesite | R(2) |
| | Kiyotaki andesite | R(1) |
| | Shin-Kaerugo-Ike pyroclastics | |
| | Choshikei andesite (11.6±0.6 Ma) | I(6) |
| | Kamikake-Yama pyroclastics | |
| | Oto-Zan andesite | N(1) |
| | Sakate volcanics | |
| | Oyayubi-Dake dacite | R(1) |
| | Miya-Yama dacite | |
| | Furue rhyolite | R(1) |
| | Kojima dacite | |
| | Sakate-Seto tuff breccia | |
| | Ino-Tani tuff | |
| | Tonosho Group | |
| Cretaceous | Ryoke complex, "Hiroshima granite" | |
| | Paleozoic sediments | |

Table 1. Summarized table of volcanostratigraphy, K-Ar ages and paleomagnetic polarity of each volcanic units. Number in parenthesis in columm of polarity shows number of site used in this study.

and Kaerugo-Ike basalt have reversed polarity. Uppermost volcanics comprising Mito andesite (11.2±0.6 Ma) and basaltic dykes and necks show again normal polarities. We can not decide NRM polarity of Hoshigajo andesite and Seihou andesite (11.1±0.6 Ma) because of highly scattered directions possibly caused by lightning. Hirooka (1963) has already reported the paleomagnetic study of Shodo-Shima Island. He mentioned about Oto-Zan andesite (normal) and Konoura basalt (normal; one of the uppermost basaltic necks in this study), and our result shows good agreement with his result.

Age determination by fission track method and further paleomagnetic study of Sakate volcanics are now under way. It is difficult to mention about the time gap represented by the unconformity between Sakate volcanics and Kankakei volcanics at this stage. So far as concerning to the Kankakei volcanics, it can be stated that the activity of them started in the period of the normal polarity and ceased next normal polarity period intervening reversed polarity period.

## References


Hirooka, K (1963): Master Thesis of Kyoto University.

Tatsumi, Y and T. Yokoyama (1978): Jour. Japan Assoc. Min. Petr. Econ. Geol., 73, 262-266.

________ and K. Ishizaka (1978): *ibid*, 73, 355-358.

________ and ________ (1979): Jour. Geol. Soc. Japan, 85, 583-585.

________ (1980): Master Thesis of Kyoto University

________, T. Yokoyama, M. Torii and K. Ishizaka (1980): Jour. Japan Assoc. Min. Petr. Econ. Geol., 75, 102-104.

________, M. Torii and K.Ishizaka (1980): Bull. Vol. Soc. Japan, 25, 171-179.

MAGNETIC ANOMALY AND PALEOMAGNETISM
OF THE HAYAMA-MINEOKA OPHIOLITE

Shyoji TONOUCH and Kazuo KOBAYASHI

Ocean Research Institute, University of Tokyo

## Introduction

The ophiolite is primarily defined as a suite of rocks consisting of serpentine, basalt, and chert. It was used by Steiman (1927) in his descriptions of rock associations occuring in the Mediterranean mountain chains. The present-day paradigm considers that the ophiolite forms as the oceanic lithosphere which is generated at midocean ridge and has been slowly migrated by ocean floor spreading toward the continental margins. At the margins the oceanic lithosphere is usually subducted beneath continent. Under some circumstances slabs of the oceanic lithosphere have become overiding the continental margins (obduction) to form outcrops of ophiolite. The mechanism of ophiolite emplacement along the continental margins have been debated.

Recently the DSDP results have indicated that siliceous muds and cherts are widespread in the bottom of sedimentary layer overlying the layer 2 of the northwest Pacific Ocean. It is largely possible that the rigid cherts can be found at many outcrops on land if such oceanic crusts are obducted. It has been generally believed that the layer 2 consists of tholeiitic basalts. The DSDP results have shown that alkali basalts also occur in the Nauru Basin and the Shikoku Basin.

## Hayama-Mineoka Zone

It has been well known that pillow basalts are exposed in the region from the Kamogawa coast of the Boso Peninsula to Kinugasa Town in the Miura Peninsula across Tokyo Bay. Gabbro and dolerite were found in the zone and cristalline schist was found in the Bentenjima at the Kamogawa coast. Ultramafic complexes are emplaced on the Mineoka Hill (Fig.1). This rock association in this area is clearly characteristic of the ophiolite. Chemical composition of these basalts are similiar to those of abyssal tholeiite (Table 1). In the Miura Peninsula the small outcrops of basalts and ultramafic complexes were found near Kinugasa southwest of Yokosuka. Microfossil can be identified in the cherts and siliceous shales, but this age has not been distinctly determined. The basalt from the Kamogawa coast is assumed to be Oligocene (Takigami et al,1980) and mica schist from the Bentenjima is dated to be 38 m.y in age (Yoshida,1974). The Hayama Group overling uncomformally the Mineoka Group is of Miocene (Fig.2).

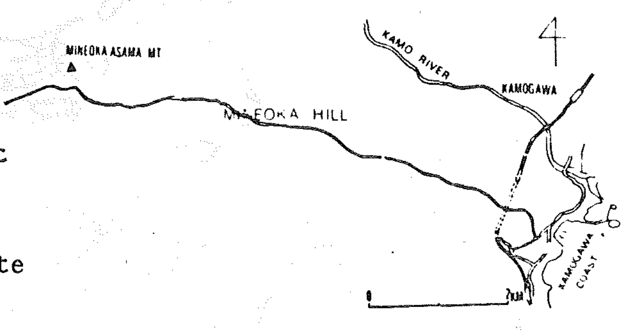


Fig.1. Index Map of Kamogawa and the Mineoka Hill.

| sample no. | 3287 | 3288 | 3290 | 3296 |
|---|---|---|---|---|
| $SiO_2$ | 48.10 | 47.72 | 43.79 | 47.80 |
| $TiO_2$ | 2.23 | 1.77 | 0.65 | 2.10 |
| $Al_2O_3$ | 13.98 | 14.22 | 18.34 | 18.21 |
| $Fe_2O_3$ | 5.70 | 4.36 | 5.58 | 6.80 |
| FeO | 6.73 | 5.58 | 3.85 | 4.61 |
| MnO | 0.22 | 0.28 | 0.17 | 0.21 |
| MgO | 6.30 | 8.02 | 7.74 | 6.17 |
| CaO | 10.78 | 9.05 | 10.76 | 10.11 |
| $Na_2O$ | 2.79 | 3.58 | 2.33 | 3.28 |
| $K_2O$ | 0.13 | 0.14 | 0.72 | 0.59 |
| $H_2O(-)$ | 1.40 | 1.65 | 1.07 | 1.57 |
| $H_2O(+)$ | 1.77 | 3.74 | 5.62 | 2.30 |
| $P_2O_5$ | 0.19 | 0.14 | 0.05 | 0.30 |
| Total | 100.32 | 100.25 | 100.40 | 100.22 |

Table 1. Chemical composition of basalts from Mineoka Group.

This may suggest that this ophiolite was emplaced during Miocene (Fig.2). Thickness of the sediment, basalt and ultramafic layers can not be determined because the rock association was not observed together in one outcrop. It seems likely that many foults occur in the folding zone to form outcrops of each layer with a restricted thickness.

In the Bouger gravity anomaly map (Fig.3), the zone of possitive anomalies (about +60mgal) lies along the Mineoka Gruop from Kamogawa through the Boso Peninsula. This data suggests that the belt of a high density rock is present in the deeper part under this region. Although the detailed gravity anomaly analyses is in progress now, this gravity data implies that occurence of ultramafic rocks in this zone is primary and not transported as rolling stones.

An aeromagnetic survey was made by Hydrographic Department Maritime Safety Agency in and around this area (Fig.4). The negative magnetic anomaly belt greater than 100$\gamma$(nT) in amplitude lies over or slightly in the northern part above the Mineoka Group.

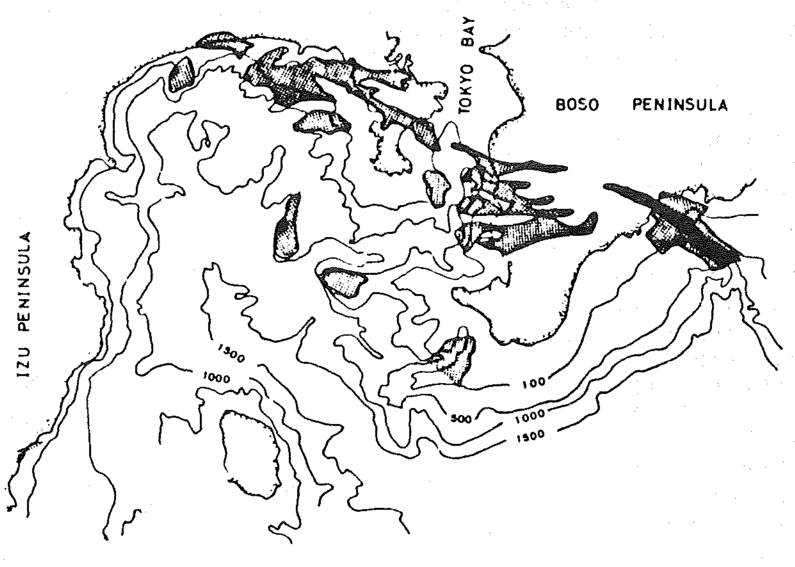


Fig.2. Geological Map of the Boso and Miura Peninsula.
■ ; Mineoka Group, ▒ ; Hayama Group.

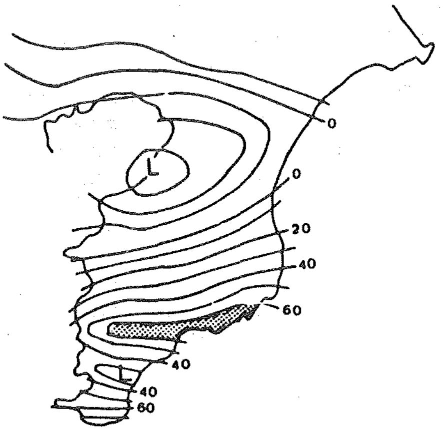


Fig.3. Bouguer gravity anomaly map of the Boso Peninsula (mgal).

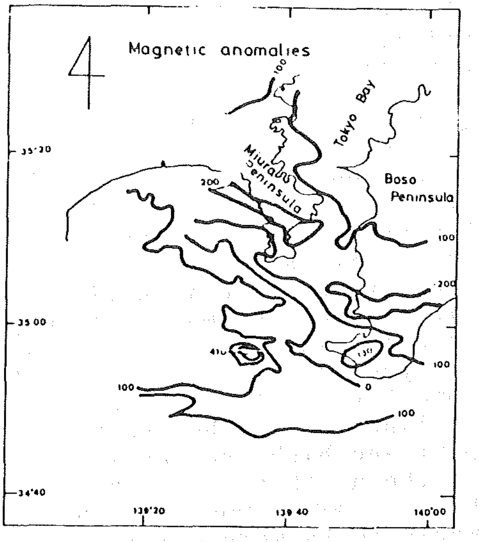


Fig.4. Magnetic anomaly map of the Boso and Miura Peninsula($\gamma$).

Paleomagnetism of the Igneous Rocks from the Hayama-Mineoka Group.

Direction and intensity of the natural remanent magnetization (NRM) of over 250 oriented samples collected 40 sites from the Boso Peninsula to the Miura Peninsula, have been measured.

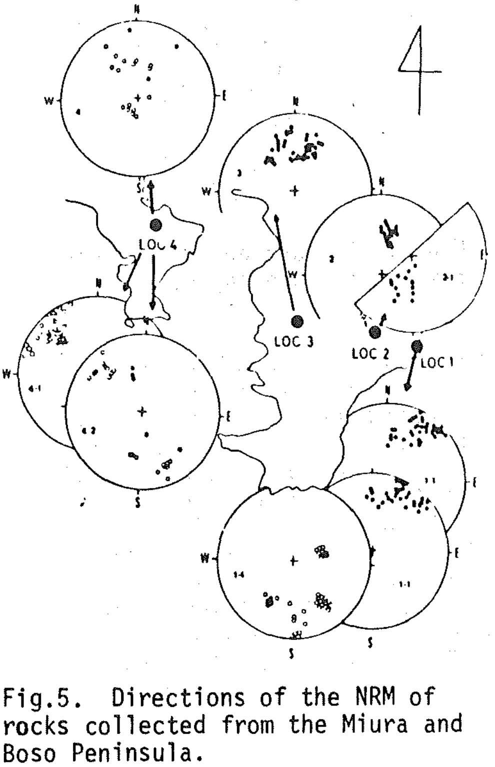


Fig.5. Directions of the NRM of rocks collected from the Miura and Boso Peninsula.

These rocks are basalt, gabbro, dunite and hartzburgite. Stability of the NRM of all samples was tested by the alternating field demagnetization and magnetic field storage test. This result shows that all samples except some ultramafic rocks can be sufficiently used for the paleomagnetic purpose. Susceptibility of the specimens was determined and the Koenigsburger ratio (Qn) was caluculated. Pillow basalts, gabbros and ultramafic rocks have the Qn-values ranging from 3 to 10. Qn of the dike basalts is however from 0.1 to 1, and their Jn and H are about one order of magnetitude smaller than those of pillow basalts. This suggests that the magnetic anomaly is caused by the NRM, regardless of the induced magnetic field parallel to the present geomagnetic field. Gabbro has the Qn-value more than 1 and has the

the NRM intensity larger than those of pillow basalt in some spesimens. Some ultramafic rocks have large Qn-value but these NRM intensities are small. However, the intensity of some serpentinized specimen is large. The directions of the NRM are concentrated if directions are plotted in the Schmit net with samples collected at several sites in one locality. Concentration is better after the specimens were demagnetized by an optimum demagnetization field, 50 or 100 (Fig.5). Although the mean directions at various localities are slight different, Kamogawa (Loc 1), the Mineoka Hill (Loc 2), the west part of the Boso Peninsula (Loc 3), the Miura Peninsula (Loc 4) have mean directions similiar to one another. In some localities rocks were clearly reversed magnetized (e.g.Loc 1-1).
Fig.6 shows the mean paleomagnetic directions averaged for each locality and their relationship with the present direction of the geomagnetic field. The NRMs of the rocks from Hayama-Mineoka zone have generally low inclination in the southern part and high inclination in the north area of the hill. If we assume that the whole rocks were originally horizontal with NRM parallel or antiparallel to the present field and tilted later as shown in Fig.8, general tendency of the observed directions of NRM can be explained. Angle of tilting seems to be about 30° to 40°.

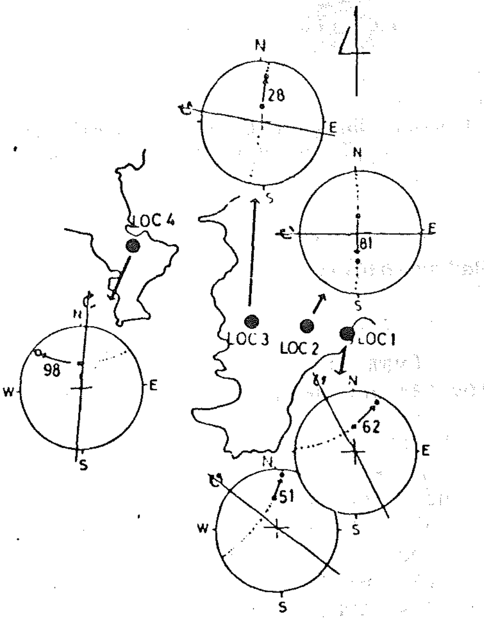


Fig.6. The average directions in respect to each layer.

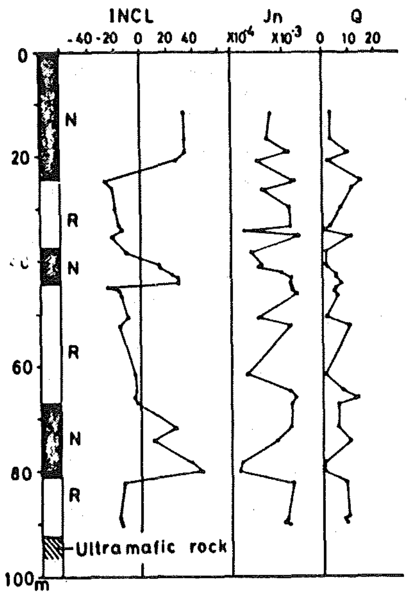


Fig.7. Paleomagnetic results of a boring core from the Mineoka Hill.

If the original inclination is shallower than the present one, as implied from the northward drift of the ocean floor, tilting in the area south of the axis is smaller and that north of it is larger given here. Such tectonic settling of this zone may be tested by examining the overall inclination of pillow surface at each locality.

The NRM of the boring core made near the crest of the

Mineoka Hill (Fig.7). This result shows that three zone of reversed magnetization exsist in the pillow basalt of 92m in thickness. The DSDP result have indicated that a pile of normal and reversed magnetization is generally present in the oceanic layer 2. In the boring core gabbro could not been obtained but serpentinized ultramafic rocks were found. Because the rocks fragmented, the NRM of ultramafic could not been determined.

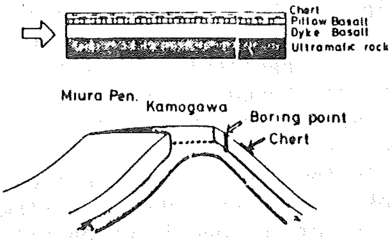


Fig.8. Sectional schematic diagram of the Hayama-Mineoka ophiolite.

Correlation of NRM Directions to Magnetic Anomaly

The belt of negative magnetic anomaly parallel but slightly south to the crest of Hayama-Mineoka ophiolite zone can be explained as a result of the nearly horizontal direction of natural remanent magnetization of basalt and gabbro in a portion south of the crest. As theoretically studied in a consideration of cause of oceanic magnetic lineations, a belt of negative magnetic anomaly is observed on a horizontal magnetic bar situated with its elongated axis trending east-west and magnetized horizontally northward.
If normal and reversed directions of magnetization of upper pillow lavas are alternating as found in the boring core, the source of anomaly lies in the lower pillows or gabbro.

Since the total amount of ophiolite body in the zone north of the crest seems to be much smaller than that in the south as expected from the graben -like topography in the northern zone, magnetic effect of the northern body may be negligible compared to that of the southern one.

Suture Belt as a Paleo-plate Boundary in Bōsō, Miura and Izu Area

From paleomagnetic results reported here and other evidences from petrological and geotectonic investigation, it seems quite likely that the ophiolite suite occurring in the Hayama-Mineoka zone is a part of remnant oceanic lithosphere (crust and uppermost mantle).
It implied that a deep ocean floor existed here at one time. Kinoshita (1980) indicated from paleomagnetic measurement of the DSDP rocks (site 445 of leg 58) that the Philippine Sea floor has drifted northward since Eocene.
It appears plansible that the southern portions of Boso and Miura Peninsulas together with Izu Peninsula were situated further south with wide ocean floor separating them from the northern portions of these peninsulas and central Honshu. As the northward drift of ocean floor proceeded, the ocean floor subducted under the northern continental mass from a paleotrench situated along the present Hayama-Mineoka zone . Mica schist found at Bentenjima was formed in this subducted lithosphere.

The southern portions of Boso and Miura Peninsulas which have the crust with continental structure drifted gradually northward and collided with the northern masses at one time. The subduction along this trench ceased and a reminder of the ocean floor was obducted to form the Hayama-Mineoka ophiolite. Exactly age of the collision is still unknown from microfossils contained in the Hayama Foramation (20 to 15 m.y BP),but it appears to be Oligocene to early Miocene overlying the ophiolite layer.

Somewhile after the collision occured, a new subduction started possibly along the present Sagami, Suruga and Nankai troughs. Direction of the present plate mortion relative to Honshu revealed by focal mechanism of earthquakes along these troughs is WNW and is quite different from at periods older than 12 m.y BP, which was derived from the paleostress analyses using shapes of intrusive bodies ( Takeuchi et al,1979).

At present the Izu Peninsula is colliding with Honshu but the line of collision may be different from that at the previous age when the southern portions of Boso and Miura Peninsulas also collided. Ishibashi (1978) suggested from seismicity data that a new subduction is being created in an area south of the Izu peninsula. If such a zone of subduction comes at work, the present Sagami and Suruga troughs become a suture zone associated with the ophiolite belt. Nankai trough will then be connected to the Japan and Izu-Bonin trenches more straightly.

In the present article a westward extension of the suture zone in the Shizuoka Prefecture, Honshu northwest of the Suruga trough has not been dealt with. A suture zone in which pillow basalts and ultramafics are exposed is also reported in this area. Paleomagnetic and geotectonic investigation is now underway by the authors.

References

Earth Monthly (1979).5
Ishibashi,K.(1978).Geodynamic Conference.
Kinoshita,H.(1980) Initial Rep. DSDP Leg 58,765.
Koike,K.(1975) Chikyu kagaku.11,1 (in Japanese).
Nasu,K.(1976) Kaiyochihitu,155.
Report of the Coordinating Committee for Earthquake Prediction(1979).
Takigami,y.,I.Kaneoka and S.Hirano(1980) Bull.Volcanol.Soc.25(in press).
Takeuchi,A.,K.Nakamura.,Y.Kobayashi and K.Hori(1979) Chikiyu.6,447.

# A PALEOMAGNETIC APPROACH TO POSSIBLE TILTING MOVEMENTS OF KITAKAMI MOUNTAINS AND OSHIMA PENINSULA OF HOKKAIDO

Haruaki ITO, Katsuyasu TOKIEDA and Yukio NOTSU

Department of Physics, Shimane University, Matsue 690

Paleomagnetic studies of Cretaceous rocks of the Kitakami mountains have been reported by several workers (Kawai et al., 1961; Kato and Muroi, 1965; Fujihara, 1966; Kawai et al., 1971). On the other hand, we reported results of preliminary paleomagnetic study of Cretaceous granitic rocks in the Oshima peninsula of Hokkaido (Ito and Tokieda, 1974). The results showed that NRM directions of granitic rocks in the Oshima peninsula are clearly different from those of Cretaceous rocks in the Kitakami mountains. To identify this difference in NRM directions between the Oshima peninsula and the Kitakami mountains, we undertook more detailed Paleomagnetic studies of Cretaceous granitic rocks in the Kitakami mountains.

Granite bodies in various dimensions of the early Cretaceous are widely exposed in the Kitakami mountains and the Oshima peninsula of Hokkaido. The granitic rocks in the Kitakami mountains were preliminary grouped into eight zones by Katada et al. (1971), and then Katada (1974) redivided them into six zones on the basis of the mode of occurrence, megascopical features and petrography. On the other hand, Kano (1978) classified them in two groups of the P-type which is plutons of mesozone in the lower Paleozoic terrain and the M-type which is plutons of epizone in the upper Paleozoic and Mesozoic terrain.

K-Ar age data reported by Shibata and Miller (1962) and Kawano and Ueda (1964, 1965) indicate that granite masses in the Kitakami mountains and the Oshima peninsula of Hokkaido were mainly emplaced in the early Cretaceous (110-125 m.y.). Accroding to Katada (1974), it seems likely that intrusive rocks of zones II, V and VI in the Kitakami mountains were emplaced after intrusions of zones I, III and IV, but a difference in the time of intrusion appears to be geologically insignificant.

Oriented hand samples for the paleomagnetic study were collected from 43 sites in 20 bodies in the Kitakami mountains as shown in Figure 1. Ten to fifteen hand samples were taken from each site. In the Oshima peninsula of Hokkaido, about one hundred hand samples were collected from 9 sites in four bodies (Ito and Tokieda, 1974). Two core samples were usually drilled from each hand sample in the laboratory and the NRM of all core samples was measured with a spinner magnetometer.

Ten or more core samples at all the sampled sites in the Kitakami mountains were magnetically demagnetized and a few core samples were thermally demagnetized. Consequently, remanent vectors of samples at 27 sites were found to be stable

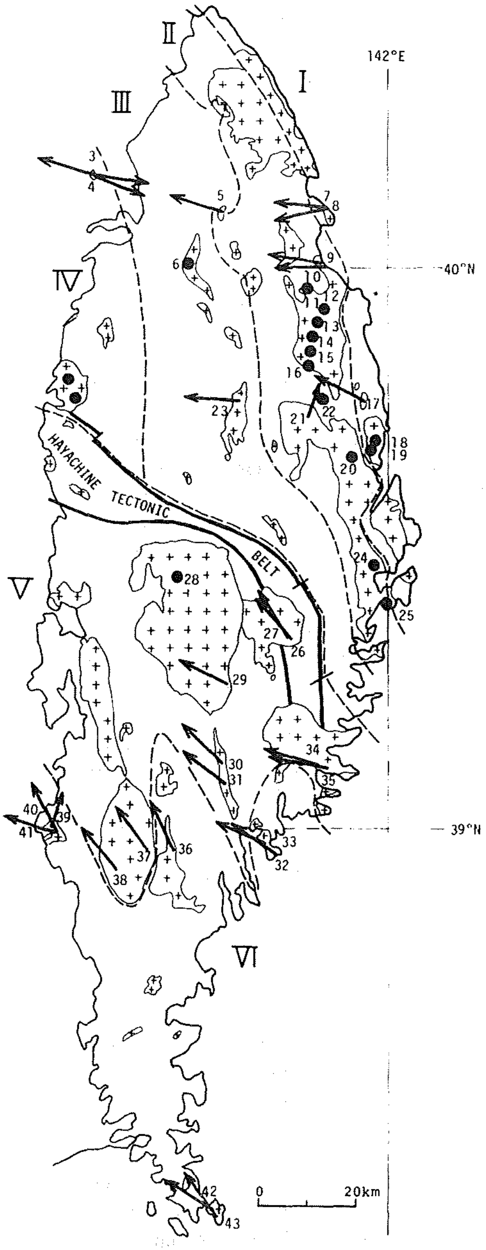


Fig. 1. Locations sampled in the Kitakami mountains. Arrows represent the declinations of site mean direction of stable sites. Closed circles represent unstable sites.

and to display intrasite consistency. Twenty three sites had circles of 95 percent confidence of less than 10.0° and four sites had those of 10.0° to 20.0°. However, the remaining sixteen sites having circles of 95 percent confidence of greater than 20.0° were excluded from the data of Table 1 and Figure 2 as unstable or inconsistent sites. Such unstable or inconsistent sites are indicated by the numbered closed circles in Figure 1. Site mean directions of NRM at the stable and consistent sites after magnetic cleaning are shown in Figure 2. The sites 21 and 39 are excluded from this figure.

As seen in Figure 2, the site mean directions at the stable sites were classified in two groups from a significant difference in direction. This would indicate that the granitic rocks in the Kitakami mountains are paleomagnetically divided into two groups of northern Kitakami region and southern Kitakami region. The boundary between these two regions is the Hayachine tectonic belt as shown in Figure 1. The site mean directions of NRM in the northern Kitakami region are extremely deflected from the geographic north to the west as seen in Figures 1 and 2. A mean paleomagnetic direction for the northern Kitakami was NW 81° in declination and 22° in inclination and that of reversed samples was SE 73° and -24°. On the other hand, the site mean directions of NRM in the southern Kitakami was also uniformly deflected to the west, and a mean paleomagnetic direction was NW 48° and 51°.

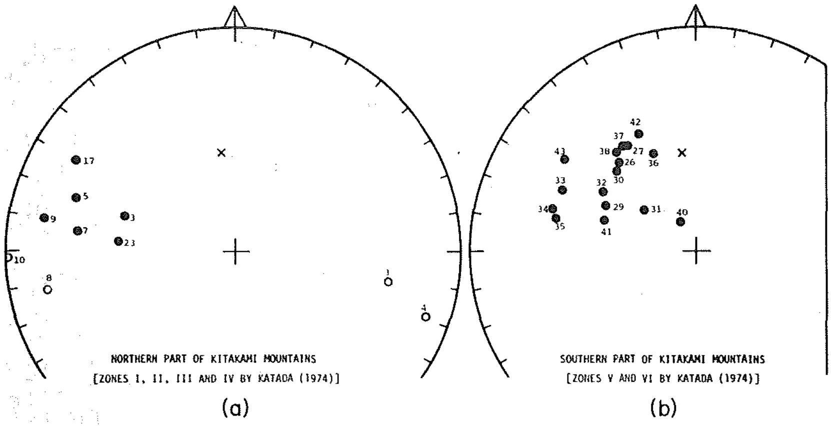


Fig. 2. Site mean directions of granitic rocks in the Kitakami mountains. Cross mark is the present field direction.

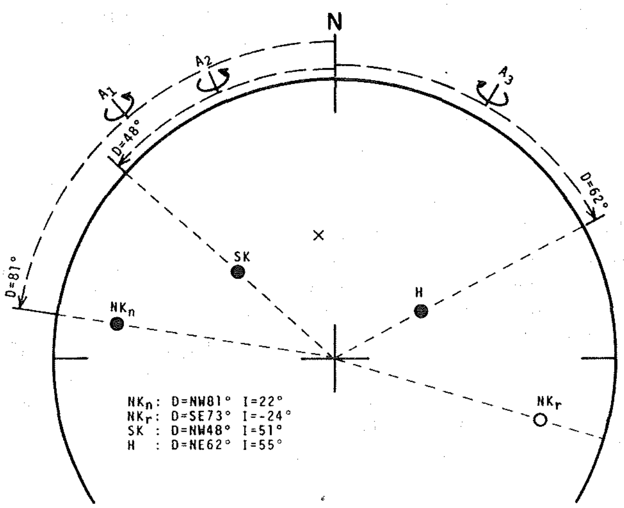


Fig. 3. Rotations about horizontal axes. $A_1$ represents a horizontal axis for the northern Kitakami region. $A_2$ represents a horizontal axis for the southern Kitakami region. $A_3$ represents a horizontal axis for the Oshima peninsula of Hokkaido. Cross mark is the present field direction.

To account for these paleomagnetic data, we discuss three general cases of tectonic rotational movements. (1) Intrusive rocks had undergone clockwise or counterclockwise rotation about earth radial or vertical axes after acquisition of magnetization as previously proposed by Kawai et al. (1961). (2) Intrusive rocks had undergone tectonic rotation about horizontal axes as proposed by Ito and Tokieda (1974). (3) Intrusive rocks had been affected by more complex rotation about inclined axes.

According to the K-Ar age data by Shibata and Miller (1962) and Kawano and Ueda (1964, 1965), the granitic rocks in the Kitakami mountains and the Oshima peninsula are considered to have almost been coeval intrusions. Therefore, we currently assume that original magnetic directions of these granitic rocks had been approximately consistent with each other and also nearly closed to the present geographic poles.

$A_1$, $A_2$ and $A_3$ in Figure 3 represent horizontal axes for the northern Kitakami, southern Kitakami and Oshima peninsula. The bisectors between the observed declinations and the geographic north were simply selected as the horizontal axes $A_1$, $A_2$ and $A_3$. The orientations of these axes $A_1$, $A_2$ and $A_3$ are NW 40°, NW 24° and NE 31° respectively. Apparent rotation angles about the horizontal axes, which may restore the observed declinations to the original one, are estimated to be 51°, 32° and 40° respectively. On the other hand, rotation angles about vertical axes are 81°, 48° and 61°. The angles are equivalent to the observed mean declinations for each region. It is accordingly evident that the rotation angles about the horizontal axes are less than those about the vertical axes. However, in the three general cases, rotation angles about inclined axes should be minimum.

Tilt is clearly produced by rotation about a horizontal or inclined axis, i. e., rotations about horizontal axes or inclined axes correspond to tilting movements of rock masses. A fact that the rotation angles about the horizontal axes are less than those about the vertical axes suggests that the Kitakami region and the Oshima peninsula region were mainly affected by some tilting movements of granite masses It was previously concluded that the granitic rocks in the Oshima peninsula had been tilted to the Japan Sea side and those in the Kitakami mountains to the Pacific Ocean side during upward movements (Ito and Tokieda, 1974). However, it may be necessary that we select two rotation axes for the Kitakami mountains as described above.

## References


Fujihara, Y. (1966); J. Fac. Sci. Hokkaido Univ., Series IV, Vol. XIII, No 3, p293.

Ito, H. and K. Tokieda (1974); Rock Mag. Paleogeophys., Vol. 2, p54.

Kano, H. (1978); J. Japan. Assoc. Min. Petr. Econ. Geol., Vol. 73, p97.

Katada, M., H. Onuki, Y. Kata, S. Kanisawa, C. Ono and M. Yoshii (1971); J. Japan. Assoc. Min. Petr. Econ. Geol., Vol. 65, p230.

Katada, M. (1974); Report No 251, Geol. Surv. Japan, p121.

Kato, Y. and I. Muroi (1965); Ann. Progr. Rept. Rock Mag. Res. Group Japan, p179.

Kawai, N., H. Ito and S. Kume (1961); Geophys. J. Roy. Astro. Soc., Vol. 6, p121.

Kawai, N., T. Nakajima and K. Hirooka (1971); J. Geomag. Geoelectr., Vol. 23, p263.

Kawano, Y. and Y. Ueda (1964); J. Japan. Assoc. Min. Petr. Econ. Geol., Vol. 51, p127.

Kawano, Y. and Y. Ueda (1965); J. Japan. Assoc. Min. Petr. Econ. Geol., Vol. 53, p143.

Shibata, K. and J. A. Miller (1962); Bull. Geol. Suv. J., Vol. 13, p709.

Table 1. Paleomagnetic data for granitic rocks in the Kitakami mountains

| Site | Number | Location Latitude | Location Longitude | N | $J_r$ (emu/gr) | Mean Direction Decl. | Mean Direction Incl. | k | $\alpha_{95}$ | Age, m.y. |
|---|---|---|---|---|---|---|---|---|---|---|
| 1 | Himekami-yama | 39°50'N | 141°14'E | - | - | - | - | - | - | 110,115 |
| 2 | Himekami-yama | 39°48'N | 141°15'E | - | - | - | - | - | - | 110,115 |
| 3 | Ichinohe | 40°13'N | 141°17'E | (4<br>4 | $6.31 \times 10^{-6}$<br>$9.74 \times 10^{-6}$ | 287.6°<br>101.3° | 47.5°<br>-30.5° | 244.7<br>21.8 | 5.9°)<br>20.0° | 106,116 |
| 4 | Ichinohe | 40°14'N | 141°17'E | 8 | $4.34 \times 10^{-6}$ | 108.8° | -10.4° | 30.2 | 10.2° | 100,107,111 |
| 5 | Numabukuro | 40°09'N | 141°36'E | 8 | $9.68 \times 10^{-6}$ | 288.4° | 26.2° | 43.8 | 8.5° | 120 |
| 6 | Hiraniwa | 40°04'N | 141°31'E | - | - | - | - | - | - | 117 |
| 7 | Kosode-kaigan | 40°11'N | 141°50'E | 10 | $4.80 \times 10^{-6}$ | 277.2° | 30.9° | 25.2 | 9.8° | 120 |
| 8 | Kosode-kaigan | 40°10'N | 141°50'E | 8 | $2.27 \times 10^{-5}$ | 257.9° | -17.1° | 214.6 | 3.8° | 120 |
| 9 | Shimoakka | 40°03'N | 141°51'E | 12 | $7.82 \times 10^{-6}$ | 279.9° | 16.0° | 11.4 | 13.5° | 112,117 |
| 10 | Ōtanabe | 40°01'N | 141°54'E | 10 | $1.66 \times 10^{-5}$ | 268.5° | - 0.3° | 89.5 | 5.1° | 112,117 |
| 11 | Akka | 40°01'N | 141°47'E | - | - | - | - | - | - | 122 |
| 12 | Sukō | 39°58'N | 141°52'E | - | - | - | - | - | - | 121 |
| 13 | Numabukuro | 39°57'N | 141°50'E | - | - | - | - | - | - | 121 |
| 14 | Hosozawa | 39°55'N | 141°49'E | - | - | - | - | - | - | 118 |
| 15 | Natsufushi | 39°53'N | 141°48'E | - | - | - | - | - | - | Cretaceous |
| 16 | Uchinosawa | 39°52'N | 141°48'E | - | - | - | - | - | - | 122 |
| 17 | Kurumihata | 39°48'N | 141°56'E | 9 | $5.66 \times 10^{-6}$ | 300.0° | 19.7° | 49.7 | 7.4° | 114 |
| 18 | Taro | 39°44'N | 141°58'E | - | - | - | - | - | - | 121 |
| 19 | Taro | 39°43'N | 141°58'E | - | - | - | - | - | - | 121 |
| 20 | Sabane | 39°42'N | 141°55'E | - | - | - | - | - | - | 112 |

Table 1. (continued)

| Site Number | Location Latitude | Longitude | N | $J_r$ (emu/gr) | Mean Direction Decl. | Incl. | k | $\alpha_{95}$ | Age, m.y. |
|---|---|---|---|---|---|---|---|---|---|
| 21 Uge | 39°45'N | 141°49'E | 6 | $7.09 \times 10^{-6}$ | 19.6° | 49.9° | 52.8 | 9.3° | 112 |
| 22 Takshimizu | 39°48'N | 141°50'E | - | - | - | - | - | - | 114,120 |
| 23 Ōkawa | 39°48'N | 141°38'E | 11 | $1.11 \times 10^{-5}$ | 275.3° | 47.0° | 36.9 | 7.6° | Cretaceous |
| 24 Yamaya | 39°30'N | 141°58'E | - | - | - | - | - | - | 123 |
| 25 Tanohama | 39°25'N | 141°59'E | - | - | - | - | - | - | Cretaceous |
| 26 Haginohora | 39°22'N | 141°46'E | 10 | $1.03 \times 10^{-5}$ | 319.7° | 46.7° | 20.4 | 11.0° | 115,122 |
| 27 Ōkuchi | 39°21'N | 141°43'E | 10 | $1.06 \times 10^{-5}$ | 327.4° | 43.5° | 38.5 | 7.9° | 120,126,129 |
| 28 Ōde | 39°28'N | 141°31'E | - | - | - | - | - | - | 114 |
| 29 Akabane-toge | 39°15'N | 141°36'E | 12 | $4.97 \times 10^{-5}$ | 297.1° | 52.8° | 111.2 | 4.1° | 119 |
| 30 Taya | 39°07'N | 141°35'E | 14 | $3.01 \times 10^{-5}$ | 315.7° | 48.8° | 85.7 | 4.3° | 112 |
| 31 Kurentsubo | 39°05'N | 141°35'E | 11 | $1.75 \times 10^{-5}$ | 309.5° | 66.1° | 92.7 | 4.8° | 112 |
| 32 Nesaki | 38°57'N | 141°43'E | 15 | $2.66 \times 10^{-5}$ | 303.1° | 49.2° | 100.6 | 3.8° | Cretaceous |
| 33 Ōyo | 38°58'N | 141°41'E | 10 | $1.05 \times 10^{-5}$ | 295.4° | 34.5° | 92.3 | 5.1° | Cretaceous |
| 34 Okirai | 39°07'N | 141°49'E | 11 | $2.81 \times 10^{-4}$ | 287.4° | 33.9° | 65.3 | 5.7° | 107,116 |
| 35 Okirai | 39°07'N | 141°50'E | 11 | $4.83 \times 10^{-5}$ | 284.3° | 36.4° | 43.0 | 7.0° | 107,116 |
| 36 Murone-san | 38°58'N | 141°27'E | 10 | $1.08 \times 10^{-5}$ | 337.3° | 50.5° | 36.0 | 8.2° | Cretaceous |
| 37 Kiyota | 38°56'N | 141°24'E | 11 | $1.53 \times 10^{-5}$ | 325.8° | 42.9° | 55.2 | 6.2° | 114,119 |
| 38 Senmaya | 38°54'N | 141°20'E | 12 | $1.33 \times 10^{-5}$ | 321.8° | 42.7° | 79.0 | 4.9° | 114,119 |
| 39 Tabashine-yama | 39°00'N | 141°11'E | 10 | $8.06 \times 10^{-5}$ | 17.0° | 47.9° | 84.3 | 5.3° | Cretaceous |
| 40 Tabashine-yama | 39°00'N | 141°11'E | 10 | $2.32 \times 10^{-5}$ | 333.8° | 78.2° | 88.7 | 5.2° | Cretaceous |

Table 1. (cintinued)

| Site Number | Location Latitude | Longitude | N | $J_r$ (emu/gr) | Mean Direction Decl. | Incl. | k | $\alpha_{95}$ | Age, m.y. |
|---|---|---|---|---|---|---|---|---|---|
| 41 Tabashine-yama | 39°00'N | 141°12'E | 11 | $2.42 \times 10^{-5}$ | 289.2° | 54.2° | 52.1 | 6.4° | Cretaceous |
| 42 Kinkasan | 38°17'N | 141°33'E | 5 | $1.82 \times 10^{-5}$ | 334.9° | 40.9° | 27.9 | 14.7° | 119,120 |
| 43 Kinkasan | 38°17'N | 141°34'E | 10 | $1.19 \times 10^{-4}$ | 305.8° | 29.2° | 81.6 | 5.4° | 109 |

N is the number of samples; $J_r$ is the intensity of natural remanent magnetization after AF demagnetization of 100 to 1200 oe; k is the Fisher's precision parameter; $\alpha_{95}$ is the semi-angle of cone of 95 percent confidence for the site mean direction.

A PALEOMAGNETIC STUDY ON TRIASSIC-JURASSIC SYSTEM IN INUYAMA AREA, CENTRAL JAPAN (PART I)

Hidetoshi SHIBUYA and Sadao SASAJIMA

Department of Geology and Mineralogy, Kyoto University, Kyoto 606

## Introduction

In Japan few systematic paleomagnetic studies were made so far pre-Cretaceous rocks. Fujiwara (1968) compiled 16 pre-Tertiary paleomagnetic results, and stated that the paleolatitude of Japan was low in the age from the Middle Devonian to the Late Triassic. The data were too few to establish this conclusion. Hattori and Hirooka (1977 and 1979) made a systematic study on Permian greenstones of the northern part of Mino belt and concluded that the paleolatitude was low on the Permian period. In a recent summary of the Japanese paleomagnetic results published so far by many scientists, one of the present writers has confirmed the low pleolatitude of Honshu during the period of Late Paleozoic to Early Jurassic (Sasajima, 1980), however, the conclusion is led from still insufficient results and much more results are being expected before the conclusion is established. This study is presented as a supplement supporting the weak conclusion.

Paleomagnetic measurements on Late Mesozoic and Cenozoic rocks in Southwest Japan have been summarized by Yaskawa and Nakajima (1974), and the paleolatitude of the Cretaceous time is estimated at about 41°N by them. It is important to determine the time when the paleolatitude became high between the Late Permian and Cretaceous periods.

Chert, mudstone and sandstone members, Triassic to Jurassic in age, are exposed along the riversides of Kiso (35°22'N, 136°58'E) in Inuyama area on the southern part of Mino belt. The different ages of the sequences were precisely identified by Yao et al. (1980) by the combination of both radiolarians and conodonts, of which result is illustrated in Fig. 1. They concluded that four sequences of thin chert beds intercalated by thinner siliceous mudstone in the area are ranging from Middle Triassic to Lower Jurassic in age, and mudstone and sandstone members are ranging from Middle to Upper Jurassic in age.

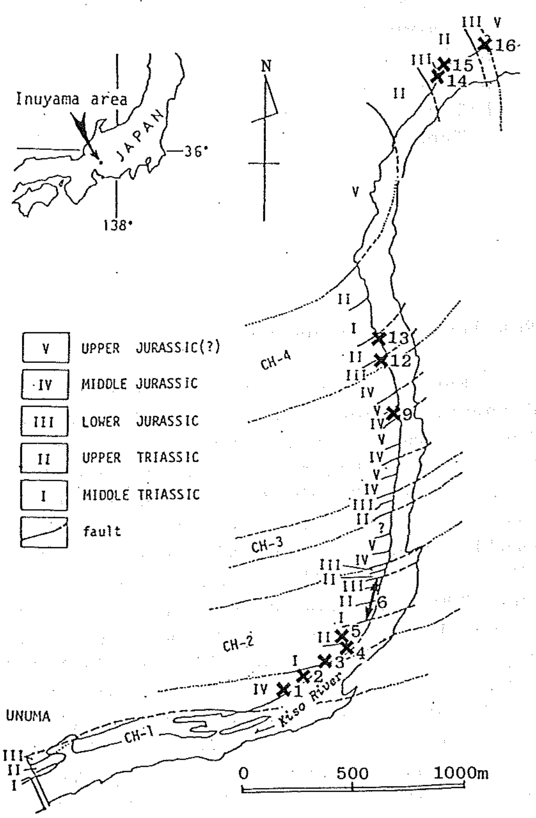


Fig. 1. Map showing the distribution of five major units along the Kiso River. Cert beds are CH-1~CH-4. Sample locations are indicated by crosses. (Modified from Yao et al., 1980)

## Experimental Procedure

About 180 hand samples of red chert and red siliceous mudstone were collected from the area. No samples were collected from the Upper Jurassic member because mudstone could not be found in the strata. The sampling sites are also indicated in Fig. 1. A few core specimens sized 22.5mm in both diameter and height were drilled from each sample in the laboratory. The paleomagnetic measurements were performed using a Schonstedt SSM-1A spinner magnetometer. The bedding plane of the strata from which each hand sample was taken was clearly measured, hence tilting correction was precisely performed in reference to the plane.

Stepwise alternating field demagnetization (A.F.D.) up to 1,000 Oe was applied to a few specimens for each site. Furthermore, one specimen at least from each sampling site was subjected to stepwise thermal demagnetization (Th.D.). Thermomagnetic analyses of the ferromagnetic minerals responsible for natural remanent magnetizations (N.R.M.s) were done under a higher field (3-5 KOe). Some typical examples are illustrated in Fig. 2.

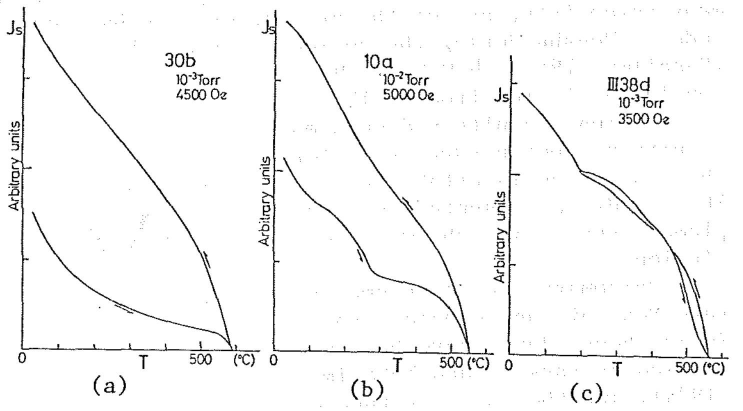


Fig. 2. Results of thermomagnetic analyses.
(a) Type A (site 6)
(b) Type B (site 6)
(c) Type D (site 9)

## Results and Discussions

Based on the remanent magnetization behaviors of the chert under A.F. demagnetization process, samples can be classified into two types, A and B. Type A samples, whose age is the Middle Triassic (sites 3, 4 and the lower half of site 6), possess a considerably large median destructive field (M.D.F.) of 200-600 Oe leaving 15% or more of their initial remanent intensity at 1,000 Oe peak field. The directional change of them is within a smaller range of several degrees while A.F. is steped up to 800 or 1,000 Oe (Fig. 3a) after the viscous remanent magnetizations are cleaned by A.F. less than 200 Oe. Contrary to this, type B samples, whose ages were estimated at the Upper Triassic or Lower Jurassic (sites 5, 12-16 and the upper half of site 6), are defined by a small M.D.F. (50-200 Oe) and unstable directional changes through the stepwise A.F.D. (Fig. 3b). The N.R.M. intensity of the chert samples is ranged in the order of $10^{-6}$ e.m.u./g.

Remanent magnetizations of the Middle Jurassic mudstone are also classified into two types, C and D. The pattern of the directional change of type C samples (sites 1 and 2) through stepwise A.F.D. is similar to that of the type A. M.D.F. of type C is within a range 600-1000 Oe. Type D samples, tuffaceous mudstone in lithology (site 9), have a relatively small M.D.F. (100-200 Oe). The remanent directions of type D samples are changed about a few tens of degrees with increasing field of the demagnetization (Fig. 3c), but they seem to converge each other into the peak field of about 300 Oe. Then, all other specimens from site 9 were demagnetized by three

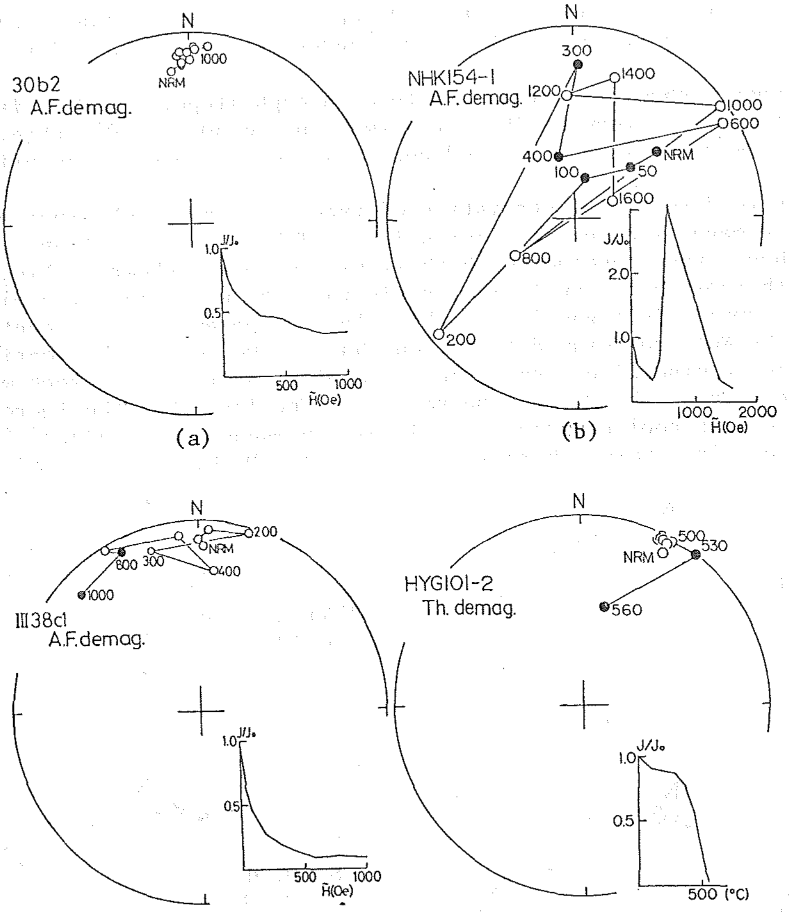


Fig. 3. Typical examples of remanent magnetization change by A.F. and Th. demagnetization. Solid circles represent positive inclination and open circles represent negative inclination.
(a) Type A (site 6) (b) Type B (site 12)
(c) Type D (site 9) (d) Type C (site 1)

| Age | Site | Dec | Inc | $\alpha_{95}$ | k | N | P.Lat. | Treatment |
|---|---|---|---|---|---|---|---|---|
| M.Jr. | 1 | 23.6 | -5.6 | 5.7 | 83.8 | 9 | -2.8 | AFD 300 Oe |
| | 2 | 5.6 | 5.1 | 7.1 | 35.0 | 13 | 2.6 | AFD 300 Oe |
| | 9 | -18.6 | -6.8 | 9.6 | 11.4 | 22 | -3.4 | AFD 300 Oe |
| M.Tr. | 3 | -12.8 | -34.0 | 6.2 | 39.0 | 15 | -18.6 | AFD 300 Oe |
| | 4 | -7.9 | -9.4 | 7.7 | 30.3 | 13 | -4.7 | AFD 300 Oe |
| | 6 (lower half) | 6.3 | -23.2 | 11.9 | 7.2 | 24 | -12.1 | AFD 200 Oe |

Table 1. The site directional statistics of tyapes A, C and D.

steps in A.F., 200, 300 and 400 Oe, in order to determine the most suitable demagnetization level in which their directions are most tightly clustered. The intensity of N.R.M. of red mudstones is in the order of $10^{-5}$ e.m.u./g.

The sample showing a stable feature through stepwise A.F.D. is also stable through the stepwise Th.D. treatment up to 500°C-550°C (Fig. 3d) where the remanence is sharply reduced to a few percents of the original value.

The site directional statistics of types A, C and D obtained after 200 or 300 Oe demagnetization are listed in the Table 1. Directions of specimens of these types together with their site mean are shown in Fig. 4.

The thermomagnetic analysis reveals that the major magnetic mineral of type D samples is magnetite of which lattice parameter was identified as 8.397Å by Nolerco X-ray diffraction chart. We could not identify the major magnetic mineral of type A and C samples, as the Js of rock was too small to determine the Curie temperature. The fact that the increasing of intensity during cooling process is due to fine magnetites produced from the reduction of fine-grained hematites (Shive and Diehl, 1977; Sasajima and

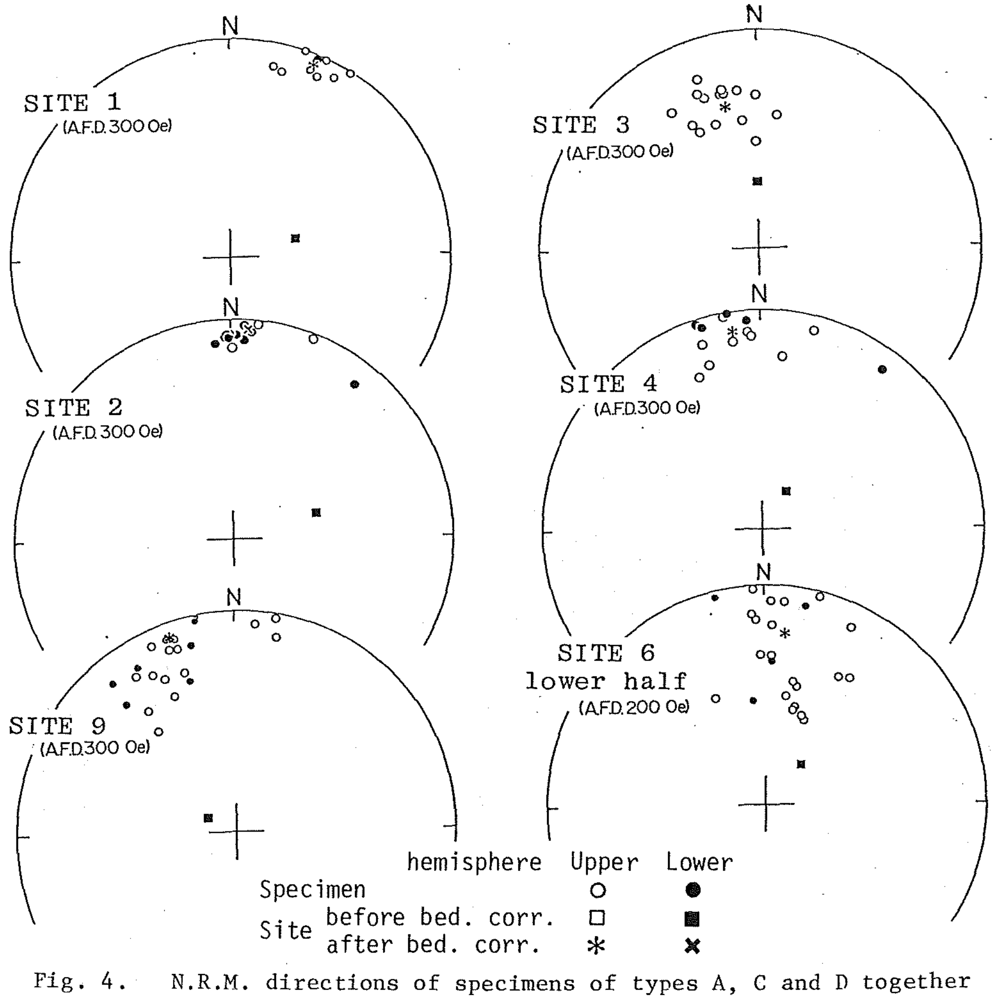


Fig. 4. N.R.M. directions of specimens of types A, C and D together with their site mean after 200 or 300 Oe demagnetization.

Torii, 1980) suggests the presence of hematites in the original specimen. We cannot find it under the microscope directly, however it is supported indirectly by the fact that hematite crystals with the size of 500Å x 2000Å were found in chert from Tanba belt with the use of Hitachi 700H 200KV Analytical Electron Microscopy (Kitamura 1980, personal communication). The high M.D.F. of these samples could be explained by fine-grained hematites. Type B sample is also suggested to include hematite, but it has a different phase whose Curie temperature is low. It may be the major cause of magnetic instability of these samples.

By the assumption that the magnetization is primary, which will be ascertained by more detailed studies, we can derive following conclusion. Considering from the fact that the Middle Jurassic time is regarded, in general, as a normal tranquil interval (Graham Interval; McElhiny and Burek, 1971), the polarity of the remanence of rocks acquired in that time would be expected to have been normal. The paleopositions of the Inuyama area of Mino belt has negative values, and is calculated to be about 11°S and 1°S in the Middle Triassic and Middle Jurassic, respectively. It seems to have become high on Late Jurassic or Early Cretaceous.

## References


Fujiwara, Y. (1968) J. Fac. Sci. Hokkaido Univ., Ser. IV, 14, 159-168.

Hattori, I. and K. Hirooka (1977) J. Japan. Assoc. Min. Pet. Econ. Geol., 72, 340-353.

Hattori, I. and K. Hirooka (1979) Tectonophys., 57, 211-235.

McElhinny, M.W. and P.J. Burek (1971) Nature, 232, 98-102.

Sasajima, S. (1980) GDP Report, A.G.U. (in press).

Sasajima, S. and M. Torii (1980) in this issue.

Shive, P.N. and J.F. Diehl (1977) J. Geomag. Geoelectr., 29, 345-354.

Yao, A., T. Matsuda and Y. Isozaki (1980) J. Geosci., Osaka City Univ., 23, 135-154.

Yaskawa, K. and T. Nakajima (1974) J. Geol. Soc. Japan, 80, 215-224. (in Japanese with English abstract)

PRELIMINARY PALEOMAGNETIC STUDIES ON THE PERMIAN AND TRIASSIC ROCKS FROM OKINAWA-JIMA, RYUKYUS, SOUTHERN JAPAN

Sadao SASAJIMA and Masayuki TORII

Department of Geology and Mineralogy, Kyoto University, Kyoto 606

## 1. Introduction

One of highlights in paleomagnetism of Honshu, main island of Japan, is concerned with a significant drift of the island. Whether it has experienced a large drift or no during some time of Pre-Tertiary is a matter for argument paleomagnetically (Nur and Ben-Avraham, 1978; Hattori and Hirooka, 1979; Sasajima, 1980).

Honshu and Ryukyu arcs embrace toward the Asian continent marginal seas, the Japan sea and East China sea, respectively. The geological structure of the two arcs is closely related in their framework intervening Kyushu island between them (Konishi, 1965; Kizaki, 1978). Under such circumstances, Pre-Tertiary paleomagnetic study on Ryukyu arc is of importance, particularly associating with that of the same period in Southwest Honshu. Results of the present study are a supplementary evidence supporting the supposition that the Honshu was situated at some lower latitude near the paleoequator during the Permian to Triassic times (Sasajima, 1980).

Tertiary paleomagnetic studies on Ryukyu arc have already been reported by one of the present authors (Sasajima and Shimada, 1965; Sasajima, 1977). One of characteristic features of the result is that the apparent polar wandering path for the southwestern subarc shows a remarkable feature similar to that for Southwest Honshu. Recently, paleomagnetic investigation of Permian and Triassic sedimentary rocks developed in the Motobu Peninsula of Okinawa-jima has been carried out. An outline of the result is presented in this paper.

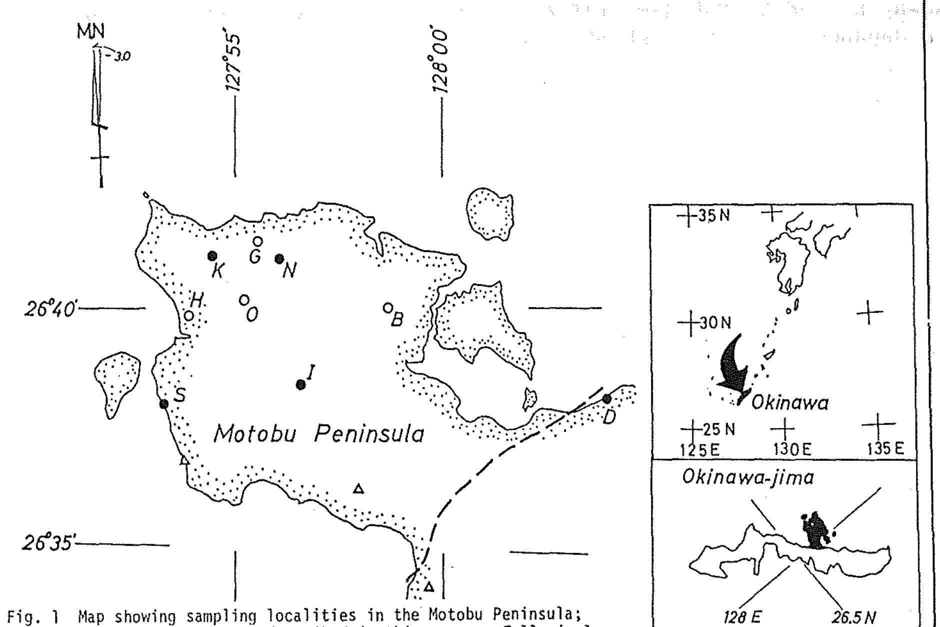


Fig. 1 Map showing sampling localities in the Motobu Peninsula; sites in the hole circle are described in this paper. Full circles, failed to obtain paleomagnetic data; triangle, site of previous report (Sasajima, 1977). B: Konshado, D: Genga, G: Gushiken, H: Hamamoto, I: Kokatsuu, K: Kitazato, N: Nakijin, O: Ufudo, S: Sakimotobu.

2. Sample and result obtained

In the Motobu Peninsula, northwestern part of Okinawa-jima, there distribute Permian to Triassic formations of which geological studies were improved by Ishibashi(1969) and Hashimoto and Nakagawa(1978). The Permian system is divided into five formations; Fukuchibaru, Bumabaru, Otowadake, Yanaza and Agaribaru formations in ascending order. Limestone samples were taken from Bumabaru and Yanaza formations because their well-bedded structure warranted the tilting correction of NRM directions. The distribution map of sample localities is shown in Fig. 1. Above-mentioned samples were taken from Site B and Site I in the figure. Besides, greenschist samples belonging to the Anne Formation of which age is assumed maybe Permian, were collected at Genga (G in Fig. 1).

The Triassic Nakijin Formation consists mainly of limestones with subordinate basic andesite lavas and tuffite intercalated in limestone beds. Among these rock kinds basic andesites and tuffites were taken from near Gushiken, Kitazato, Hamamoto, Sakimotobu and Ufudo (G,K,H,S and O, respectively). Bedded limestones, which are estimated to be *Carnian* in age as deduced from numerous characteristic ammonoids and *Halobia*, were also sampled from the southern road cutting of the Nakijin ancient castle. This submember is assumed to be lower horizon relative to the igneous submember mentioned above (Ishibashi, 1969).

By the stepwise AF demagnetization treatment of some pilot specimens, the optimum AF peak fields of cleaning for all other specimens were determined. As a result, limestone samples of Permian Yanaza and Triassic Nakijin Formations were not useful for paleomagnetism because they showed internal scatter of directions though each specimen was exceedingly stable against demagnetization field up to 1,000 Oe (MDF>1,000 Oe). Greenschist samples from Genga, of possible Permian age, and pale green tuffites from Sakimotobu of Triassic age altogether were so weak in NRM intensity and further, too soft in AF coercivity for the paleomagnetic purpose.

Contrasting to these hopeless samples, directions of NRMs from Ufudo and a part of Gushiken show reversed ones having approximately antipodal nature to the normal directions obtained from Hamamoto,

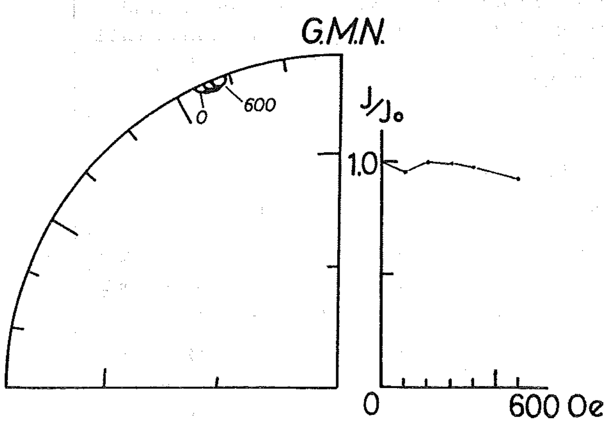


Fig. 2. An extraordinarily stable behavior of the Bumabaru limestone for AF cleaning up to 600 Oe (0.6T).

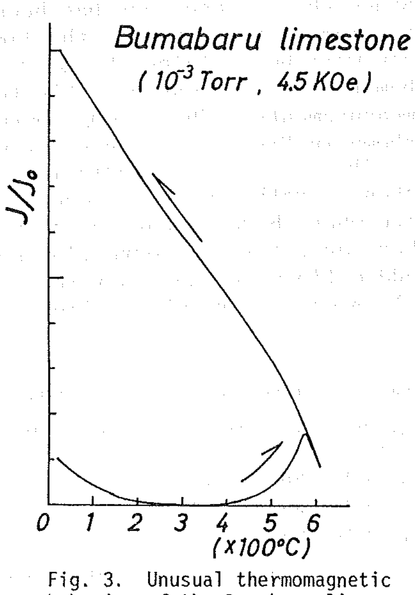


Fig. 3. Unusual thermomagnetic behavior of the Bumabaru limestone sample under vacuum $10^{-3}$ Torr., suggesting presumable reduction of the contained fine-grained hematites to a transitional state of magnetites(quasi-stable).

qualifying their high reliability as paleomagnetic data. The number of samples showed the reversed NRM is slightly fewer than those with the normal NRMs. The reversed direction of NRMs is, of course, inversed for computation as given in Table 1,basing on the assumption that these rocks acquired the original NRMs under the geomagnetic field of normal polarity during the Triassic time. The gray limestone sample of the Bumabaru formation, Middle Permian in age, shows a highly stable character for AF cleaning up to 600 Oe. A typical example is shown in Fig. 2. Considering from the result obtained, the MDF of the stable RM is supposed to be fur larger than 600 Oe.

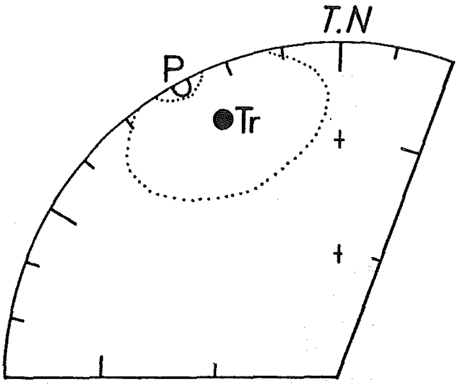


Fig. 4. Permian and Triassic mean directions of NRMs after appropriate AF demagnetization.

To make clear of responsible ferromagnetic minerals for such an exceedingly high stability, the thermomagnetic analysis has been extensively carried out. A typical example of measurements is shown in Fig. 3. As illustrated in the heating curve, a ferromagnetic character is so weak and obscure even with a high sensitivity condition of the thermomagnetic quartz balance, while at the temperature 450°C or more rather sharp increse of magnetization due to some chemical reaction takes place resulting in the Curie point similar to pure magnetite; the reaction product become more evident by the cooling process. Then, we have made experimentally a cross check of the unusual thermomagnetic phenomenon behaved by some minerals under vacuum state made with oil rotary pump. Such phenomenon was found originally by Schwartz (1969) and examined experimentally in detail by Shive and Diehl(1977). Since their reasonings has been confirmed experimentally again by us, the thermomagnetic curve of the limestone specimen in Fig. 3 (Bumabaru Formation) can well be explained by existence of a relatively small amount of very fine hematites which was not able to identify directly with a thermomagnetic measurements. The strong coercivity under AF cleaning of the same sample shown in Fig. 2 is consistent with the hematite origin mentioned above.

The structural deformation of the formations in which our samples were taken is rather weak in general, and in addition samples were taken from the site where bedding correction seemed rather easy except for basic andesites. Therefore, tilting correction seems satisfactorily performed, especially for bedded limestone and tuffite; correction angle is ranged 20-50 degrees. Paleomagnetic result is listed in Table 1.

Table 1. Paleomagnetic results of Triassic and Permian of Motobu Peninsula

| SITE | AGE | ROCK TYPE | DEC | INC | $A_{95}$ | k | N | VLAT | VLON | dp | dm | PL | AFD |
|---|---|---|---|---|---|---|---|---|---|---|---|---|---|
| G | U.Tr | basaltic andesite | -31.3 | 27.9 | 22.6 | 12.4 | 5 | 58.5 | 22.3 | 13.5 | 24.8 | 14.8 | 300 |
| O | U.Tr | basaltic andesite | -15.1 | 4.4 | 33.1 | 8.7 | 4 | 61.7 | 341.2 | 16.6 | 33.2 | 2.2 | 200 |
| H | U.Tr | basic tuff | -25.8 | 15.1 | 26.3 | 7.4 | 6 | 59.0 | 5.0 | 13.9 | 27.0 | 7.7 | 200 |
| | *U.Tr in toto* | | -23.8 | 15.9 | 21.9 | 32.8 | 3* | 60.8 | 3.0 | 11.6 | 22.5 | 8.1 | |
| B | M.P | limestone | -31.6 | - 0.7 | 4.9 | 150.6 | 7 | 49.4 | 1.6 | 2.5 | 4.9 | - 0.4 | 600 |

N*: number of site, VLAT, VLON: latitude and longitude of virtual geomagnetic pole position,
PL: paleolatitude, symbols in site as same in Fig. 1

## 3. Discussion

As shown in the Table, grouping of directions of remanent magnetization (RM) are poor and number of site is also inadequate to lead paleomagnetic conclusions, however, it is of interest that the obtained low paleolatitudes for the Motobu area are roughly in good accordance with those for Southwest Honshu that was estimated to have been near the paleoequator during the Permian and Triassic periods (Fujiwara, 1968; Hattori and Hirooka, 1979; Sasajima, 1980). Although the present result is only from Okinawa-jima, and it cannot be the representative of the entire Ryukyus, it is presumed, based on the similar latitudinal changes of both regions, that the pre-Tertiary basement rocks in the Ryukyus at least in Okinawa-jima might have formed nearly the present assemblage of Honshu and Ryukyus before the middle Triassic time. This could be in good conformity with the close zonal relation of pre-Tertiary basements structure between Southwest Honshu and North Ryukyus (Konishi, 1965).

It is impossible to decide each sence of polarities of the Permian and Triassic geomagnetic fields while the samples acquired their NRMs, but one of alternatives is to prefer solely the normal polarity for both periods as being adopted in the region has been subjected to more than 20° anticlockwise rotation accompanied by about 20° northward drift since the late Triassic until the Eocene time (Sasajima, 1977). Second alternative is to prefer solely the reversed one, in this case it is interpreted that the region has been subjected to about 156° clockwise rotation accompanied by about 36° northward drift during the same period. The average rate of the land rotation, ~1°/m.y. may be unusually large excepting for the instance of Southwest Honshu during the Paleogene (Sasajima, 1980). The other two alternatives which are combined the opposed polarities in the Permian and Triassic times to the above-stated alternative cases are possible, but they are omitted in this argument.

As concluding remarks, it is noted that, 1) some kinds of limestones possess potent characters for the paleomagnetic usage and, 2) the Triassic paleomagnetic pole for Okinawa-jima is almost consistent with that for Inuyama area, Central Japan (Shibuya and Sasajima, in this issue), and 3) during the period since the Middle Permian through the Eocene to the Recent, Okinawa-jima might have experienced the geotectonic evolution with the similar latitudinal movement accompanied some rotational movements to Honshu, forming one chain like as at present.

## References


Fujiwara, Y. (1968): J. Fac. Sci., Hokkaido Univ., Ser. 4, 14, 159

Hashimoto, S. and H. Nakagawa (1978): Geological Studies of the Ryukyu Islands 3, ed. K. Kizaki, 23.

Hattori, I and K. Hirooka (1979): Tectonophysics, 57, 211.

Ishibashi, T. (1969): Mem. Fac. Sci., Kyushu Univ., Ser. Geol., 19, 373.

Kizaki, K. (1978): Geological Structure of the Ryukyu Islands, 3, ed. K. Kizaki, 228.

Konishi, K. (1965): J. Geol. Soc. Japan, 71, 437.

Nur, A. and Z. Ben-Avraham (1978): J. Phys. Earth, 26, suppl., 21.

Sasajima, S. (1977): Rock Mag. Paleogeophys., 4, 108.

__________ (1980): Final report of GDP, A.G.U. (in press)

__________ and M. Shimada (1965): Mem. Coll. Sci., Univ. Kyoto Ser. B, 32, 89.

Schwarz, E. J. (1969): Earth Planet. Sci. Lett., 5, 333.

Schive, P. N. and J. F. Diehl (1977): Geophys. Res. Lett., 4, 159.

# PALEOMAGNETISM OF PERMIAN RED CHERT IN THE TAMBA BELT, SOUTHWEST JAPAN (PRELIMINARY REPORT)

Ikuo KATSURA*, Junichi NISHIDA** and Sadao SASAJIMA*

* Department of Geology and Mineralogy, Faculty of Science, Kyoto University, Kyoto 606, Japan
** Institute of Natural Science, Otani University, Kyoto 603, Japan

## Introduction

First attempts of pre-Cretaceous paleomagnetic study in Japan were reported by Minato and Fujiwara(1967, 1968). Shimada et al.(1967) reported the change of paleolatitude for southwest Japan from Carboniferous to Cretaceous time. They suggested that southwest Japan was situated at lower latitude at pre-Cretaceous. Recently, Hattori and Hirooka(1977, 1979) presented paleomagnetic results of some Permian greenstones in the northern part of Mino Zone, central Japan. They suggested that Japanese upper Paleozoic strata might have been formed at equatorial region and they have migrated toward the present situation. This presumption shoud be confirmed on the other pre-Cretaceous strata in Japan.

The Tamba Belt composes one of important Paleozoic unit in the structural framework of Japan. Geology of Tamba Belt around Ohmori area, which is located northwestern part of Kyoto City, was reported by Tamba Belt Research Group(1974). They reported that there expose schalestein and red chert. The greater part of the formations in this district is regarded to be lower to middle Permian.

It is our purpose to study Japanese pre-Cretaceous paleomagnetism by using many rock facies, especially red chert. Red chert is not known of its origin of remanence and the usage for paleomagnetic purpose. The result of examination on the problem whether red chert is available for paleomagnetic research or not is presented.

## Sample used

Rock samples were collected from the southern wing of the Ohmori syncline region in the Tamba Belt located on the northern area of Kyoto Prefecture (Tamba Belt Research Group, 1974).

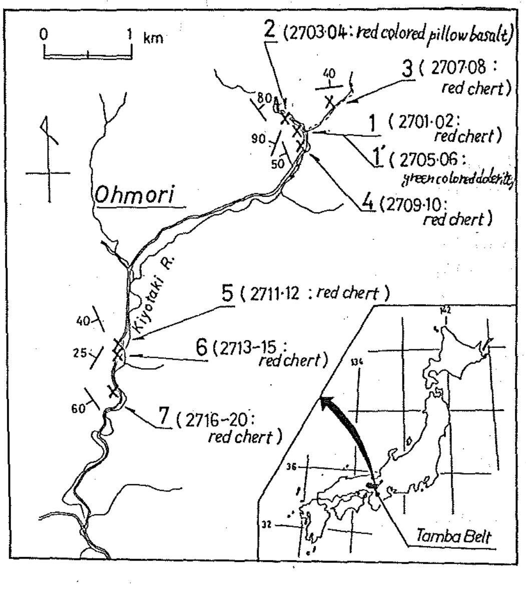


Fig.1 Sampling sites of the Ohmori area in the Tamba Belt, southwest Japan. Site numbers, sample numbers and rock facies are represented with strike and dip of bedding plane.

Most samples are red chert, and additional samples are red colored pillow basalt and green colored dolerite. Localities of samples are shown in Fig.1. Fusulina in limestone lens included in schalestein and radiolaria in chert indicate that the formation, which comprises our samples, may be lower to middle Permian age. A stratigraphic succession cropped out along Site 5 to 7 is considered to be a sequence of banded red cherts of a few tens meters thickness with minor folds. The bedding planes of red chert samples were clearly recognized, but that of volcanic rocks were not so clear in general. Hence, the precision of tilting correction for red cherts seems considerably high.

Paleomagnetic measurement

Paleomagnetic measurements were carried out on cylindrical cored specimen (about 1 inch in diameter, 1 inch in length) by means of spinner magnetometer(Schonstedt SSM-1A).

Paleomagnetic results

Alternating field demagnetization

Firstly, one pilot specimen from every block hand sample was subjected to the stepwise alternating field(AF) demagnetization up to 1,000 or 1,600 Oe.

NRM of red cherts did not notably changed their remanent directions during AF demagnetization of which examples are shown in Fig.2. Based on the modes of intensity change against AF demagnetization, red chert can be divided into two groups. One type shows so slow decrease in intensity

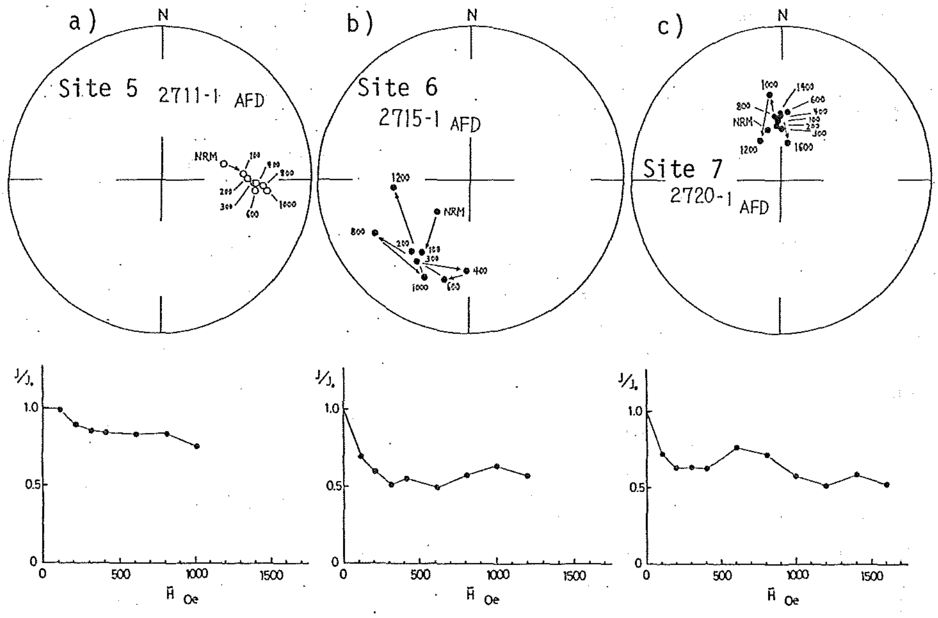


Fig.2 Diagrams representing typical results of progressive AF demagnetization of red cherts from Site 5-7. Remanent directions are plotted on Schmidt's equal area projection and represented by directions before bedding correction (open circle; upper hemisphere, solid circle; lower hemisphere).

change that it is impossible to decide the median destructive field(MDF) with the limit of our apparatus. Another type shows 30-40 % intensity reduction below peak AF of 200-400 Oe and after application of higher fields the intensity reduces gently. In this case, MDF is about 500-600 Oe. Therefore, all red chert specimens were cleaned in the optimum peak AF of 200-400 Oe.

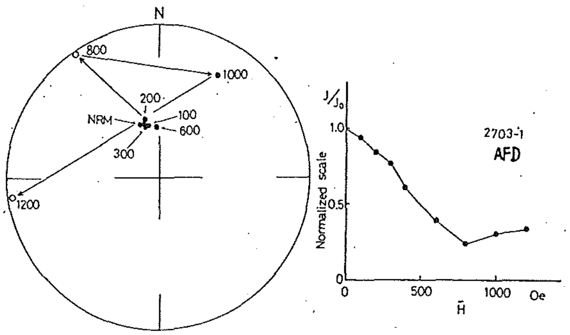


Fig.3 Diagram representing the result of AF demagnetization of red colored pillow basalt.

NRM of red colored pillow basalt showed a little change both in direction and in intensity through AF demagnetization process up to peak AF of 600 Oe. Its MDF was about 500 Oe. And the direction of NRM changed considerably when the applied AF was higher than 600 Oe (Fig.3). As a result, we chose 200 Oe of peak AF as the optimum demagnetization field.

NRM of green colored dolerite samples changed their direction randomly accompanied by a rapid reduction of remanent intensity after the similar AF treatment. Therefore, these rock samples were excluded from further paleomagnetic study.

Thermal demagnetization

One pilot specimen from every site was examined their stability for

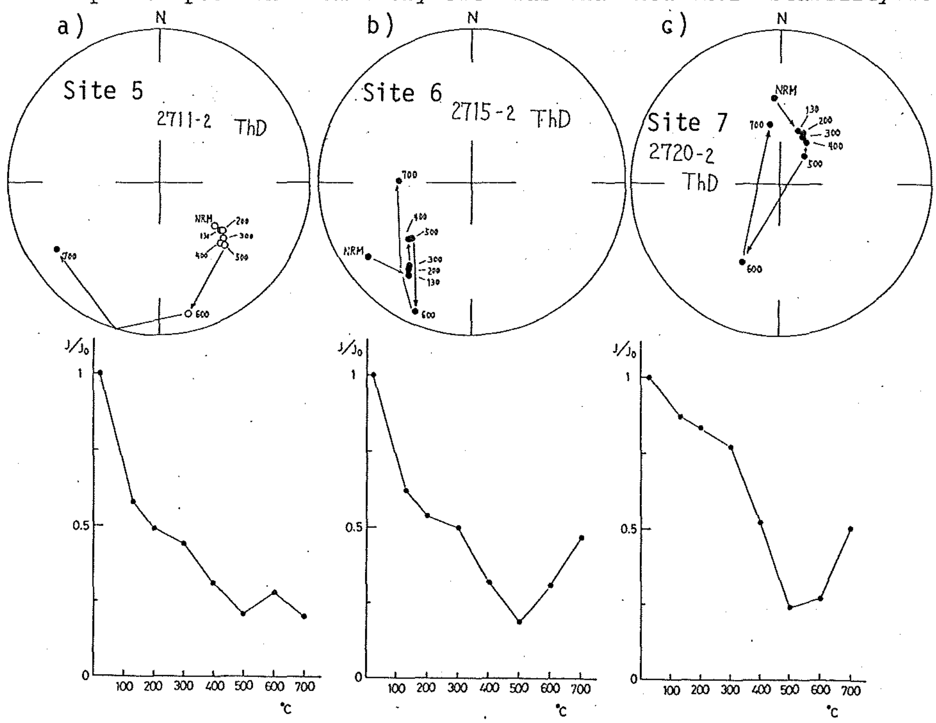


Fig.4 Diagrams representing the results of thermal demagnetization of red chert. Remanences are represented by directions before bedding correction.

stepwise thermal demagnetization(ThD) up to 700°C.

In Fig.4 is shown the result of thermal demagnetization of chert except for Site 3 and 4. It is noticed that the direction of NRM of red chert is very stable and the intensity decreases linearly up to 500°C. It may be safely stated that the remanence of red chert is paleomagnetically reliable from the examination of AF and Th demagnetization. In Table 1 are summarized the remanent directions after bedding correction with other paleomagnetic parameters and remanent intensities before AF demagnetization.

Table 1. Paleomagnetic data from Permian red chert in Tamba Belt

| Site | Rock type | N | NRM intensity (emu/g) | ODF(Oe) | D | I | $\alpha_{95}$ | k | Paleo-latitude |
|---|---|---|---|---|---|---|---|---|---|
| 5 | red chert | 3 | $4.69\times10^{-6}$ | 400 | 97.5 | 0.5 | 23.0 | 30 | 0.3 |
| 6 | red chert | 6 | $9.59\times10^{-7}$ | 200~300 | -145.1 | 24.3 | 8.0 | 71 | 13 |
| 7 | red chert | 9 | $2.30\times10^{-6}$ | 200~400 | -102.4 | 34.4 | 9.6 | 30 | 19 |

N=number of specimens; ODF=optimum demagnetization field; D and I=declination and inclination after bedding tilt correction (site mean);k and $\alpha_{95}$=Fisher's parameter

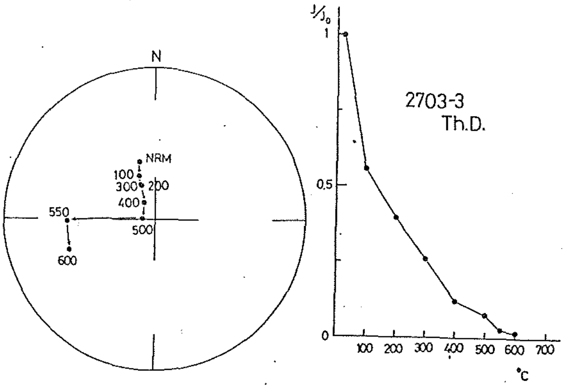


Fig.5 Diagram of the result of thermal demagnetization of red colored pillow basalt.

Red colored pillow basalt was also thermally demagnetized and the result is shown in Fig.5. Compared with the result of AF demagnetization, it is noticed that the intensity of NRM reduced rapidly with considerable directional change. As the remanent magnetization is not stable against thermal treatment and the bedding plane at the sampled locality is not clear, the red colored pillow basalt is excluded from paleomagnetic consideration.

Magnetization of red chert

The intensity of red chert (initial state) is about $10^{-6}$ emu/g. The carrier of remanence have been presumed hematite from its thermomagnetic and AF demagnetization behaviors. Red chert, which contains red pigment in microcrystalline quartz and fossils of radiolaria, had scarcely been used for paleomagnetic purpose so far. The carrier of remanence has not been detected, as we have failed to identify directly the Curie temperature of ferromagnetic mineral by thermo-magnetic analysis. By using the trial proposed by Shive and Diehl(1977), we have indirectly regarded hematite as being responsible for the NRM; such an actual example is shown in the paper of this issue by Sasajima and Torii(1980).

Kitamura(Kyoto University) tried to find out iron oxide minerals in red chert from Ohmori area(Site 5) by using Hitachi 700H 200KV Analytical Electron Microscopy (personal communication). He found the existence of iron mineral which have an euhedral tabular shape about 2,000 Å long and 500 Å width. This iron mineral is supposed to be hematite crystal as a carrier of the remanence.

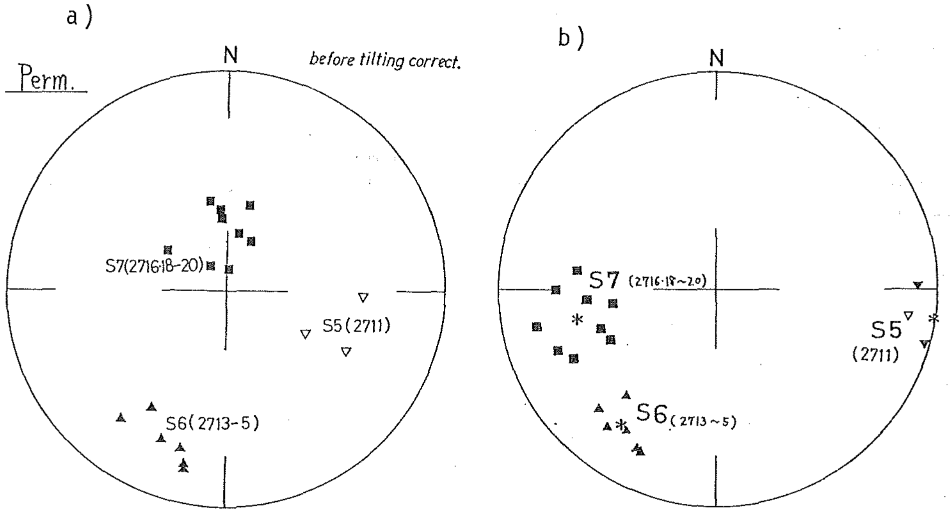


Fig.6 Paleomagnetic results of red cherts after optimum AF demagnetization. a) remanent directions before bedding correction, b) remanent directions after bedding correction. Inverted triangle; Site 5, triangle; Site 6, square; Site 7.

## Discussion

As the plunge axis in Ohmori area cannot be determined precisely, the direction of NRM is corrected merely using dip angle of the bedding plane at sampling locality. It is noticed that the obtained declination does not truely reflect the declination of the past geomagnetic field. The directions of NRM of red chert obtained in this study are shown in Fig.6.

Isozaki and Matsuda(1980) estimated the sedimentation rate of Tamba Group in Nishiyama, Kyoto as 1.4 mm/1000 yrs. The other estimations for the banded chert are about some tens or some millimeters per thousand years (Iijima et al., 1978; Yao et al., 1980). If this sedimentation rate and the average frequency of geomagnetic reversals of about $10^6$ years (Cox, 1975) are simply applicable to this study, we may expect a normal reverse transition of remanent polarities in a few tens meters thick of strata. The strikes and dips of Site 5-7 are similar and the overturn of chert sequences was not observed near these sites. Red cherts in these sites are supposed successive strata of a few tens meters with minor folds. We can regard the antipodal directions of Site 5 and Site 7 as a reasonable result of the geomagnetic reversal. It is noticed that the remanence of chert is exceedingly stable against AF and thermal demagnetizations. Then we are able to expect that chert has reliable paleomagnetic records.

If the remanence was acquired at or just after the deposition of chert, the shallow inclinations obtained strongly suggest that the chert sequences in the Tamba Belt had existed at low latitude in lower to middle Permian. This explanation agrees well with the presumption of the Japanese northward drift(Hattori and Hirooka, 1979).

## References

Cox, A. (1975) Rev. Geophys. Space Phys., 13, 35.
Fujiwara, Y. (1967) J. Fac. Sci. Hokkaido Univ., Ser.4, 13, 395.
Fujiwara, Y. (1968) J. Fac. Sci. Hokkaido Univ., Ser.4, 14, 159.

Hattori, I. and Hirooka, K. (1977) J. Japan. Assoc. Min. Petr. Econ. Geol., 72, 340.
Hattori, I. and Hirooka, K. (1979) Tectonophysics, 57, 211.
Iijima, A., Kakuwa, Y., Yamazaki, K. and Yanagimoto, Y. (1978) J. Fac. Sci. Univ. Tokyo, Sec.2, 19, 369.
Isozaki, Y. and Matsuda, T. (1980) J. Geosci. Osaka City Univ., 23, 115.
Minato, M. and Fujiwara, Y. (1964) Proc. Japan Acad., 40, 116.
Minato, M. and Fujiwara, Y. (1965) J. Assoc. Geol. Coll. Japan, no.78, 21.
Sasajima, S. and Torii, M. (1980) in this issue.
Shimada, M., Nishida, J. and Sasajima, S. (1967) J. Geol. Soc. Japan, 73, 93. (in Japanese)
Shive, P. N. and Diehl, J. F. (1977) J. Geomag. Geoelectr., 29, 345.
Tanba Belt Research Group (1974) J. Assoc. Geol. Coll. Japan, 28, 57. (in Japanese with English Abstract)
Yao, A., Matsuda, T. and Isozaki, Y. (1980) J. Geosci. Osaka City Univ., 23, 135.

AUTHOR INDEX


AKAI, Hiroshi see FURUYA, J.
DOMEN, Haruo 59
FUJIWARA Yoshiki, S. MUKOYAMA and T. KOSHIMIZU 49
FURUTA, Toshio see FURUYA, J.
FURUYA, Jun, H. AKAI and T. FURUTA 82
HAMANO, Yozo see KONO, M.
HASE, Yasushi see HYODO, M.
HAYASHIDA, Akira 85
HEKI, Kohsuke 72
HIROOKA, Kimio 78
HIROOKA, Kimio see NAKAJIMA, T.
HIROOKA, Kimio see SASAJIMA, S.
HYODO, Masayuki, T. ISHIZAWA, Y. HASE, H. INOKUCHI, N. ISEZAKI, and K. YASKAWA 36
INOKUCHI, Hiroo, H. MORINAGA and K. YASKAWA 68
INOKUCHI, Hiroo see ISEZAKI, N.
INOKUCHI, Hiroo see HYODO, M.
ISEZAKI, Nobuhiro, J. MATSUDA, H. INOKUCHI, and K. YASKAWA 30
ISEZAKI, Nobuhiro see HYODO, M.
ISHIZAWA, Toshiki see HYODO, M.
ITO, Haruaki, K. TOKIEDA and Y. NOTSU 113
KANEOKA, Ichiro, H. MEHNERT, S. ZASHU and S. KAWACHI 100
KATSURA, Ikuo, J. NISHIDA and S. SASAJIMA 130
KATSURA, Ikuo see OTOFUJI, Y.
KAWACHI, Shimpei see KANEOKA, I.
KOBAYASHI, Kazuo see SATO, T.
KOBAYASHI, Kazuo see TONOUCHI, S.
KONO, Masaru, Y. HAMANO, T. NISHITANI and T. TOSHA 22
KOSHIMIZU, Tatsuji see FUJIWARA, Y.
MAENAKA, Kazuaki 94
MATSUBARA, Yoshikazu and J. MATSUDA 1
MATSUDA, Jun-ichi see MATSUBARA, Y.
MATSUDA, Jun-ichi see ISEZAKI, N.
MEHNERT, Harald see KANEOKA, I.
MORINAGA, Hayao see INOKUCHI, H.
MUKOYAMA, Sakae see FUJIWARA, Y.
NAKAJIMA, Tadashi and K. HIROOKA 52
NISHIDA, Junichi see KATSURA, I.
NISHIMURA, Susumu see SASAJIMA, S.
NISHITANI, Tadashi see KONO, M.
NOTSU, Yukio see ITO, H.
OTOFUJI, Yo-ichiro, I. KATSURA and S. SASAJIMA 40
SAKAI, Hideo 8, 61
SASAJIMA, Sadao, S. NISHIMURA and K. HIROOKA 90
SASAJIMA, Sadao and M. TORII 126
SASAJIMA, Sadao see OTOFUJI, Y.
SASAJIMA, Sadao see SHIBUYA, H.
SASAJIMA, Sadao see KATSURA, I.
SATO, Takaharu and K. KOBAYASHI 16
SHIBUYA, Hidetoshi and S. SASAJIMA 121
TATSUMI, Yoshiyuki see TORII, M.
TOKIEDA, Katsuyasu see ITO, H.
TONOUCHI, Shyoji and K. KOBAYASHI 107
TORII, Masayuki and Y. TATSUMI 105
TORII, Masayuki see SASAJIMA, S.

| | | |
|---|---|---|
| TOSHA, Toshiyuki | see KONO, M. | |
| YASKAWA, Katsumi | see ISEZAKI, N. | |
| YASKAWA, Katsumi | see HYODO, M. | |
| YASKAWA, Katsumi | see INOKUCHI,H. | |
| YOSHIDA, Mitsuo | | 46 |
| ZASHU, Shigeo | see KANEOKA, I. | |